The characterization of adaptor protein homologues in *Plasmodium falciparum*

Sandra Allison Meredith

Thesis Presented for the Degree of
DOCTOR OF PHILOSOPHY
in the Department of Pharmacology
UNIVERSITY OF CAPE TOWN
October 2008

Supervisor
Dr Heinrich Hoppe

Declaration

I, Sandra Meredith, hereby declare that the work on which this thesis is based is my original work (except where acknowledgements indicate otherwise) and that neither the whole work nor any part of it has been, is being, or is to be submitted for another degree in this or any other University.

I empower the University to reproduce, for the purpose of research, either the whole or any portion of the contents in any manner whatsoever.

Signed signature removed

Date 10/07/09

Abstract

Sandra Allison Meredith

The characterization of adaptor protein homologues in *Plasmodium falciparum*

October 2008

Plasmodium falciparum is becoming increasingly more resistant to regular antimalarial drugs, making it necessary to identify novel drug candidates and drug targets. Components of the endocytic and secretory pathway in asexual stage parasites are attractive targets because they play fundamental roles in the normal processes of parasite metabolism. Adaptor protein complexes are components of protein coats that associate with transport vesicles of the endocytic and secretory pathways in mammalian cells. Homologues of several adaptor protein subunits are encoded by the parasite genome. Their presence suggests that the parasite experiences clathrin-mediated transport processes. This study reports the cloning and characterization of three medium (μ) chain adaptin protein homologues and two sigma (σ) chain homologues. The malaria gene sequences were amplified by RT-PCR and expressed in *E. coli*. The recombinant proteins, as well as synthetic peptides derived from the σ proteins, were used to generate antisera. Monospecificity of the antisera was confirmed by Western blotting of parasite lysates and the subcellular localization of the adaptor homologues in the parasite was determine by immunofluorescence and immuno-electron microscopy assays. The μ1 and μ2 adaptins co-localize to a ribbon-like structure in the parasite cytosol which appears as tubulovesicular profiles under electron microscopy and is morphologically suggestive of a secretory compartment such as the Golgi. This conclusion is further supported by the extensive co-localization of μ1 and *Pf*rab6, a Golgi marker in the parasite. In contrast, the μ4 adaptin homologue is associated with the plasma membrane and digestive vacuole. Plasma membrane localization is co-incident with that of the parasite clathrin heavy chain. These results suggest that μ1 and μ2 form part of parasite adaptor complexes that are analogous to mammalian AP-3 and AP-4 which mediate clathrin-independent secretion from the Golgi. In turn, μ4 may be part of a parasite adaptor complex, similar to mammalian AP-2, involved in clathrin-mediated endocytosis from the plasma membrane and trafficking at the food vacuole. Further Western blotting and co-localization experiments suggest that the μ1 and μ4 adaptins are complexed with the smaller σ1 and σ4 adaptins respectively, in a complex that does not dissociate under standard SDS-PAGE conditions.

Abstract

Plasmodium falciparum is becoming increasingly more resistant to regular antimalarial drugs, making it necessary to identify novel drug candidates and drug targets. Components of the endocytic and secretory pathway in asexual stage parasites are attractive targets because they play a fundamental role in the normal processes of parasite metabolism. Adaptor protein complexes are components of protein coats that associate with transport vesicles of the endocytic and secretory pathways in mammalian cells. Homologues of several adaptor protein subunits are encoded by the parasite genome. The presence of these genes suggests that the parasite experiences clathrin-mediated transport processes. This study reports the cloning and characterization of selected malarial homologues of these adaptor proteins, namely three medium (μ) chain adaptin homologues and two sigma (σ) chains. The malaria gene sequences were amplified by RT-PCR and expressed in *E. coli*. The recombinant proteins, as well as synthetic peptides derived from the σ proteins, were used to generate antisera. Monospecificity of the antisera was confirmed by Western blotting of parasite lysates. The antisera were used in immunofluorescence and immuno-electron microscopy assays to determine the subcellular localization of the adaptor protein homologues in the parasite. The μ1 and μ2 adaptins co-localize to a ribbon-like structure in the parasite cytosol which appears as tubulovesicular profiles under electron microscopy and is morphologically suggestive of a secretory compartment such as the Golgi. This conclusion is further supported by the extensive co-localization of μ1 and *Pf*rab6, an acknowledged Golgi marker in the parasite. In contrast, the μ4 adaptin homologue is associated with the plasma membrane and digestive vacuole. The plasma membrane localization is co-incident with that of the parasite clathrin heavy chain. These results suggest that μ1 and μ2 form part of parasite adaptor complexes that are analogous to mammalian AP-3 and AP-4 which mediate clathrin-independent secretion from the Golgi. In turn, μ4 may be part of a parasite adaptor complex, similar to mammalian AP-2, involved in clathrin-mediated

endocytosis from the plasma membrane and trafficking at the digestive vacuole. Further Western blotting and co-localization experiments suggest that the μ1 and μ4 adaptins are complexed with the smaller σ1 and σ4 adaptins respectively, in a complex that does not dissociate under standard SDS-PAGE conditions. In addition to coat recruitment, adaptor proteins select protein cargo for inclusion into transport vesicles in mammalian cells. The results presented here constitute the first evidence that endocytosis in parasites may be mediated by clathrin-associated adaptor complexes, while selective targeting of proteins in the secretory pathway may proceed via adaptor protein cargo selection.

Publications arising from this work

Peer-reviewed Journals

- Hoppe, H.C., van Schalkwyk, D.A., Wiehart, U.I.M., Meredith, S.A., Egan, J., and Weber, B.W. (2004). Antimalarial quinolines and artemisinin inhibit endocytosis in *Plasmodium falciparum*. *Antimicrobial Agents and Chemotherapy*. **48**(7), 2370-2378.

Conference presentations

Oral presentations

- University of Cape Town Medical Research Day, 2005
  The characterization of adaptor protein homologues in *Plasmodium falciparum*.

Acknowledgments

I owe a great dept of gratitude to my supervisor Dr Heinrich Hoppe for his support, enthusiasm, and expertise.

A heartfelt thanks to past and present members of the Department of Pharmacology, especially Associate Professor Pete Smith, Dr Susan Yeh, Dr Ursula Wiehart, Dr Donelly van Schalkwyk, Dale Taylor, Wynand Smythe, Professor Marc Blockman and Noor and Sumaya Salie.

A huge thank you to my friends and family, especially my parents, for their continued love and support.

I would like to acknowledge and thank Dr Nicole Struck for the co-localization experiment with ERD2-GFP expressing parasites and Andrew Kessler for his help with the mitochondria staining and imaging. Furthermore, I'd like to thank Dr Tim Gilberger for the gift of rabbit antibodies to *Pf*Bip and for the GFP-μ1 data.

Lastly, I would like to thank the following funding agencies for their financial support during the completion of my degree: The University of Cape Town, The Medical Research Council, The Harry Crossley Foundation, The Marion Beatrice Waddell Foundation, The Duncan Baxter Foundation, The KW Johnston Bequest Foundation and The Benfara Foundation.

Table of Contents

List of Figures and Tables

List of Tables

List of Abbreviations

A	adenine
AP	adaptor protein
N-terminal	amino-terminal
BFA	brefeldin A
BLASTN	basic local alignment search tool (nucleotide)
BLASTX	basic local alignment search tool (protein)
BSA	bovine serum albumin
C-terminal	carboxyl-terminal
cDNA	complementary deoxyribonucleic acid
°C	degrees Celsius
C	cytosine
CGN	*cis*-Golgi network
DAPI	4',6-Diamidino-2-phenylindole Dihydrochloride
DEPC	diethyl pyrocarbonate
dH_2O	distilled deionised water
DMSO	dimethyl sulfoxide
DNA	deoxyribonucleic acid
dNTPs	deoxynucleoside triphosphate
DTT	dithiothreitol
DV	digestive vacuole
E. coli	*Escherichia coli*
EBA	erythrocytic binding antigen
EDTA	ethylene diamine tetra acetic acid
ELISA	enzyme-linked immunosorbent assay
EM	electron microscopy
ER	endoplasmic reticulum
ERGIC	ER-Golgi intermediate compartment
F	forward
FCS	foetal calf serum
Fig.	figure
FITC	fluorescein isothiocyanate
FPIX	ferriprotoporphyrin IX
g	gram
G	guanine

GDA	gluteraldehyde
gDNA	genomic DNA
GFP	green fluorescent protein
GST	glutathione-S-transferase
hct	haematocrit
HEPES	hydroxyethane piperazine sulphonic acid
hrs	hours
MHC-II	histocompatibility complex type II
IFA	immunofluorescence assay
IPTG	isopropyl-β- D- thiogalactopyranoside
kb	kilobase
kDa	kilodalton
L	litre
M	molar
mA	milli-Amps
mg	milligrams
mL	milli-Litre
mM	milli-Molar
mRNA	messenger ribonucleic acid
µl	micro-litre
µm	micro-meter
Tm	melting temperature
nm	nano-meter
OD_{260}	optical density at 260 nm
OD_{280}	optical density at 280 nm
OPD	phosphate-citrate buffer containing o-phenylenediamine and hydrogen peroxide
P. falciparum	*Plasmodium falciparum*
NC	parasite nucleus
PAGE	polyacrylamide gel electrophoresis
PBS	phosphate-buffered saline
PCR	polymerase chain reaction
PEMS	parasitophorous vacuolar membrane-enclosed merozoite structures
PEXEL	*Plasmodium* export element
PFA	paraformaldehyde
pH	negative algorithm of the hydrogen concentration ion
PMSF	phenylmethylsulfonyl fluoride
PPM	parasite plasma membrane
PRD	proline-rich domain
pst	parasitaemia
PV	parasitophorous vacuole

PVM	parasitophorous vacuolar membrane
RACE	rapid amplification of cDNA ends
rcf	relative centrifugation factor
RBC	red blood cell
R	reverse
RNA	ribonucleic acid
RNAi	RNA interference
RNase	ribonuclease
rpm	revolutions per minute
RT-PCR	reverse transcription polymerase chain reaction
SDS	sodium dodecyl sulphate
SDS-PAGE	sodium dodecyl sulphate- polyacrylamide gel electrophoresis
SERA	secondary ER
SH3	Src homology 3
SS	signal sequence
T	thymine
TAE	tris/acetate (buffer)
TBE	tris/borate (buffer)
TdT	terminal deoxynucleotidyl transferase
TE	tris/EDTA (buffer)
TEMED	*N,N,N¢,N¢*-tetramethyl-ethylenediamine
tER	transitional ER
TGN	*trans*-Golgi network
T. gondii	*Toxoplasma gondii*
Tris	Tris (hydroxymethyl) methylamine
TVM	tubovesicular membrane
TVN	tubulovacuolar network
U	units
UAP	universal adaptor primer
UV	ultraviolet
V	volt
VTS	vacuolar transport signal
v/v	volume/volume
w/v	weight/volume
X-gal	5-bromo-4-chloro-3-indolyl-β-D-galactoside

CHAPTER 1 – General Introduction

1.1. Endocytosis and secretion in eukaryotic cells

Vesicular trafficking in eukaryotic cells consists of the exocytic system, where proteins are exported through the secretory pathway, and the endocytic system, where proteins are internalized from the extracellular medium (Mellman *et al.*, 1986). In mammalian cells, newly synthesized proteins and lipids destined for secretion are translocated into the endoplasmic reticulum (ER) prior to being transported in coated vesicles from the ER to the Golgi complex for processing and sorting, and finally to the plasma membrane. Three different coat protein complexes participate in vesicle formation. These include the clathrin-coat, the COPI-coat and the COPII-coat. The coat proteins mediate cargo selection and membrane curvature (Rothman *et al.*, 1994, Kreis *et al*, 1995, Harter, 1995). Chaperone proteins that assist the folding and maturation of secretory proteins, reside in the ER lumen. These proteins must be retained in the ER to sustain the important functions of the compartment. Resident proteins are recovered from post-ER compartments by means of retrieval signals via COPI-coated vesicles (Kreis *et al*, 1995, Janson *et al.*, 1998). COPI-coats also mediate intra-Golgi vesicle trafficking (Crottet *et al.*, 2002).

Proteins that do not contain a retrieval signal are transported on microtubule tracks to the Golgi in COPII-coated vesicles. Ribosome-free regions of the ER, termed the transitional ER (tER), are the specialized budding sites for COPII-coated vesicles (Gürkan *et al.*, 2006, Kirk and Ward, 2007, Lee *et al.*, 2008). The COPII vesicles then fuse with a tubulovesicular system which links the ER and the Golgi complex, known as the ER-Golgi intermediate compartment (ERGIC), to deliver cargo proteins. Proteins exit the ERGIC and are transported to the Golgi (Hauri and Schweizer, 1992, Baines and Zhang, 2007). The Golgi complex, the most important morphological component of the secretory pathway, sorts proteins and targets them to other organelles. The Golgi is comprised of

three cisternal membranes organized into stacks; the *cis*, *medial* and *trans* compartments. These sub-compartments differ in composition and function, and are linked in a continuous system. A network of tubules and vesicles is present on either side of the stack and are referred to as the *cis*-Golgi network (CGN) and *trans*-Golgi network (TGN), respectively (Rothman *et al.*, 1984, Shorter *et al.*, 1999, Sheiner and Soldati-Favre, 2008). The *trans*-Golgi network plays a key role in the sorting and targeting of secreted proteins to the correct destination. Proteins may be directed to organelles within the cell, such as secretory granules, to early or late endosomes and lysosomes, or may be secreted to the plasma membrane, or in the case of polarized epithelial cells, to the basolateral or apical membrane surface (Salamero *et al.*, 1990, Traub and Kornfeld, 1997. Nelson and Yeaman, 2001).

Converse to secretion, cells are able to internalize extracellular fluid and macromolecules from the surrounding environment by endocytosis. This occurs at specialized sites or invaginations of the plasma membrane to form coated transport vesicles which carry cargo molecules into the cell (Fig. 1) (Kirchhausen *et al.*, 1999). Two types of endocytosis exists; phagocytosis, for the uptake of large particles, and pinocytosis, to allow fluid and small solutes to enter the cell. Pinocytosis occurs in all cell types, whereas phagocytosis is restricted to specific mammalian cells. Actin plays a crucial role in these internalization events (Conner and Schmid, 2003a, Engqvist-Goldstein and Drubin, 2003, Lazarus *et al.*, 2008). In phagocytosis, membrane extensions develop in an actin-dependent process to engulf the entire particle destined for internalization. The formation of the protrusions and vesicle fission is driven by actin polymerization, which is regulated by two Rho-family GTPases, Cdc42 and Rac (May and Machesky, 2001, Niedergang and Chavrier, 2004). In addition to its involvement in endocytosis at the plasma membrane, actin is required for the movement of transport vesicles derived from Golgi membranes, for membrane fusion, as well as for secretion at the plasma membrane (Eitzen *et al.*, 2003, Egea *et al.*, 2006, Lanzetti *et al.*, 2007).

Pinocytosis involves the invagination of the plasma membrane. There are several pathways by which pinocytosis occurs in mammalian cells, determined by the size and characteristics of the extracellular particles. These pathways include macropinocytosis and three receptor-mediated pathways; clathrin-mediated, caveolae-mediated and

clathrin- and caveolae-independent endocytosis (Conner and Schmid, 2003a, Lefkir *et al.*, 2004).

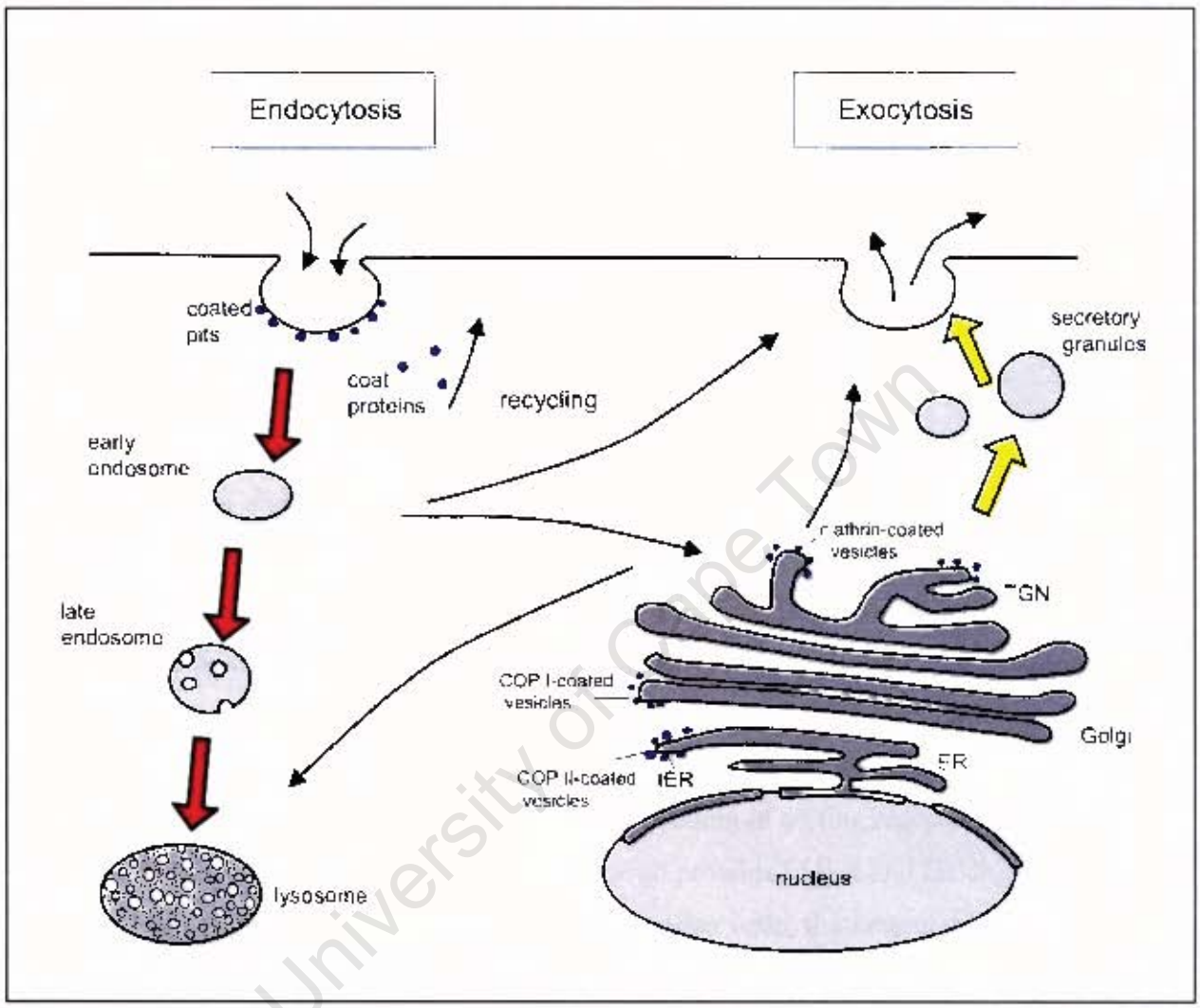

Figure 1. Vesicular trafficking in eukaryotic cells.

The endocytic route in eukaryotic cells involves the invagination of the plasma membrane to form membrane-bound transport vesicles for the delivery of cargo molecules to organelles within the cell. The exocytic route involves the secretion of nascent proteins from the *trans*-Golgi network (TGN) to other destinations within the cell and to various membrane surfaces.

Macropinocytosis is a GTPase regulated process whereby actin-driven membrane protrusions engulf the extracellular environment (Araki *et al.*, 1996, Conner and Schmid 2003a). Caveolae-dependent mechanisms, less common than clathrin-mediated processes,

take place at small, flask-shaped invaginations at lipid-rafts in the plasma membrane of numerous mammalian cells. Lipids and protein-lipid interactions compartmentalize the membrane into lipid-based microdomains. Lipid-rafts are detergent-resistant cholesterol and sphingolipid-rich domains which interact with cholesterol-binding proteins called caveolin, the main protein component of caveolae (Nichols and Lippincott-Schwartz, 2001, Parton and Richards, 2003, Echarri *et al.*, 2007). Caveolae-mediated endocytosis is dependent on dynamin for vesicle scission (Le and Nabi, 2003). Clathrin- and caveolae-independent endocytosis is less well defined and also involves lipid-rafts for the internalization of lipids and fluids. Internalization is a transient, cargo-activated process that is dependent on cholesterol and the actin cytoskeleton, but independent of dynamin (Damm *et al.*, 2005, Kirkham and Parton, 2005).

Clathrin-mediated endocytosis is the most extensively characterized route of particle internalization and is accountable for a large portion of vesicular traffic to endosomal compartments. Clathrin-mediated pathways function to maintain homeostasis of the cell and are essential for nutrient uptake and receptor recycling (Owen and Luzio, 2000, Takei and Haucke, 2001). Actin is involved in the recruitment of endocytic machinery to the plasma membrane and has a mechanical role in membrane invagination, vesicle fission and internalization of nascent vesicles into the cytosol (Merrifield, 2004, Yarar *et al.*, 2005). Vesicle formation is triggered by the binding of sorting receptors in the protein coat with sorting signals of transmembrane cargo proteins (Allan and Balch, 1999). Two types of cargo-binding receptors exist in mammalian cells; the heterotetrameric adaptor protein (AP) complexes, of which there are four, and the Golgi-localized, γ-ear-containing, ARF-binding (GGA) proteins. In addition to cargo selection, these adaptors function in binding clathrin and other accessory proteins implicated in vesicle formation. The GGA proteins contain domains homologous to the adaptins of the AP complex (Boehm and Bonifacino, 2001, Chapuy *et al.*, 2008).

Clathrin is a trimeric protein arranged in a triskelion composed of three heavy chains closely associated with three light chains. It is recruited to membranes by AP complexes and self-assembles on the inner surface of the plasma membrane to form a polyhedral lattice. The clathrin lattice provides a mechanical means to distort the membrane, forcing it to invaginate to form a coated pit. This pit enlarges to eventually form a clathrin-coated

vesicle. Unaided, clathrin has no affinity for membranes (Takei and Haucke, 2001, Traub, 2005).

AP complexes associate with the cytoplasmic face of organelles of the secretory and endocytic pathways. The complex is comprised of two large adaptin subunits, a β-chain and a divergent chain (either γ/ α/ δ/ ε depending on the complex), one medium adaptin, the μ-chain, and one small adaptin, the σ-chain (Boehm and Bonifacino, 2001). The β, μ and σ adaptins are highly conserved among the complexes, whereas the divergent chains are very different to each other (Kirchhausen *et al.*, 1999). The general organization of the complex consists of a core or 'head' region attached to two small appendages or 'ears' by flexible hinges (Fig. 2). The core comprises the amino-terminal (N-terminal) domains of the large adaptins, as well as the medium and small adaptins, and the appendages consist of the carboxyl-terminal (C-terminal) domains of the large adaptins (Robinson and Bonifacino, 2001, Page and Robinson, 1995). There is no evidence of direct contact between the small and medium chains. However, strong interactions exist between the two large adaptins, between the N-terminal domain of the β-chain and the μ-chain, and between the N-terminal domain of the divergent adaptin and the σ-chain. All four subunits are required for a completely stable assembly of the complex (Heldwein *et al.*, 2004).

Analogous subunits of the four AP complexes have high homology and are therefore structurally related to each other and thought to serve similar functions. Each adaptin chain has specific functions (Bonifacino and Traub, 2003). The β-adaptin interacts with the N-terminal binding sequence of the clathrin heavy chain via its hinge domain to recruit clathrin to membranes and promote clathrin assembly (Wakeham *et al.*, 2000, Owen *et al.*, 2000, Robinson and Bonifacino, 2001). The main role of the divergent adaptin is targeting the complex to specific membranes (Lewin and Mellman, 1998). Localization of the adaptor complex at the membrane depends on an interaction between the N-terminal domain of the divergent adaptin with phosphoinositides present in the membrane. Phosphoinositides are lipids that regulate the trafficking of transport machinery to desired membranes. On binding to the AP complex, phosphoinositides direct AP assembly and enhance their affinity for tyrosine-based sorting signals. Phosphoinositides also bind dynamin to trigger vesicle budding (Rapoport *et al.*, 1997, Takei and Haucke, 2001, Collins *et al.*, 2002, Heldwein *et al.*, 2004). In addition to

membrane targeting, the C-terminal appendage domain of the divergent adaptin contains binding sites for endocytic accessory proteins such as amphiphysin, auxilin, dynamin and ADP-ribosylation factor (ARF), and a clathrin-binding domain in its N-terminal and hinge regions (Wang *et al.*, 1995, Lewin and Mellman, 1998, Hinners and Tooze, 2003). Amphiphysin is a dimer of two very similar proteins, amphiphysin 1 and 2, and is involved in clathrin-mediated endocytosis by linking clathrin-coated budding vesicles with dynamin for membrane fission (Takei *et al.*, 1999, Yoshida, *et al.*, 2004). ARF, a small GTPase protein, regulates the recruitment of different coat proteins from the cytosol to the correct membrane in a GTP-dependent manner by interacting with the core domain of the adaptin (Black and Pelham, 2001, Shinotsuka *et al.*, 2002).

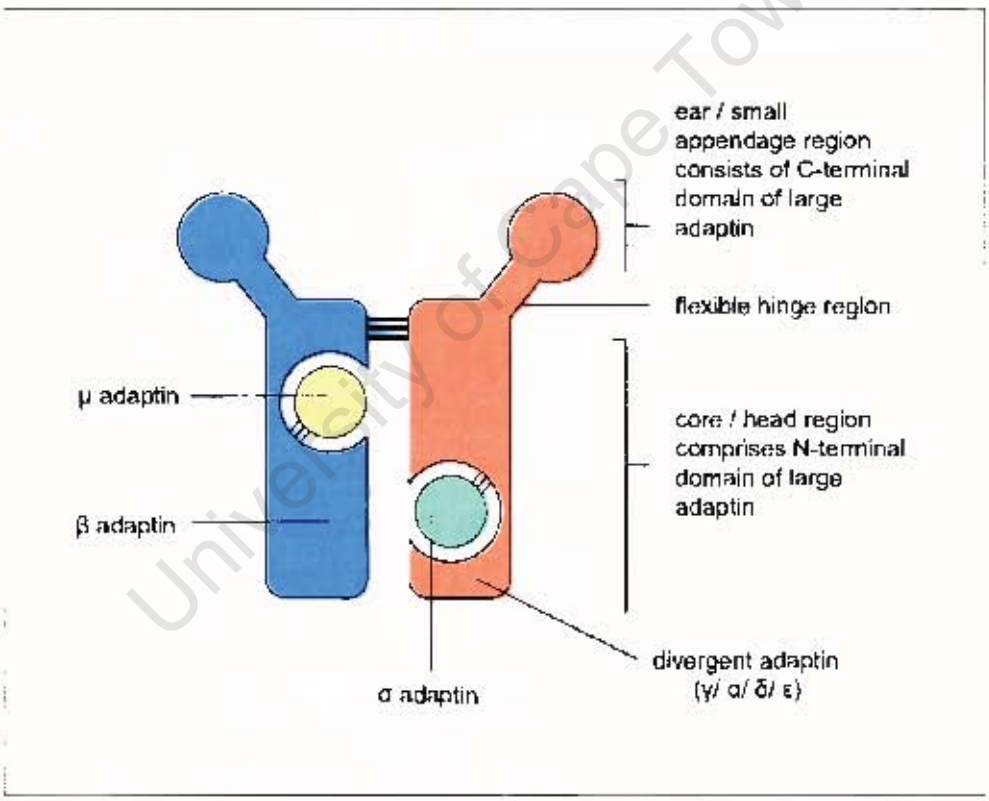

Figure 2. Schematic representation of the AP complex.

The AP heterotetramer consists of two large adaptins, a medium adaptin and a small adaptin. The specific divergent adaptin depends on the particular AP complex (AP-1: γ, AP-2: α, AP-3: δ and AP-4: ε). The head or core region consists of the amino-terminal domains of the large adaptins, plus the medium and small subunits. The carboxyl-terminal domains of the large adaptins form the ears, which are connected to the head by flexible hinges. The three parallel lines indicate interactions between the subunits.

The exact role of the σ-chain has not been determined, although it has been implicated in a number of functions including stabilization of the complex, recruitment of the complex to the appropriate membrane and cargo recognition (Boehm and Bonifacino, 2001, Collins *et al.*, 2002, Chapuy *et al.*, 2008). The μ-chain adaptin binds tyrosine-based sorting signals in the cytoplasmic domain of transmembrane cargo proteins to select and concentrate them into clathrin-coated pits by coupling them to the clathrin coat (Wakeham *et al.*, 2000, Collins *et al.*, 2002, Conner and Schmid, 2003b). In addition, the μ-chain is thought to be involved in complex assembly and conformation stabilization, as well as adaptor targeting to membranes and for the correct targeting of cargo molecules to their desired location (Lewin and Mellman, 1998, Nesterov *et al.*, 1999, Lefkir *et al.*, 2003).

Tyrosine-based sorting signals conform to the YXXΦ motif, where Y denotes a tyrosine residue, X is any amino acid, and Φ represents a bulky, hydrophobic residue. The motif confers sorting information to the cargo protein (Ohno *et al.*, 1996, Bonifacino and Traub, 2003). The tyrosine residue is essential for function and signal recognition. The X residue and the amino acids flanking the signal motif determine the affinity and specificity of the interaction with the μ-chain. The various μ-chains of AP complexes display different preferences for certain sorting signals. The position of the signal motif in the cytosolic tail of transmembrane proteins and the identity of the Φ residue in the signal are also important determinants of μ-chain specificity (Kirchhausen *et al.*, 1997, Traub and Kornfeld, 1997, Ohno *et al.*, 1998). Accessibility of the Φ residue enhances the interaction with the μ-chain (Ohno *et al.*, 1996).

The structure of the μ-chain is arranged into two functional parts, an N-terminal domain that covers one-third of the protein and a carboxyl-terminal domain comprising the remaining two-thirds of the protein. The N-terminal domain, consisting of a 5-stranded β-sheet flanked by two α-helices, is positioned within the β core and associates with the β-chain via hydrophobic interactions (Aguilar *et al.*, 1997, Bonifacino and Traub, 2003). The C-terminal domain exhibits a concave platform of a 16-stranded β-sheet that extends outward from the core to interact with tyrosine-based sorting motifs through the YXXΦ-binding site (Aguilar *et al.*, 1997, Heldwein *et al.*, 2004, Höning *et al.*, 2005). The two functional domains are connected by a linker sequence and are active independently of each other. The tyrosine and Φ residue fit into two hydrophobic pockets in the C–

terminal domain. These pockets are positioned in a way that when binding of a target molecule occurs, extensive interactions are made between the peptide and the binding site (Aguilar *et al.*, 1997, Owen and Evans, 1998). The position of the C-terminal domain however, is unfavourable as the YXXΦ-binding site is partially obstructed by the large β-chain core. Phosphorylation of the μ-chain by kinase activity, as a result of AP binding to clathrin cages, results in a conformational change to displace the C-terminal domain by approximately 90°, thereby improving accessibility of the binding site and enhancing binding to sorting signals (Kirchhausen *et al.*, 1997, Bonifacino and Traub, 2003, Heldwein *et al.*, 2004). In addition to increasing the binding affinity for internalization motifs, phosphorylation also regulates clathrin assembly and AP recruitment to membranes. An adaptor-associated kinase, AAK1, is responsible for phosphorylation of the adaptin (Ricotta *et al.*, 2002, Conner and Schmid, 2003b). AP σ-chains have significant homology to the N-terminal domain of the μ-chain, suggesting that a large section of the chain may participate in interactions with the divergent adaptin, while the C-terminal domain may be involved in another function (Aguilar *et al.*, 1997).

Each adaptor complex functions at a specific intracellular location. In mammalian cells, AP-1 is found in the cytosol and in association with vesicles derived from the TGN. It functions in sorting events from the TGN to endocytic compartments such as endosomes, as well as in retrograde transport from endosomes to the TGN (Dell'Angelica *et al.*, 1999, Boehm and Bonifacino, 2001, Lefkir *et al.*, 2003). The AP-2 adaptor complex is involved in the formation of endocytic vesicles at the plasma membrane for internalization of extracellular molecules and cell surface-receptors (Le Borgne and Hoflack, 1998, Takatsu *et al.*, 2001). AP-3 and AP-4 associates with the TGN and endosomes, and mediates lysosomal delivery (Le Borgne and Hoflack, 1998, Dell'Angelica *et al.*, 1999, Robinson and Bonifacino, 2001). AP-1 and AP-2 participates in clathrin-mediated sorting events, whereas AP-4 is a constituent of a non-clathrin coat. Studies have shown that the β and ε adaptins of the AP-4 complex lack the binding motifs for clathrin (Dell'Angelica *et al.*, 1998, Hirst *et al.*, 1999, Robinson and Bonifacino, 2001). AP-3 has been shown to interact with clathrin in mammalian cells and is likely to function as a clathrin adaptor similar to AP-1 and AP-2; however no association has been established in *Saccharomyces cerevisiae*, and in support of this finding, it was establish that the β-chain of *S. cerevisiae* AP-3 does not contain a clathrin-binding motif (Dell'Angelica *et al.*, 1998, Hirst *et al.*, 1999, Boehm and Bonifacino, 2001, Robinson and Bonifacino, 2001).

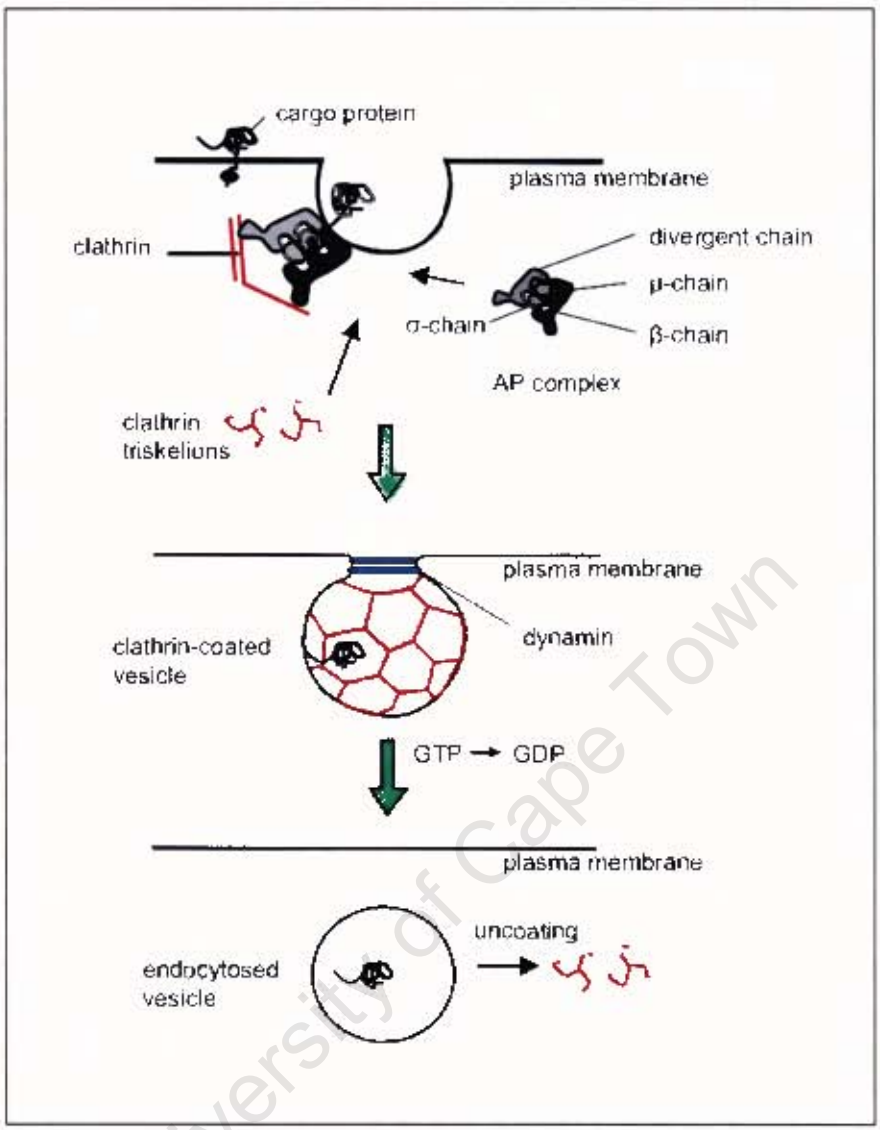

Figure 3a. Clathrin-mediated endocytosis.

Clathrin coat assembly at membrane invaginations is mediated by adaptor protein (AP) complexes. Clathrin triskelions consist of light and heavy chains. Transport vesicles pinch-off from the membrane by dynamin's GTPase activity and clathrin removed from liberated vesicles by Hsc70 and auxilin. Cargo is subsequently transported to sites within the cell.

In addition to cargo recognition and clathrin recruitment and assembly at the plasma membrane, AP complexes are required for the recruitment of dynamin. Following clathrin assembly and vesicle formation, dynamin, a large GTPase protein, is recruited to coated pits by binding amphiphysin present in the membrane (Cavalli *et al.*, 2001, Hill *et al.*, 2001). Dynamin assembles into helical rings at the neck of invaginated coated pits on

phosphorylation of the bound GDP. GTP hydrolysis results in a conformational change in dynamin causing the neck to constrict to catalyze membrane fission (Bottomley *et al.*, 1999, Sever, 2002). The C-terminal region of amphiphysin contains the Src homology 3 (SH3) domain which binds the SH3-binding motifs of the proline-rich domain (PRD) region of dynamin. The central region of amphiphysin binds the clathrin heavy chain and the AP complex (Cavalli *et al.*, 2001, Hill *et al.*, 2001).

Nascent clathrin-coated vesicles are uncoated by the ATP hydrolysis-driven processes of Hsc70 and its molecular chaperone, auxilin, by dissociating the clathrin triskeleton (Zinsmaier and Bronk 2001, Newmyer *et al.*, 2003). AP complexes are still retained on the membrane following removal of clathrin from coated vesicles (Hirst and Robinson, 1998). The endocytosed vesicle and its contents are delivered to early endosomes for sorting. The mildly acidic environment of the endosome leads to the uncoupling of receptor-ligand complexes. The endocytosed material will either be recycled back to the cell surface or transported further into the cell cytoplasm to late endosomes. Lysosomes containing hydrolytic enzymes fuse with the late endosomes to form organelles responsible for digestion (Mellman *et al.*, 1986, Luzio *et al.*, 2000).

The four adaptor complexes are expressed in most eukaryotic cells. However, genes for the AP-4 subunits are absent in yeast (*S. cerevisiae* and *Schizosaccharomyces pombe*), the nematode (*Caenorhabditis elegans*) and the fruit fly (*Drosophila melanogaster*) (Boehm and Bonifacino, 2001, Robinson and Bonifacino, 2001), and the *Toxoplasma gondii* genome does not contain genes for the AP-3 subunits (Ngô *et al.*, 2003). Adaptor identification in these and other organisms is accomplished by comparisons with mammalian counterparts, as well as by biochemical and genetic evidence (Robinson and Bonifacino, 2001). Yeast, mouse (*Mus musculus*), amoeba (*Dictyostelium discoideum*), *C. elegans* and *T. gondii* AP-1 has functions analogous to mammalian AP-1 in anterograde transport from the Golgi to endocytic organelles. In addition, AP-1 mediates the targeting of rhoptry proteins from post-Golgi organelles to the rhoptries in *T. gondii* (Boehm and Bonifacino, 2002, Lefkir *et al.*, 2003, Ngô *et al.*, 2003). AP-2 is essential for endocytosis in *C. elegans*, but not for endocytosis in *S. cerevisiae* (Boehm and Bonifacino, 2002). *S. cerevisiae* AP-3 is presumed to function as a coat protein at the late Golgi or TGN (Stepp *et al.*, 1997). In *D. melanogaster*, AP-2 has a role in the recycling of synaptic vesicle membranes and AP-3, in targeting to melanosomes (Lewin and

Mellman, 1998, Boehm and Bonifacino, 2002). AP-2 and AP-3 are also involved in sorting to the endocytic pathway in *D. discoideum*. The function of AP-4 in *Dictyostelium* has not yet been characterized (Bennett *et al.*, 2008).

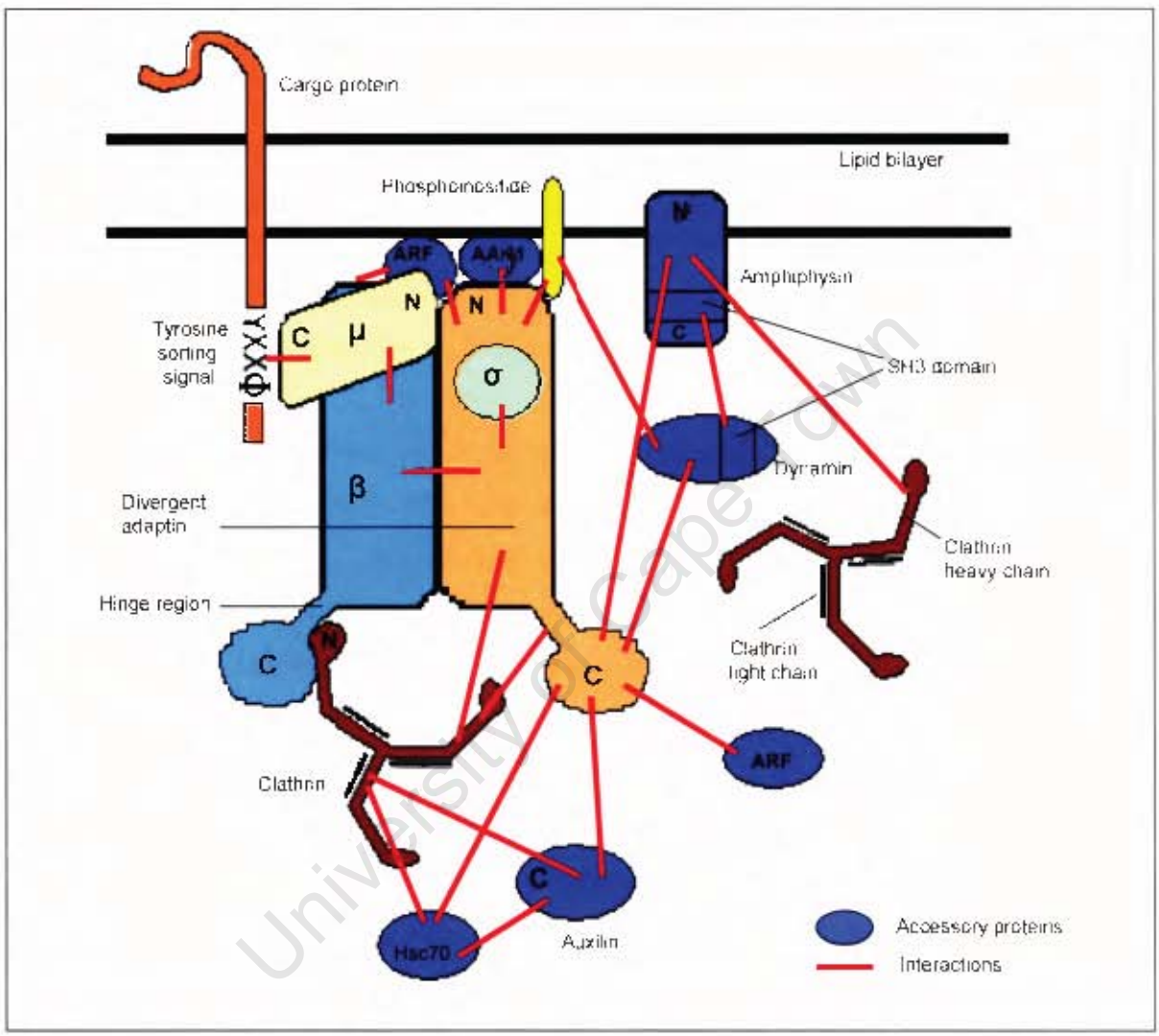

Figure 3b. Schematic description of interactions between components of the endocytic pathway. Interactions between adaptor protein components, clathrin and accessory proteins are represented by the thick red line. Amino- and Carboxyl-terminal domains are indicated with the symbol N and C respectively.

1.2. Malaria

Malaria is a tropical, mosquito-borne disease and is the world's most important parasitic infection. The malaria parasite infects more than 500 million people and causes over a million deaths each year with the highest mortality rate occurring among young children. Aside from malaria mortality and severe morbidity, the disease negatively impacts the economy and contributes to poverty in the developing world (Gallup and Sachs, 2001). Nevertheless, the disease is curable if diagnosed and treated correctly (Land, 2003, Greenwood *et al.*, 2008). However, the decline in efficacy of affordable anti-malarials due to drug resistance makes it increasingly more difficult for developing countries to access alternative, inexpensive treatments and poses a major threat to the global effort to eradicate the disease (Yeung *et al.*, 2004).

The causative agent of malaria is an obligate intracellular parasite belonging to the phylum Apicomplexa, genus *Plasmodium*. There are five species that are able to infect humans. These include *Plasmodium falciparum*, *Plasmodium ovale*, *Plasmodium malariae*, *Plasmodium vivax* and *Plasmodium knowlesi*. Of these, *P. falciparum* is the major cause of malaria morbidity and mortality in humans (Cortes *et al*, 2003, Tonkin *et al.*, 2006, Sahu *et al.*, 2008, Cox-Singh and Singh, 2008). In addition, it has emerged recently that *P. knowlesi* infection in humans can be fatal (Cox-Singh *et al.*, 2008).

The complex life cycle of the malaria parasite is split between the human host and the *Anopheles* mosquito vector. *Anopheles gambiae* is the chief vector of *Plasmodium falciparum*, although there are many species that transmit the disease (Walliker *et al.*, 1987, Kanzokand and Zheng, 2003, Moffett *et al.*, 2007). Infection in humans begins when sporozoite stage parasites, present in the saliva of infected mosquitoes, are injected into the bloodstream via a mosquito bite and are transported to the liver microcirculation (Taylor-Robinson, 2001, Rathore *et al.*, 2002). Inside the liver, sporozoites invade hepatocytes. To begin with, the sporozoite forms a moving junction with the hepatocyte which aids uptake of the parasite within a parasitophorous vacuole (PV), a process called cell invasion. This is necessary for sporozoite differentiation into asexual stage merozoites before rupture from the liver. Sporozoites also traverse several host cells, including hepatocytes, before settling in a final hepatocyte. Studies using *Plamsodium berghei*, a species that infects rodents, suggests cell traversal is important for preventing

parasite destruction by phagocytic cells in liver sinusoids and circumventing infection of other non-phagocytic cells within a PV. Furthermore, cell infection is necessary to silence cell traversal activity to allow infection of the final hepatocyte (Krettli *et al.*, 2001, Amino *et al.*, 2008). Once inside the hepatocyte, they undergo radical changes and asymptomatically multiply over the following two weeks to produce thousands of asexual stage merozoites, before rupturing out of the liver (Taylor-Robinson, 2001, Rathore *et al.*, 2002).

Released merozoites are transported in merosomes, vesicles covered by host cell membrane, to the peripheral circulation. The merosome ensures parasite survival by protecting the merozoite from destruction by Kupffer and other phagocytic cells by inhibiting exposure of a phosphatidylserine (PS) residue signal, an indicator displayed on the outer leaflet of the membrane of dying cells (Strum *et al.*, 2006). Once in the peripheral circulation, free merozoites invade circulating erythrocytes and undergo several phases of development, structurally and morphologically, to produce more merozoites. The invasion of red blood cells (RBC) by merozoites is a very intricate process and entails precise receptor-ligand interactions. Differential expression of proteins and multiple parasite ligands provides the parasite with a number of different invasion pathways. The process begins with the initial attachment of the merozoite to the erythrocyte, mediated by a glycosylphosphatidylinositol (GPI) anchored membrane protein, MSP-1. MSP-1 is the most abundant antigen on the merozoite surface. Following this, re-orientation occurs to position the merozoite's apical end adjacent to the erythrocyte for direct contact with the erythrocyte membrane. Several proteins stored in the apical organelles (rhoptries and micronemes) are discharged onto the erythrocyte membrane and facilitate invasion. One such protein is the apical membrane antigen 1, AMA-1, which is transported to the merozoite surface and is important for apical interaction with the erythrocyte. Once apical attachment occurs, a tight junction is formed involving ligand-receptor interactions, which moves from the apical end to the posterior end of the merozoite, thereby engulfing the parasite. At the same time parasite proteases facilitate the removal of ligands and the surface coat covering the merozoite. Invasion is powered by the parasite's actin-myosin motor and is thought to involve two protein families, the duffy binding-like (DBL) proteins and the parasite's reticulocyte binding protein homolog (Rh) (Kariuki *et al.*, 2005, Cowman and Crabb, 2006, Richard *et al.*, 2009). EBA-175, a DBL protein, attaches to the sialic acid residues of glycophorin A of

the erythrocyte membrane and causes a localized deformation in the surface of the RBC, which results in the invagination of the membrane (Pasvol and Wilson, 1982, Singh *et al.*, 2002, Pattnaik *et al.*, 2007). This leads to the uptake of the merozoite enclosed in a new PV which is separated from the erythrocyte by a parasitophorous vacuole membrane (PVM) (Shin and Abraham, 2001, Tonkin *et al.*, 2006).

The first phase of the intra-erythrocytic asexual lifecycle is the ring stage, in which the parasite begins to metabolize haemoglobin to fulfil its nutrient needs. Secretory proteins are synthesized and exported across the parasite's plasma membrane and the PVM to the RBC for modification of the RBC membrane and cytosol (Adisa *et al.*, 2001, Bannister and Mitchell, 2003, Taraschi *et al.*, 2003). These alterations aid nutrient uptake and cause cytoadherence of the infected RBC to the endothelium of capillaries. The retention and accumulation of infected RBCs protects the parasites from destruction as they avoid immune clearance by the spleen (Haldar, 1998, Wiser *et al.*, 1999, Kirchgatter and del Portillo, 2002, Kyriacou *et al.*, 2006). A parasite protein, *P. falciparum* erythrocyte protein 1 (PfEMP1) encoded by the *var* gene family, is expressed and exported to the surface of infected RBCs and mediates binding to several host receptors (Miller *et al.*, 2002). Generally, binding to vascular endothelium does not lead to pathogenesis, but occasionally the infection may become serious and cause high levels of sequestration of infected erythrocytes within capillaries in the brain, resulting in cerebral malaria (Elford *et al.*, 1997, Smith *et al.*, 2000, Sam-Yellowe *et al.*, 2004, Cooke *et al.*, 2004).

Ring stage parasites develop into more rounded trophozoites. Trophozoite stage parasites further modify the RBC and digest most of the host haemoglobin in preparation for the reproduction of merozoites, as well as to synthesize protein, DNA and RNA (Bannister *et al.*, 2000, Lazarus *et al.*, 2008). Trophozoites mature to form schizonts which engage in intense protein synthesis and undergo nuclear division. During schizogony, each parasite divides within the vacuole to produce 16 to 32 merozoites that rupture from the infected cell enclosed in little sacs called parasitophorous vacuolar membrane-bound structures (PEMS) (Delplace *et al.*, 1988, Salmon *et al.*, 2001, Bannister and Mitchell, 2003).

Although egress of merozoites from the erythrocyte is known to be a two-step process, some controversy surrounds the order of these two steps. One model suggests that merozoites escape from the schizont within the parasitophorous vacuole and then upon

exit from the erythrocyte they are released from the vacuole (Salmon *et al.*, 2001). An alternative model suggests that merozoites first ruptures from the vacuole while still within the erythrocyte, followed by the secondary rupture of the erythrocyte to release free merozoites. Proteases have been implicated in both erythrocyte and parasitophorous vacuole lysis (Wickham *et al.*, 2003). One erythrocytic cycle lasts approximately 48 hours (Salmon *et al.*, 2001, Bannister and Mitchell, 2003). Other human-infecting species have different periodicities. *P. knowlesi* has a 24 hour life cycle and *P. malariae* a 72 hour cycle. *P. vivax* and *P. ovale* have a life cycle similar to *P. falciparum* of 48 hours (Collins and Jeffery, 2005, Collins and Jeffery, 2007, Vargas-Serrato *et al.*, 2003). The time from infection of liver cells by *P. falciparum* to the development of the disease is usually about 10 to 15 days (Omonuwa and Omonuva, 2002, Giobbia *et al.*, 2005). The brief period between egress of merozoites from an infected RBC and the re-infection of a new RBC is immunologically important as it provides the opportunity for blocking parasite entry into the erythrocyte. Parasite receptor-binding domains that mediate erythrocyte invasion are excellent candidates for vaccine development (Kisilevsky *et al.*, 2002, Singh *et al.*, 2002).

The asexual erythrocytic stages of parasite development are responsible for malaria pathogenesis. The clinical symptoms of the disease, such as chills and fever, are associated with the synchronous rupture of infected erythrocytes when merozoites are liberated (Murphy *et al.*, 2006, Tripathi *et al.*, 2006). The progressive breakdown of RBCs leads to anaemia, and changes in the adhesive properties of the RBC results in the sequestration of infected red blood cells to the blood-brain barrier endothelia and other organs. Infected erythrocytes develop surface protrusions known as knobs that form junctions with endothelial cells resulting in attachment of the RBC to the endothelial cells and ultimately the obstruction of capillaries, a speciality of *P. falciparum* (Leech *et al.*, 1984). In extreme cases, this may result in severe anaemia, cerebral malaria and organ failure (Guerin *et al.*, 2002). Cerebral malaria is caused by increased permeability of the blood-brain barrier, resulting in neurological complications and local inflammation (van den Steen *et al.*, 2008). Other human-infecting parasite species are characterized by different biological features. The most distinguishing features of *P. vivax* are the enlarged parasite-infected erythrocyte and the stippling of the RBC cytoplasm, termed Schüffer's dots (Udagama *et al.*, 1988). These granules are also exhibited by *P. ovale*-infected erythrocytes (Collins and Jeffery, 2005). *P. malariae* does not alter the host erythrocyte

in anyway, however a feature associated with infection is the thickening of the glomerular basement membrane of the kidney which may lead to renal disease (Collins and Jeffery, 2007). Similarly, *P. knowlesi*-infected erythrocytes do not develop any protrusions, but are still sequestered in the vasculature. Congregation of RBC is believed to be a result of the infected erythrocytes becoming less deformable (Miller *et al.*, 1971, Vargas-Serrato *et al.*, 2003).

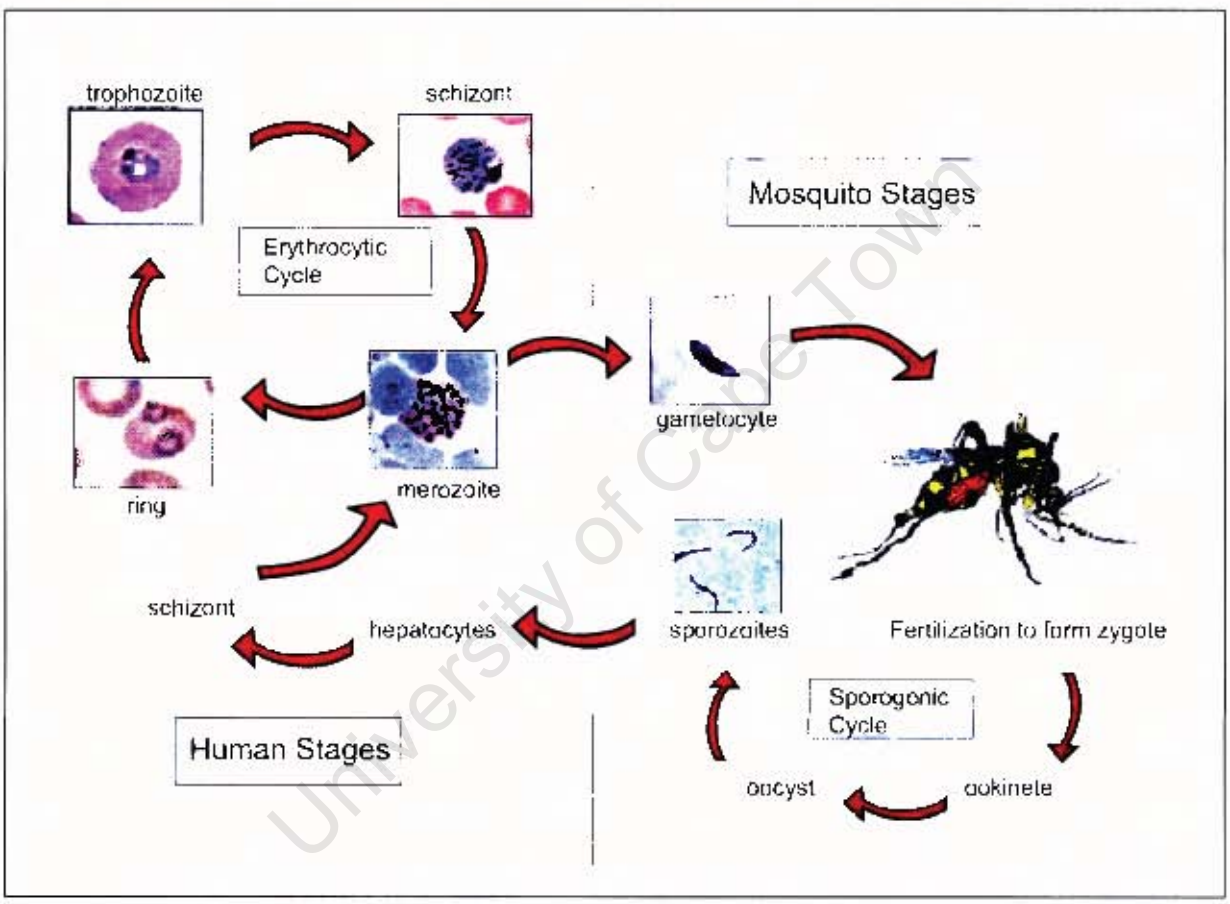

Figure 4. *P. falciparum* life cycle.

The malaria parasite has a complex life cycle involving several morphologically distinct stages in the human host and mosquito vector. The erythrocytic stages can be maintained *in vitro* by standard tissue culture procedures.

Merozoites that do not follow the normal asexual cycle described above differentiate into male and female sexual forms, macrogametocytes and mircogametocytes respectively, which are taken up by other mosquitoes during a blood meal (Kooij and Matuschewski, 2007). Fertilization of the gametes occurs in the mosquito midgut to form zygotes, which

further differentiate into mobile ookinetes that transverse epithelial cells and develop into an oocyst on the exterior of the gut wall. Here the oocyst matures and produces thousands of infective sporozoites. Eventually the oocysts burst, releasing sporozoites that travel to the mosquito salivary glands and are available for injection into a new human host to complete the lifecycle (Gouagna *et al.*, 1998, Kooij and Matuschewski, 2007).

1.3. Endocytosis and secretion in *Plasmodium falciparum*

To sustain rapid intra-erythrocytic growth the parasite acquires nutrients from the host RBC and extracellular environment by several routes. Firstly, the erythrocyte cytoplasm, consisting largely of haemoglobin, is endocytosed through a specialized invagination of the parasite plasma membrane and the PVM, known as the cytostome (Olliaro and Goldberg, 1995, Goodyer *et al.*, 1997, Robibaro *et al.*, 2001). The cytostome is notable by the presence of an electron-dense collar flanking the cytostome neck (Lazarus *et al.*, 2008). Double-membrane transport vesicles, containing the host cytosol, pinch off from the membrane and are transported to the digestive vacuole (DV), the parasite equivalent of the mammalian lysosome. These vesicles fuse with the acidic digestive vacuole (ph between 5.0 and 5.4) and deliver the cytoplasm for degradation. The mechanism of haemoglobin uptake and transport to the digestive vacuole is unknown, and it is uncertain whether these transport vesicles are coated with clathrin (Goldberg, *et al.*, 1990, Francis *et al.*, 1997, Robibaro *et al.*, 2001, Hempelmann *et al.*, 2003, Elliott *et al.*, 2008). Actin is thought to play a role in cytostome formation and stabilization, assisting the recruitment of protein complexes involved in endocytosis to the plasma membrane, similar to what is found in other eukaryotic systems, as well as in the trafficking of haemoglobin vesicles (Elliott *et al*, 2008, Lazarus *et al.*, 2008, Smythe *et al.*, 2008). An alternative pathway for haemoglobin uptake by early ring-stage parasites has been proposed, where it is believed that the digestive vacuole can also originate from a solitary, haemoglobin-filled double-membrane bound vacuole created by the parasite in an event termed the 'Big Gulp'. The inner membrane of the vacuole is removed prior to the vacuole becoming the digestive vacuole. Additional uptake processes involving the cytostome contributes to the volume of this haemoglobin-filled vacuole (Elliott *et al.*, 2008).

Once haemoglobin enters the digestive vacuole, it is initially degraded by two aspartic proteases, plasmepsin I and II, and a calcium-dependent cysteine protease, falcipain. The plasmepsin proteases initiate the cleavage of the native haemoglobin tetramer while two members of the falcipain family, falcipain-2 and falcipain-3, digest the denatured substrate to small peptides that at are exported for terminal degradation (Hanspal *et al.*, 2002, Asojo *et al.*, 2003, Klemba *et al.*, 2004). A third member of the falcipain family, falcipain-1, has a role in invasion and parasite release from the RBC (Greenbaum *et al.*, 2002, Rosenthal, 2004).

The plasmepsin proteases are synthesized as integral membrane proenzymes in the ER. The prodomain is thought to play a role in targeting the enzyme to the digestive vacuole. Proplasmepsins are transported through the secretory pathway and processed by plasmepsin convertase activity in the digestive vacuole to release mature, active plasmepsin (Klemba *et al.*, 2004, Tonkin *et al.*, 2006). Plasmepsin I is synthesized and processed in the early stages of parasite development, while plasmepsin II is produced during the later stages when haemoglobin digestion is at a maximum (Francis *et al.*, 1997). Plasmepsin trafficking to the digestive vacuole utilizes the haemoglobin endocytic pathway. The plasmepsins are transported from the ER to the cytostome where they accumulate and are incorporated into endocytic vesicles and delivered to the digestive vacuole along with the haemoglobin. (Francis *et al.*, 1994. Klemba *et al.*, 2004, Tonkin *et al.*, 2006). It is thought that some proteolytic digestion may already occur in the transport vesicle (Hempelmann *et al.*, 2003, Elliott *et al.*, 2008).

An alternative model for haemoglobin uptake has been proposed that contradicts the prevailing model that endocytic vesicle bud off from the plasma membrane and are transported into the parasite cytosol. The new model suggests that transport vesicles are not required for haemoglobin transport. It proposes that cytostomes containing haemoglobin expand and extend into the cytosol, to eventually reach and fuse with the digestive vacuole. At the time of fusion, the cytostome is simultaneously pinching off from the membrane (Lazarus *et al.*, 2008).

Within the digestive vacuole, haemoglobin is hydrolyzed to globin and haem (ferroprotoporphyrin IX or FP-Fe II). Amino acids obtained from the globin portion are transported to the parasite cytoplasm, while the haem is immediately oxidized to

ferriprotoporphyrin IX (FPIX or FP-Fe III) or haematin. FPIX is toxic to the parasite as it affects protein synthesis by destabilizing barrier properties of membranes and disturbing ion homeostasis (Egan *et al.*, 2002, Hempelmann *et al.*, 2003). To protect against the lethal effects of haem, the ferriprotoporphyrin is incorporated into an insoluble, crystalline pigment called haemozoin (Wiser *et al.*, 1999, Krugliak *et al.*, 2002, Tripathi *et al.*, 2002). Haemozoin comprises dimers of β-haematin linked by hydrogen bonds between the iron group of one FPIX and the carboxyl group of another. Although haemoglobin digestion and haemozoin structure is well characterized, the process of haemozoin formation is still under investigation (Hempelmann *et al.*, 2003, Egan *et al.*, 2006, Elliott *et al.*, 2008).

Haemoglobin is degraded to supply the parasite with nutrients for protein synthesis and energy metabolism to sustain rapid growth. The globin portion of haemoglobin provides the parasite with all but five of the essential amino acids. Although the majority of haemoglobin in the infected RBC gets degraded, only a fraction of the amino acids liberated are utilized. Protein synthesis relies on additional amino acid contributions from the extracellular medium. In addition to nutrient acquisition, haemoglobin is digested to make space for parasite growth within the erythrocyte (Goldberg *et al.*, 1990, Francis *et al.*, 1997, Krugliak *et al.*, 2002, Tonkin *et al.*, 2006).

Besides haemoglobin ingestion, the parasite is able to obtain macromolecules from the extracellular medium surrounding the erythrocyte. Mechanisms by which the parasite imports these nutrients have been the subject of much debate (Pouvelle *at al.*, 1991, Taraschi and Nicolas, 1994, Elford *et al.*, 1997). A pathway supported by several research groups is the non-specific permeation pathway whereby parasite-induced permeability changes in the erythrocyte membrane allow access of small molecules. The increase in membrane permeability is brought about either by parasite-induced channels or by structural defects of the membrane due to insertion of parasite proteins or lipids (Desai *et al.*, 1993, Elford *et al*, 1997, Ramya *et al.*, 2002, Saliba *et al.*, 2006). Furthermore, low molecular weight compounds are able to reach the parasite through an extensive tubovesicular membrane (TVM) network that extends from the PVM into the red blood cell cytoplasm (Haldar, 1998, Robibaro *et al.*, 2001, Ramya *et al.*, 2002).

In addition to nutrient uptake, intra-erythrocytic parasites traffic proteins to organelles within its cytosol and to the cytosol and plasma membrane of the host cell. The main destinations of parasite secretory proteins include the digestive vacuole for haemoglobin digestion, the host RBC for modification purposes, the apical secretory organelles (consisting of the micronemes, rhoptries and dense granules) involved in host cell invasion, and the apicoplast (Haldar, 1998, Tonkin *et al.*, 2006). The apicoplast is a non-photosynthetic, relic plastid found in apicomplexan parasites. It is essential for parasite survival and although its exact function is unclear, evidence suggests it plays a role in lipid biosynthesis, isoprenoid biosynthesis and some aspects of haem biosynthesis. It is presumed that synthesis of fatty acids is necessary for the formation of the parasitophorous vacuole during invasion of the host RBC (Jomaa *et al.*, 1999, McFadden and Roos, 1999, Wilson, 2002, Waller and McFadden, 2005). The apicoplast contains its own genome and expresses a small number of genes involved in protein expression. Nevertheless, most proteins functioning within the apicoplast are nuclear encoded and post-translationally targeted to the organelle via the parasite's secretory pathway (Wilson *et al.*, 1996, Waller *et al.*, 1998, Ralph *et al.*, 2004, Kobayashi *et al.*, 2006).

The morphology of the rhoptries, such as internal membranes, vesicles and transmembrane proteins, suggest that the rhoptries may resemble the multivesicular bodies (MVB) of higher eukaryotic cells. MVB in eukaryotic cells are endosomes that function as transport vesicles for delivery of their cargo to late endosomes for degradation, as well as having the role of secretory lysosomes. Endosomal sorting complexes required for transport (ESCRT) are the machinery responsible for the network of interactions involved in sorting to lysosomes (Yang *et al.*, 2004, Nevin and Dacks, 2009). Firstly, ESCRT-I, a complex consisting of Vps23 / Vps28 and Vps37, recognize ubiquitous cell surface receptors and on binding them triggers the ESCRT-II complex consisting of Vps22 / Vps25 and Vps36. The activated ESCRT-II directs the assembly of ESCRT-III on membranes. The ESCRT-III complex, consisting of Vps2 / Vps24 and Vps20 / Snf7, facilitates the removal of ubiquitin from the cargo prior to their inclusion into vesicles (Yang *et al.*, 2004, Williams and Urbé, 2007). Lastly, Vps4, part of the ATPase complex, is recruited to membranes by ESCRT-III (Vps2 / Vps24) to induce disassembly of the ESCRT components. Vps4 has an essential role in MVB formation. Although a homologue of Vps4 and all components of ESCRT-III have been detected in the *P. falciparum* genome, subunits of ESCRT-I and II are absent (Yang *et al.*, 2004,

Slater and Bishop, 2006, Williams and Urbé, 2007). Studies using Vps4 as an endocytic pathway marker suggests MVBs are formed in the parasite, possibly along the endocytic pathway (Yang *et al.*, 2004). Furthermore, phosphatidylinositol-3-phosphate (PI3P), a lipid found in membranes of eukaryotic cells, has an essential role in recruiting regulatory proteins of the endocytic trafficking system to membranes. These effector proteins typically contain either a FYVE or PX motif that mediates ligand binding. A single effector protein containing the FYVE domain has been identified in the parasite and been found to localize to the digestive vacuole (Birkeland and Stenmark, 2004, McIntosh *et al.*, 2007).

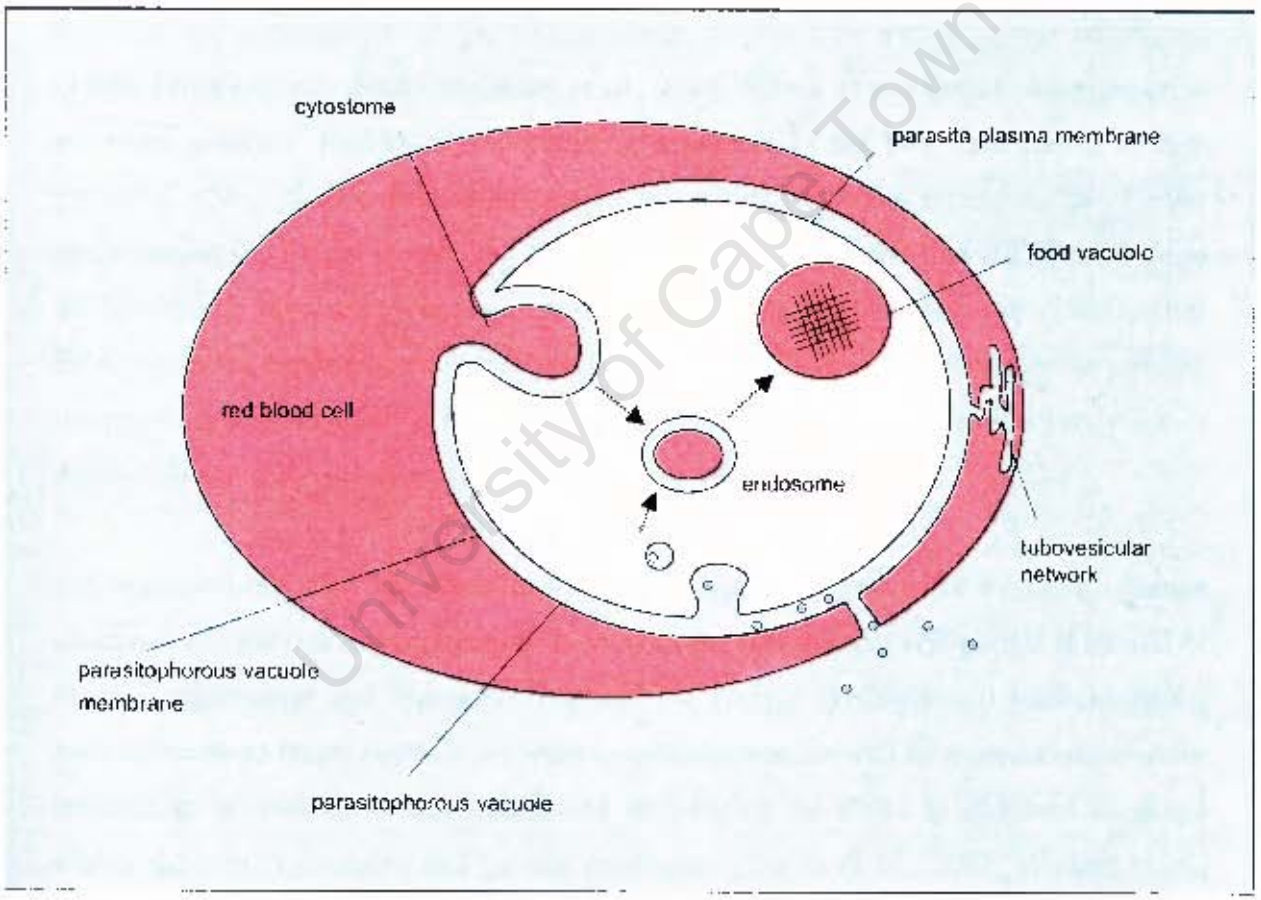

Figure 5. Nutrient uptake pathways in *P. falciparum*.

Within the erythrocyte, the parasite resides in a parasitophorous vacuole which is separated from the RBC cytoplasm by a parasitophorous vacuole membrane (PVM). The diagram illustrates the different routes by which trophozoite stage parasites acquire nutrients from the human host to sustain rapid growth.

The mechanisms of protein trafficking in *P. falciparum* are poorly understood. Secretory proteins are either transported to sites within the parasite, or are exported across the parasite plasma membrane to the RBC. The existence of the classical secretory pathway similar to that found in eukaryotes involving the ER and Golgi has been suggested for the parasite. A Golgi has been identified, although its organization and morphology remains unclear and is cause for debate (Taraschi *et al.*, 1998, Struck *et al.*, 2008). Some researches suggest the Golgi is unstacked, with a tubulovesicular organization consisting of distinct compartments (van Wye *et al.*, 1996, Bannister *et al.*, 2000). Studies using *Pf*rab6, an established *trans*-Golgi marker in the parasite, *Pf*GRASP, a *cis*-Golgi marker, and *Pf*ERD2, an ER and *cis*-Golgi marker, suggest that there is a close association between the compartments, supporting a more complex organization and contradicting the dispersed arrangement of the compartments proposed by van Wye and colleagues (1996) (Struck *et al.*, 2005, de Castro *et al.*, 1996, Struck *et al.*, 2008). An alternative secretory pathway, presumably specializing in export to the host cell, has also been proposed, although its existence has not been supported by more recent studies. Earlier studies using the fungal metabolite, brefeldin A (BFA), suggested that the ER and Golgi are not directly involved (Ward *et al.*, 1997, Wiser *et al.*, 1999, Cortes *et al.*, 2003). After BFA treatment, exported proteins accumulate in a subcellular compartment at the parasite periphery, morphologically similar but distinct from the ER, called the secondary ER of Apicomplexa (sERA) (Cortes *et al.*, 2003).

Alterations of the RBC are essential for parasite survival in terms of avoiding immune clearance and for nutrient acquisition. In view of the fact that the erythrocyte is devoid of internal membranes and organelles required for protein synthesis and trafficking, the parasite needs to target proteins involved in modification, as well as proteins required for trafficking, beyond its plasma membrane and across the PVM to different locations within the RBC cytoplasm and plasma membrane (Cortes *et al.*, 2003, Wickert *et al.*, 2003, Wiser *et al.*, 1997, Lee *et al.*, 2008). These export proteins contain a two part host targeting motif; the N-terminal signal sequence (SS) for translocation into the PV via the ER, Golgi, and parasite plasma membrane, and the *Plasmodium* export element (PEXEL) or the vacuolar transport signal (VTS) which targets proteins across the PVM into the erythrocyte, a process less well understood. It is thought that trafficking into the erythrocyte is either exclusively by vesicles or is through an interconnected membranous structure called the tubulovacuolar network (TVN) (Elford *et al.*, 1997, Taraschi *et al.*,

2001, Horrocks and Muhia, 2005, Tonkin *et al.*, 2006, Chang *et al.*, 2008). This network is also termed the tubovesicular membranes by other research groups (Elmendorf and Haldar, 1993, Elford *et al.*, 1995, Haldar *et al.*, 2001, Horrocks and Muhia, 2005). In addition to the TVN, the parasite establishes disc-shaped, membranous structures termed Maurer's clefts at the RBC periphery. Maurer's clefts are intermediate trafficking compartments for proteins destined for the host cell membrane; however its role in protein transport remains unclear. It had been suggested that the clefts may be the equivalent of an extracellular Golgi since it morphologically resembles the Golgi of higher eukaryotes (Knuepfer *et al.*, 2005, Przyborski, 2008, Spycher *et al.*, 2008).

The protein secretory pathway and the processes and sites of haemoglobin degradation and haem crystallization are attractive targets for anti-malarial drugs (Francis *et al.*, 1994, Klemba *et al*, 2004, Tonkin *et al.*, 2006). *Plasmodium falciparum* is becoming increasingly more resistant to regular anti-malarials, making it necessary to identify novel drug candidates and drug targets. Understanding parasite biology, transport processes and the protein transport machinery involved in these processes is of importance to identify novel parasite enzymes and metabolic pathways as potential targets for drug development to ultimately eradicate the disease. Slow progress in this field arises from the technical difficulties of manipulating the parasite by standard molecular techniques. The high AT content of the parasites genome is responsible for poor protein expression in heterologous systems and limited molecular approaches (Hume *et al.*, 2003, La Count *et al.*, 2005, Greenwood *et al.*, 2008), while transfection efficiencies with transgene expression and heterologous recombination constructs are poor. Post-transcriptional silencing by antisense RNA and RNAi approaches have also met with limited success.

The completion of the *P. falciparum* genome sequencing project has enabled a better understanding of the biology of this organism and has revealed key players in the metabolic and biosynthetic pathways, allowing a rational approach to drug design. Components of the endocytic and secretory pathways in asexual stage parasites are excellent targets because they play a fundamental role in parasite survival (Krishna *et al.*, 2002, Greenwood *et al.*, 2008). Homologues of a number of components involved in trafficking pathways in other organisms are encoded by the *P. falciparum* genome (Ward *et al.*, 1997). The presence of some of these components (e.g. Clathrin, adaptor subunits and dynamin) suggests the parasite experiences clathrin-mediated transport processes. In

addition, these proteins are known to have additional functions in other cellular events in mammalian cells. Therefore it is likely that they may have additional or alternative functions in the parasite (Ewan, 2004, Royle and Lagnado, 2006).

1.4. Aims and Objectives

Protein trafficking within the parasite and beyond its plasma membrane is vital for parasite growth and survival. Apart from morphological descriptions, the molecular mechanisms by which these pathways occur in the parasite are predominantly poorly understood. The main aim of this project was to initiate characterization of the medium (μ) chain homologues of adaptor protein complexes expressed by blood stage parasites. The goal was to localize the μ-chain homologues in the parasite by immunohistochemical methods, to assess whether they possibly play roles in endocytosis in the parasite or whether they are involved in other trafficking events, such as secretion or cytokinesis. To this end, three μ-chain adaptin homologues were characterized. In addition, two σ-chain homologues and the parasite Rab6 protein (*Pf*rab6) were examined. *Pf*rab6 is a known marker of the *trans*-Golgi. Identification of the parasite protein homologues was achieved by consulting the sequence data contained in the *P. falciparum* sequence database, PlasmoDB (Bahl *et al.*, 2002). Selection of these homologues was motivated by their convincing predicted amino acid sequence homology to their mammalian counterparts and their well established roles in endocytosis. Transcript presence in blood stages of malaria parasites was determined by reverse transcriptase PCR (RT-PCR) on RNA isolated from trophozoites. Gene sequences were cloned and expressed in *Escherichia coli* (*E. coli*), and in some cases, antigenic peptides were manufactured. Antisera to the purified recombinant proteins and antigenic peptides were raised in mice and rabbits respectively. Proteins were localized in the parasite by immunofluorescence assays (IFA), and further resolution of the μ-chains subcellular localization was achieved by immuno-electron microscopy.

CHAPTER 2 – Identification and Characterization of Adaptor Protein μ-chain Homologues

2.1. Introduction

The first step in vesicle trafficking from the plasma membrane during endocytosis and from the *trans*-Golgi network (TGN) during secretion is cargo recognition by heterotetrameric adaptor protein (AP) complexes in association with regulatory molecules. This is followed by AP-mediated recruitment of clathrin to the membrane for budding and vesicle formation (Hirst *et al.*, 2001, Heldwein *et al.*, 2004). Of the four AP complexes, AP-2 mediates endocytosis from the plasma membrane while AP-1, AP-3, and AP-4 mediate sorting events at the TGN and endosomes (Le Borgne and Hoflack, 1998, Ngô *et al.*, 2003). AP-1 and AP-2 function in conjunction with clathrin, whereas AP-4 appears to participate in clathrin-independent vesicle formation. A requirement of clathrin for AP-3 mediated trafficking is controversial (Dell'Angelica *et al.*, 1998, Hirst *et al.*, 1999, Boehm and Bonifacino, 2001). The AP complex consist of two large adaptins (~100 kDa); a divergent subunit (Ap-1: γ, AP-2: α, Ap-3: δ and Ap-4:ε) and a β-chain (β1-4 respectively), one medium-sized adaptin, the μ-chain (μ1-4 respectively, ~50 kDa), and one small adaptin, the σ-chain (σ1-4 respectively, ~20 kDa). Generally the subunits of different complexes are not interchangeable, apart from β1 and β2 which could be a constituent of both AP-1 and AP-2 (Boehm and Bonifacino, 2001, Heldwein *et al.*, 2004). The subunits are closely associated and require powerful denaturing conditions for their dissociation (Hirst and Robinson, 1998). The β subunit is important for clathrin binding and has been implicated in cargo selection, the γ and α adaptins target the AP complexes to specific membranes, and the μ-adaptin recognizes and binds cargo for selection into clathrin-coated vesicles via distinct sorting signals (Ohno *et al.*, 1995, Hirst and Robinson, 1998, Collins *et al.*, 2002). To date there is no definite function assigned to the

σ subunits, although several functions have been suggested (Takatsu *et al.*, 2001, Aguilar *et al.*, 2001).

Tyrosine-based sorting signals interact directly with the μ-adaptin of all four adaptor complexes (Heldwein *et al.*, 2004). This interaction results in selective incorporation of the integral membrane proteins into coated vesicles that carry proteins to different destinations within the cell. AP-1 is responsible for the delivery of proteins from the TGN to the endosomal-lysosomal system, as well as from endosomes to the TGN (Lefkir *et al.*, 2003), whereas AP-2 mediates rapid internalization of endocytic receptors from the plasma membrane (Collins *et al.*, 2002). Recent studies suggest that AP-3 is involved in an alternative pathway of protein transport from the TGN or endosomes to lysosomal compartments. The intracellular distribution of the AP-4 complex to the TGN and endocytic compartments indicates it may play a role in the sorting of cargo proteins from the TGN and early endosomes. Of the four adapters, AP-4 it is situated most closely to the nucleus (Hirst *et al.*, 1999).

In *Plasmodium falciparum*, secretory proteins synthesized during the intra-erythrocytic stages may either be transported to other sites within the parasite or exported beyond the confines of the plasma membrane, across the parasitophorous vacuolar membrane (PVM) and to the erythrocyte (Foley and Tilley, 1998, Templeton and Deitsch, 2005, Epp and Deitsch, 2006). Protein trafficking within the parasite is generally assumed to occur via the conventional vesicle-mediated pathway involving the ER and the Golgi, whereas the export of proteins beyond the parasite plasma membrane, to the erythrocyte membrane, is largely uncharacterized but is thought to involve either an alternative BFA-insensitive pathway or a direct protein-translocation pathway (Foley and Tilley, 1998).

One approach to elucidating trafficking pathways in the parasite is to characterize proteins potentially associated with them, based on homology to mammalian counterparts. Three convincing homologues of human μ1, μ2 and μ4 adaptins were identified by BLAST searches of the *P. falciparum* genome. Expression of these genes in parasite blood stages was confirmed by RT-PCR and fragments of the coding sequences cloned, expressed and purified from *E. coli*, then used to immunize mice to produce antisera for immunohistochemical purposes.

2.2. Results

2.2.1. Identification of predicted *P. falciparum* homologues of human μ-chain adaptins

A search of the *P. falciparum* sequence database, PlasmoDB (http://www.plasmodb.org), was preformed with the amino acid sequences of *Homo sapiens* homologues of μ1, μ2 and μ4 (accession numbers Q9BXS5, Q96CW1 and O00189 respectively) using the BLAST algorithm (Fig. 6a). The search revealed predicted *P. falciparum* proteins (PF13_0062, PFL0885w, PF11_0202) with significant sequence similarities to human AP-1 complex subunit μ1 (60 % identity and 80 % positives over a 422 amino acid sequence), human AP-2 complex subunit μ2 (35 % identity and 60 % positives over a 429 amino acid sequence) and human AP-4 subunit μ4 (30 % identity and 60 % positives over a 430 amino acid sequence). These three predicted *P. falciparum* open reading frames are the only ones to show significant sequence homology to human μ-chain subunits (Fig. 6a).

```
μ1
1     .MSASAVYVLDLKGKVLICRNYRGDVDMSEVEHFMPILMEKEEEGMLSPILAHGGVRFMW
1     MACISAIFIIDLKGKVIINRNYRGEVNVNLTEVFYNCVIDQEDN.LIKPIFHVNGLTYCW

60    IKHNNLYLVATSKKNACVSLVFSFLYKVVQVFSEYFKELEEESIRDNFVIIYELLDELMD
60    VAHNNIYFLAVTRKNSNATLIIAFLYKLIQVLKDYFKVLEEESIKDNFVITYELLDEMID

120   FGYPQTTDSKILQEYITQEGHKLETGAPRPPATVTNAVSWRSEGIKYRKNEVFLDVIESV
120   NGFPQLSEVKILREYIKNKAHQLTVNNFKIPSALTNSVSWRSEGIKYKKNEIFLDVVESL

180   NLLVSANGNVLRSEIVGSIKMRVFLSGMPELRLGLNDKVLFDN...........TGRGKS
180   NIIISSNGTVLRSEILGCLKMKSYLSGMPELKLGLNDKLLFNKNLNNYPNSSNNNLNNKT

229   KSVELEDVKFHQCVRLSRFENDRTISFIPPDGEFELMSYRLNTHVKPLIWIESVIEKHSH
240   KLVELEDIKFHQCVRLSKFENDRTISFIPPDGIFNLMTYRLSTHVKPLFWLDINITKKSL

289   SRIEYMIKAKSQFKRRSTANNVEIHIPVPNDADSPKFKTTVGSVKWVPENSEIVWSIKSF
300   TKIEYNVKAKSQFKNKSIANNVEFHLPVPADVDSPHFQTYIGTVKYYPDKDILIWKIKQF

349   PGGKEYLMRAHFGLPSVEAEDKE...GKPPISVKFEIPYFTTSGIQVRYLKIIEKSGYQA
360   QGQKEYIMNAQFGLPSIVSNENKDLYYKRPVNVKFEIPYFTVSGITVRYLKIIEKSGYQA

406   LPWVRYITQNGDYQLRTQ
420   LPWVRYITQNGDYQVRMS


μ2
1     MIGGLFIYNHKGEVLISRVYRDDIGRNAVDAFRVNVIHARQQVRSPVTNIARTSFFHVKR
1     MIDALYIFFINGQLLIQRNYRDTTKRTDLTQYINKYIKTKRFYENPIVEINNVFFINVNI

61    SNIWLAAVTKQNVNAAMVFEFLYKMCDVMAAYFG.KISEENIKNNFVLIYELLDEILDFG
61    NEIVITVLTRSNSNICLIFNFIYKFIEILKYFFNNELSGINIVNNFVLIYEICDEIIDYG

120   YPQ.....................................................
121   YPQTLEVNILKNSLLNKVKYYSKTSRYFQKISNELLNVNSVIEDIVHDPHIHNRTSNNKK

123   NSETGALKTFITQQGIKS..........................QHQTKEEQSQITS
181   NKSNNKIRDFYNTKSVKNKNTYDLNETNKLKYIGKETLNRIKNKIINNNNNNNKTANHFN

154   QVTGQIGWRREGIKYRRNELFLDVLESVNLLMSPQGQVLSAHVSGRVVMKSYLSGMPECK
241   YITGNCTWRNNNIYYKKNEIYIDILEILNVTINSN.NLIYAHINGKVTLKCHLSGMPLCE

214   FGMNDKIVIEK...QGKGTADETSKSGK...........................
300   LSTNNKINLLKNILAGSNTSNNNNNTSNNNNKTNQGNALRGSCGSNSLVNNKVMQNNLKK

239   .........QSIAIDDCTFHQCVRLSKFDSERSISFIPPDGEFELMRYRTTKDIILPFRV
360   KYTLDEKDNEEIIIDNCIFHHCVTLSKYENNKVITFTPPDGTFELMKYTITKNIQIPFHI

290   IPLVR...EVGR.....................TKLEVKVVIKSNFKPSLLAQKIE
420   LAIYNPILEYSKNVEKKFSLKKLTTNNKSIYGEYKNTNKYEYSVTIKSNYKGNMHASDVL

322   VRIPTPLNTSGVQVICMK.GKAKYKASENAIVWKIKRMAGMKESQISAEIELLPTNDKKK
480   IKIPIYKFSENVQVKYKSIGKTEFNNIDSLVIWRIKKFLSSSEHNIKIHLTLENHNQIYS

381   ........................WARPPISMNFEVP.FAPSGLKVRYLKVFE
540   NMNNTQKVDDLSKVVLQVHKIKNMNTVKFLNTYKMPITLSFKIPMFTSSGMYIRYLKVFE

409   PKLNYSDHDVIKWVRYIGRSGIYETRC
600   ....KSNYKIIKWIKYLTESGIYQYK.
```

```
μ4
  1     .MISQFFILSSKGDPLIYKDFRGDSGGRDVAELFYRKLTGLPGDESPVVMHHHGRHFIHI
         :||||:||| :|| :| :|||||      ||:|:| :    | ::| | : :| :| ::
  1     MVISQFYILSPRGDTIINRDFRGDIIKG.SAEVFFRNVKLYKG.DAPPVFYLNGINFTYL

 60     RHSGLYLVVTTSENVSPFSLLELLSRLATLLGDYCGSLGEGTISRNVALVYELLDEVLDY
        : : || |||:  |:||  |:||| ||  :  |:|| : |  |  |  |:||::||::||
 59     KSNSLYFVVTSLFNISPSYLIELLHRLLKIFKDFCGQITEELIRTNFILIYEIIDEIIDY

120     GYVQTTSTEMLRNFIQTEAVVSKPFSLFDLSSVGLFGAETQQSKVAPSSAASRPVLSSRS
        ||:| ::|| ::| |  |   :   ::   :::  |  :   :   ||:|: :|:  :
119     GYLQNSNTEYIKNLIHNEIATNN.NTVKKFANLPNFSIKN..TNTLPSNASQKPIQIN..

180     DQSQKNEVFLDVVERLSVLIASNGSLLKVDVQGEIRLKSFLPSGSEMRIGLTEEFCVGKS
           :|||:|:|:||:::::: ||| ::   : | |::||:|     ::| | ::  :
174     ..DKKNEIFIDIVEKINLIMNSNGEIVYSYIDGVIQIKSYLLGNPFIKIALNDDLYIKNI

240     ELRGYGPGIRVDEVSFHSSVNLDEFESHRILRLQPPQGELTVMRYQLSDDLPSPLPFRLF
                | :|: :|:  ||| :||  :|| |  | ||  :| |:::::  :  ||:::
232     HHD.NSNNIIIDDCNFNHLVNLSQFEKDKILSLYQPDGECVLMNYRINNNFKA..PFKIY

300     PSVQWDRGSGRLQVYLKLRCDLLSKSQALNVRLHLPLPRGVVSLSQELSSP....EQKAE
         :| :::    ::: :::| |: |:    || ::  | : : ::  :|::       :
289     ANVIYNQN.HTVELCIRIRLDIPSQYTCTNVFVYCNLCKHITNVHLDLNTNSDLFSAQYI

356     LAEGALRWDLPRVQGGSQLSGLFQMDVPGPPGPPSHGLSTSASPLGLGPASLSFELPRHT
          |  | | : : :|  : |   :: :      | :  |        ||  : ||:|
348     SNENKLLWTIKKFKGEHEYSIRSKITLS.....PHYAFSKRD....FGPIYILFEIPMFN

416     CSGLQVRFLRLAFRPCGNANPHKWVRHLSHSDAYVIRI.
         | |:::::|:       :| |:|||::: | :|| |:
399     LSKLRIKYLRIIEN.YKTSNTHRWVRYITQSSSYVYRLN
```

Figure 6a. μ-chain sequence alignments.

Protein sequence alignment of human (upper sequence) and *P. falciparum* (lower sequence) μ-chain adaptins using a DNAMAN© alignment program. Identical residues are shown with a blue vertical line. Conserved amino acid substitutions are denoted by colon symbols (:), and a dot (.) represents a sequence gap, introduced for optimal alignment.

Homology amongst these three parasite μ-chains is approximately 12 % at the amino acid level (Fig. 6b). The identity between μ1 and μ2 over 136 residues is in the region of 38 %, the identity between μ1 and μ4 over 449 residues is 31 %, and between μ2 and μ4 over 153 residues is 26 % (individual alignments not shown).

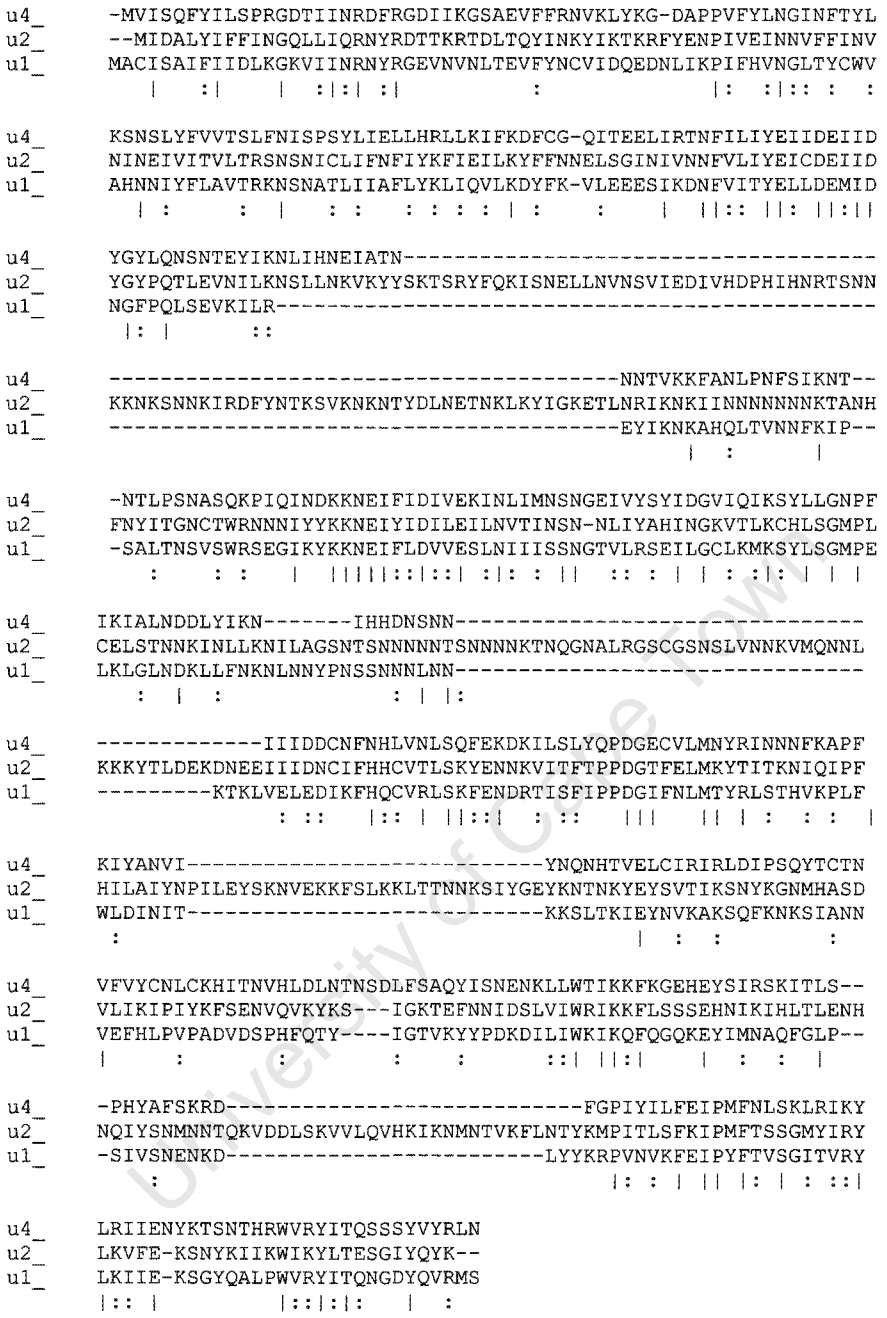

Figure 6b. Sequence homology amongst *P. falciparum* μ-chains.

Protein sequence alignment of parasite μ-chain adaptins using a DNAMAN© alignment program. Homology amongst the μ-chains is 12 % over 630 amino acid residues. Identical residues are shown with a blue vertical line, conserved amino acid substitutions are denoted by colon symbols (:), and a dash (-) represents a sequence gap introduced for optimal alignment.

2.2.2. RNA isolation and cDNA synthesis

As a first step to characterizing the μ-chain homologues it was important to confirm that they are present during the erythrocytic cycle of the parasite, as opposed to, for example, the mosquito or liver stages. For this reason, RNA was isolated for subsequent detection of μ-chain mRNA by RT-PCR.

Maximum RNA yield was obtained from late trophozoite stage parasites harvested from 50 ml cultures with a haematocrit (hct) of 4 % and a parasitaemia (pst) of 10 to 20 %. The RNAgents® Total RNA Isolation System from Promega was used and the yield of total RNA was determined spectrophotometrically at 260 ηm, where one absorbance unit (A_{260}) is equivalent to 40 μg of single-stranded RNA per ml sample. RNA yield was usually in the range of 40 to 120 μg. RNA isolated with the RNAgents® System is generally free of DNA and contaminating protein; however trace amounts of genomic DNA was removed by DNAse digestion while preserving the integrity of the RNA. The accepted range of a pure RNA preparation by A_{260}/A_{280} ratio is usually between 1.9 and 2.0. RNA isolated had ratio values falling within this range. The RNA was used as a template for single-stranded complementary (cDNA) synthesis by RNA-dependent DNA polymerase using the ThermoScript™ RT-PCR kit reagents from Invitrogen.

2.2.3. RT-PCR

cDNA was used as a template for gene amplification by PCR. Primers were designed to amplify the full-length coding sequence of μ1 and truncated versions of μ2 and μ4 (See Chapter 6- Materials and Methods, and Appendix A-1), and contained appropriate restriction sites to facilitate subsequent cloning. Expected sizes of amplification products are shown in Table 1.

Size (bp)		
μ1	μ2	μ4
1314	1031	852

Table 1. Expected sizes of PCR products.

Predicted sizes of PCR products based on genome sequences obtained from PlasmoDB.

The amplification reactions followed standard PCR protocols and yielded DNA products of the correct size when evaluated by gel electrophoresis on agarose gels and compared with a 1 kb DNA marker (Fig. 7). Successful amplification of the products confirmed that the mRNAs for μ1, μ2 and μ4 are transcribed in the trophozoite stage of *P. falciparum* in agreement with the microarray data for PF13_0062, PFL0885w and PF11_0202 (studies by the Derisi lab, Core Facility for Genomics and Proteomics, UCSF) available in PlasmoDB (Reference for the datasets: Le Roch *et al.*, 2003). The resulting product samples generally contained only the band of interest; however, for subsequent cloning samples were purified by excising the band from the gel and extracting the DNA to remove any residual primers, nucleotide bases or non-specific PCR products.

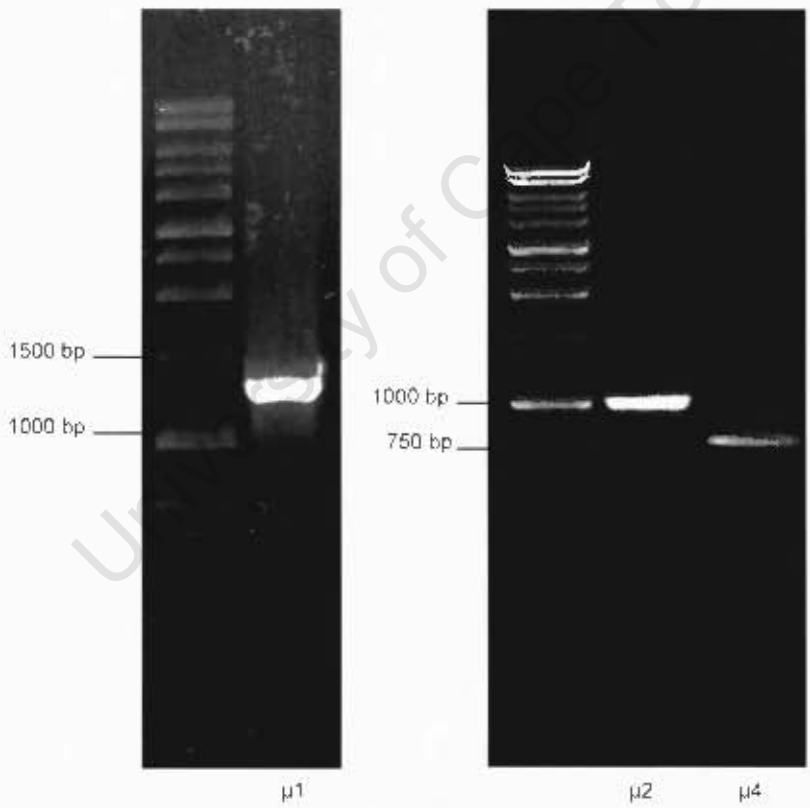

Figure 7. RT-PCR products.

Agarose gel electrophoresis (1 % gel) showing RT-PCR products alongside a 1 kb DNA ladder. μ1 gene product (1314 bp) is shown on left-hand gel. μ2 (1031 bp) and μ4 (852 bp) shown on the right-hand gel.

2.2.4. Cloning

Once the coding sequences were obtained by RT-PCR and the correct size and purity established, the products were cloned into *E. coli* to create a permanent and abundant source. Purified PCR products were either diluted or concentrated to the correct volume, and then ligated to the pGEM®-T Easy vector. Competent DH5alpha™ *E. coli* cells were transformed with the recombinant plasmid DNA. Blue/white selection of transformed bacteria on agar plates enabled the selection of single colonies containing the plasmid with insert DNA. These colonies were grown in liquid broth cultures and the plasmids isolated. Restriction digest analysis confirmed that the plasmids contained inserts of the expected size (not shown).

After verifying the presence of inserts, digests were carried out on a large scale with specific restriction enzymes to obtain the insert DNA from the pGEM®-T Easy vector for sub-cloning. BamH1 and EcoR1 were used to digest plasmids with the μ1 insert, BamH1 and Not1 for plasmids containing the μ4 insert, and BamH1 and Xho1 for μ2 containing plasmids. The excised insert DNA was purified by agarose gel purification and then cloned into the pGEX-4T-1 expression vector digested with the corresponding restriction enzymes (i.e. BamH1/EcoR1, BamH1/Not1 and BamH1/Xho1, See Appendix A-2). The restriction sites were chosen to ensure that the gene is cloned into the plasmid in-frame and in the correct orientation.

After growing *E. coli* colonies transformed with the pGEX-4T-1 ligations overnight, the recombinant plasmids were isolated and restriction digests performed to confirm that the correct insert was incorporated in the plasmid (Fig. 8-10). BamH1 restriction enzyme was used in each instance, with an additional enzyme predicted to cut within each gene based on the genome sequence; Spe1 for μ1, Nsi1 for μ2 and EcoR1 for μ4 (See Appendix A-2). All digests yielded fragments of the expected size. DNA sequencing was performed by Inqaba Biotechnical Industries (South Africa) on plasmids containing the inserts to confirm the presence of the correct inserts (data not shown).

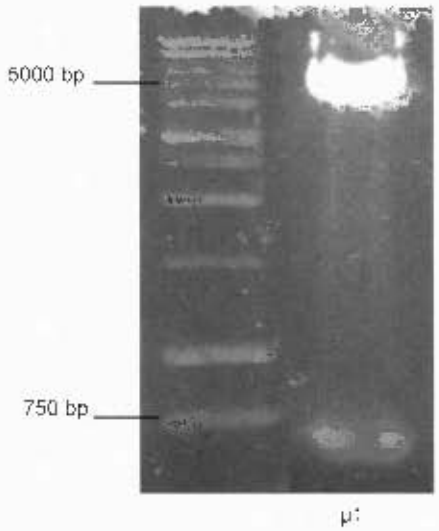

Figure 8. Plasmid digest (μ1).

1 % agarose gel showing part of the μ1 insert excised from the pGEX-4T-1 plasmid. The plasmid was digested with restriction enzymes BamH1 and Spe1. The BamH1 restriction site was introduced into the μ1 sequence with the forward primer and Spe1 cuts within the sequence, resulting in a predicted DNA fragment of 720 bp. The plasmid containing the remaining part of the insert has a size of approximately 5490 bp.

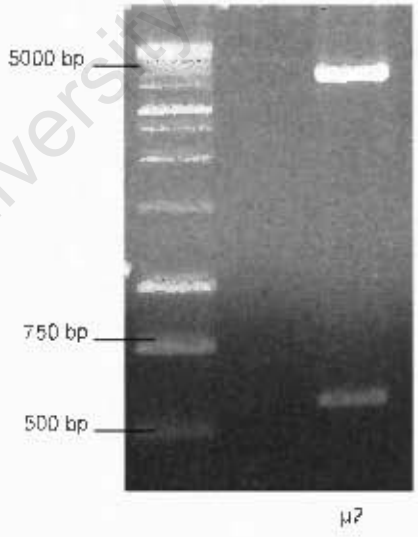

Figure 9. Plasmid digest (μ2).

1 % agarose gel showing part of the μ2 sequence excised from the pGEX-4T-1 plasmid. The plasmid was digested with restriction enzymes BamH1 and Nsi1. The restriction site for BamH1 was included in the forward primer and Nsi1 cuts within the insert sequence, resulting in a predicted fragment of 586 bp. The plasmid and remaining part of the insert has a size of approximately 5340 bp.

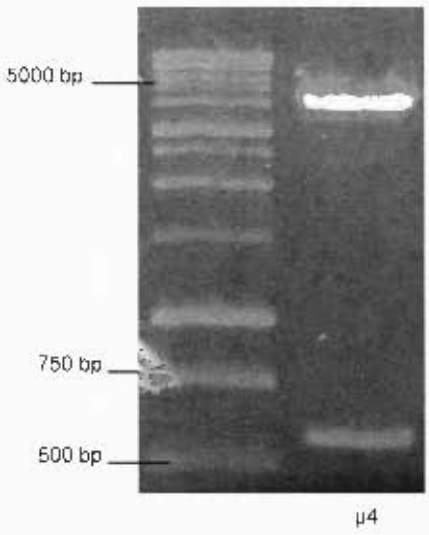

Figure 10. Plasmid digest (μ4).

1 % agarose gel showing part of the μ4 gene excised from the pGEX-4T-1 plasmid. The plasmid was digested with restriction enzymes BamH1 and EcoR1. The restriction site for BamH1 is found at the 5' end of the insert sequence and EcoR1 within the insert, resulting in a fragment of 572 bp. The plasmid with the remaining part of the gene has a size of approximately 5180 bp.

The pGEX-4T-1 plasmids containing the correct insert DNA were initially transformed into DH5alpha™ *E. coli*. For improved protein expression yields, the plasmids were subsequently used to transform BL21 Star™(DE3) *E. coli*. BL21 Star™ strains are high-performance cells designed for improved protein expression in T7 promoter-based expression systems.

2.2.5. Expression of recombinant proteins

The cloned genes were expressed to obtain recombinant protein for antibody production through immunization. The pGEX-4T-1 expression vector contains an IPTG-inducible promoter region upstream of the multiple cloning site. In addition, it produces an N-terminal fusion to glutathione-S-transferase (GST) to facilitate expression, solubility and purification. Bacteria possessing the correct plasmids were grown overnight in LB containing Ampicillin and expression induced with IPTG for three hours. To confirm that the bacteria have expressed the fusion proteins, *E. coli* were lysed using standard lysozyme / Triton lysis (Chapter 6- Materials and Methods). In all cases, the recombinant

protein was present in the insoluble pellet in inclusion bodies and an attempt was made to solubilize them with sarkosyl. The sarkosyl lysates and remaining insoluble pellets were run on SDS polyacrylamide gels and stained with Coomassie. When compared to bacteria that have not been induced with IPTG, a prominent new band of the appropriate size was visible in all cases (Fig. 11-13).

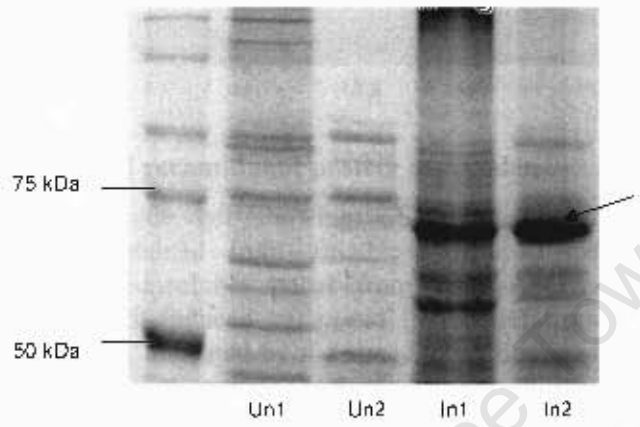

Figure 11. GST-μ1 recombinant protein expression.

Extracts of *E. coli* expressing GST-μ1 recombinant protein were electrophoresed on a 10 % polyacrylamide gel against a broad range protein molecular weight marker. Un1; sarkosyl lysate of lysozyme / Triton insoluble pellet obtained from uninduced BL21 Star™(DE3) *E. coli* (control sample), Un2; remaining sarkosyl-insoluble pellet from uninduced cells (control sample), In1; sarkosyl lysate from IPTG-induced cells, and In2; pellet from induced cells. The additional band in both the lysate and pellet induced samples, indicated by the arrow, migrates with an estimated molecular weight of 72 kDa.

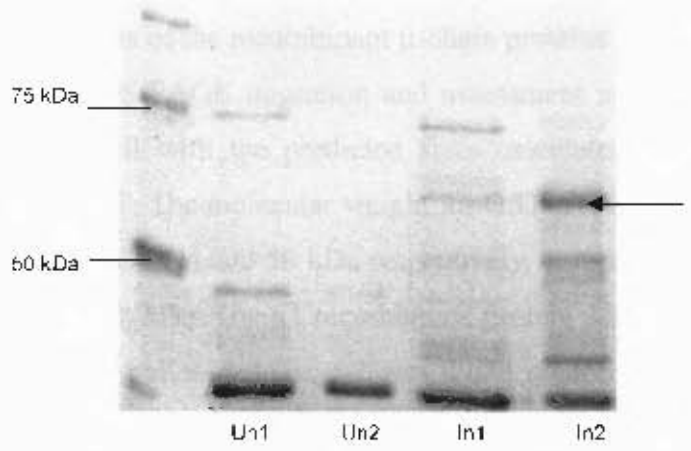

Figure 12. GST-μ2 recombinant protein expression.

10 % polyacrylamide gel showing GST-μ2 expression. Un1; sarkosyl lysate obtained from uninduced *E. coli* cells, Un2; remaining sarkosyl-insoluble pellet from uninduced cells, In1; sarkosyl lysate from induced cells, and In2; pellet from induced cells. Expressed μ2, indicated by the arrow, is predominantly found in the sarkosyl pellet sample and migrates with an apparent molecular weight of approximately 63 kDa.

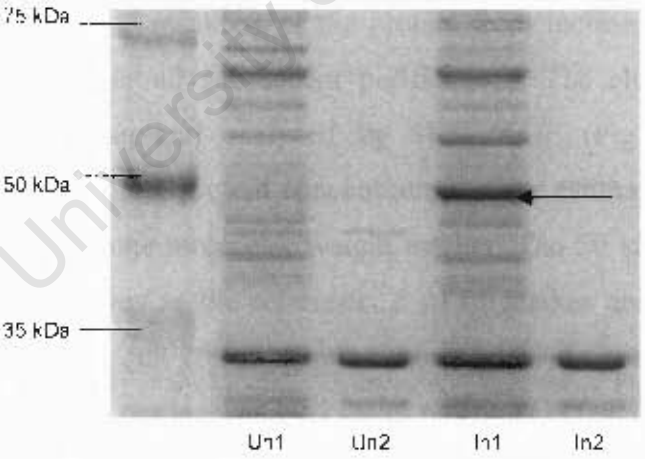

Figure 13. GST-μ4 recombinant protein expression.

10 % gel showing GST-μ4 expression. Un1; sarkosyl lysate obtained from uninduced cells, Un2; remaining sarkosyl-insoluble pellet from uninduced cells, In1; sarkosyl lysate from induced cells, and In2; pellet from induced cells. The GST-μ4 protein, present in the sarkosyl lysate, migrates with an apparent molecular weight of approximately 50 kDa, indicated by the arrow.

The apparent molecular weights of the recombinant μ-chain proteins in the IPTG-induced *E. coli* extracts, based on SDS-PAGE migration and assessment against the molecular weight marker, compared well with the predicted sizes calculated for the respective coding sequences fused to GST. The molecular weight for GST-μ1, GST-μ2 and GST-μ4 were approximately 72 kDa, 63 kDa and 50 kDa respectively, compared to the predicted sizes of 76 kDa, 65 kDa and 58 kDa. The μ1 recombinant protein was present in both the sarkosyl lysate and remaining pellet samples, μ2 was found predominantly in the pellet sample and μ4 only in the sarkosyl lysate sample. These samples were used for subsequent protein purification procedures.

When comparing the induced and uninduced samples, it is notable that there is little or no bacterial protein of similar size to the adaptins in the uninduced sample. This is significant when selecting the appropriate purification technique as the electro-elution method relies on the excision of the protein band from the gel. Purification was initially carried out using both affinity chromatography with glutathione-agarose columns and electro-elution from gel slices. The glutathione agarose method yielded pure recombinant proteins; however yields were less than that achieved by electro-elution, presumably due to inefficient solubilization and refolding of the protein from inclusion bodies. Electro-elution was therefore used for all subsequent purifications. The eluted proteins were concentrated by freeze-drying and analyzed by SDS-PAGE (Fig. 14-16). For the purposes of antibody preparation, protein concentrations were estimated by comparison with proteins of the broad range molecular weight marker. The 50 kDa protein band is present at 0.3 μg/μl and serves as the reference. 5 μl of marker and 15 μl of protein sample were loaded onto the gel. 200 ml broth cultures yielded approximately 1 μg/μl purified GST-μ1 and GST-μ4 proteins, and 0.1 μg/μl purified GST-μ2 protein.

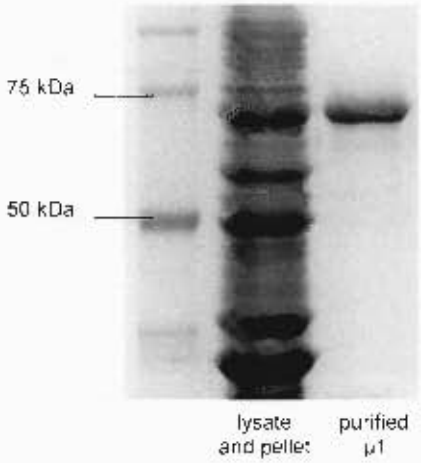

Figure 14. Electro-eluted GST-μ1 recombinant protein.

SDS-PAGE showing the purified GST-μ1 recombinant protein alongside the combined induced sarkosyl lysate and pellet samples.

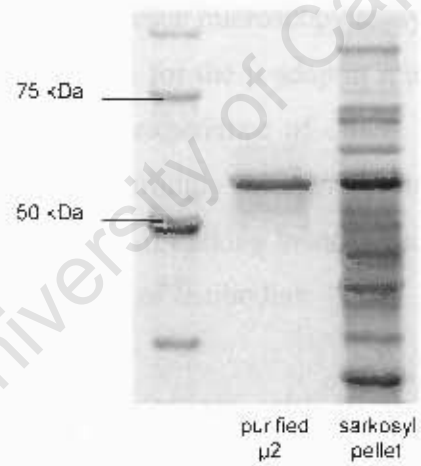

Figure 15. Electro-eluted GST-μ2 recombinant protein.

Purified GST-μ2 recombinant protein alongside the induced sarkosyl pellet sample.

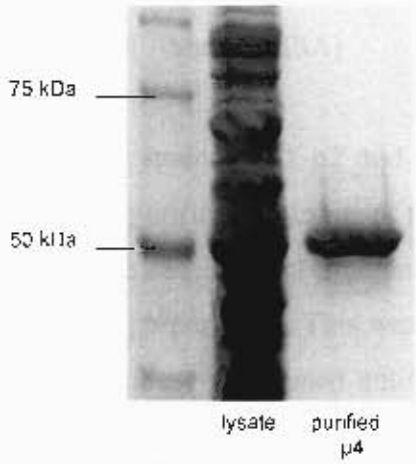

Figure 16. Electro-eluted GST-μ4 recombinant protein.

Purified GST-μ4 recombinant protein alongside the induced sarkosyl lysate.

Mice were immunized with the purified proteins and antisera collected and stored for use in Western blotting, immunofluorescence microscopy assays (IFA) and immuno-electron microscopy (EM). Mice were chosen for the μ-adaptin immunizations instead of rabbits for two reasons. Firstly, from past experience of others and ours, rabbit sera tend to contain antibodies that cross-react strongly with irrelevant malaria proteins. Secondly, mice immunization offers the option of making monoclonal antibodies, which provides a permanent and highly specific source of antibodies.

Five mice were immunized for each antigen, with 30 μg protein in complete Freund's adjuvant administered to each mouse. Booster immunizations were done with incomplete Freund's adjuvant every three weeks and blood collected from the tail vein one week after each booster immunization. The serum collected was stored at - 80 °C with sodium azide.

2.2.6. Enzyme-Linked Immunosorbent Assay (ELISA)

Serial dilutions of the antisera raised against GST-μ2 and GST-μ4 were initially tested for reactivity with the corresponding purified recombinant protein by ELISA. Wells of a microtitre plate were coated with the recombinant antigens, washed of excess antigen, blocked and probed with the antisera preparations. This was followed by incubation with a goat anti-mouse Horseradish peroxidase-conjugated antibody, after which peroxidase activity was quantitated with OPD colorimetric substrate. As the substrate was hydrolyzed by the enzyme conjugate, a coloured product, proportional to the amount of antibody in the sera, was generated and detected by a microtitre plate reader. The graphs illustrate antibody response for pooled post-immune sera relative to no response observed for the control where no primary sera were used (Fig. 17 and 18). These results suggest that the antisera recognize the respective recombinant proteins with which the mice were immunized.

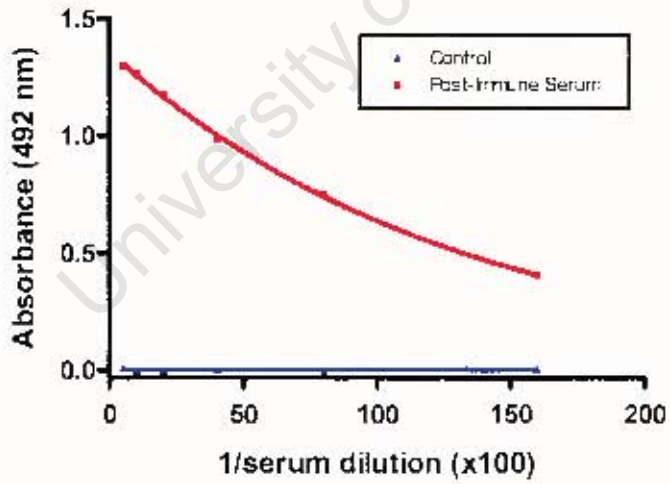

Figure 17. ELISA performed on pooled GST-μ2 bleeds.

The graph illustrates the strong immune response of the antisera (red) relative to the negative control (blue).

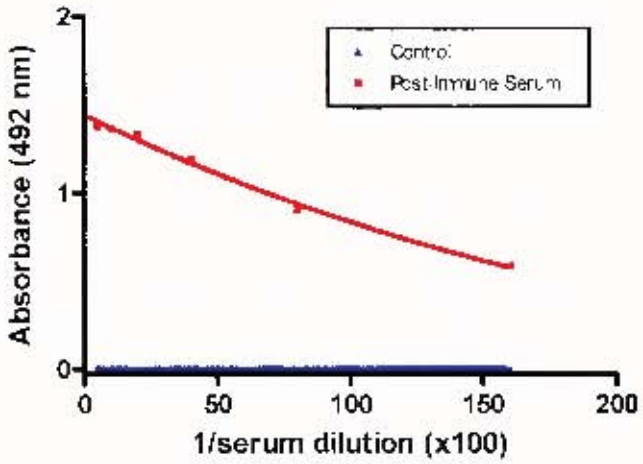

Figure 18. ELISA performed on pooled GST-μ4 bleeds.

The graph illustrates the strong immune response of the antisera (red) relative to the negative control (blue).

2.2.7. Western blotting

In order to determine if the antisera recognize the corresponding parasite proteins and to assess their specificity, Western blotting was performed. Trophozoite stage parasites were released from infected erythrocytes by saponin lysis and the lysate solubilized in sample buffer and run on SDS-PAGE gels. The separated proteins were transblotted onto membranes, membranes cut into strips, and each strip incubated with the respective antisera followed by peroxidase-conjugated anti-mouse antibodies, and detected with a chemiluminescent peroxidase substrate. Additional strips were also incubated with pre-bleed sera as controls. As shown in Figure 19a, the antisera obtained for μ1, μ2 and μ4 recognize specific proteins. A protein of approximately 70 kDa was detected by the μ1 antisera and proteins of 63 kDa and 70 kDa by μ2 and μ4 antisera respectively. No specific proteins were detected with the pre-bleed sera.

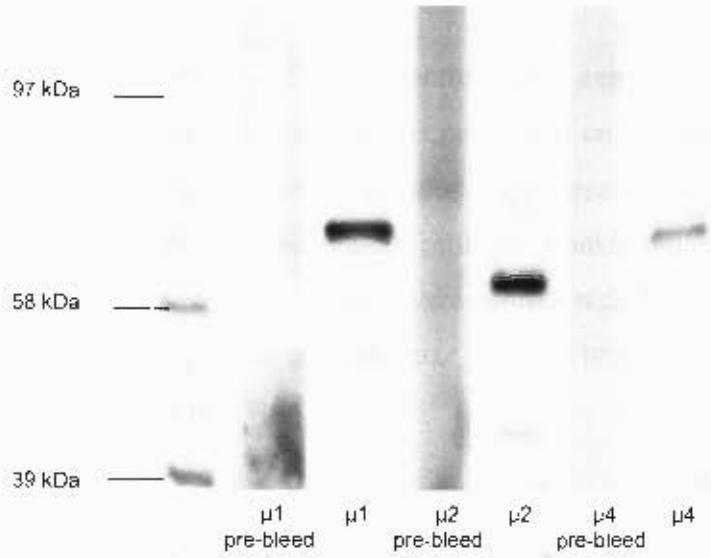

Figure 19a. Western blot of *P. falciparum* lysate using antisera raised in mice. Strips of membrane were probed with pre-bleed sera and the specific antisera. μ1 antiserum recognizes a parasite protein with an apparent molecular weight of approximately 70 kDa. A protein of approximately 63 kDa is recognized by μ2 antiserum and 70 kDa by μ4. No parasite proteins were detected with the pre-bleeds.

Encouragingly, the antisera appeared mono-specific and reacted strongly with parasite proteins on the blot. However, the apparent sizes of the parasite proteins did not agree with the sizes predicted by the gene sequences in PlasmoDB (Table 2). The μ1 and μ4 antisera recognized proteins approximately 20 kDa larger than what was expected, while the μ2 adaptin is predicted to have a size of around 73 kDa, about 10 kDa larger than what is observed on the blot.

	Molecular weight values	
	SDS-PAGE (kDa X 10^{-3})	calculated (kDa)
μ1	70	50812
μ2	63	72902
μ4	70	51137

Table 2. Apparent and calculated molecular weights.

The apparent molecular weights estimated by SDS-PAGE compared with the molecular weight values predicted by the gene sequences in the malaria genome database, PlasmoDB.

To determine if the different μ-chain adaptins are expressed throughout the intraerythrocytic cycle, Western blot analysis was performed on different parasite stages. Parasites lysates from ring, trophozoite and schizont stage parasites were subject to SDS-PAGE in adjacent wells and the separated proteins transferred onto membranes. Membranes containing the three parasite stage were probed with the respective antisera. The antisera obtained for μ1, μ2 and μ4 recognize specific proteins in trophozoite and schizont stage parasites only (Fig. 19b).

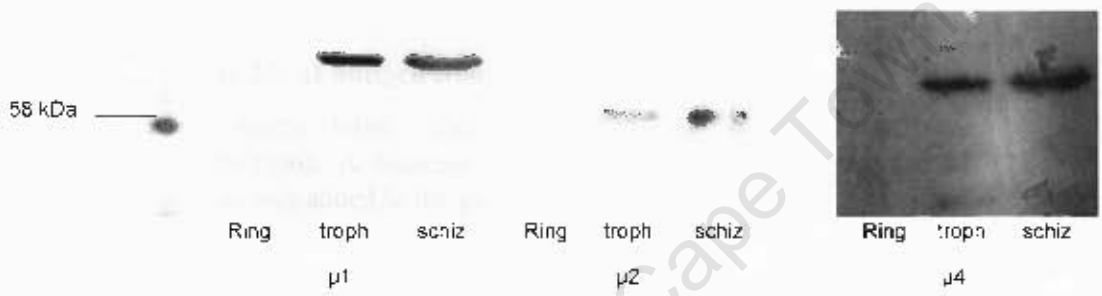

Figure 19b. Western blot of *P. falciparum* extracts at different parasite stages. Membrane containing ring, trophozoite and schizont stage parasites were probed with the specific antisera. All three μ-chains recognized the corresponding protein in trophozoite and schizont stage parasites. No protein was detected in ring stage parasites.

To verify that the μ1 antisera is specific for the recombinant μ1 antigen, antigen competition experiments were performed by running parasite lysate on a gel, transferring the protein to a membrane, and cutting the membrane into strips. Two 5 ml antiserum solutions of the same dilution (1:1000) were prepared. To one of these solutions 10 μg purified μ1 antigen was added. Both solutions were incubated at room temperature for one hour. The preparations were used separately on two strips of membrane and standard Western blot procedure carried out. A visible reduction in Western blot signal was observed when the antibody solution was incubated with the μ1 antigen when compared with the strip probed with antisera alone (Fig. 20). The result confirms that the prominent 70 kDa parasite protein is recognized by antibodies that cross-react with recombinant μ1.

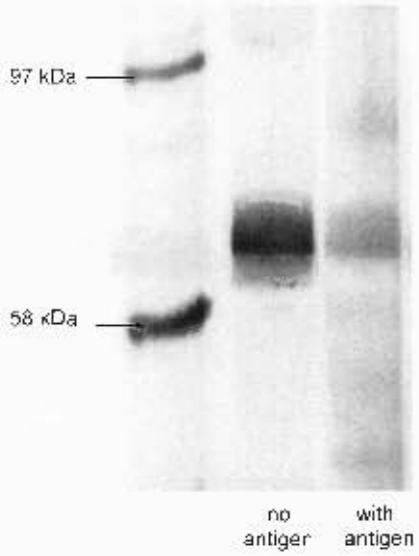

Figure 20. μ1 antigen competition.

The same band was recognized by the two antisera preparations. A decrease in band intensity occurred when the μ1 antigen was added to the μ1 antisera.

To further explore the size discrepancies, additional Western blotting analyses of the μ1 antisera was carried out. To test for cross-reactivity of the antisera with different cell types, a Western blot was performed on membranes containing total protein extract of mammalian cos-1 cells and *Toxoplasma gondii* (*T. gondii*) RH strain parasites, along with *P. falciparum* parasite lysate (Fig. 21). Distinct single bands of approximately 45 kDa and 70 kDa were observed with mammalian cos-1 cells and *Toxoplasma* RH2 cells respectively. The results suggest that the antiserum cross-reacts with the mammalian μ1 homologue of cos-1 cells, known to migrate as a 47 kDa species on SDS-PAGE gels (Sorkina *et al.*, 1999), while the μ1 homologue of the more closely related apicomplexan parasite, *T. gondii*, also migrates as a 70 kDa band.

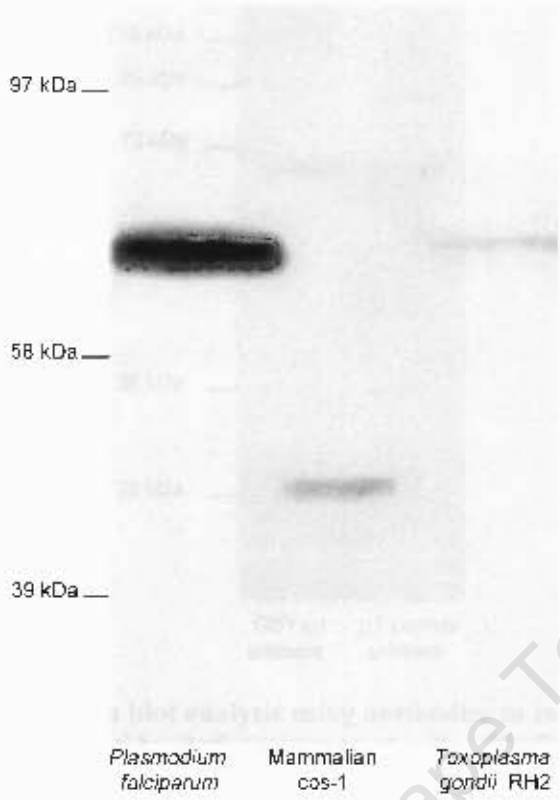

Figure 21. Western blot analysis of total protein extracts from different cell types. *P. falciparum* μ1 antisera cross-reacts with a 70 kDa protein in *T. gondii* and a 45 kDa protein in mammalian cells.

In addition to antisera raised against the recombinant protein, antibodies to a synthesized peptide predicted to be a μ1 epitope were raised in rabbits by GeneScript Corporation (USA) (See Chapter 6- Materials and Methods, and Appendix A-1 and A-3) to further support the notion that the mouse derived antisera recognize the parasite μ1 adaptin. Western blot analysis, completed on strips of membrane containing parasite proteins and probed in parallel with the two μ1 antisera, revealed that the most prominent band recognized by the anti-peptide antisera co-migrated with the single band recognized by antisera raised to the bacterially expressed μ1 protein (Fig. 22). The results substantiate the notion that *P. falciparum* μ1 migrates as a 70 kDa band by SDS-PAGE, despite the 50 kDa size predicted by the genome sequence. Other non-specific parasite proteins were detected with the peptide-derived antiserum, which is a problem commonly experienced with rabbit antisera used in parasite blots.

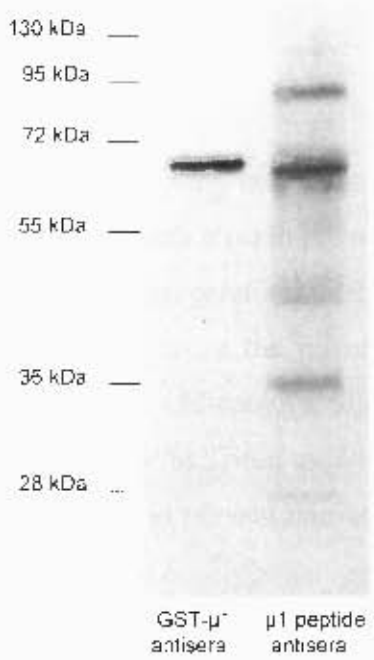

Figure 22. Western blot analysis using antibodies to recombinant μ1 and to a μ1 peptide. Both antisera react with a 70 kDa protein in *P. falciparum*.

To further verify that the μ1 antiserum is specific for the recombinant μ1 antigen, an attempt to specifically silence μ1 expression by an RNAi approach was performed. Parasites were incubated with double-stranded RNA corresponding to the μ1 coding sequence. This led to a 30% decrease in the intensity of the 70 kDa band recognized by the μ1 antisera by Western blotting. However, the results could not be reproduced with additional controls and are therefore presented in the Appendix (A-6). Furthermore, an attempt was made to identify any irregularities in the predicted μ1 mRNA open reading frame experimentally by RACE PCR. Although 3' RACE was successful, several attempts at 5' RACE was unsuccessful. A description of the RACE experiments is detailed in the Appendix (A-7).

2.2.8. Immunofluorescence microscopy assays (IFA)

2.2.8.1. Localization of μ1, μ2 and μ4

The subcellular localization of the μ-adaptins was determined by immunofluorescence microscopy on parasites released with saponin (to improve fixation and antibody access), immobilized on poly-lysine and fixed with paraformaldehyde (PFA) and glutaraldehyde (Fig. 23a). The mouse antisera raised against the recombinant adaptins were used as primary antibodies and Alexa Fluor® 488-conjugated anti-mouse antibodies as the secondary. Fixed parasites were treated with Triton to permeabilize membranes and with glycine to quench free aldehyde groups to prevent non-specific binding of antibodies to the parasite.

Figure 23a shows representative parasites in each case, clearly visible in the phase-contrast panels. Note that the surrounding host erythrocyte is not visible, due to saponin lysis prior to fixation to improve antibody access to parasite subcellular structures. The location of the digestive vacuole in each parasite can easily be inferred from the prominent haemozoin crystal in the phase-contrast panels. Parasite nuclei are identifiable by DAPI staining. Note that some parasites have two nuclei, indicating that they are at the late trophozoite / early schizont border. Both μ1 and μ2 antisera recognized a convoluted, extended structure in the parasite cytoplasm (Fig. 23a A and B, respectively). The structure is further depicted in Figure 25, where two adjacent parasites reacted with μ1 antisera were photographed at successive focal plains, 1 μm apart. Negative controls containing secondary antibodies alone display only weak background fluorescence (an example is shown in Fig. 23b). By contrast, two different staining patterns were discernable for the μ4 adaptin, as represented in the first and second rows of Figure 23 C. μ4 appeared to localize to regions along the parasite plasma membrane (first row) and associated with the digestive vacuole (second row).

To examine the labelling profile of the adaptins at different stages of development, IFA was performed on ring, trophozoite and schizont stage parasites with the μ2 and μ4 antisera (Fig. 24). No fluorescence was detected in ring stage parasites for either adaptin. Trophozoite and schizont stage parasites show bright fluorescence at the digestive vacuole, and in some cases, at the plasma membrane with the μ4 sera. Similarly, the

elongated ribbon pattern seen with μ2 is maintained throughout the mature stages of the life cycle.

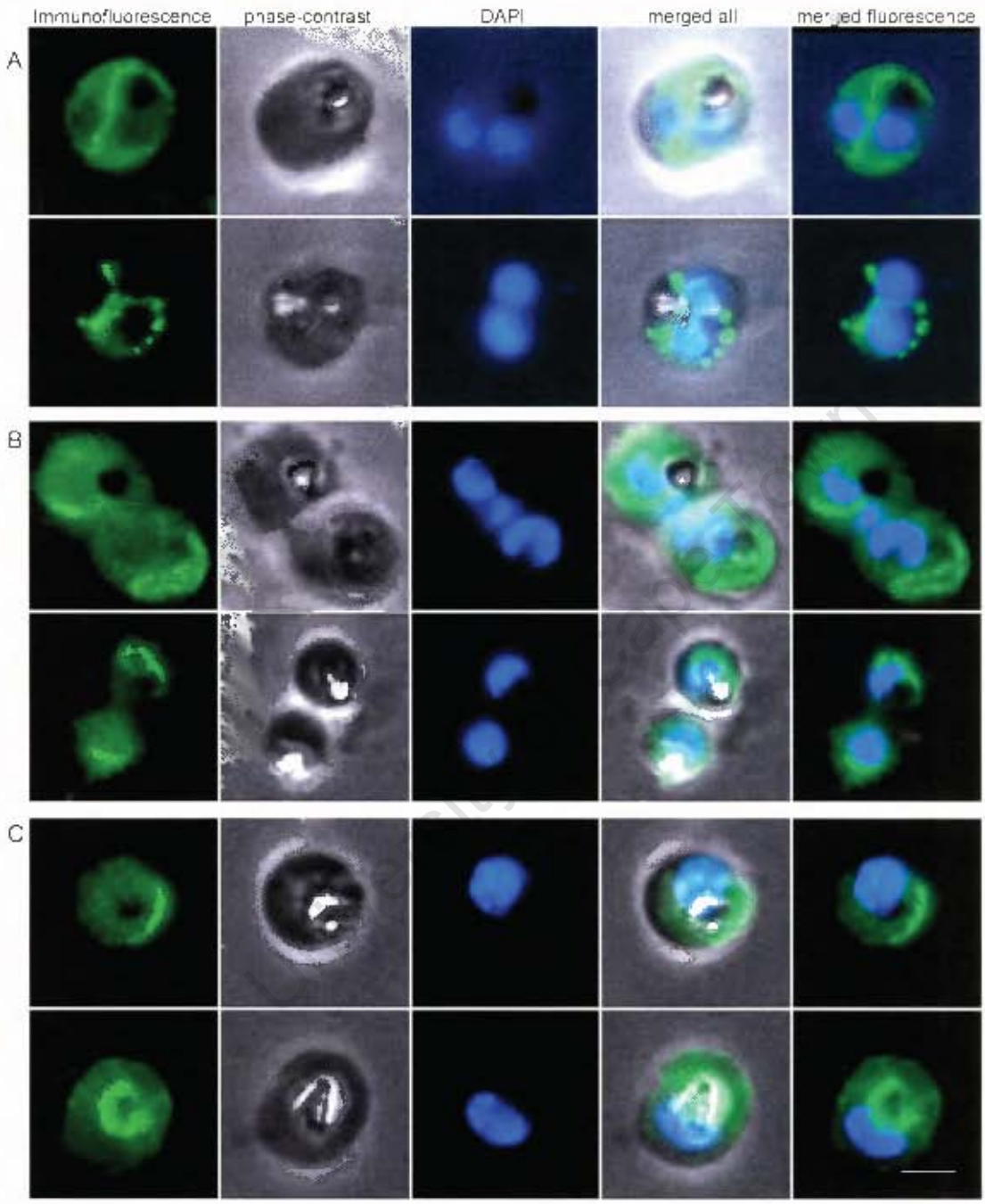

Figure 23a. IFA localization of μ-chain adaptins in *P. falciparum* trophozoites. Parasites were fixed with paraformaldehyde supplemented with glutaraldehyde. Two different parasites are shown for each adaptin (two rows per adaptin); (A) Intracellular localization pattern of μ1 in the parasite, (B) μ2 distribution, and (C) μ4. The panels illustrate from left to right: the immunofluorescence image obtained using μ-adaptin antisera and an Alexa Fluor® 488-conjugated secondary antibody (green), the corresponding phase-contrast image, the DAPI stained nuclei (blue), the merged image of the three, and the merged image of fluorescence and DAPI. Bar, 2 μm.

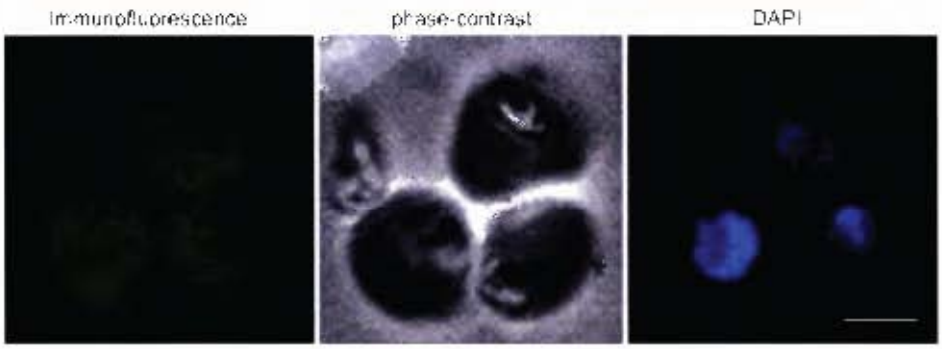

Figure 23b. Immunofluorescence control.

The first panel shows three parasites probed with Alexa Fluor® 488-conjugated secondary antibodies (green) in the absence of primary antiserum. Only faint background fluorescence is visible. The second and third panels show a phase-contrast image of the parasites and the nuclei stained with DAPI, respectively. Bar, 2 μm.

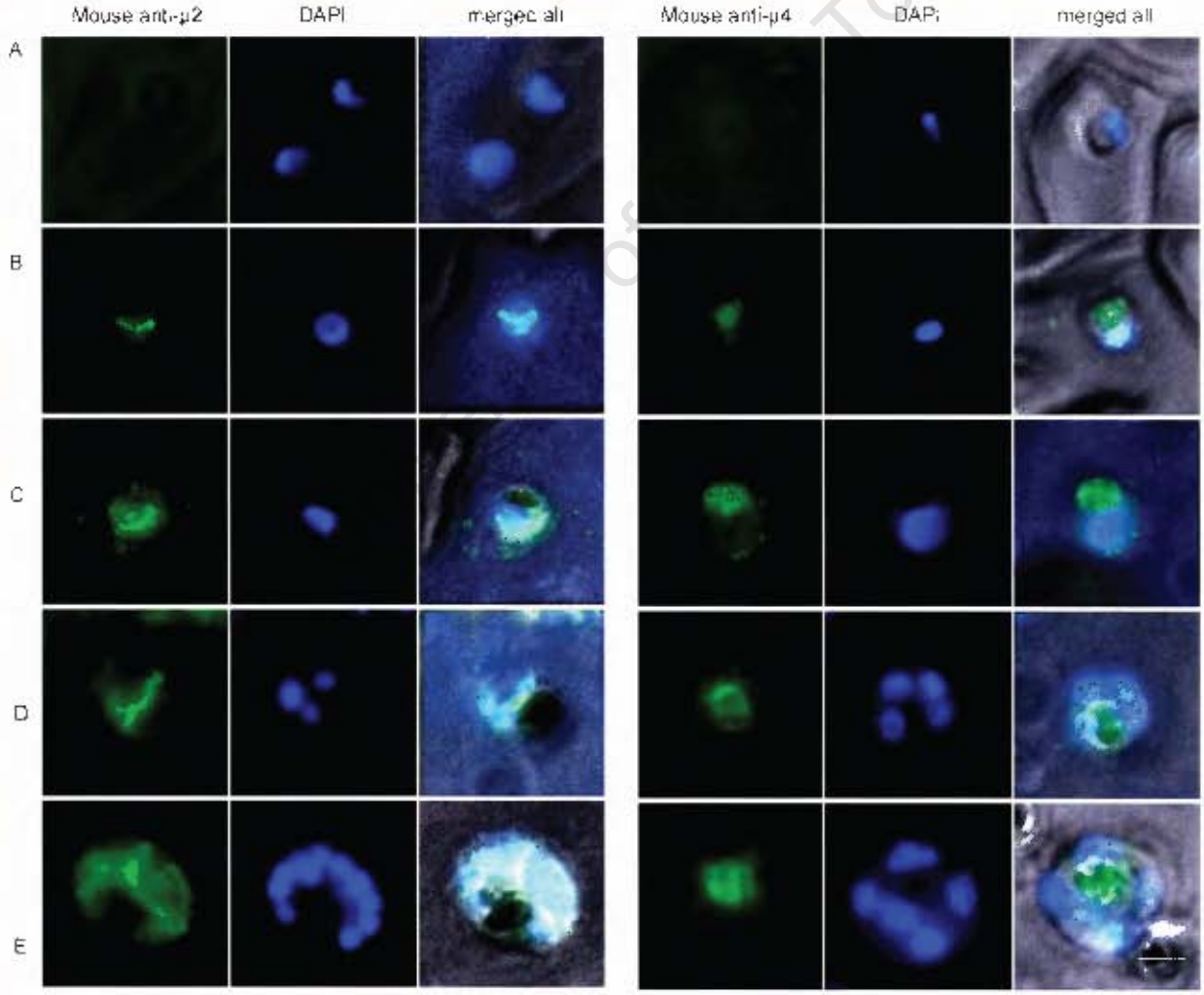

Figure 24. IFA localization of μ2 and μ4 in different parasite intraerythrocytic stages. No fluorescence was detected in the ring stage parasite for either adaptin (A). Early and late trophozoite (B and C) and schizont (D and E) stage parasites show bright fluorescence. Bar, 2 μm.

Figure 25. Serial focal plains of parasites labelled with μ1 antisera. Each panel contains a different focal plain of the same two parasites. Images were taken at 1 μm intervals along the z-axis. Bar, 2 μm.

2.2.8.2. Co-localization of μ1 and μ2

The immunofluorescence images suggested that μ1 and μ2 might localize to similar sites within the parasite (compare Fig. 23a A and B). Co-localization experiments using anti-μ1 and anti-μ2 were performed to determine if these structures are the same (Fig. 26). Parasites that were fixed in paraformaldehyde and permeabilized with Triton were first incubated with anti-μ1 antiserum, followed by Alexa Fluor® 488-conjugated goat anti-mouse secondary antibodies. The antibodies were fixed in place with PFA / glutaraldehyde, where after samples were incubated with anti-μ2 antiserum and TRITC-conjugated anti-mouse secondary antibodies. The different fluorescent channels were used to view the different fluorescent tags. The two fluorescent images were merged and regions where the signals overlap appear yellow. The images suggest that the adaptins localize to similar sites within the parasite cytosol.

Negative controls were performed by the same procedure, with the only difference being that the anti-μ2 antiserum step was excluded (Fig. 27). The results show that no specific localization was obtained when probing with the TRITC-conjugated anti-mouse secondary antibody, verifying that the glutaraldehyde fixing step between antibody incubations is sufficient to prevent recognition of the first primary antibody, anti-μ1, by the TRITC-conjugated anti-mouse secondary, thus preventing spurious co-localizations.

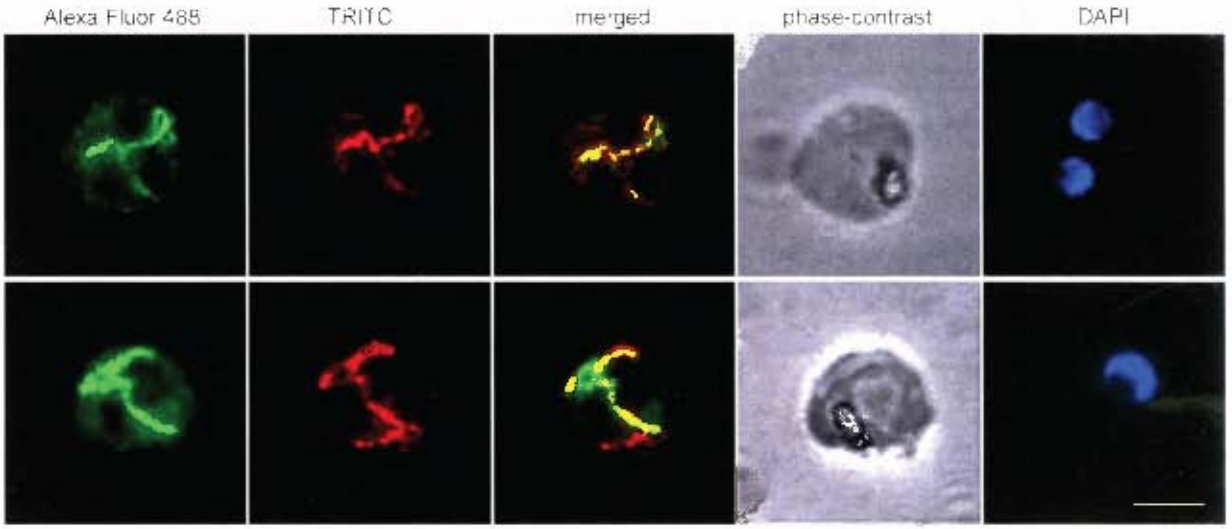

Figure 26. Co-localization of μ1 and μ2 adaptins in *P. falciparum* trophozoites. In each row, the Alexa Fluor® 488-conjugated secondary antibodies (green) correspond to μ1 and the TRITC-conjugated secondary antibodies (red) to μ2. In the merged images, areas of overlap between the green and red signals display as yellow. Phase-contrast and DAPI staining show the position of the digestive vacuole and nuclei, respectively. Bar, 2 μm.

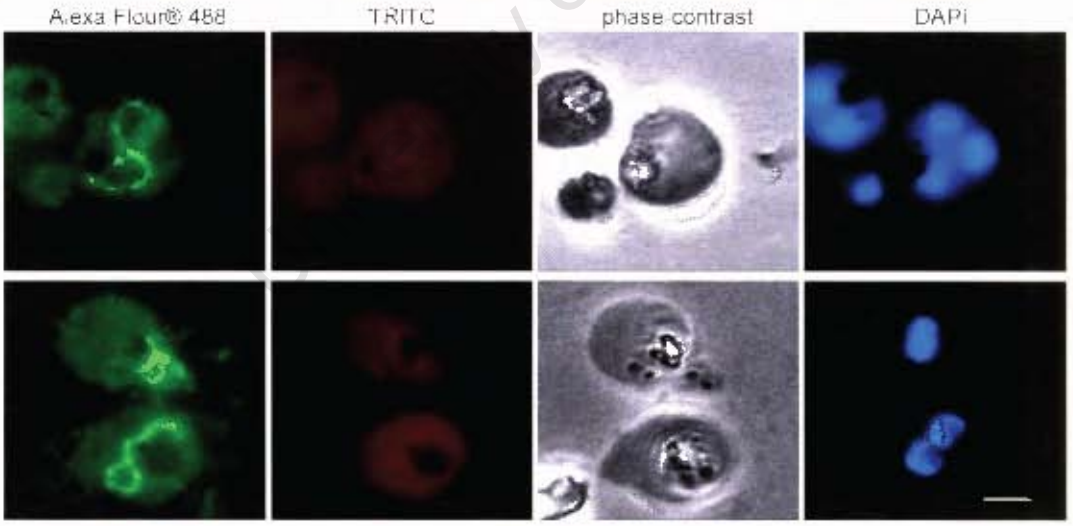

Figure 27. Co-localization control for μ1 and μ2.

Fixed and permeabilized parasites were incubated sequentially with μ1 antiserum, Alexa Fluor® 488-conjugated anti-mouse secondary antibodies, PFA / glutaraldehyde and TRITC-conjugated anti-mouse secondary antibodies. The first panels show two parasites, viewed in the Alexa Fluor® 488 channel, showing typical μ1 localization patterns, and the second panels show the same view through the TRITC channel, with only weak background fluorescence. Bar, 2 μm.

2.2.8.3. Co-localization of mouse anti-μ1 and rabbit anti-μ1 peptide antisera

Co-localization experiments using anti-μ1 antiserum derived from mice immunized with recombinant GST-μ1 and rabbit antiserum to the μ1 peptide were performed to determine if these antisera recognize the same structures (Fig. 28), as suggested by the earlier Western blotting experiment which shows both antisera recognizing a prominent 70 kDa parasite protein (Fig. 22). Parasites were prepared as previously described and were incubated with both primary antisera, followed by both Alexa Fluor® 488-conjugated goat anti-mouse and TRITC-conjugated goat anti-rabbit secondary antibodies. The images suggest extensive co-localization by the two antisera, consistent with the notion that both antisera are specific for the μ1 adaptin. To rule out the possibility of spurious co-localization due to species cross-reactivity in the secondary antibodies, controls were performed for each antiserum where the primary antibody was excluded during the incubation step (Fig. 29). In the first control (Fig. 29 A), rabbit anti-μ1 peptide antiserum was excluded, and in the second (Fig. 29 B), mouse anti-μ1 antiserum was omitted. Only faint background fluorescence was observed in either case when the relevant primary antiserum was absent. This confirms species specific recognition of the primary antibodies by the secondary antibodies.

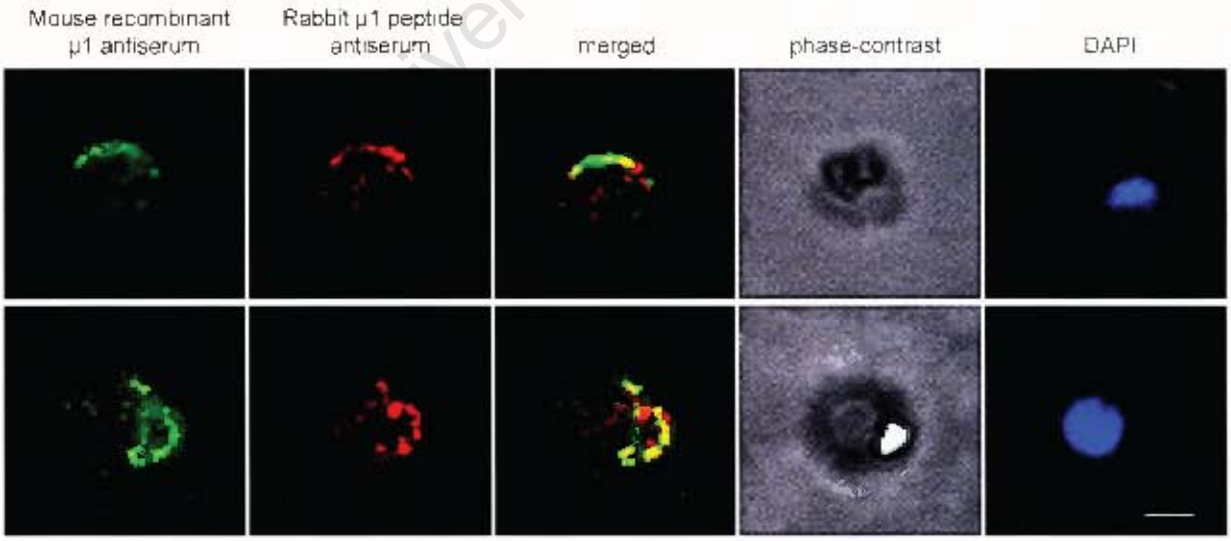

Figure 28. Co-localization using mouse antiserum to recombinant μ1 and rabbit antiserum to a μ1 peptide. A mixture of anti-mouse Alexa Fluor® 488-conjugated secondary antibody (green) and anti-rabbit TRITC-conjugated secondary antibody (red) was used to recognize the two antisera respectively. Bar, 1 μm.

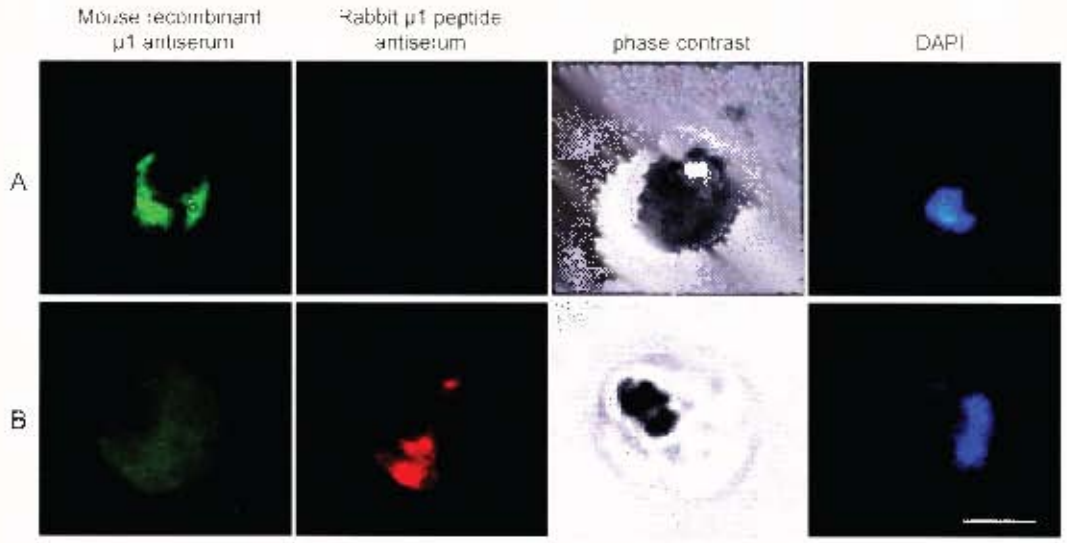

Figure 29. Co-localization controls for recombinant μ1 and μ1 peptide antisera. The first Control (A), where rabbit anti-μ1 peptide antiserum was excluded, shows μ1 recognized by anti-mouse Alexa Fluor® 488-conjugated secondary antibodies (green). No distinct localization is seen for the anti-rabbit TRITC-conjugated secondary antibodies. (B) illustrates the control where the mouse recombinant anti-μ1 antiserum was omitted. The first panel shows no localization with anti-mouse Alexa Fluor® 488. The second panel shows rabbit anti-μ1 peptide antiserum recognized by TRITC-conjugated anti-rabbit secondary antibodies (red). Bar, 2 μm.

2.2.8.4. Dual labelling with antibodies recognizing the clathrin heavy chain

Immunofluorescence microscopy results suggest that μ4 localizes to plasma membrane and digestive vacuole sites in the parasite (Fig. 23a C). Similar plasma membrane-like localization was also previously found with rabbit antiserum raised to a recombinant fusion of GST and the C-terminal hub domain of the *P. falciparum* clathrin heavy chain homologue (PFL0930w) (H. Hoppe and B. Weber, unpublished results). Co-localization IFA was therefore performed using the mouse anti-μ4 antiserum (this study) and rabbit anti-*Pf*clathrin (H. Hoppe and B. Weber) to assess a possible association between *P. falciparum* μ4 and clathrin (Fig. 30a). Anti-μ4 displayed significant co-localization with antigens detected by the clathrin antibody at the peripheral sites.

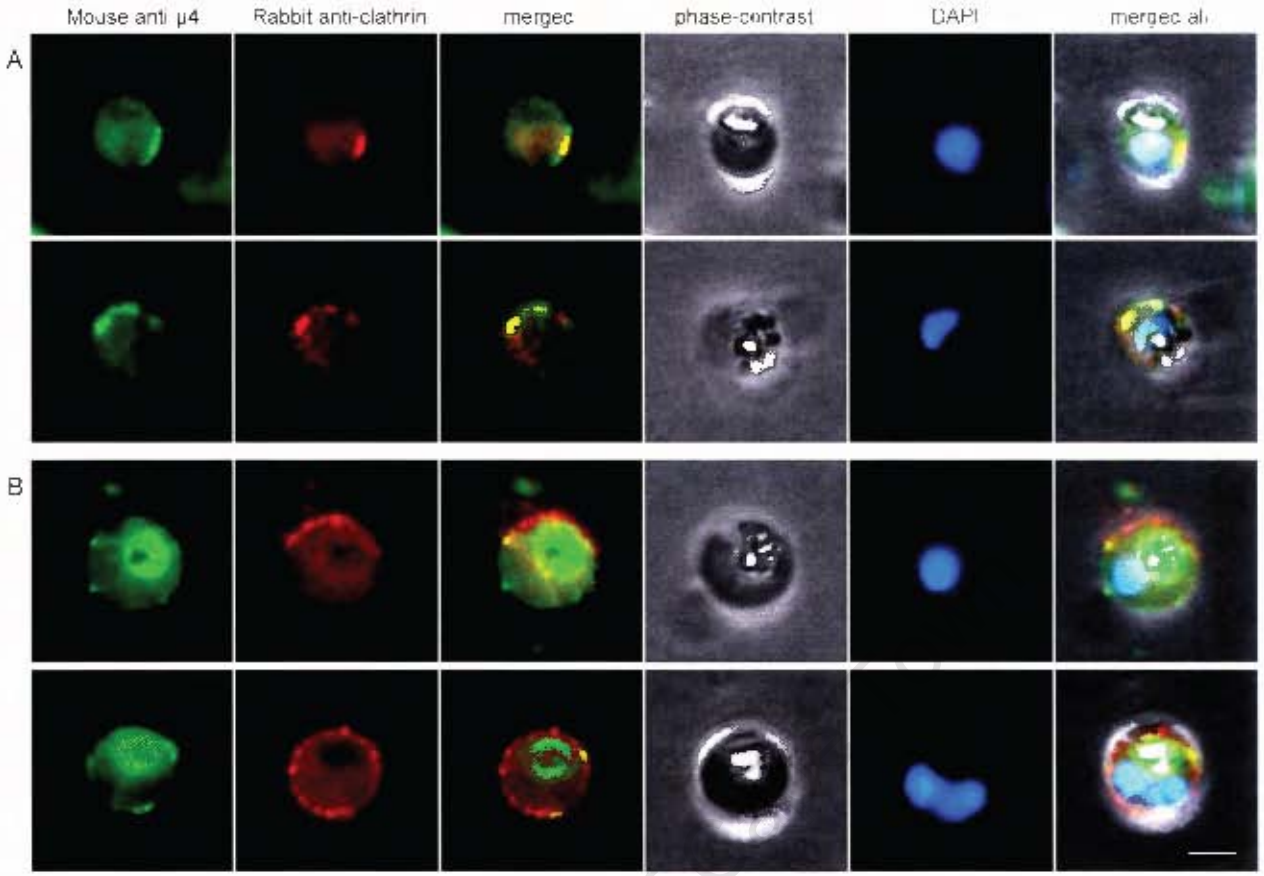

Figure 30a. Dual labelling in *P. falciparum* trophozoites with anti-μ4 and anti-clathrin. Alexa Fluor® 488-conjugated anti-mouse antibodies (green) and TRITC-conjugated anti-rabbit antibodies (red) were used to detect anti-μ4 and anti-clathrin, respectively. Areas of overlap (merged image), are display as yellow. Phase-contrast and DAPI staining show the position of the digestive vacuole and nuclei, respectively. (A) Co-localization of μ4 and clathrin is seen at the plasma membrane. (B) The digestive vacuole is labelled by μ4, but not by anti-clathrin. Bar, 2 μm.

Controls were performed by the same method discussed previously. In the first instance (Fig. 30b A), the rabbit anti-clathrin antibody was left out of the protocol, and in the second instance (Fig. 30b B), the anti-μ4 antibody was omitted. No fluorescence was detected in either case when probing with the respective secondary antibody, confirming species specific recognition of the primary antibodies by the secondary antibodies.

The ribbon-like structure to which μ1 localizes (Fig. 23a A), as opposed to the peripheral localization of μ4 and clathrin, suggests that μ1 is not associated with clathrin. IFA co-localization was performed to explore this (Fig. 31). As expected, no co-localization was observed between μ1 and the clathrin heavy chain.

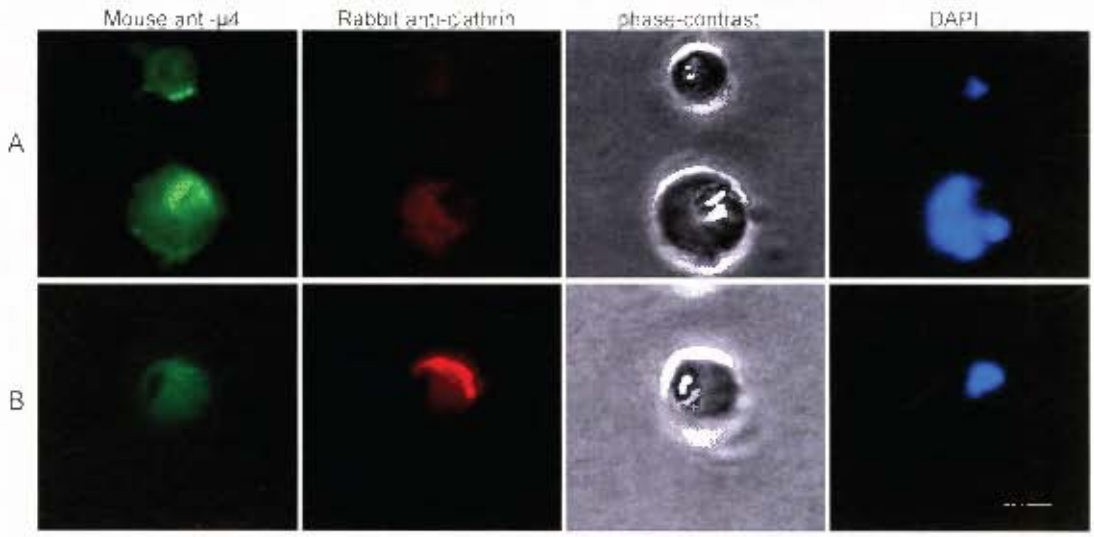

Figure 30b. Dual labelling controls for μ4 and clathrin.

Two different controls were performed. (A) illustrates the control where the anti-clathrin antibody was excluded. The first panel shows μ4 recognized by Alexa Fluor® 488-conjugated secondary antibodies (green). The second panel shows no distinct localization when incubated with TRITC-conjugated secondary antibodies (red). The digestive vacuole and nuclei are shown in the phase-contrast and DAPI-staining (third and fourth panels) respectively. (B) depicts the control where the anti-μ4 antibody was omitted. The first panel shows no localization when probed with the secondary antibodies. This confirms specificity between the corresponding primary and secondary antibodies. Bar, 2 μm.

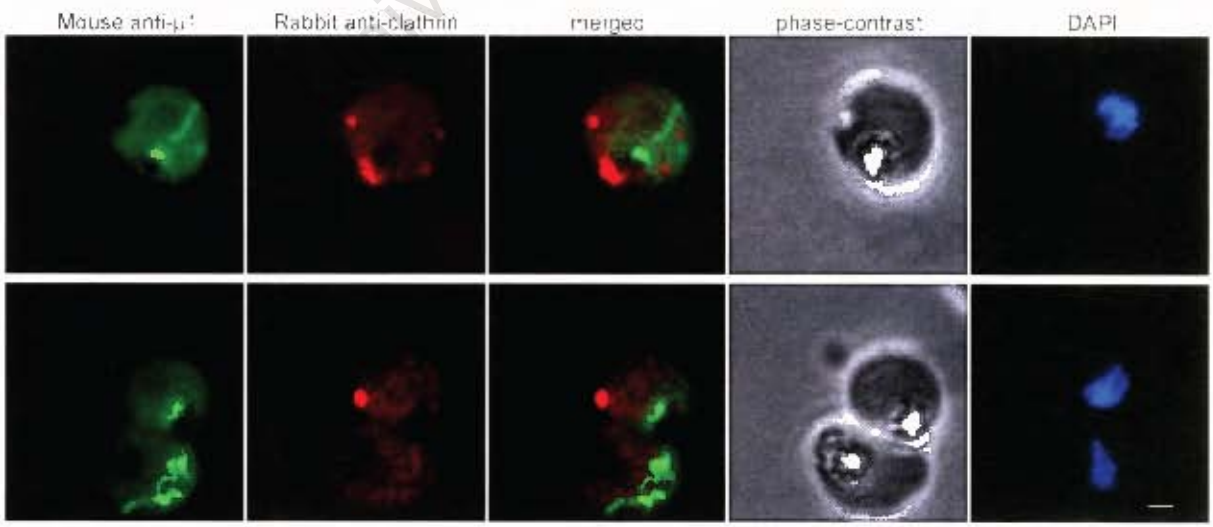

Figure 31. Dual labelling of μ1 and clathrin in *P. falciparum* trophozoites. The secondary antibody used for μ1 is Alexa Fluor® 488-conjugated anti-mouse (green) and for clathrin is TRITC-conjugated anti-rabbit (red). Bar, 1 μm.

2.2.8.5. Dual labelling of μ2 and the mitochondrion

Fluorescence images of mitochondria in trophozoite stage parasites reported by other research groups (Biagini *et al.*, 2006, del Pilar Crespo *et al.*, 2008) show a similar localization pattern to that obtained by the μ1 and μ2 antisera, suggesting the adaptins may be found at the mitochondria. To investigate this, dual localization using anti-μ2 and MitoTracker, a mitochondrion-selective stain, was performed (Fig. 32). μ2 fluorescence was not co-localized with MitoTracker.

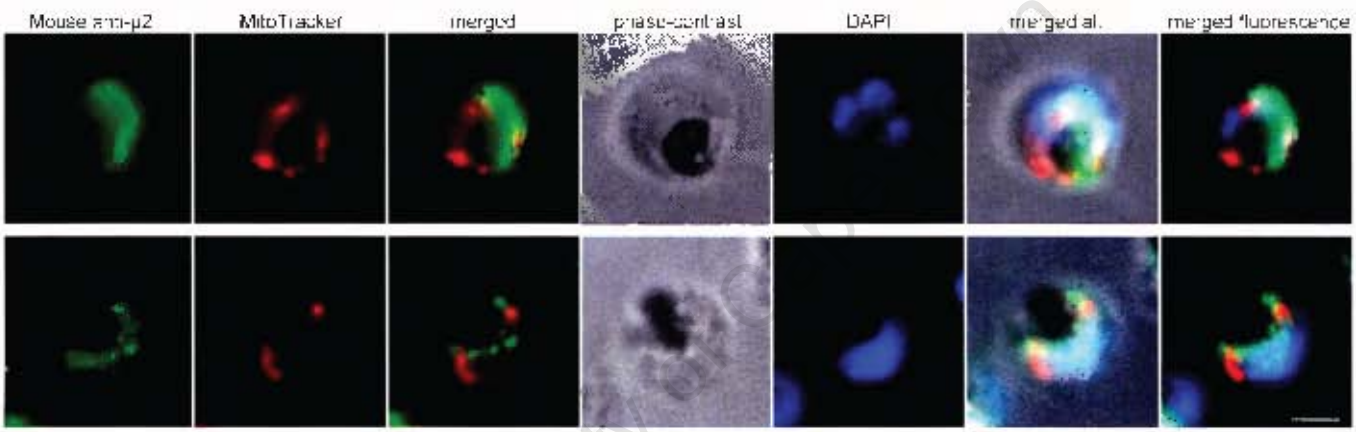

Figure 32. Dual labelling of μ2 and the mitochondrion in *P. falciparum* trophozoites. Live parasites where incubated with MitoTracker® Red CMXRos, a stain that labels the mitochondrion, fixed and labelled with anti-μ2. The secondary antibody used for μ2 is Alexa Fluor® 488-conjugated anti-mouse (green). The TRITC channel corresponds to MitoTracker. Bar, 1 μm.

2.2.8.6. Dual labelling of μ2 and the endoplasmic reticulum

To investigate whether μ2 (and by inference μ1) localizes to the endoplasmic reticulum (ER), dual localization experiments were performed with the ER marker, *Pf*Bip (gift from Dr Tim Gilberger) (Fig. 33a). *Pf*Bip is a chaperone protein reported to reside in the lumen of the plasmodial ER. As reported in the literature, *Pf*Bip labels a perinuclear ring. No co-localization was seen with the μ2 antisera and *Pf*Bip. Controls were performed by the same method discussed previously (Fig. 33b).

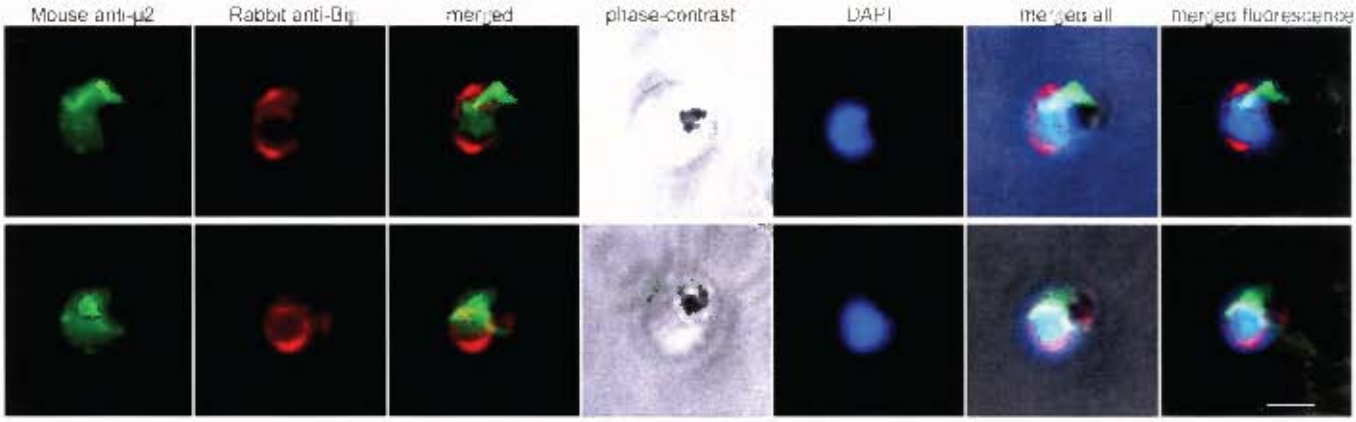

Figure 33a. Dual labelling of μ2 and the endoplasmic reticulum in *P. falciparum* trophozoites. Alexa Fluor® 488-conjugated anti-mouse antibodies (green) and TRITC-conjugated anti-rabbit antibodies (red) were used to detect anti-μ2 and anti-Bip, respectively. DAPI staining shows the position of the nuclei, respectively. Bar, 2 μm.

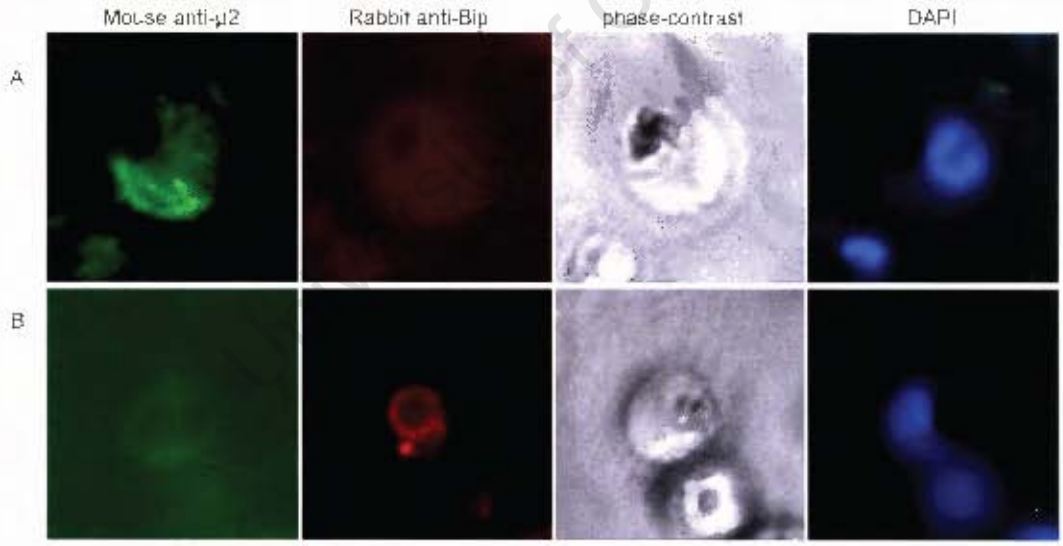

Figure 33b. Dual labelling controls for μ2 and Bip.

Two different controls were performed. (A) anti-Bip antibody was excluded, and (B) the anti-μ4 antibody was omitted. In panel (A), the first frame shows μ2 recognized by Alexa Fluor® 488-conjugated secondary antibodies (green) and the second panel shows no distinct localization when incubated with TRITC-conjugated secondary antibodies (red). In panel (B), the first panel shows no localization when probed with the secondary antibodies and the second frame shows Bip localization. This confirms specificity between the corresponding primary and secondary antibodies. Bar, 1 μm.

2.2.9. Immuno-electron microscopy (EM)

To further refine μ-adaptin localization in *P. falciparum*, trophozoite stage parasites where examined by immuno-electron microscopy using the μ1, μ2 and μ4 antisera. Labelling by μ2 was not convincing and is not included. Ultra-thin sections of *P. falciparum* parasites were immobilized on nickel grids and initially labelled with the relevant antisera, followed sequentially by rabbit anti-mouse antiserum and gold-conjugated goat anti-rabbit antiserum. Bound antibodies were fixed with glutaraldehyde and sections contrasted by incubation in uranyl acetate and lead acetate.

Although the parasite's morphology has not been entirely defined, the parasite nucleus, digestive vacuole (easily recognized due to the presence of haemozoin crystals) and plasma membrane are relatively easy to identify in the EM images. These organelles were used for morphological comparison to identify the structures occupied by the proteins.

Positive controls were performed on parasites using mouse antisera to GST-plasmepsin II (prepared by B. Weber) which localizes primarily to the digestive vacuole (Fig. 34). Plasmepsin II is a protease found in the digestive vacuole which initiates the degradative process of haemoglobin (Francis *et al.*, 1997).

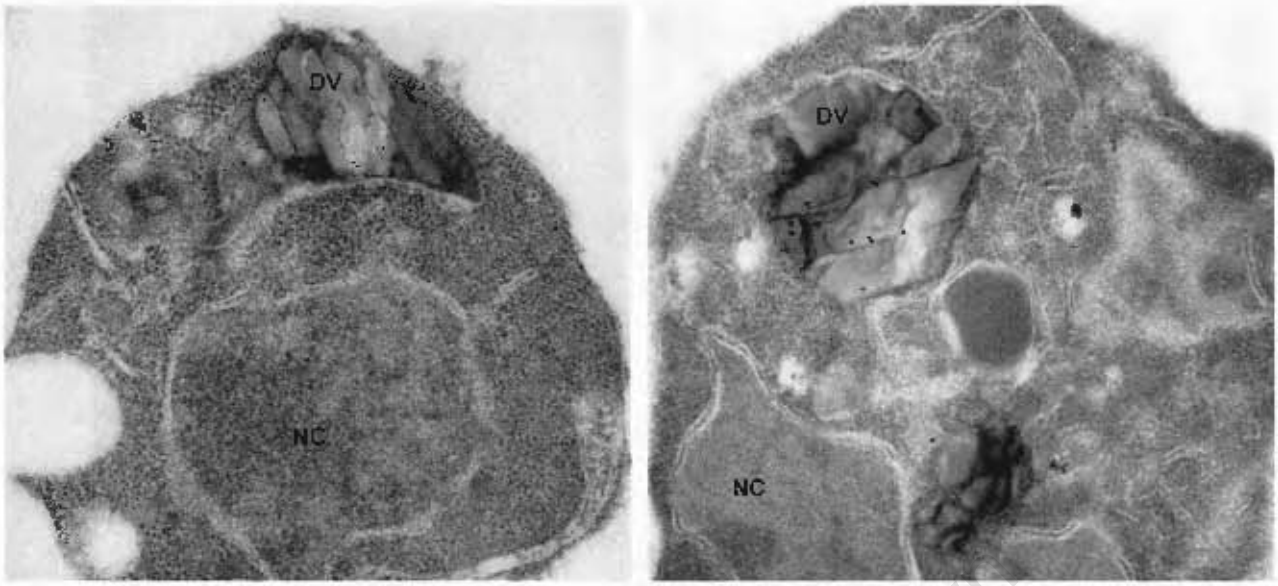

Figure 34. Transmission electron micrographs of a cross section of trophozoite stage parasites with anti-plasmepsin. Labelled structures are the parasite nucleus (NC) and digestive vacuole (DV). The gold particles, viewed as black dots, are localized to the digestive vacuole.

Anti-μ1 seems to localize to a distinct structure or structures within the cytosol (Fig. 35). This corroborates the findings of IFA. Defining the exact sites of localization is difficult due to the lack of information regarding the organization and repertoire of parasite organelles. However, the images are suggestive of extended tubulovesicular structures typically associated with secretory organelles. By contrast, and in agreement with the IFA images, the μ4 adaptin localizes to regions along the plasma membrane, as well as along the edge of the digestive vacuole (Fig. 36).

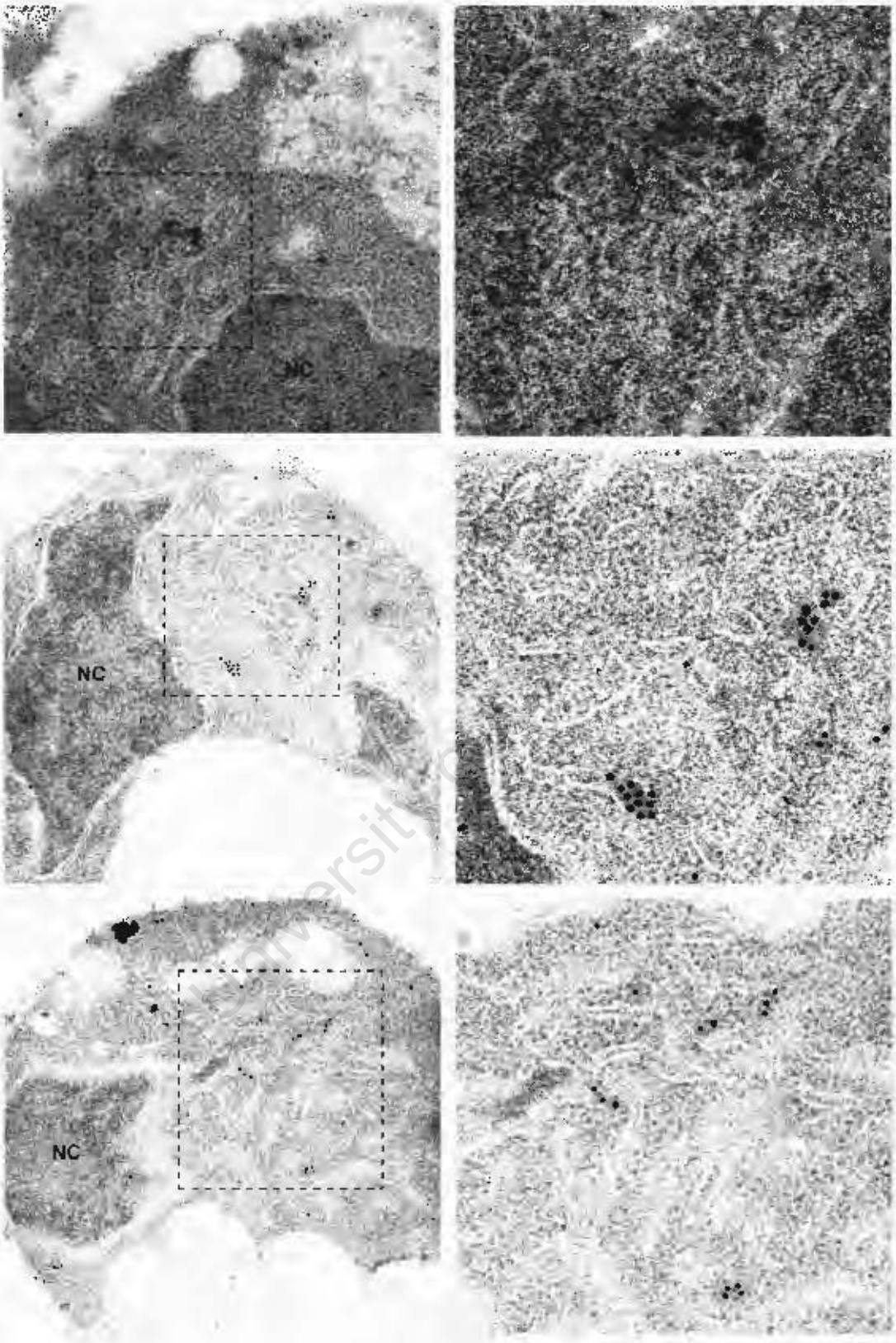

Figure 35. Immuno-EM localization of μ1.

The labelled structures, seen by dense accumulation of the gold particles, have been enlarged (boxed area). The second panels depict the region magnified.

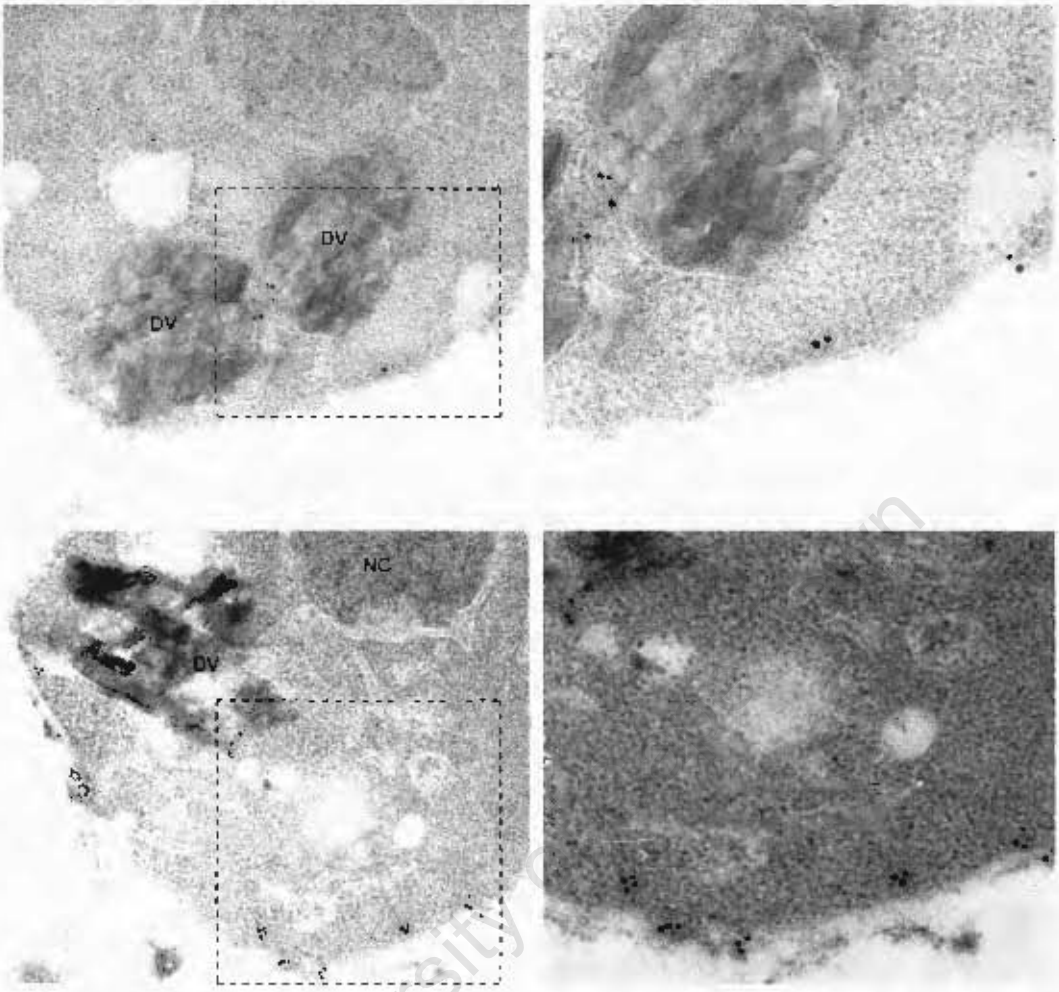

Figure 36. Immuno-EM localization of μ4.

The gold particles, representing μ4 localization, localize to sites at the parasite plasma membrane, as well as to the digestive vacuole (DV). Magnification of the region of gold accumulation is depicted in the right-hand panels.

2.3 Discussion

The identification and characterization of the μ-chain adaptin gene homologues of *Plasmodium falciparum* is valuable for investigating the components and organization of the parasite's trafficking pathways, given the central role they play in selecting cargo in mammalian cell types (Hirst and Robinson, 1998). The selection of these proteins was motivated by their close sequence homology to the mammalian adaptin counterparts known to be involved in endocytosis and secretion. DNA sequences were amplified by RT-PCR from purified parasite RNA as some genes were predicted to contain introns, as well as to provide confirmation of expression in blood-stage parasites.

The expression of malaria genes in heterologous systems is a pre-requisite for the production of recombinant antigens and the generation of antibodies. Expression in *E. coli* is notoriously difficult due to the unusual AT-rich codon preference of malaria sequences (Sayers *et al.*, 1995). It has been shown that certain amino acids such as arginine, glycine and isoleucine, which are more commonly found in *P. falciparum*, are less frequently used by *E. coli* (Baca and Hol, 2000). For instance, the presence of AGA and AGG codons (arginine residues) in the open reading frame seems to slow gene translation relative to genes that contain the CGU codon (Sayers *et al.*, 1995). Serendipitously, it was found that a GST N-terminal fusion greatly improved expression levels of *P. falciparum* sequences, for example μ1, clathrin and dynamin (H. Hoppe, personal communication), a phenomenon also noted by others (Esposito and Chatterjee, 2006). In addition, expression was achieved for μ2 and μ4 by amplifying them as truncated sequences to reduce the number of certain codons and improve primer design, bearing in mind that antiserum production does not require preparation of a full-length functional protein.

Sufficient expression was obtained for the adaptins, as judged by Coomassie stained SDS-PAGE. The molecular weight estimated from the gel for GST-μ1, when compared to the molecular weight marker, is approximately 72 kDa. The predicted size based on the amino acid composition of GST and μ1 is in the region of 76 kDa. This small discrepancy in size is also apparent for GST-μ2 and GST-μ4, although to varying degrees. The estimated size on the gel for GST-μ2 is 63 kDa compared to the predicted size of 65 kDa, and GST-μ4 is 50 kDa compared to 58 kDa. The diminished size of the

expressed proteins may be due to the fact that certain proteins migrate aberrantly in SDS-PAGE gels. This abnormal migration is usually a consequence of a high proportion of basic or charged amino acids associated with atypical binding of SDS (Takano *et al.*, 1988, Cooke *et al.*, 2004). An additional likely explanation may be the well-known tendency of *E. coli* to prematurely terminate translation of proteins from plasmodial sequences, due to codon incompatibilities (Flick *et al.*, 2004).

The expressed proteins were present in *E. coli* as insoluble aggregates, or inclusion bodies. This is a very common phenomenon in expressing malaria genes in *E. coli* (Yadava and Ockenhouse, 2003). For antibody production, it may be advantageous since aggregated or denatured proteins often improve immune presentation and antibody titres. A potential disadvantage though, is that the predominant antibodies in the antisera may recognize linear epitopes that are not exposed in the native, folded proteins. Inclusion bodies may also simplify purification since the major protein in the aggregates often consists of the expressed recombinant protein. Nonetheless, the contaminating bacterial proteins needed to be removed before immunization. The Triton-insoluble pellets were partially solubilized in sarkosyl, an ionic detergent, and then purified by two different methods; electro-elution from SDS-PAGE gel slices or affinity chromatography on glutathione columns. For affinity chromatography, the soluble lysates were diluted in PBS prior to their addition to the glutathione-agarose columns to allow for protein refolding. Refolding is essential as GST loses its ability to bind glutathione resin when denatured. Although a refolding protocol was attempted, yields from affinity chromatography were generally lower than that obtained from electro-elution.

Following purification, mice were used to raise antibodies to the specific recombinant proteins since rabbits were generally found to generate sera that cross reacted strongly with some malaria proteins in Western blotting assays (H. Hoppe, personal communication). Initial mouse bleeds for μ2 and μ4 were tested for immune response by ELISA to determine if the immunization protocol was effective. The antibody titre curves generated indicated that a strong immune response was obtained for both sera. This encouraged us to proceed directly to Western blotting for subsequent characterization of the μ2 and μ4, as well as the μ1 antisera.

Western blotting against *P. falciparum* proteins revealed that the antisera strongly recognized specific parasite proteins, which supported the RT-PCR conclusion that all the μ-chain adaptins are expressed in blood-stage parasites. However, there were some inconsistencies in the sizes of the recognized parasite proteins. The genome sequence predicted a molecular weight for μ1 of 50.8 kDa which was significantly lower than the value estimated from the western blot (70 kDa). This large discrepancy in size was also apparent for μ4 where the protein recognized by the antisera also had a molecular weight of 70 kDa, considerably larger than the value calculated from the genome database (M_r 51137). There could be several explanations for the size discrepancies which are covered in the latter half of this discussion. A discrepancy in size was also observed for the μ2 adaptin; however the size predicted (M_r 72902) is about 10 kDa larger than what is observe on the blot (63kDa). Western blot analysis of parasite extracts at different parasite stages revealed that the μ-chains were expressed in the trophozoite and schizont stages. Limited or no expression was detected in the lysates of ring stage parasites, suggesting that the μ-chain genes are only expressed in the later stages when haemoglobin digestion is at a maximum.

An Immunofluorescence microscopy approach was employed to determine the subcellular localization of the μ-adaptins. The IFA data suggests digestive vacuole and plasma membrane localization for the μ4 adaptin, which raises the possibility that μ4 may mediate endocytosis and trafficking in the endocytic pathway. Localization appears to vary between the digestive vacuole and plasma membrane, and in many individual parasites no distinct localization was found besides a general cytoplasmic fluorescence. The reason for this could be that recruitment of adaptins to membranes is transient, with the μ4 protein being predominantly present in a diffuse cytoplasmic pool. In eukaryotic cells, some known coat proteins are peripherally and transiently associated with membranes (Lewin and Mellman, 1998). Localization at the digestive vacuole was prominent throughout the trophozoite and schizont stages, whereas no μ4 was present in ring stage parasites as established previously with Western blot analysis.

By contrast, μ1 and μ2 localize to intracellular sites that suggest alternative or additional roles. This is not surprising given the fact that typical endocytosis homologues have been found to have variant functions, such as secretion and cytokinesis, in other cell types. In mammalian cells, the μ2 adaptin forms part of the AP-2 adaptor complex required for

endocytosis, whereas AP-1, AP-3 and AP-4 play a role in secretion from the *trans*-Golgi network to endosomes and lysosome-like organelles (Robinson and Bonifacino, 2001). The elongated ribbon pattern seen with μ2 is maintained throughout the mature stages of the intraerythrocytic life cycle.

Based on the localization data, and by analogy to mammalian systems, it therefore appears that *P. falciparum* μ4 forms part of a parasite adaptor complex that, like AP-2, mediates endocytosis. This hypothesis is significantly strengthened by the co-localization of μ4 with the *P. falciparum* clathrin heavy chain, as judged by IFA. In mammalian cells, AP-2 recruits clathrin to the plasma membrane to initiate endocytosis (Boehm and Bonifacino, 2001). It further suggests that the molecular mechanisms of endocytosis in the parasite may be related to clathrin-dependent endocytosis of higher cells. There is currently no experimental evidence that comprehensively describes trafficking of haemoglobin along the endocytic pathway in the parasite and its overall organisation. Therefore, a practical initial working hypothesis would be that it conforms to the organization of a basic endocytic pathway in eukaryotic cells where endocytic vesicles containing haemoglobin pinch off from the parasite plasma membrane and are trafficked to the digestive vacuole where they fuse and deliver haemoglobin for digestion (Klemba *et al.*, 2004, Smythe *et al.*, 2008). By the same rationale, although there is no evidence for a retrieval pathway as demonstrated in mammalian cells, given the proclivity of recycling of endocytosed components in eukaryotes, arguably there is a pathway to recycle membrane components back to the plasma membrane from the digestive vacuole. This could be the explanation for the presence of μ4 at the digestive vacuole, admittedly in the absence of direct experimental evidence for such a pathway.

The digestive vacuole, where haemoglobin degradation takes place, is the parasite equivalent of a lysosome (Rosenthal *et al.*, 1988, Reeves *et al.*, 2006). In mammalian cells, AP-1, AP-2 and AP-3 have been shown to localize to endosomes and lysosomes (Theos *et al.*, 2005). For example, AP-1 and AP-2 are involved in the trafficking of the major histocompatibility complex type II (MHC-II), found on the surface of antigen-presenting cells, to lysosome for degradation (McCormick *et al.*, 2005). In addition, AP-2 and AP-3 have significant roles in the delivery of lysosome-associated membrane proteins (Lamps), glycosylated transmembrane proteins present in lysosome membranes, to late endosomes and lysosomes (Janvier and Bonifacino, 2005). It has been shown that

certain adaptor complexes also play a role in recycling. AP-1, in association with clathrin, is involved in the basolateral recycling of transferrin receptors from endosomes to the plasma membrane (Pagano *et al.*, 2004), whereas AP-2 binds synaptotagmin 1 receptor for clathrin-mediated recycling of synaptic vesicle membranes (Lewin and Mellman, 1998).

Additional assays to further explore the hypothesis that *P. falciparum* μ4 forms part of a parasite adaptor complex that, like AP-2, mediates endocytosis, would include knockdown (silencing) experiments. A disruption or deviation in the localization of haemoglobin digesting proteases, plasmepsin I and II, could be assessed in parasites where μ4 has been silenced by an RNA interference (RNAi) approach. This would indicate whether μ4 is involved in endocytosis since transmembrane precursors of these proteases are thought to reach the digestive vacuole via the plasma membrane by endocytosis. Similarly, the effect of μ4 knockdown on the relative quantity of the plasmepsin precursor, proplasmepsin, and mature plasmepsin by quantitive Western blotting assays would indicate the involvement of μ4 in endocytosis since maturation of the enzyme relies on transport to the digestive vacuole (Francis *et al.*, 1997). In addition, quantitative assays for endocytosis could be carried out by determining the effect μ4 knockdown would have on haemoglobin levels in the parasite by means of Western blot, quantitating immunofluorescence intensity in the digestive vacuole using anti-haemoglobin antibodies, and counting haemoglobin transport vesicles by immuno-electron microscopy or IFA (Roberts *et al.*, 2008).

In *Toxoplasma gondii* a mutational strategy and an RNAi strategy (antisense mRNA) was undertaken to implicate AP-1 (and adaptin μ1 chain) in the process of delivery of rhoptry proteins from the TGN to the rhoptries. An epitope tagged version of μ1 was engineered and used to generate dominant mutants. The mutations were introduced into the predicted tyrosine-binding motif of μ1. Overexpression of these constructs resulted in the accumulation of rhoptry proteins in post-Golgi compartments. Inhibition of μ1 expression using an antisense mRNA approach generated swollen Golgi cisternae, immature rhoptries and multivesicular endosomes (Ngô *et al.*, 2003).

Given the controversy surrounding the functionality of RNAi in the parasite and the absence of machinery essential for the RNAi pathway in the genome of Plasmodium (Ullu *et al.*, 2004, Baum *et al.*, 2009), alternative methods for gene function analysis

could also be considered. These include: (i) targeted gene alterations, where exogenous DNA (a generated knockout construct) is integrated into the parasite chromosome by crossover events between homologous regions (Wu *et al.*, 1996, Krnajski *et al.*, 2002); and (ii) FKBP destabilization domain (ddFKBP) system whereby the target gene is fused to a mutant domain of the human rapamycin-binding protein FKBP12, promoting degradation of the fusion protein in a ligand dependent manner. The destabilization domain suppresses protein levels to allow function assessment (Armstrong and Goldberg, 2007).

Immunoprecipitation experiments could also clarify whether μ4 is part of an adaptor complex similar to AP-2. Binding partners may be identified by immunoprecipitation after digitonin lysis, followed by Western blotting and LC-MS/MS protein sequencing. Digitonin is a mild detergent that permeabilizes cell membranes while preserving macromolecular complexes (Silvie *et al.*, 2006). Co-precipitation with clathrin would indicate that μ4 forms part of a complex that associates with clathrin, and thus could be implicated in clathrin-mediated endocytosis given that mammalian adaptor complexes AP-1 and AP-2 bind clathrin to mediate vesicle budding (Robinson and Bonifacino, 2001). In addition, it would allow the identification of other members of the μ4-containing adaptor complex, as well as co-regulatory proteins.

The μ1 and μ2 adaptins seem to localize primarily to a ribbon-like structure found within the cytosol of the parasite. A working hypothesis would be that μ1 and μ2 form part of parasite adaptor proteins that are analogous to mammalian AP-1, AP-3 and AP-4. These adaptor complexes mediate secretion from the *trans*-Golgi network in mammalian cells as opposed to endocytosis / endocytic trafficking. It may therefore be proposed that the structure recognized by the antisera represents a secretory compartment such as the Golgi, and could suggest the proteins play a role in secretion.

IFA images can be expanded by z-sectioning and deconvolution. It was anticipated that 3D reconstruction would be achieved; however, owing to *P. falciparum's* small size, image clarity was poor which made it impossible to achieve deconvolution and produce a clear 3D image. Therefore, images were merely captured at different focal plains through the parasite to more accurately depict the ribbon-like structure to which μ1 localizes.

Co-localization of μ1 and μ2 indicate that the homologues localize to similar intracellular sites, but that these sites do not always overlap completely. This suggests that the two adaptins have similar roles and perhaps additional complementary roles. For instance, in addition to being associated with transport structures from the *trans*-Golgi network to endosomes, and endosomes to the *trans*-Golgi network in mammalian cells, AP-1 has been implicated in the transport of transferrin receptors from apical to basolateral membranes in epithelial cells, as well as transport from the TGN to basolateral membranes, demonstrating that AP-1 functions at more than one location (Crottet *et al.*, 2002, Lefkir *et al.*, 2003).

In contrast to μ4, there was no overlap of μ1 localization with clathrin. In mammalian cells, AP-1 associates with clathrin to mediate secretion at the *trans*-Golgi network. However, AP-4, and in some cases AP-3, form part of non-clathrin coats. It is therefore likely that parasite adaptor complexes that contain μ1 and μ2 are analogous to mammalian AP-3 and AP-4, and mediate secretion by clathrin-independent vesicular budding mechanisms.

Co-localization experiments, using known markers of intracellular parasite organelles, may help determine the compartments to which the proteins localize. ERD2 is a Golgi marker protein that is concentrated in the *cis*-Golgi in mammalian systems, and in *P. falciparum*, the *Pf*ERD2 homologue has been shown to localize to the perinuclear region (Elmendorf and Haldar, 1993). For this reason, the μ1 antiserum was sent to Dr Tim Gilberger's laboratory and dual localization experiments with ERD2-GFP expressing parasites were carried out by Dr Nicole Struck (See Appendix A-4). Her findings show that *Pf*ERD2 and μ1 localization are distinct from each other, with some overlap seen in one instance. This suggests that μ1 does not localize to the *cis*-Golgi element of *P. falciparum*, but possibly to distal Golgi membranes. Dual localization of GFP fused to μ1 and anti-GRASP has recently been accomplished, confirming a Golgi localization for μ1 (Dr Tim Gilberger, Personal communication).

In higher eukaryotic cells, the Rab6 gene product is localized to the *medial* and *trans*-Golgi cisternae, and *trans*-Golgi network, but not to the *cis*-Golgi. A Rab6 homologue has been identified in the parasite and is a marker of the parasite *medial* and *trans*-Golgi (van Wye *et al.*, 1996). It was shown that the dispersed localization of Rab6 in the

parasite is distinct from that of ERD2. Rab6 could thus be used as a potential marker to address whether μ1 localized to a parasite equivalent of a *medial* or *trans*-Golgi. The cloning, expression and immunization of Rab6, as well as co-localization studies with μ1, are detailed in Chapter 4. Briefly, the co-localization studies show that μ1 localizes to sites similar to Rab6. Fluorescence images of mitochondria in trophozoite stage parasites reported by Biagini and colleagues (2006, Fig. 2c, d, and e) and del Pilar Crespo and colleague (2008, Fig. 7a, c and d) show a similar morphology to the structure to which the μ1 and μ2 antisera localize, suggesting that the adaptins may be found at the mitochondria. However, dual labelling with anti-μ2 antiserum and the dye, MitoTracker® Red CMXRos, refutes this suggestion. MitoTracker® is a specific stain that accumulates in active mitochondria and is retained after aldehyde fixation. Furthermore, μ2 (and by inference μ1) fluorescence was not co-localized with *Pf*Bip, a molecular chaperone reported to reside in the lumen of the plasmodial endoplasmic reticulum.

Determining exact sites of localization of parasite proteins with the light microscope is difficult due to the small size of the parasites and resolution limits, as well as paucity of subcellular markers. It is therefore important to redefine and validate findings obtained by immunofluorescence assays with higher resolution microscopes, such as immuno-electron microscopy. Unfortunately, the poorly characterized subcellular morphology of parasites often hampers unambiguous assignment of protein location by electron microscopy as well. Nonetheless, the immuno-EM images obtained with the μ4 antiserum strongly suggests that this adaptin localizes to regions of the digestive vacuole periphery and the plasma membrane. Unlike many other organelles, the digestive vacuole is readily identifiable due to the presence of prominent haemozoin crystals within them, as also demonstrated by the positive control EM images obtained with the anti-plasmepsin II antiserum. The EM results for μ4 substantiate the IFA results obtained for this protein and, together with the clathrin IFA co-localization data, further supports the possibility that μ4 may be part of a parasite adaptor complex involved in endocytosis from the plasma membrane and trafficking at the digestive vacuole.

It could be anticipated from the ribbon-like structure seen by IFA with μ1 and μ2 antisera that EM localization could be difficult to interpret. Nonetheless, μ1 localization is very suggestive of tubulovesicular profiles typical of secretory sites, for example the *trans*-

Golgi network in higher cells. Comparisons with EM images by Witola and colleagues (Witola *et al.*, 2006) supports the theory that the structure to which μ1 localizes is the Golgi (see Appendix A-5). Immuno-EM localization of μ2 was less satisfactory with the existing antisera and accurately identifying the sites of localization was not possible. The staining intensity with the μ2 antiserum was generally weak in comparison with μ1, and suggests that the relevant μ2 epitopes recognized by the antiserum do not survive the EM sample preparation conditions well.

In summary, mouse antisera raised against gel-purified recombinant GST-μ-chain fusion proteins strongly recognize single parasite proteins by Western blotting. IFA and immuno-EM localization suggests that, in common with the known functions of adaptor proteins in mammalian cells, parasite μ1 and μ2 are associated with a late secretory compartment, whilst μ4 is found at the plasma membrane and digestive vacuole, suggestive of a role in endocytosis. The μ1 antiserum cross-reacts with a 45-kDa protein in COS-1 cells which corresponds to the size of mammalian μ1. Recognition of the endogenous μ1 in this monkey kidney fibroblast cell line is not unexpected, given the extensive sequence homology between the predicted plasmodial protein and its human counterpart (60% amino acid identity). Puzzlingly, the apparent size of the parasite μ1 counterpart in the Western blots is approximately 20 kDa larger than predicted by the annotated gene sequence (PF13_0062). Although μ4 has a different intracellular distribution and presumably forms part of a separate adaptor complex, it displays an increase in apparent size by the same 20 kDa margin, suggesting a common origin for the size increase for both parasite μ-chain homologues. The specificity of the μ1 antiserum was explored by an antigen competition Western blot assay in which pre-incubation of the antiserum with purified recombinant GST-μ1 strongly reduced recognition of the single 70 kDa parasite protein on the blots, suggesting that the protein is recognized by antibodies raised to the immunogen. More importantly, rabbit antiserum raised to a predicted peptide epitope of the μ1 sequence also strongly recognized a 70 kDa parasite protein and co-localized with the mouse antiserum by IFA. In an attempt to specifically silence μ1 expression by an RNAi approach, parasites were incubated with double-stranded RNA corresponding to the μ1 coding sequence, which led to a 30% decrease in the intensity of the 70 kDa band recognized by the μ1 antisera by Western blotting. However, the results could not be reproduced with additional controls. The RNAi experiments are detailed in the Appendix (A-6).

Aberrant migration on SDS-PAGE gels is a potential source of discrepancies between apparent and predicted protein molecular weights (Hawthorne *et al.*, 2004). However, it seems unlikely that μ1 and μ4, which differ extensively in amino acid sequence (31 % amino acid identity), would migrate abnormally to the same extent. This may however, be the reason for the reduced size of plasmodial μ2. Post-translational modification may also account for increased apparent protein size of μ1 and μ4 on SDS-PAGE gels, but has not been reported for μ-chain adaptins in other cell types and is unlikely to result in such a large shift in mobility, except for extensive glycosylation, which is limited to secretory proteins and is not found in malaria parasites. A further possibility is that the annotation of the two genes (μ1 and μ4) in the PlasmoDB database is incorrect and that the actual mRNA open reading frames are longer. However, the likelihood of such a misinterpretation for both μ-chains is small, and further minimized by the extensive homology of the μ-chains to their mammalian counterparts (especially μ1) and the absence of open reading frames in the respective upstream intergenic regions large enough to account for the 20 kDa increase in size. An attempt was made to explore the μ1 mRNA open reading frame experimentally by RACE PCR. 3' RACE of the μ1 mRNA confirmed the presence of the stop codon in the expected position and the absence of coding sequence between the stop codon and poly-A tail to account for the increased size. Despite several attempts, 5' RACE was unsuccessful. A description of the RACE experiments is detailed in the Appendix (A-7).

Alternatively, the increased apparent size of μ1 and μ4 may be caused by their association with similar, smaller protein partners in complexes that fail to dissociate under denaturing SDS-PAGE conditions, considering the fact that μ-chains form part of larger heterotetrameric adaptor complexes in other cell types. Predicted homologues of the two larger components of mammalian adaptor complexes (the α- and β-chains) are present in the parasite genome, as are four parasite homologues of the smaller σ-chains. The latter adaptor components have sizes of approximately 20 kDa. Tight, SDS-PAGE-resistant binding of parasite μ1 and μ4 to the respective σ-chain components of the adaptor complexes may be able to account for their increased apparent sizes. This postulate is explored in the following experimental chapter.

An additional explanation for the reduced size of the μ2 adaptin could be due to early termination of protein translation in the particular *P. falciparum* strain used, that being D10. It has been established that *P. falciparum* strains differ in certain phenotypes. An example of this phenomenon is shown with *P. falciparum* normocyte binding protein 1 (*Pf*NBP1), a protein expressed at the apical end of merozoites to facilitate invasion of erythrocytes by binding the trypsin-resistant invasion receptor, Receptor Y. Two *P. falciparum* strains, 3D7 and 7G8, express truncated *Pf*NBP1 proteins. The lack of certain domains however, does not affect expression or correct localization of the protein (Rayner *et al.*, 2001). Further work on other strains such as K1, HB3, W2 and 7G8 would need to be carried out to ascertain whether this could be the cause of the diminished size of μ2. Thus far, the reduced size was also seen on Western blots loaded with 3D7 strain parasite. Alternatively, the reduced apparent size of μ2 may be caused by post-translational proteolytic cleavage of the protein, generating the 63 kDa protein as well as a smaller protein. A faint lower molecular weight protein can be seen on the gel (Fig. 19b). The combined size of these proteins exceeds the size predicted by the μ2 gene sequence. However, since the apparent size of both μ1 and μ4 in the Western blot are approximately 20 kDa larger than predicted, it is possible that μ2 may also be larger. Post-translational proteolytic cleavage has been reported to account for the size difference of other *P. falciparum* proteins. For example, *Pf*RPA1, the parasite homologue of the eukaryotic replication protein A (RPA) essential for DNA metabolism, and *Pf*CDS, a protein involved in phospholipid synthesis, are both smaller than their orthologues in higher eukaryotes as a result of proteolytic processing due to presence of several Asn-rich stretches in their gene sequences (Martin *et al.*, 2000, Voss *et al.*, 2002). Asn-rich stretches are present in the μ2 sequence; however, additional work is required to determine if μ2 undergoes post-translational processing.

CHAPTER 3 – Identification and Characterization of Adaptor Protein σ-chain Homologues

3.1. Introduction

The adaptin subunits of the AP complexes are directly associated with each other and require powerful denaturing conditions for their dissociation. In mammalian cells the two large adaptins interact with each other, the divergent subunit (γ/ α/ δ/ ε) interacts with the small chain (σ1-4 respectively) and the β subunit interacts with the μ-chain (Robinson and Bonifacino, 2001, Page and Robinson, 1995). An interaction between the medium and small chains has not been reported conclusively, but immunoprecipitation studies suggest that there is likely an interaction between them (Page and Robinson, 1995). Each adaptin performs a different function (Kirchhausen *et al.*, 1999).

Transmembrane proteins generally contain two types of sorting signals in their cytosolic tails; tyrosine-base motifs and dileucine-based motifs. The μ-chain adaptin has been shown to interact with tyrosine-containing motifs, while it is thought the recognition site for dileucine motifs is on the β-chain (Haft *et al.*, 1998, Rapoport *et al.*, 1998). The exact role of the σ-adaptin has yet to be determined, although it has been suggested that the adaptin may facilitate recruitment of the complex to the correct membrane and may interact with the divergent adaptin to stabilize the complex which is fundamental to AP function (Boehm and Bonifacino, 2001, Aguilar *et al.*, 2001). It has also been proposed that the σ subunit may be implicated in the recognition of dileucine-based sorting signals (Janvier *et al.*, 2003).

As discussed in Chapter 2, the μ1 and μ4 adaptin antisera recognize parasite proteins with an apparent molecular weight approximately 20 to 25 kDa larger than the size calculated from the predicted gene sequence. Of the several possible explanations for this, one

possibility is that the μ-chains bind to a smaller molecular weight partner, and that this complex does not dissociate under standard SDS-PAGE conditions. The fact that the μ-chains form part of adaptor protein complexes in other cell types and that the σ-chain adaptins of these complexes have a molecular weight of 20 to 25 kDa (Hirst and Robinson, 1998), supports this possibility. To explore this hypothesis, a characterization of *P. falciparum* σ-chain adaptins was undertaken. Homologues of human σ1 and σ4 adaptins were identified by BLAST searches of the *P. falciparum* genome. Expression of these genes in parasite blood stages was confirmed by RT-PCR, and fragments of the coding sequences cloned, expressed and purified from *E. coli*, then used to immunize mice to produce antisera for immunochemical characterization purposes. Disappointing results by this approach prompted the preparation of rabbit antisera to synthetic peptides derived from the σ1 and σ4 sequences.

3.2. Results

3.2.1. Identification of predicted *P. falciparum* homologues of human σ-chain adaptins

Consultation of sequence data contained in the PlasmoDB database (http://www.plasmodb.org) revealed the gene sequences for *P. falciparum* σ1 and σ4 homologues, designated PF11_0187 and PFD1090c respectively. The selection of these genes was motivated by the close homology of their predicted amino acid sequence to their counterparts, *Homo sapiens* σ1 and σ4 (accession numbers P61966 and Q9BVE7 respectively). Sequence alignment by DNAMAN© (Fig. 37) revealed significant sequence similarities of parasite σ-chains (σ1 and σ4 respectively) to human AP-1 complex subunit σ1 (54 % identity and 78 % positives over a 155 amino acid sequence) and human AP-4 subunit σ4 (47 % identity and 69 % positives over a 145 amino acid sequence).

```
σ1

1     MMRFMLLFSRQGKLRLQKWYLATSDKERKKMVRELMQVVLARKPKMCSFLEWRDLKVVYK
      |: |:|| ||||| || |||:  | ||: |::||  |: | | ||:|:|:|||: |:|:|
1     MIHFVLLISRQGKTRLAKWYIPLSQKEKAKIIRETSQITLNRTPKLCNFVEWREYKLVFK

61    RYASLYFCCAIEGQDNELITLELIHRYVELLDKYFGSVCELDIIFNFEKAYFILDEFLMG
      |||||:|   |:  ||||||||:|| |||:||||||:|||||:|||| |||::||| |:
61    RYASLFFIACIDKGDNELITLEIIHHYVEILDKYFGNVCELDLIFNFHKAYYLLDEILVT

121   GDVQDTSKKSVLKAIEQADLLQEEDESPRSVLEEMGLA
      |::|::|||::|: :   | | |:::: : :   :
121   GEMQESSKKTILRIVAAQDSLMEDNKTTKKLGALI...

σ4

1     MIKFFLMVNKQGQTRLSKYYEHVDINKRTLLETEVIKSCLSRSNEQCSFIEYKDFKLIYR
      ||:| ||||||||||||:|| |: | ::|:|| |:|: |||| : ||||::|:::|:|||
1     MIEFLLMVNKQGQTRLSQYYNHLSIEEKTILEGELIRKCLSRVDYQCSFLQYREYKIIYR

61    QYAALFIVVGVNDT.ENEMAIYEFIHNFVEVLDEYFSRVSELDVSFFNTVFHSTWQMHSG
      :||:|:::|||:|   || || | ||| :|:||:|:  | |||: |   :  : : :
61    RYASLYLIVGVSDQDVNEFAILEMIHNIIEILDKYYENVCELDIMFN..IDKTHFIIDEI

120   PYQEPIDELPKICSALEPQQTCFSPDSSSFKGAASTTPIY
          | :: |   | |       |  | |
119   ICNGEICDMNKTN.VLRP...ILLMDKVSLKM........
```

Figure 37. σ-chain sequence alignments.

The alignment of human σ-chain sequences (upper sequence) with *P.falciparum* σ-chains (lower sequence) using a DNAMAN© alignment program. Identical residues are shown with a blue vertical line. Conserved amino acid substitutions are denoted by colon symbols (:) and a dot (.) represents a sequence gap, introduced for optimal alignment.

3.2.2. RNA isolation, cDNA synthesis and RT-PCR

DNA sequences encoding regions of the σ-chains were amplified by RT-PCR from purified parasite RNA and the products evaluated by gel electrophoresis against a 1 kb DNA marker on agarose gels (Fig. 38). PCR from cDNA confirms expression of the σ-adaptins during the parasite's erythrocytic stages. Trophozoite stage parasites were collected from 50 ml cultures (4 % hct and 10 to 20 % pst) and RNA isolated using a RNAgents® Total RNA Isolation System (Promega). Total RNA yield, determined spectrophotometrically at 260 ηm, was between 40 to 120 μg and the purity determined to be within the appropriate range ($A_{260}/A_{280} \sim 1.9$).

Gene specific primers, containing BamH1 and Xho1 restriction sites in the forward and reverse primers respectively, were designed to amplify truncated versions of the adaptins (See Chapter 6-Materials and Methods, and Appendix A-1). To obtain the best possible priming site, the forward primer in each instance was designed to anneal to a portion of the gene slightly downstream from the start codon, but in-frame with the codon reading frame from the pGEX-4T-1 expression vector, where the presence of the GST fusion partner provides the initiation signal. Expected sizes of the amplification products are shown in Table 3. DNA products were purified by excising the band from the gel and extracting the DNA to remove any residual primers, nucleotide bases or non-specific PCR products.

Size (bp)	
σ1	σ4
387	408

Table 3. Expected sizes of PCR products.

Predicted sizes of σ-chain PCR products determined from the gene sequences contained in PlasmoDB (PF11_0187 and PFD1090c).

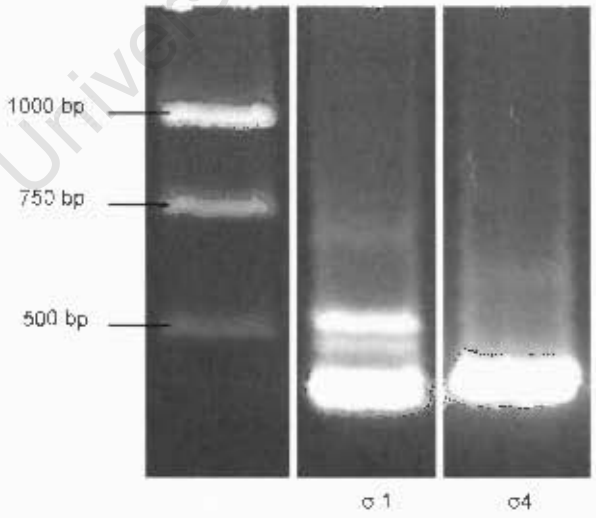

Figure 38. RT-PCR products.

Agarose gel electrophoresis (1 % gel) showing amplified gene products from cDNA along side a 1 kb DNA ladder (Lane 1). Lane 2 contains the σ1 gene product (387 bp) and Lane 3, σ4 (408 bp). The less intense, non-specific bands seen in lane 2 were removed by gel purification.

3.2.3. Cloning

Purified PCR products were ligated to the pGEM®-T Easy vector and the recombinant plasmid cloned into competent DH5alpha™ *Escherichia coli* cells. Bacteria were grown overnight in the presence of Ampicillin and blue/white selection was used to select single colonies containing the plasmid with insert DNA. Plasmids were isolated from these colonies and restriction digest with BamH1 and Xho1 restriction enzymes confirmed that the plasmids contained inserts of the expected size. Inserts were then removed from the pGEM®-T Easy vector by overnight digestion with BamH1 and Xho1, and the gel purified DNA inserts sub-cloned into the pGEX-4T-1 expression vector previously digested with BamH1 and Xho1 (See Appendix A-2). DH5alpha™ *E. coli* were transformed with the pGEX-4T-1 ligations. Plasmids purified from Ampicillin-resistant colonies were again digested with BamH1 and Xho1 to confirm the presence of the correct inserts (Fig. 39). Isolated plasmids were subsequently used to transformed BL21 Star™(DE3) *E. coli* to improve expression yields.

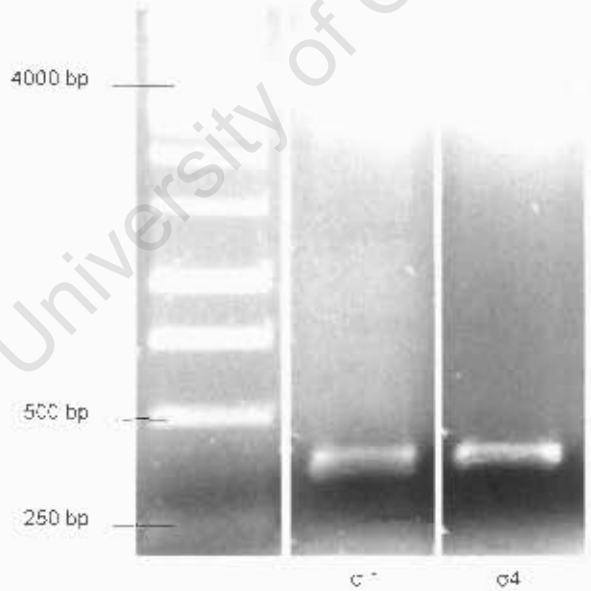

Figure 39. pGEX-4T-1 plasmid digests.

Agarose gel electrophoresis (1 % gel) showing pGEX-4T-1 plasmids digested with restriction enzymes BamH1 and Xho1. BamH1 and Xho1 restriction sites were introduced into inserts with the forward and reverse primers, respectively. Lane 1: 1 kb DNA ladder; Lane 2: σ1 DNA insert (387 bp); and Lane 3: σ4 DNA insert (408 bp). The plasmid remaining after the inserts were removed has an approximate size of 4900 bp.

3.2.4. Expression of recombinant proteins

The cloned genes were expressed as GST fusion proteins in BL21 Star™(DE3) cells to obtain recombinant protein for antibody production through immunization. The GST fusion tag improves expression and assists purification of the proteins by affinity chromatography. Expression was induced with the addition of IPTG during log-phase growth. To verify expression, *E. coli* were lysed using lysozyme / Triton lysis (Chapter 6-Materials and Methods) and the soluble and insoluble fractions were run on SDS polyacrylamide gels and stained with Coomassie. Comparison with bacteria that have not been induced with IPTG revealed a prominent new band for σ1 and σ4 in the insoluble pellet samples (Fig. 40). The molecular weights for GST-σ1 and GST-σ4 were approximately 35 kDa and 33 kDa respectively, compared to the predicted sizes of 40 kDa and 41 kDa. Truncation of heterologous proteins upon expression in *E. coli*, usually due to premature cessation of translation, is often found with non-codon optimized plasmodial sequences (see also the GST-μ-chain expressed proteins, Chapter 2, section 2.2.5) (Flick *et al.*, 2004, Zhou *et al.*, 2004).

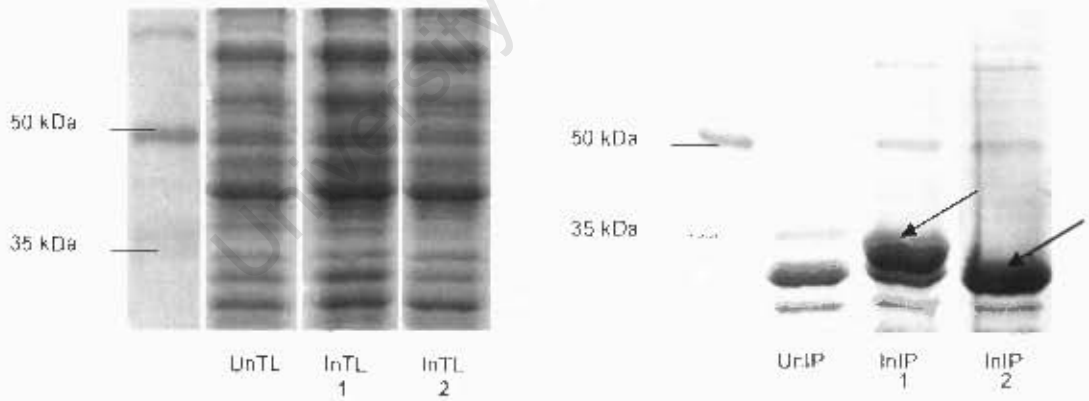

Figure 40. Recombinant protein expression.

Extracts of *E. coli* expressing the GST-σ recombinant proteins were electrophoresed on a 10 % polyacrylamide gel against a broad range protein molecular weight marker. UnLT (control sample); Triton lysate obtained from uninduced BL21 Star™(DE3) *E. coli*, InTL1; Triton lysate from IPTG-induced cells containing the σ1 recombinant plasmid and InTL2; σ4. The second gel contains insoluble pellet extracts (IP) alongside the uninduced control sample (UnIP). The additional band in the σ1 (InIP1) and σ4 (InIP2) fractions, indicated by arrows, migrates with an estimated molecular weight of 35 kDa and 33 kDa respectively.

Since a full-length functional and soluble expressed protein is not a requirement for antiserum production, protein purification procedures were carried out on the insoluble pellets for σ1 and σ4. The insoluble fractions, resuspended in water and diluted in PBS (see Chapter 6- Materials and methods), were purified using affinity chromatography with glutathione-agarose columns. The GST fusion tag is able to specifically bind the glutathione-agarose, allowing the recombinant protein to be retained on the column. Proteins were eluted with free glutathione, concentrated by freeze-drying and analyzed by SDS-PAGE (Figure 41).

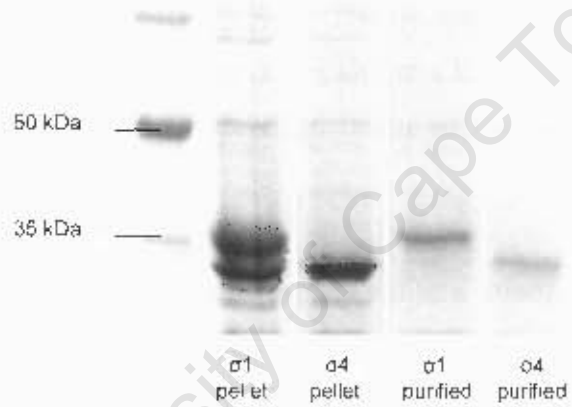

Figure 41. Purified σ recombinant proteins.

SDS-PAGE showing purified σ1 and σ4 recombinant proteins against crude, insoluble pellet samples.

For the purpose of mouse immunization, protein concentrations were estimated by comparison with the staining intensity of the 50 kDa protein of the broad range molecular weight marker and found to be in the range of 0.1 μg/μl to 0.5 μg/μl. Mice were immunized with approximately 30 μg purified protein and antisera collected and stored for use with Western blotting and IFA.

3.2.5. Anti-peptide antisera

Western blotting was performed to determine if the mouse antisera recognize the corresponding parasite proteins. Saponin-released trophozoite parasites were solubilized in sample buffer and run on SDS-PAGE gels. Proteins were transblotted onto membranes and incubated consecutively with the mouse antisera and peroxidase-conjugated anti-mouse antibodies. Detection was carried out with a chemiluminescent peroxidase substrate. Despite repeated booster immunizations and bleeds, the mouse antisera failed to react with parasite proteins. A different immunization strategy was therefore followed. Predicted antigenic peptides derived from the σ1 and σ4 sequences were synthesized and used to immunize rabbits (preformed by GeneScript Corporation (USA)) (See Chapter 6-Materials and Methods, and Appendix A-1). The σ1 and σ4 peptides were 14 and 15 residues in length respectively and were conjugated to a KLH carrier protein. In addition, ELISA was completed by GeneScript Corporation to test the anti-peptide antibody immune response (see Appendix A-3).

To investigate the specificity of the anti-peptide antisera raised, antisera were analysed by Western blotting. Trophozoite stage parasites were released from erythrocytes by saponin lysis, solubilized in sample buffer and run on SDS-PAGE gels. The separated proteins were transblotted to membranes and the membranes probed with the antibodies. Anti-peptide antiserum to σ1 and σ4 both bound to parasite proteins of approximately 70 kDa (Fig. 42). The sizes estimated from the gel differ considerably to the sizes predicted by the gene sequences in PlasmoDB, 18.2 and 17.5 kDa respectively. The antisera recognize proteins approximately 50 to 55 kDa larger than what is expected. The σ1 antisera cross-reacted with other parasite proteins, the most prominent one having a size of approximately 90 kDa.

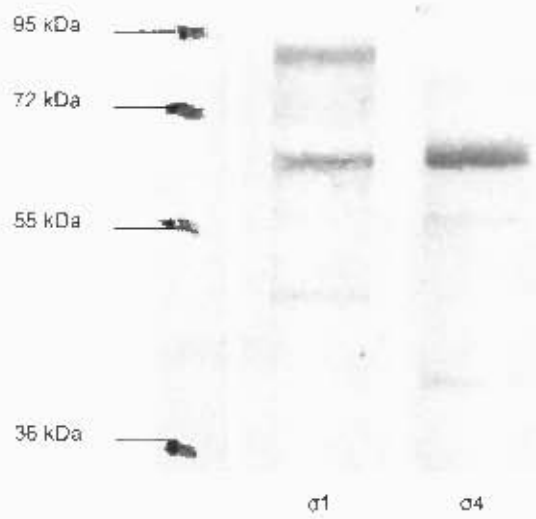

Figure. 42. Western blot of *P. falciparum* lysate using anti-peptide sera raised in rabbits. Antisera to σ1 and σ4 recognized parasite proteins with apparent molecular weights of approximately 70 kDa.

To explore the hypothesis that the size difference for the μ1 and σ1 antisera, and μ4 and σ4 antisera, is attributed to the σ adaptin being bound to the μ adaptin in a complex that does not dissociate under SDS-PAGE conditions, the size of the proteins recognized by each serum was compared. Western blots were performed on strips of membranes containing parasite protein extracts, and the strips probed with anti-μ1 antiserum raised in mice, μ1 anti-peptide antiserum raised in rabbits and σ1 anti-peptide antiserum raised in rabbits (Fig. 43). The most prominent band for the anti-peptide antisera were similar in size (approximately 70 kDa) to the single band recognized by antisera raised to the bacterially expressed μ1 protein. The results suggest that the antisera to μ1 and σ1 recognize the same protein, presumably a complex consisting of the μ1 and σ1 adaptins. A larger parasite protein, approximately 90 kDa in size, is detected with both rabbit anti-μ1 and rabbit anti-σ1. This protein could be a non-specific protein due to cross-reactivity of the sera or could potentially be an even higher molecular weight complex of the adaptins.

Similarly, Western blot strips probed with anti-μ4 antiserum raised in mice and σ4 anti-peptide antiserum raised in rabbits (Fig. 44) suggest that the antisera to μ4 and σ4 recognize the same protein complex, approximately 70 kDa in size, comprising the μ4 and σ4 adaptins.

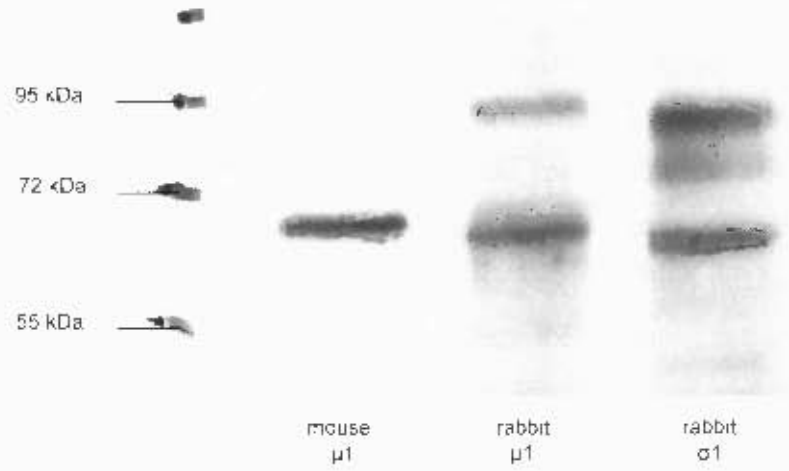

Figure. 43. Western blot of *P. falciparum* lysate using antisera raised in mice and rabbits. Strips of the same membrane were probed with anti-μ1 antiserum raised in mice, μ1 anti-peptide antiserum raised in rabbits and σ1 anti-peptide antiserum raised in rabbits. Each antiserum recognized a parasite protein of comparable size.

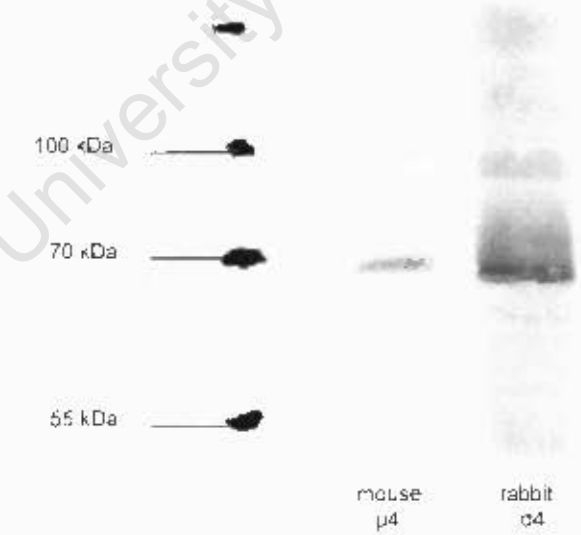

Figure. 44. Western blot of *P. falciparum* lysate using antisera raised in mice and rabbits. Strips were probed with anti-μ4 antiserum raised in mice and σ4 anti-peptide antiserum raised in rabbits. The antisera recognized a parasite protein of similar size.

3.2.6. Immunofluorescence microscopy assays (IFA)

The subcellular localization in the parasite as determined by immunofluorescence microscopy was attempted for the σ-adaptins. Trophozoite stage parasites were fixed with either paraformaldehyde (PFA) and glutaraldehyde, permeabilized with Triton, and treated with glycine to quench free aldehyde groups, or fixed in ice-cold methanol. Parasites were incubated with antisera raised to the peptides, then incubated with anti-rabbit TRITC-conjugated secondary antibodies. Only the σ1 anti-peptide antisera gave distinct localization in parasites fixed with PFA (Fig. 45), to an elongated structure within the cytosol that in some cases extends to regions along the parasite periphery. The position of the digestive vacuole can be seen in the phase-contrast and fluorescence images due to the presence of the large haemozoin crystal.

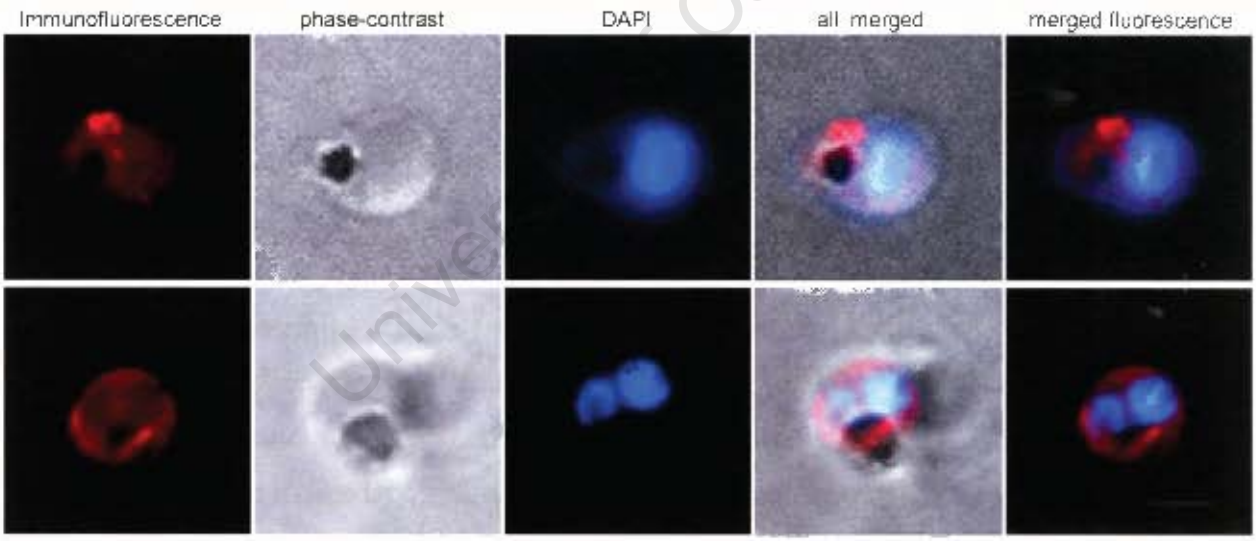

Figure 45. IFA localization of antibodies raised to the σ1 peptide in *P. falciparum*. A single parasite, fixed with PFA and glutaraldehyde, is shown in each row. From left to right, the panels illustrate the immunofluorescence image obtained using σ1 anti-peptide antisera and anti-rabbit TRITC-conjugated secondary antibody (red), the corresponding phase-contrast image, the DAPI stained nuclei (blue), the merged image of all three preceding frames, and the merged immunofluorescence and DAPI image. Bar, 2 μm.

A negative control was performed by the same procedure using pre-immune antiserum obtained from the same rabbit prior to immunization (Fig. 46). The control showed no specific localization in the parasite.

Figure 46. Localization control for σ1.

The first panel shows a parasite probed with pre-immune rabbit antiserum and TRITC-conjugated secondary antibodies (red). No distinct localization is seen, only faint background fluorescence. The second and third panels show the phase-contrast image and the nucleus stained with DAPI, respectively. Bar, 2 μm.

Western blot data for σ1 (Fig. 42) and the immunofluorescence images of σ1 and μ1 localization (Fig. 45 and Chapter 2, Fig. 23a A) suggest that the antisera may recognize similar sites within the parasite. Co-localization experiments with the two sera were performed to determine if these structures are the same (Fig. 47). Parasites were prepared as previously described and were incubated with both antisera, followed by both Alexa Fluor® 488-conjugated goat anti-mouse secondary antibodies and TRITC-conjugated goat anti-rabbit secondary antibodies. The merged images show co-localization of parasite σ1 with μ1, suggesting that the two antisera recognize the same structure, possibly containing a complex of the μ1 and σ1 adaptin.

A negative control was carried out by the same procedure discussed in Chapter 2, where the σ1 anti-peptide antiserum was excluded during the primary incubation (Fig. 48). No fluorescence was detected through the TRITC channel, confirming the secondary antibodies are specific for the respective primary antibodies.

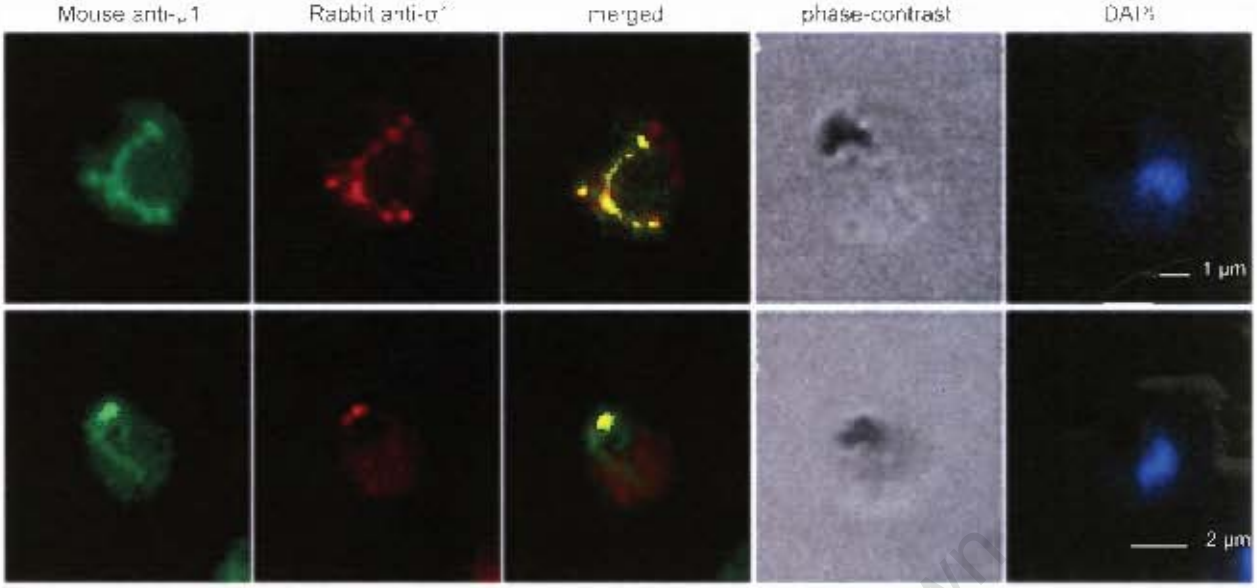

Figure 47. Co-localization of μ1 and σ1 in *P. falciparum* trophozoites. The first image shows localization with the μ1 antiserum and the second, localization with σ1. The secondary antibody used for μ1 is mouse Alexa Fluor® 488-conjugated (green) and σ1 is rabbit TRITC-conjugated secondary antibody (red). The merged image (third panel) shows co-localization (yellow).

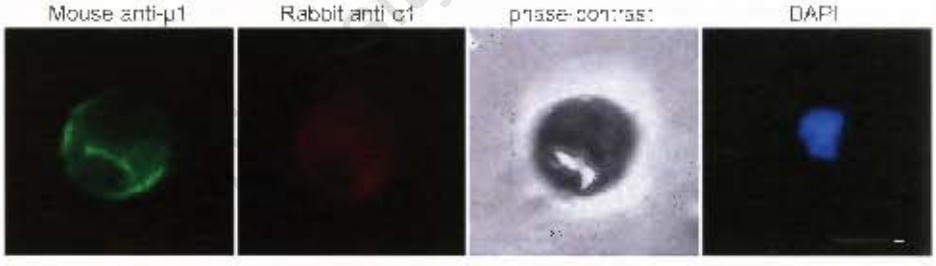

Figure 48. Co-localization controls for μ1 and σ1.

The σ1 antiserum was omitted during the primary antibody incubation. The first panel shows μ1 recognized by Alexa Fluor® 488-conjugated secondary antibodies (green). The second panel shows no distinct localization when incubated with TRITC-conjugated secondary antibodies (red). The digestive vacuole and nuclei are shown in the phase-contrast and DAPI-stained images (third and fourth panels) respectively. Bar, 2 μm.

3.3 Discussion

The characterization of the σ-chain adaptin gene homologues of *Plasmodium falciparum* was undertaken to explore the possibility that the μ-chains (μ1 and μ4) may be complexed with their smaller molecular weight adaptor protein partners, the σ-chains, and that this complex is able to withstand dissociation under standard SDS-PAGE conditions thus explaining the 70 kDa size observed for the μ-chains by Western blot. In Mammalian cells, the μ-chain and σ-chain adaptins form part of adaptor protein complexes (Robinson and Bonifacino, 2001).

The selection of the σ proteins was based on homology to mammalian counterparts. Homologues of human σ1 and σ4 adaptor protein partners of μ1 and μ4 were identified by BLAST searches of the *P. falciparum* genome. Expression of the genes during the blood stages of the parasite lifecycle was confirmed by RT-PCR. DNA sequences were amplified, cloned and expressed in BL21 Star™(DE3) *E. coli*. High levels of recombinant GST-σ1 and GST-σ4 were expressed as insoluble products, as determined by Coomassie stained SDS-PAGE. Comparisons with the molecular weight marker estimated the molecular weight of the recombinant GST-σ1 protein to be approximately 35 kDa and GST-σ4 approximately 33 kDa, which is smaller than the predicted 40 kDa and 41 kDa respectively. The discrepancies in molecular weight for the adaptins are comparable to the differences seen with the expressed recombinant GST-μ chains (Chapter 2). Although the production of recombinant fusion proteins in *E. coli* is well established, several factors may obstruct the efficient translation of certain proteins. Codon bias in *E. coli* hosts is the most significant basis for unsuccessful expression, especially in the case of AT-rich sequences like those found in *P. falciparum*; arginine and proline codons most frequently affect bacterial gene expression and can result in tRNA exhaustion, ribosome pausing and premature termination.. To overcome this obstacle and rescue gene expression, an alternative host strains could be used (Goldman *et al.*, 1995). An example of a host strain for AT-rich genes is BL21-CodonPlus-RIL *E. coli* which contains a plasmid that encodes extra copies of the arginine, leucine and isoleucine tRNA genes (Zhang *et al.*, 2005). Alternatively, codon optimization or harmonization may be attempted. Codon optimization entails the synthesis of the plasmodial coding region with a codon usage that corresponds to the most frequently

used *E. coli* codons. Harmonization entails preparing a synthetic gene composed of *E. coli* codons that reflect the codon usage frequency of the plasmodial sequence (i.e. a low frequency *P. falciparum* codon is replaced with a low frequency *E. coli* codon). This results in appropriate movement and pausing of the translational machinery during translation, allowing correct folding of the elongating polypeptide chain (Angov *et al.*, 2008). Lastly, unsuccessful *in vitro* protein expression may occur when secondary structures are present in the mRNA, which could affect ribosomal binding and hinder translation (de Smit and van Duin, 1990). Another known cause for failed expression could be an inadequate concentration of IPTG used at induction, although attempts using higher concentrations were also ineffective. Attempts were not made to improve expression by using lower *E. coli* growth temperatures or inducing at different phases of *E. coli* growth.

Expressed proteins were purified from the insoluble pellets by affinity chromatography with glutathione-agarose columns. Fortuitously, the recombinant proteins were partially solubilized by resuspending the inclusion body pellets in water. The samples were diluted in PBS and run through a column repeatedly. Mice were immunized with the purified proteins eluted from the columns with glutathione, and the antisera raised to the individual adaptins analyzed by Western blotting.

In view of the fact that σ1 and σ4 antisera did not detect any malarial proteins, an alternative approach for generating antibodies to the σ-adaptins was employed. The ability of antibodies to react with epitopes isolated from a native protein allows for an anti-peptide approach to antibody production. Anti-peptide antibodies are able to recognize the denatured form of the protein from which their sequence was derived. However, the ability of anti-peptide antibodies to react with intact, native proteins depends on whether the peptide sequence is displayed on the surface of the native protein. Algorithms are used to predict potentially exposed sequences for the selection of antigenic peptides for peptide synthesis (Xu and Ellington, 1996, Richardson *et al.*, 1997).

It is generally recommended that synthetic peptides be conjugated to immunogenic protein carriers since they are too small to elicit an immune response by themselves. These carrier proteins contain many epitopes that stimulate T-helper cells, which help

induce the B-cell response. The most commonly selected carriers are keyhole limpet hemocyanin (KLH) and bovine serum albumin (BSA). The higher immunogenicity of KLH often makes it the preferred choice. Although antibodies will also be generated to the carrier molecule, this will not pose a problem as they are not expected to have any specificity for parasite proteins (van Houten *et al.*, 2006). Immunization with the peptide-carrier molecule allows the generation of protein-reactive polyclonal antibodies. Where monoclonal antibodies react with a single epitope or antigenic determinant making them highly specific, polyclonal antisera contain antibodies that are able to recognize several epitopes on a single antigen. However, due to their multiple specificity, cross-reactivity can frequently occur (Fieser *et al.*, 1987). Anti-peptide antibodies are useful for Western blot analysis since the proteins probed are denatured by SDS and all epitopes are accessible by the sera. Conversely, antibodies to anti-peptides are not always useful for IFA purposes since protein structure is generally preserved and certain antibodies would not be able to react with epitopes buried in the interior of the intact protein (Spangler, 1991).

Antigenic peptides were synthesized and rabbits immunized to produce anti-peptide sera. Western blotting against *P. falciparum* proteins revealed that the antisera strongly recognized specific parasite proteins. Both the σ1 and σ4 rabbit antisera recognized proteins of approximately 70 kDa. Further Western blotting assays on parasite proteins revealed that the 70 kDa protein recognized by the σ1 antiserum co-migrated with the major 70 kDa protein recognized by the antisera to recombinant μ1 as well as the μ1 peptide. In addition to the 70 kDa protein, a larger protein of approximately 90 kDa was detected with both anti-peptide sera raised in rabbits. This could be due to non-specific cross reactions with malarial proteins often seen with antibodies derived from rabbits (H. Hoppe, personal communication), or could potentially be an even higher molecular weight complex of the adaptins. Similarly, Western blots using anti-σ4 and anti-μ4 show that both antisera recognize a 70 kDa parasite protein.

The fact that the σ-chains form part of adaptor protein complexes in other cell types and that the combined molecular weights of the σ-adaptin and μ-adaptin is predicted to be approximately 70 kDa (Hirst and Robinson, 1998) supports the proposed hypothesis that the μ1 and μ4 adaptins are complexed with the smaller molecular weight protein, the σ1 and σ4 chains. The finding that both μ1 and μ4, as well as σ1 and σ4, are approximately

70 kDa in size, suggests that μ1 and μ4 are bound to either σ1 or σ4 in a complex that does not dissociate under standard SDS-PAGE conditions. There are other instances of protein complexes able to withstand dissociation by SDS and heat. For example, secretin multimers in the bacterium *Klebsiella oxytoca* do not separate in the presence SDS or at temperatures as high as 100 °C (Guilvout *et al.*, 2006). Likewise, αβ-chains of MHC class II heterodimers in macrophages (Ullrich *et al.*, 2000) and transmembrane core proteins, Syndecan dimmers and multimers, in *Drosophila* (Kramer and Yost, 2003) are able withstand dissociation by SDS. To dissociate these persistent complexes, treatment with a variety of other detergents could be attempted (Rhinehart-Jones and Greenwalt, 1996).

In mammalian cells, the general organization of the adaptor complex consists of a core region and two ear appendages. In the core, the N-terminal of the β subunit interacts with the μ-chain and the N-terminal of the divergent subunit (γ/ α/ δ/ ε) interacts with the σ-chain (Robinson and Bonifacino, 2001). The *P. falciparum* genome sequence has revealed malaria homologues to other adaptor complex subunits: a β-chain homologue (PF1400c), an α-chain (PFF0830w), a γ-chain (PF14_0529) and an ε-chain homologue (PFI0200c). Although all the members of the typical adaptor complex are present, adaptin interactions may be different in the parasite where a stronger association between the small adaptins may exist that is able to endure SDS dissociation. It suggests that the 3D organization and intermolecular association in plasmodial adaptor complexes may differ considerably from those of their mammalian counterparts.

Proteomic analysis may be carried out to confirm the complexing of the plasmodial μ and σ-chains in SDS-PAGE gels, beyond the co-migration of bands on the Western blots and the co-localization obtained by IFA. One approach would be to attempt immunoprecipitation of the adaptor complexes from parasite lysates, followed by amino acid sequencing of internal peptides generated by proteolysis. Alternatively, a comprehensive MS-assisted analysis of all the malarial proteins in the 70 kDa region of SDS-PAGE gels may be carried out and analyzed for the presence of μ-chain and σ-chain sequences. A third approach may be Western blotting of 2D-PAGE gels of plasmodial proteins with the μ-chain antisera, followed by tryptic digestion and MS-analysis of the corresponding regions of the gel recognized by the antisera.

Immunofluorescence microscopy was employed to determine the subcellular localization of the σ-adaptins in the parasite. Distinct localization was solely achieved for the σ1-chain. The IFA images depict localization to an elongated structure within the cytosol, occasionally extending to regions along the parasite periphery. It is not unusual that antiserum to the other σ-chain peptide, σ4, did not give localization in the parasite. In some instances, anti-peptide antibodies are able to recognize the denatured recombinant protein on Western blots but not the native protein as seen in IFA. The ability of the anti-peptide antibody to interact with the native form depends on the folded structure of the intact protein and the location of the region to which the peptide was designed (Xu and Ellington, 1996). Co-localization of σ1 and μ1 indicates that they localize to similar intracellular sites. This is consistent with the possibility that μ1 and σ1 are bound together in a complex, resulting in the increased molecular weight of the adaptins as judged by Western blots. It suggests that the σ1 and μ1 adaptins form part of the same adaptor complex with a possible role in secretion. The same may be true for μ4 and σ4; however the inability of the σ4 antiserum to recognize the native σ4 protein by IFA prevents a definite conclusion.

CHAPTER 4 –Characterization of *Pf*rab6

4.1. Introduction

The classical secretory pathway of eukaryotes involves the movement of newly synthesized proteins to their final destinations via several membrane-bound compartments, the most important being the Golgi complex (Rothman *et al.*, 1984, Struck *et al.*, 2008). The compartments of the Golgi are organized into stacks by Golgi reassembly and stacking proteins (GRASPs) (Li *et al.*, 1995, Thyberg and Moskalewski, 1999, Mogelsvang *et al.*, 2004). GRASPs include GRASP55, a *medial*-Golgi matrix protein and GRASP65, a *cis*-Golgi protein (Shorter *et al.*, 1999, Wang *et al.*, 2005). A homologue of mammalian GRASP, *Pf*GRASP, has been identified and characterized in *P. falciparum* (Struck *et al.*, 2005).

The correct localization of chaperone proteins in the ER is fundamental for maintaining the functions of subcellular compartments (Janson *et al.*, 1998). These proteins perform essential functions in the ER related to protein folding, assembly and maturation, and are retained in the ER by means of C-terminal retrieval signals: KDEL in mammalian cells and HDEL in yeast (Sanchez-Lopez *et al.*, 1998, Majoul *et al.*, 2001). ER retention-defective complementation group 2 (ERD2) recognizes these signals and binds proteins that have escaped to the *cis*-Golgi to return them to the ER. Consequently, ERD2 is concentrated in the *cis*-Golgi but is also found in the ER (Aoe *et al.*, 1997, Janson *et al.*, 1998). The immunoglobulin-binding protein (BiP) is an ER resident chaperone protein involved in the folding of secretory proteins (Elmendorf and Haldar, 1993).

In eukaryotes, the G-protein superfamily includes proteins that control a variety of biological processes. The Rab family of proteins is a member of this superfamily, and is a highly conserved group of small GTPases that regulate vesicular trafficking (Pereira-Leal and Seabra, 2000, Chattopadhyay *et al.*, 2000). Rabs localize to the surface of specific

membrane-bound organelles and cycle between an active GTP-bound form associated with membranes, and the cytosolic GDP-bound inactive form. GTP binding triggers a conformational change in the Rab protein to catalyze membrane fusion (Martinez *et al.*, 1994, Chattopadhyay *et al.*, 2000). Rab6 GTPase regulates intracellular transport at the level of the Golgi complex. It is associated with *medial* and *trans*-Golgi elements, and to a degree with the *trans*-Golgi network (TGN). It is responsible for retrograde transport from the Golgi to the ER and transport between endosomes and the Golgi (Zahraoui *et al.*, 1994, van Wye *et al.*, 1996).

Plasmodium falciparum has a secretory pathway similar to eukaryotes although a typical Golgi stack has not been described. A functional, less developed Golgi with single cisternae has been proposed (Elmendorf and Haldar, 1993, Chattopadhyay *et al.*, 2000, Struck *et al.*, 2008). The lack of a morphologically defined Golgi may be attributable to inadequate fixation conditions that poorly preserve membranes and organelles (Struck *et al.*, 2005). Mammalian Rab proteins have specific subcellular distributions and serve as useful markers of different intracellular compartments. The homologue of mammalian Rab6 in *P. falciparum*, *Pf*rab6, has been characterized and is an accepted *trans*-Golgi marker in the parasite (de Castro *et al.*, 1996, Struck *et al.*, 2008). *Pf*rab6 has been shown to localize at multiple sites, suggesting that Golgi elements are not stacked (van Wye *et al.*, 1996). A parasite homologue of ERD2 (*Pf*ERD2) has also been described (Elmendorf and Haldar, 1993). *Pf*ERD2 is localized to the perinuclear region of the *cis*-Golgi and is concentrated in a defined area distinct from *Pf*rab6 (van Wye *et al.*, 1996). Additional markers of parasite *cis*-Golgi, *Pf*GRASP, and parasite ER, *Pf*BiP, have been described (Struck *et al.*, 2005).

The use of molecular markers characteristic of compartments involved in protein trafficking is a logical approach to identifying the organelle to which μ1 localizes. Given that several mammalian adaptor complexes (AP-1, AP-3 and AP-4) are associated with the *trans*-Golgi (Robinson and Bonifacino, 2001), that IFA and immuno-EM results obtained with μ1 is suggestive of Golgi localization, and that *Pf*rab6 is an acknowledged Golgi marker, it was decided to explore the co-localization of μ1 and *Pf*rab6 in the parasite by IFA. The parasite homologue of human Rab6 has previously been described (de Castro *et al.*, 1996). A fragment of the *Pf*rab6 coding sequence was obtained by RT-PCR, cloned, expressed and purified from *E. coli*. It was anticipated that mice would be

immunized for antisera production; however, purified recombinant protein yield was insufficient for mice immunization. Therefore an anti-peptide approach was followed. Rabbits were immunized with a synthesized peptide coupled to a carrier molecule, KLH, and the resultant anti-peptide antiserum was used in co-localization assays with μ1.

4.2. Results

4.2.1. The *P. falciparum* homologue of human Rab6

The *P. falciparum* sequence database, PlasmoDB, contains a previously described Rab6 homologue, *Pf*rab6 (PF11_0461). Using the BLAST algorithm, the predicted *P. falciparum* protein has significant sequence similarities to human Rab-6A (63 % identity and 78 % positives over a 205 amino acid sequence) (Fig. 49).


```
1     MSTGGDFGNPLRKFKLVFLGEQSVGKTSLITRFMYDSFDNTYQATIGIDFLSKTMYLEDR
      |    : |  | |:|||||||||:|||||:||||||||:||| ||:||||||||||||:||::
1     MDEFQNSG..LNKYKLVFLGEQAVGKTSIITRFMYDTFDNNYQSTIGIDFLSKTLYLDEG

61    TVRLQLWDTAGQERFRSLIPSYIRDSTVAVVVYDITNVNSFQQTTKWIDDVRTERGSDVI
      |||||||||||||||||||||||||||  |:||||||||  ||: |||||  |:  ||| |||
59    PVRLQLWDTAGQERFRSLIPSYIRDSAAAIVVYDITNRQSFENTTKWIQDILNERGKDVI

121   IMLVGNKTDLADKRQVSIEEGERKAKELNVMFIETSAKAGYNVKQLFRRVAAALPGMEST
      | |||||||| | |:|: ||| :||:| | || |||||||:|:| ||:::|: || :::|
119   IALVGNKTDLGDLRKVTYEEGMQKAQEYNTMFHETSAKAGHNIKVLFKKIASKLPNLDNT

181   QDRSREDMIDIKLEKP..QEQPVSEGGCSC
       : :  :::||:|     :        | |
179   NN.NEANVVDIQLTNNSNKNDKNMLSKCLC
```

Figure 49. *Pf*rab6 sequence alignment.

Protein sequence alignment of human Rab6 (hrab6, accession number P20340), upper sequence, and *P. falciparum* Rab6 (*Pf*rab6), lower sequence, using a DNAMAN© alignment program. Identical residues are shown with a blue vertical line. Conserved amino acid substitutions are denoted by colon symbols (:) and a dot (.) represents a sequence gap, introduced for optimal alignment

4.2.2. RNA isolation, cDNA synthesis and RT-PCR

RNA was isolated for subsequent amplification of the *Pf*rab6 coding sequence by RT-PCR. Late trophozoite stage parasites were harvested from 50 ml cultures (4 % het and 10 to 20 % pst) and RNA isolated with RNAgents® Total RNA Isolation System from Promega. Total RNA yield, determined spectrophotometrically at 260 nm, was in the range of 40 to 120 µg and the A_{260}/A_{280} ratio was between 1.9 and 2.0. The RNA was used as a template for cDNA synthesis and the cDNA used as a template for gene amplification by PCR.

Rab6 primers, designed to amplify a truncated version of the protein (See Chapter 6-Materials and Methods, and Appendix A-1), contained appropriate restriction sites to facilitate subsequent cloning. Amplification followed the standard PCR protocol and yielded a DNA product of the correct size (405 bp) when evaluated by gel electrophoresis on agarose gels (Fig. 50). The PCR product was purified by excising the band from the gel and extracting the DNA, and used in subsequent cloning procedures.

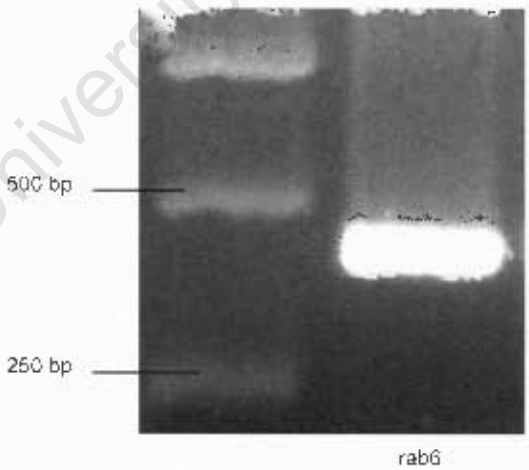

Figure 50. RT-PCR product.

Agarose gel electrophoresis (1 % gel) showing the *Pf*rab6 RT-PCR product along side a 1 kb DNA ladder. Rab6 gene product is 405 bp in size.

4.2.3. Cloning

The gene obtained by RT-PCR was diluted with water to the correct volume, ligated to the pGEM®-T Easy vector, and then cloned into *E. coli*. Competent DH5alpha™ *E. coli* cells were transformed with the recombinant plasmid DNA and the bacteria grown to a suitable extent in the presence of Ampicillin. Blue/white selection ensured the selection of colonies containing the plasmid with insert DNA. Plasmids were isolated and restriction digestion analysis, with BamH1 and Xho1 restriction enzymes, confirmed that the plasmids contained inserts of the expected size. After confirmation, purified plasmids were digested overnight with BamH1 and Xho1 to extract the insert DNA from the pGEM®-T Easy vector. The excised DNA was purified by agarose gel purification and sub-cloned into the pGEX-4T-1 expression vector digested with BamH1 and Xho1 (See Appendix A-2). These restriction sites guaranteed that the gene was cloned into the plasmid in-frame and in the correct orientation. *E. coli* colonies transformed with the pGEX-4T-1 ligations were grown overnight and the recombinant plasmids isolated. Additional digests with BamH1 and Xho1 were performed to confirm that the correct insert was incorporated in the plasmid (Fig. 51).

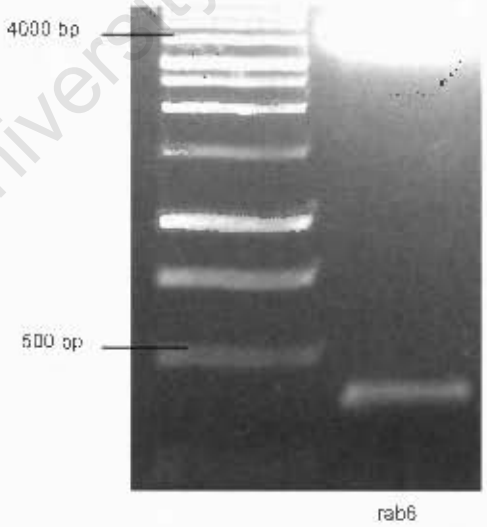

Figure 51. pGEX-4T-1 plasmid digest.

1 % agarose gel showing the *Pf*rab6 insert (405 bp) excised from the pGEX-4T-1 plasmid (4900 bp). The plasmid was digested with restriction enzymes BamH1 and Xho1. The BamH1 restriction site was introduced into the sequence with the forward primer and Xho1 with the reverse primer.

pGEX-4T-1 plasmids containing the correct insert DNA were originally transformed into DH5alpha™ *E. coli*. To enhanced protein expression yields, the plasmids were re-isolated from DH5alpha™ *E. coli*, as described in previous chapters, and used to transform BL21 Star™(DE3) *E. coli*.

4.2.4. Expression of recombinant protein

The cloned gene was expressed to obtain recombinant protein for antibody production through mouse immunization. The pGEX-4T-1 expression vector produces a recombinant protein with an N-terminal fusion to GST to facilitate expression, solubility and purification. For protein expression, bacterial cells harbouring the recombinant plasmid were grown overnight in LB medium containing Ampicillin. When the desired log-phase density of the culture was reached, IPTG was added and the culture grown for 3 hrs post-induction. To confirm that the bacteria have expressed the fusion protein, *E. coli* were lysed using standard lysozyme / Triton lysis techniques. The recombinant protein was present in the insoluble pellet, presumably in inclusion bodies. The Triton lysate and insoluble pellet remaining after Triton treatment were solubilized with sample buffer and run on an SDS polyacrylamide gel, then stained with Coomassie. When compared to bacteria that have not been induced with IPTG, a new band of the appropriate size was visible just below a prominent bacterial band in the insoluble pellet fraction (Fig. 52).

Figure 52. *Pf*rab6 recombinant protein expression.

Extracts of *E. coli* expressing GST-*Pf*rab6 recombinant protein were electrophoresed on a 10 % polyacrylamide gel against a broad range protein molecular weight marker. UnTL; Triton lysate obtained from uninduced BL21 Star™(DE3) *E. coli* (control sample), InTL; Triton lysate from IPTG-induced cells, UnIP; remaining insoluble pellet after Triton lysis from uninduced cells (control sample), and InIP; insoluble pellet from induced cells. The additional band in the induced, insoluble pellet sample, almost obscured by the prominent bacterial protein, is indicated by the arrow and migrates with an estimated molecular weight of 32 kDa.

The trend observed with the μ-chain GST fusions was repeated here; the apparent molecular weight of the recombinant *Pf*rab6 protein in the IPTG-induced insoluble pellet extract, based on SDS-PAGE migration compared to the molecular weight marker, was smaller than the predicted size calculated for the coding sequence fused to GST. The apparent molecular weight was approximately 32 kDa compared to the predicted size of 40 kDa. Despite the reduced size of the product, likely due to premature termination of translation as seen with other malaria sequences, the insoluble pellet sample was used for protein purification procedures.

Since the expressed recombinant protein was similar in size to a bacterial protein, the electro-elution protein purification technique could not be used. Purification was therefore carried out using affinity chromatography with glutathione-agarose columns. The glutathione-agarose method yielded pure recombinant proteins, illustrated by SDS-PAGE (Fig. 53). However, low yields, presumably due to inefficient solubilization and refolding of the protein from the insoluble pellet into a form capable of binding glutathione, made mouse immunization impractical. For this reason, a *Pf*rab6 peptide was synthesized for antisera production in rabbits.

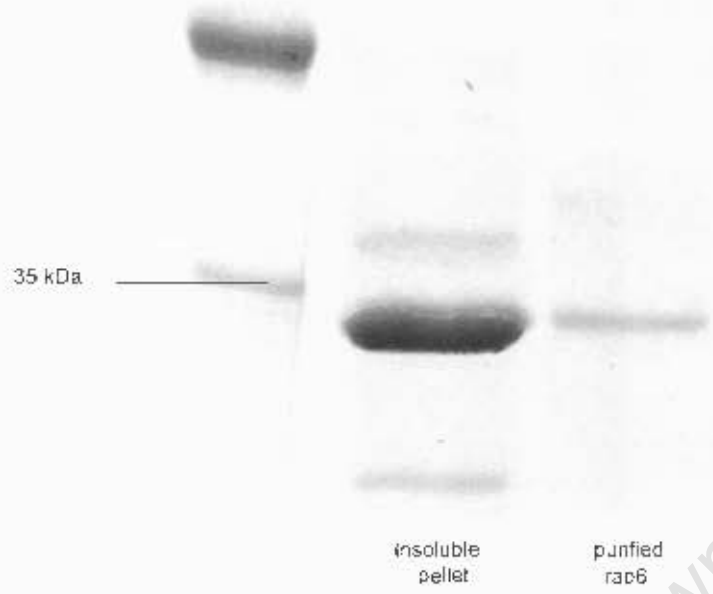

Figure 53. Purified GST-*Pf*rab6 recombinant protein.

SDS-PAGE showing the purified GST-*Pf*rab6 recombinant protein alongside the insoluble pellet sample.

4.2.5. Peptide synthesis and antiserum production

Since the *E. coil* expression approach for manufacturing *Pf*rab6 antigen for antibody production was unsuccessful, a peptide fragment of *Pf*rab6 was synthesized, coupled to a carrier molecule (KLH) and used to immunize rabbits (performed by GeneScript Corporation (USA)) (See Chapter 6- Materials and Methods, and Appendix A-1). The synthetic peptide corresponded to amino acids 71-84 of the coding region of *Pf*rab6, predicted to be an immunogenic epitope by GeneScript algorithms. GeneScript Corporation also tested antibody reactivity by ELISA (see Appendix A-3).

4.2.6 Western blotting

The specificity of the *Pf*rab6 peptide antiserum was determined by Western blot analysis. Parasites were released from erythrocytes with saponin, solubilized with sample buffer, and run on SDS-PAGE gels. The proteins were then transblotted onto a membrane. The blot indicates that the anti-peptide antisera developed to *Pf*rab6 specifically recognize a

protein with a molecular weight of approximately 24 kDa in parasites (Fig. 54), which correspond well to the size predicted by the gene sequence in PlasmoDB (23.6 kDa).

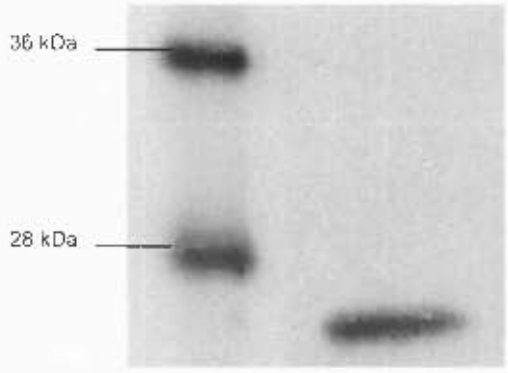

Figure 54. Western blot of *P. falciparum* lysate using anti-peptide sera raised in rabbits. The antiserum recognizes a parasite protein with an apparent molecular weight of approximately 24 kDa.

4.2.7. Immunofluorescence microscopy assays (IFA)

4.2.7.1. Localization of *Pf*rab6 using rabbit anti-peptide antiserum

*Pf*rab6 subcellular localization was determined by immunofluorescence microscopy on parasites fixed with paraformaldehyde and glutaraldehyde, permeabilized with Triton and treated with glycine (Fig. 55). The parasites were initially incubated with the *Pf*rab6 anti-peptide rabbit antiserum and then with TRITC-conjugated anti-rabbit Ig secondary antibodies. The sera recognize an elongated, ribbon-like structure that extends through the parasite cytosol.

A negative control was performed by the same procedure using pre-immune antiserum obtained from the same rabbit prior to immunization (Fig. 56). The control showed no specific localization in the parasite.

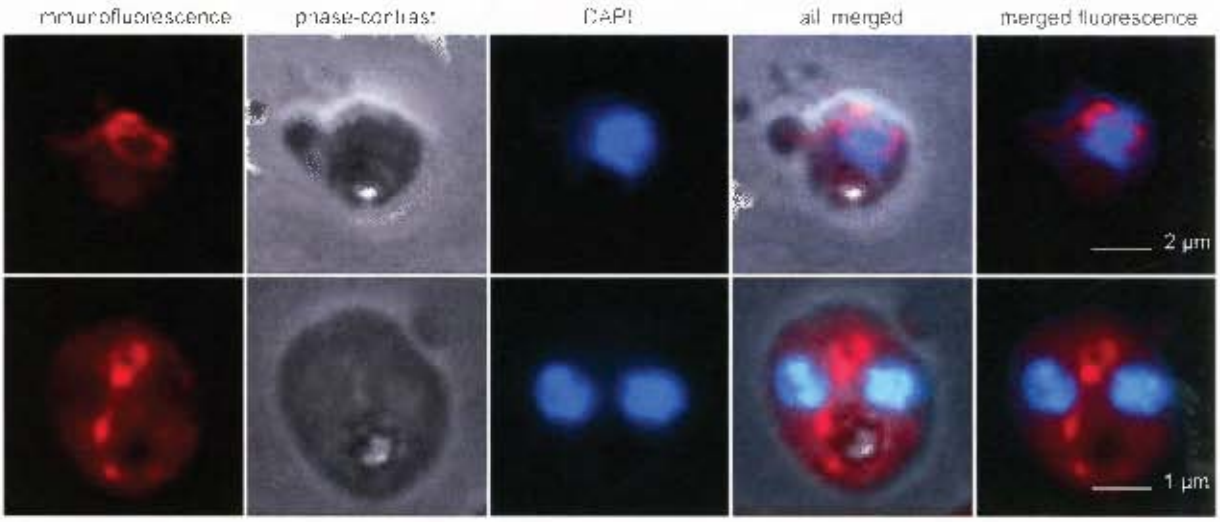

Figure 55. IFA localization of *Pf*rab6 in *P. falciparum* trophozoites with rabbit anti-peptide antiserum. A different parasite is shown in each row. The three panels illustrate (from left to right) the immunofluorescence image obtained using *Pf*rab6 anti-peptide antisera and rabbit TRITC-conjugated secondary antibody (red), the corresponding phase-contrast image and DAPI stained nuclei (blue). The digestive vacuole is identifiable due to the presence of the prominent haemozoin crystal in the phase-contrast image.

Figure 56. Localization control for *Pf*rab6.

The first panel shows a parasite probed with pre-immune rabbit antiserum and TRITC-conjugated secondary antibodies (red). No distinct localization is seen, only faint background fluorescence. The second and third panels show the phase-contrast image and the nucleus stained with DAPI, respectively. Bar, 1 µm.

4.2.7.2. Co-localization of µ1 and *Pf*rab6

The apparent similarities of the ribbon-like structure previously observed with the µ1 antiserum and that obtained for *Pf*rab6 (compare Fig. 55 and Fig. 23a A) suggested that the antisera may recognize similar sites within the parasite. Co-localization experiments with the two sera were performed to determine if these structures are the same (Fig. 57). Parasites were prepared as previously described and were incubated with both antisera, followed by both FITC-conjugated goat anti-mouse secondary antibodies and TRITC-conjugated goat anti-rabbit secondary antibodies. The merged images show co-localization of parasite *Pf*rab6 with µ1, suggesting that the two antisera recognize the same structure.

Two different controls were carried out by the same procedure discussed previously. In the first control (Fig. 58 A), the *Pf*rab6 anti-peptide antibody was left out and in the second control (Fig. 58 B), the anti-µ1 antibody was omitted. No fluorescence was detected in either case when probing with the relevant secondary antibody, confirming the secondary antibodies are specific for the respective primary antibodies.

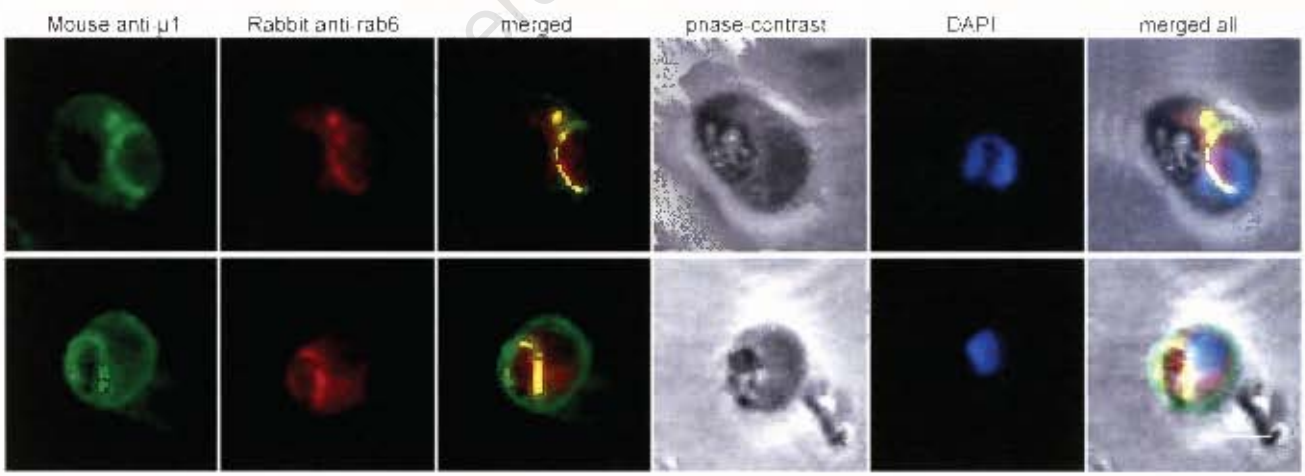

Figure 57. Co-localization of µ1 and *Pf*rab6 in *P. falciparum* trophozoites. The secondary antibody used for µ1 is FITC-conjugated anti-mouse (green), and for *Pf*rab6 is TRITC-conjugated anti-rabbit secondary antibody (red). The merged image shows co-localization (yellow). Bar, 2 µm.

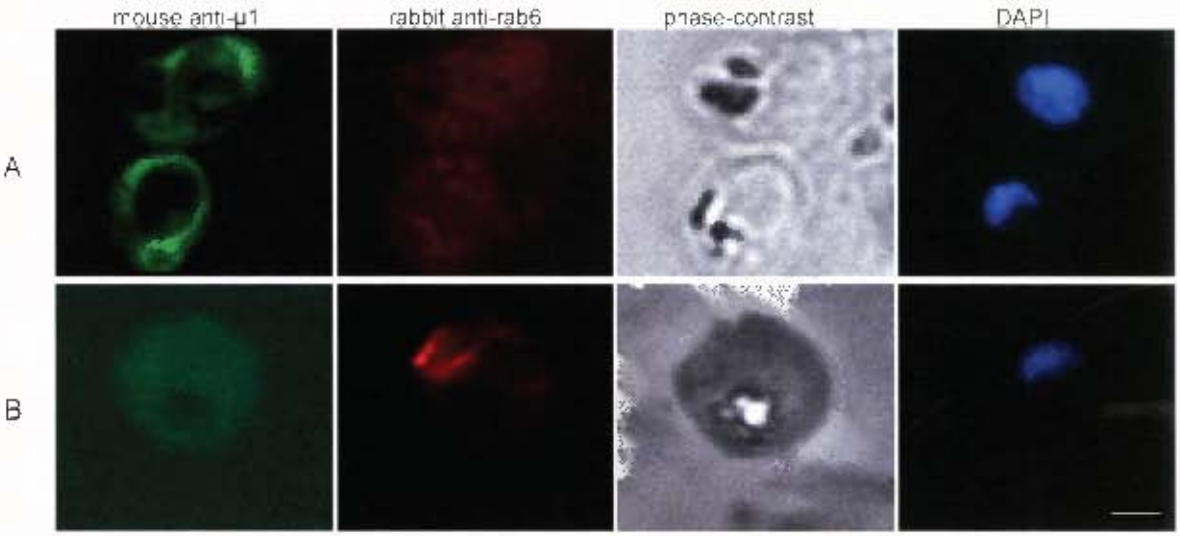

Figure 58. Co-localization controls for μ1 and *Pf*rab6.

(A) The images illustrate the control where the *Pf*rab6 antibody was excluded. The first panel shows μ1 recognized by FITC-conjugated secondary antibodies (green). The second panel shows no distinct localization when incubated with TRITC-conjugated secondary antibodies (red). The digestive vacuole and nuclei are shown by phase-contrast and DAPI-staining (third and fourth panels), respectively. (B) Illustrates the control where the anti-μ1 antibody was omitted. The first panel shows no localization when probed with FITC-conjugated secondary antibodies. The second panel shows *Pf*rab6 recognized by TRITC-conjugated secondary antibodies (red). This confirms specific recognition of the primary antibodies by the secondary antibodies. Bar, 1 μm.

4.3 Discussion

A characterization of the Rab6 gene homologue of *Plasmodium falciparum* was undertaken to explore the possibility that the μ1 adaptin has a close association with parts of the Golgi, by establishing if it localizes to the same structure as *Pf*rab6. In eukaryotes, Rab6 localizes to *medial* and *trans*-Golgi elements, and the *trans*-Golgi network, to regulate vesicular transport (Goud *et al.*, 1990). Rab proteins are conserved among eukaryotes and function at precise locations (Ali *et al.*, 2004). The GTP binding and catalytic sites of *Pf*rab6 are almost identical to that of human Rab6. *Pf*rab6 is a useful marker for Golgi membranes in *P. falciparum* (Van Wye *et al.*, 1996).

A sequence alignment revealed that *Pf*rab6 has 63 % amino acid identity with human Rab6. DNA sequences were amplified by RT-PCR from purified parasite RNA to verify previous reports (Van Wye *et al.*, 1996, de Castro *et al.*, 1996) that *Pf*rab6 is expressed in parasite intra-erythrocytic stages. As a first approach to producing anti-*Pf*rab6 antisera, an attempt was made to express it as a GST-fusion protein in *E. coli* and to purify the recombinant protein for mouse immunization purposes. The gene was amplified as a truncated sequence to improve primer design and facilitate expression.

Coomassie-stained SDS-PAGE suggested sufficient expression of a GST-fusion protein in an insoluble form in *E. coli*. However, the molecular weight was estimated to be approximately 32 kDa based on migration, compared to a predicted size of 40 kDa. This is most likely a reflection of the tendency of non-codon optimized *P. falciparum* sequences to be truncated in *E. coli*. The inconsistency in size may also be attributed to the fact that certain proteins migrate aberrantly in SDS-PAGE gels due to unusual SDS binding (Takano *et al.*, 1988).

Given that migration of the recombinant *Pf*rab6 protein on the gel was similar to that of a bacterial protein, protein purification could not be preformed by electro-elution. Purification was therefore carried out using affinity chromatography with glutathione-agarose columns. Triton-insoluble pellets were partially solubilized in sarkosyl, and then diluted in PBS to allow for protein refolding, necessary for binding of the GST to the glutathione resin. Elution with glutathione yielded pure recombinant protein. However the yield was insufficient for mouse immunization, possibly attributed to inefficient solubilization and refolding of the protein. Based on the truncated size and the poor yield of the recombinant GST-*Pf*rab6, an alternative approach was chosen for preparing anti-*Pf*rab6 antiserum. Consequently, a *Pf*rab6 peptide was synthesized for antisera production in rabbits by GeneScript Corporation (USA).

The peptide corresponds to 15 amino acids of the *Pf*rab6 coding region and was cross-liked to keyhole limpet hemocyanin (KLH). KLH is a carrier protein used to improve antibody titres by encouraging an immune response. Usually the peptide alone is insufficient to generate a response (Lankford *et al.*, 2006). The reactivity of the resultant antiserum was tested by ELISA, also completed by GeneScript Corporation, and the titre

curve generated indicated a strong immune response. This prompted further analysis of the sera by Western blotting.

Western blotting results indicate that the antiserum developed to the *Pf*rab6 peptide specifically recognizes a 24 kDa protein expressed in early and late trophozoite stage parasites, likely the Plasmodial homologue of Rab6 given that the genome sequence predicts a molecular weight for *Pf*rab6 of 23.6 kDa.

*Pf*rab6 is an established marker of the *trans*-Golgi in the parasite (de Castro *et al.*, 1996 Struck *et al.*, 2005). Feinstein and Linstedt (2008) and Mogelsvang and colleagues (2004) have described the mammalian Golgi as a ribbon-like structure consisting of interconnected cisternal stacks. By contrast, van Wye and colleagues (1996) have shown localization of *Pf*rab6 in *P. falciparum* parasites, by IFA and immuno-EM, to elongated, tubulovesicular structures extending through the parasite cytosol, and suggest that Golgi membranes are not cisternal but tubulovesicular or unstacked. De Castro and colleagues (1996) observed that the *Pf*rab6 localization pattern in the parasite differs with the progression of the erythrocytic cycle, the distribution becomes more disperse with parasite maturation. Struck and colleagues (2008) support an unstacked Golgi arrangement and provide evidence for a close association between the *cis*-Golgi, *trans*-Golgi and tER, contrary to a dispersed organization reported by van Wye *et al* (1996). In this study, subcellular localization of *Pf*rab6 was determined by immunofluorescence microscopy. The antisera recognize a ribbon-like structure that extends through the parasite cytosol. These findings are consistent with the reported observations regarding the tubulovesicular structure of the parasite Golgi. However, the fluorescence pattern becoming more punctate as the parasite matures was not found. It is possible that the antibody is not specific for rab6, but is cross-reacting with another Rab family protein of similar molecular weight. The likelihood of this occurring may be ameliorated by the fact that the peptide sequence used to generate rab6 antisera has a homology of less than 20 % to any of the other Rab proteins (see Appendix A-8).

Co-localization assays using μ1 and *Pf*rab6 antisera suggest that the two antisera recognize the same structure. This strengthens the notion that μ1 is part of a parasite adaptor protein complex, similar to mammalian AP-1, AP-3 and AP-4, that mediates secretion from the Golgi.

CHAPTER 5 – Conclusion

The re-emergence of malaria as a public health threat has prompted the discovery of new drug candidates and drug targets. The completion of the malaria genome has significantly increased our understanding of parasite biology, although information about the molecular processes involved in trafficking within the parasite itself and to locations within the host red blood cell remains limited. Components of the endocytic and secretory pathways in *P. falciparum* may yield attractive targets for the design of novel therapeutics as they play a vital role in parasite survival. The secretory pathway is required to re-model the infected red blood cell to allow nutrient acquisition and to facilitate immune evasion through sequestration, while extensive endocytosis of host cell haemoglobin provides amino acid building blocks and allows parasite expansion within the confines of the host cell. Although malaria parasites are evolutionarily widely separated from mammalian cells, have complex developmental cycles and unusual organelles (e.g. rhoptries, micronemes, apicoplast), the picture emerging from basic studies in widely divergent and more tractable model organisms (e.g. mammalian cells, plants, yeast, amoebae, kinetoplastida and *Toxoplasma gondii*) appears to be that the basic cell biological machinery and pathways of eukaryotic cells are conserved across phylogenetic boundaries. In other cell types, adaptor protein complexes play a central role in secretion, endocytosis and general protein trafficking by mediating coat recruitment, transport vesicle formation and cargo protein selection.

The identification and characterization of the adaptor complex components and the elucidation of the roles they play in transport processes in the parasite will contribute to the knowledge base surrounding molecular trafficking in the malaria parasite. This may be fundamental to efforts to ultimately eradicate this disease. The main aim of this study was to determine the subcellular distribution of adaptor protein components in the parasite in order to assess their possible functions by reference to higher cells. The protein components characterized in this study were selected due to their close sequence

homologue to their mammalian counterparts. The adaptor complex μ-chains were expressed as GST fusion proteins, whereas antigenic peptides to the σ-chains and *Pf*rab6 were synthesized for use in polyclonal antiserum preparation prior to immuno-localization. Molecular weight discrepancies of the expressed recombinant proteins were observed. These discrepancies are likely a result of either premature termination of protein translation, a phenomenon common when expressing malaria genes in *E. coli*, or anomalous behaviour of proteins in SDS-PAGE related to their amino acid composition (Takano *et al.*, 1988, Flick *et al.*, 2004). Although protein truncation (due to premature translation termination) and expression as insoluble inclusion bodies should not necessarily hinder subsequent use for immunization and antiserum production, increased yields of full-length soluble protein may be obtained by using synthetic codon-optimized coding sequences, *in vitro* translation or alternative expression hosts (Birkholtz *et al.*, 2008). One such expression host could be the slime-mould amoeba, *Dictyostelium discoideum*, as it has a similar AT-rich codon bias and is more easily genetically manipulated (Sharp and Devine,1989, Vervoort *et al.*, 2000). Expression in *Dictyostelium* can also be used for further functional characterization of the malaria proteins since *Dictyostelium* organelles are well characterized and have recognized markers, as well as established endocytosis and secretion assays (Adessi, *et al.*, 1995, Charette and Cosson, 2008).

An alternative general approach to protein localization may avoid the difficulties of heterologous expression and purification, antibody preparation, and potential artefacts and difficulties during immunofluorescence microscopy sample preparation. This approach would involve the overexpression of GFP-tagged sequences in the parasite, and allows one to track activities of proteins and view interactions between different organelles (Tilley *et al.*, 2007). Despite the comparative inefficiency of *P. falciparum* transfection and gene manipulation (Balu and Adams, 2007), this approach has been used to localize several plasmodial proteins (e.g. Tonkin *et al.*, 2004). However, fusion with GFP would disrupt the inclusion of the μ-chains and other adaptin components in tightly associated functional adaptor protein complexes. Even the fusion of a smaller C- or N-terminal epitope tag prevents μ-chains from associating with adaptor complexes in mammalian cells (Nesterov *et al.*, 1999). Additionally, expression of these fusion proteins could lead to mistargeting of the protein (Tilley *et al.*, 2007). Although knowledge of the 3D domain organization of the adaptins may allow the design and

preparation of expression constructs containing an internal epitope tag, fixation and localization by IFA using commercial antibodies can't be avoided.

The intracellular localization of the μ-chains in the malaria parasite was determined by immunofluorescence microscopy. The IFA data shows the co-localization of the μ1 and μ2 adaptins to a ribbon-like structure found within the cytosol of the parasite, suggestive of a secretory compartment. Utilizing known subcellular marker proteins in the parasite, the structure to which μ1 localizes was determined. Possible Golgi localization of μ1 was shown by co-localization with the *trans*-Golgi marker *Pf*rab6, which supports the notion that μ1 and μ2 are incorporated into parasite adaptor protein complexes similar to mammalian AP-1, AP-3 and AP-4 that mediate secretion from the *trans*-Golgi. Further analysis by co-localization experiments with the *cis*-Golgi marker, *Pf*ERD2, established that μ1 localization is distinct from the *cis*-Golgi. Co-localization experiments with μ1 and clathrin heavy chain antisera further suggest that μ1 (and by inference μ2) is part of adaptor complexes that mediate secretion by clathrin-independent mechanisms. In this respect, the parasite adaptor complexes may be more analogous to mammalian AP-3 and AP-4, both of which have been found to function in clathrin-independent trafficking events from the *trans*-Golgi. EM localization suggested that μ1 associates with extended tubulovesicular membranous structures, highly characteristic of secretory sites. Comparisons with images reported in studies by Witola and colleagues (2006) identify these structures as Golgi membranes. The possibility that μ1 is a minor constituent of other structures, as in mammalian cells (e.g. endosomes), can not be ruled out. It is further tempting to speculate that μ1 and μ2 form part of adaptor complexes that mediate protein trafficking to different subcellular destinations in the parasite. Despite their overall co-localization to the same organelle as inferred from the IFA results, the possibility remains that they may localize to distinct domains and mediate trafficking from different exit sites.

By IFA, the μ4 adaptin displays digestive vacuole and plasma membrane localization. This is strongly supported by the immuno-EM results and suggests that the adaptin plays a role in endocytosis and endocytic trafficking in the parasite, analogous to the μ2 component of the mammalian AP-2 adaptor complex. This is supported by the IFA co-localization of μ4 with the parasite clathrin heavy chain which suggests that the molecular mechanisms of endocytosis in the parasite may be related to clathrin-

dependent endocytosis of higher cells. Although typical clathrin-coated pits, characteristic of endocytosis sites in mammalian cells, have not been observed in malaria parasites, they are also absent in yeast where there is a clear requirement for clathrin in endocytosis (Munn, 2001). It is interesting in this regard that the parasite genome does not appear to encode a clathrin light chain component, which is required for clathrin cage formation in mammals (Newpher *et al.*, 2006). Furthermore, in mammalian cells the μ-chains recognize tyrosine-based sorting motifs in the cytoplasmic tails of transmembrane proteins, which allows them to mediate the targeting of transmembrane proteins to specific subcellular sites during secretion and receptor-mediated endocytosis. Receptor-mediated endocytosis and tyrosine-dependent targeting have not been demonstrated in malaria parasites, but have been shown in the apicomplexan parasite *Toxoplasma gondii* (Hoppe *et al.*, 2000). The location of *P. falciparum* μ-chains at potential sites of receptor-mediated endocytosis and intracellular targeting (i.e. the plasma membrane and the Golgi) suggest that tyrosine-dependent sorting may be important in malaria parasites as well.

The characterization of the *P. falciparum* σ1 and σ4 adaptins show that they are likely associated with either μ1 or μ4 in a stable complex that is not dissociated by SDS. Co-localization shows that μ1 and σ1 localize to similar sites in the parasite. Although it has been established that the general organization of the adaptor complex in mammalian cells consists of the μ-chain interacting with the large β-chain and the small σ-chain interacting with the large, divergent adaptin (either γ/ α/ δ/ ε depending on the adaptor complex), it may be possible that the intermolecular arrangement of the adaptin subunits in *P. falciparum* adaptor complexes differs from what is found in mammalian cells. A β-chain homologue (PF1400c), an α-chain homologue (PFF0830w), a γ-chain homologue (PF14_0529) and an ε-chain homologue (PFI0200c) are present in the *P. falciparum* genome sequence. One possibility is that characterization of these adaptins by immunoprecipitation assays (e.g. immunoprecipitation after digitonin lysis of parasites, followed by Western blotting and/or LC-MS/MS protein sequencing) may facilitate the identification of the binding partners in each adaptor complex. Additional accessory proteins that act in conjunction with the adaptor complexes (e.g. clathrin or dynamin) may also be identified in this fashion.

Although the localization reported here is highly suggestive, functional confirmation is required to explore whether *P. falciparum* μ4 forms part of a parasite adaptor complex similar to mammalian AP-2 that mediates endocytosis. In principle, this may be accomplished by disruption of the expression levels of the protein by dsRNA-mediated gene silencing, followed by cell biological assays. Reports of successful gene silencing by RNAi in malaria parasites have been sporadic (e.g. Siau *et al.*, 2007) and there is controversy whether it is a viable approach in this organism (Ullu *et al.*, 2004, Baum *et al.*, 2009). Alternative methods for gene function analysis could be considered. These include: (i) targeted gene alterations, where a generated knockout construct is incorporated into the parasite chromosome (Wu *et al.*, 1996, Krnajski *et al.*, 2002); and (ii) FKBP destabilization domain (ddFKBP) system whereby the target gene is fused to the small molecule, promoting degradation of the fusion protein in a ligand dependent manner (Armstrong and Goldberg, 2007).

Successful silencing can be assessed by semi-quantitative RT-PCR and Western blot analysis of μ4 mRNA and protein levels, respectively. Quantitative assays for endocytosis in the parasite following dsRNA silencing of μ4 may include a quantitation of haemoglobin levels by Western blotting, enumerating haemoglobin transport vesicles by IFA or EM, and assessing the levels of a macromolecular tracer, FITC-dextran, by IFA and fluorimetry in parasites occupying RBC pre-loaded with the tracer (Roberts *et al.*, 2008). Additional assays may include an assessment of plasmepsin II localization and its maturation from the precursor proplasmepsin. Plasmepsin is thought to reach the digestive vacuole via the plasma membrane by endocytosis at the cytostome (Francis *et al.*, 1997). Quantitative Western blotting to determine the relative amount of proplasmepsin and mature plasmepsin would indicate to what extent plasmepsin maturation in the endocytic vesicles has occurred (Klemba *et al.*, 2004).

Silencing experiments may also be required to functionally link μ1 and μ2 to secretion events, e.g. to the infected host red blood cell, the plasma membrane and specialized invasion organelles. Disruption of host cell targeting may be monitored by evaluating the integrity and number of parasite-derived structures by EM, by IFA localization of markers of some of these structures, and by Western blot analysis of levels of secreted marker protein in the RBC. Additionally, Western blotting assessment and IFA using antibodies to plasmepsin and its precursor would also facilitate secretion assays since

proplasmepsins are secreted to the plasma membrane, and subsequently to the endocytic pathway. Furthermore, trafficking to apical secretory organelles, such as mirconemes and rhoptries, can be studied by evaluating their morphology and quantity by EM and by IFA localization of marker proteins, such as AMA-1 and RAP-1 (Singh *et al.*, 2007, Haase, *et al.*, 2008).

Since adaptor complexes may also be involved in cytokinesis (Kita *et al.*, 2004), cell division assays could involve knockdown by dsRNA coupled with the examination of the number of merozoite or ring stage parasites formed after shizogony by thin-blood smears. A more direct approach would be to isolate and count the number of merozoites released from the infected erythrocytes.

Early termination of protein translation in certain *P. falciparum* strains has been established. An example of this is shown in two *P. falciparum* strains, 3D7 and 7G8, that express truncated normocyte binding protein 1 (*Pf*NBP1) while maintaining correct localization of the protein (Rayner *et al.*, 2001). To expand on the examination of the μ2 adaptin and determine the exact cause for its smaller size in the parasite, Western blotting on other strains such as K1, HB3, W2 and 7G8 could be carried out. Thus far, the reduced size was also seen on Western blots loaded with 3D7 strain parasite. Furthermore, additional work is required to determine if the reduced size of μ2 is caused by post-translational proteolytic cleavage. Post-translational processing has been reported for other *P. falciparum* proteins, such as *Pf*RPA1 (Voss *et al.*, 2002) and *Pf*CDS (Martin *et al.*, 2000) even though no cleavage of their orthologues in higher eukaryotes is observed.

In conclusion, the data in this study suggests that μ1 and μ2 localize to the Golgi and are possibly constituents of parasite adaptor complexes analogous to mammalian AP-1, AP-3 or AP-4 that mediate secretion from the *trans*-Golgi in a process independent of clathrin. Comparisons between the EM images obtained in this study and images reported by another research group (Witola *et al.*, 2006) confirm their localization to Golgi membranes. The findings further suggest that μ4 is part of an adaptor protein complex similar to mammalian AP-2 that associates with clathrin, and is most likely involved in clathrin-mediated endocytosis from the plasma membrane and trafficking at the digestive vacuole.

CHAPTER 6 – Materials and Methods

6.1. Continuous culture of *Plasmodium falciparum*

A chloroquine sensitive strain of *P. falciparum*, D10, was used throughout this project. Initial stocks were obtained from the Walter and Eliza Hall Institute of Medical Research in Melbourne, Australia, and were cultured continuously under sterile conditions in laminar flow hoods using a modified version of the method proposed by Trager and Jensen (1976). All Equipment was sterilized by autoclaving and reagents sterilized by filtration through a 0.22 µm filter unit. All solutions were prepared using purified distilled deionized water. The parasites were maintained in 50 ml RPMI 1640 culture medium (Cambrex, East Rutherford, NJ) supplemented with 25 mM sodium bicarbonate, 50 µg/L gentamycin sulphate, 22 mM glucose, 25 mM hydroxyethane piperazine sulphonic acid (HEPES), 5 g/L Albumax II (Invitrogen, Carlsbad, CA) and 323 µM hypoxanthine. Cultures were maintained at a haematocrit (hct) of between 2 and 4 % in sterile 75 cm^2 flasks. The parasitaemia (pst) was monitored using Giemsa-stained thin blood smears and maintained at 5 to 10 % by diluting with freshly prepared O^+ human erythrocytes (Western Province Blood Transfusion Service, Cape Town, South Africa). The red blood cells (RBC) were prepared by washing the blood three times in RPMI 1640 to remove serum and leukocytes. The blood smears were fixed on glass slides with methanol and stained with 10 % Giemsa stain (Merck, Darmstadt, Germany) in phosphate-buffered saline (PBS, 8 g/L $NaCl_2$, 0.2 g/L KCl_2, 1.15 g/L di-sodium hydrogen phosphate and 0.2 g/L potassium dihydrogen phosphate) for three minutes. The slides were rinsed with water and dried before viewing under a Leitz laborlux 12 microscope fitted with an oil immersion objective at 1500x magnification. Cultures were gassed with filtered gas containing 3 % O_2, 4 % CO_2 and 93 % N_2 and incubated at 37°C in an Air-Jacket CO_2 incubator (NUAIR™). Culture medium was replaced daily and parasites diluted with RBCs during the trophozoite stage. Parasites were pelleted by centrifugation

at 750 rcf (relative centrifugation force) in a Centrifuge 5804 (Eppendorf, Hamburg, Germany) for 3 minutes.

Ring phase parasite cultures were synchronised using the D-sorbitol method described by Lambros and Vanderberg (1979). Suspensions were centrifuged at 750 rcf for 3 minutes and the remaining pellet incubated in 5 volumes of 5 % D-sorbitol (Sigma-Aldrich, Steinheim, Germany) for 10 minutes at 37 °C. After another centrifugation, the parasite pellet was resuspended in complete medium, resulting in osmotic lysis of erythrocytes infected with mature stage parasites. Following sorbitol treatment, cultures consisted primarily of ring stage parasites.

6.2. RNA isolation and cDNA synthesis

Polymerase chain reaction (PCR) was done by RT-PCR from purified parasite RNA isolated from trophozoites, as some genes were predicted to contain introns. This excludes the non-coding regions and thus eliminates the process of splicing the introns out before protein translation. Amplification from the cDNA confirms that all the genes of interest are expressed during the erythrocytic cycle of the parasite, as opposed to exclusive expression in the mosquito, gametocyte or liver stages. Nuclease-free water was used for all preparations and reactions, except were indicated differently. 1.5 ml eppendorf tubes were used at all times, unless otherwise stated.

6.2.1. Trophozoite isolation from erythrocytes by saponin lysis

Mature parasites, generally in the trophozoite stage, were isolated form host erythrocytes by saponin lysis. Parasite cultures of a high parasitaemia (10 to 20 %) were centrifuged at 750 rcf for 3 minutes and the supernatant aspirated off. The remaining pellet of parasitized erythrocytes was resuspended in 20 mL PBS containing 0.1 % (w/v) saponin (Sigma-Aldrich, Steinheim, Germany) and incubated at room temperature for 5 minutes. After a second centrifugation, the pelleted free trophozoites were washed three times with PBS to remove lysed erythrocytes and excess haemoglobin. The pellets were stored at -20°C.

6.2.2. RNA extraction from isolated trophozoites

The thawed pellet was resuspended in 600 µl ice-cold denaturing solution (RNAgents® Total RNA Isolation System, Promega, Madison, WI). 60 µl 2 M sodium acetate was added and the suspension vortexed. RNA extraction was achieved by adding an equal volume of phenol:chloroform:isoamyl alcohol to the pellet suspension (Promega, Madison, WI), shaking the sample vigorously for 10 seconds, incubating it on ice for 15 minutes and briefly centrifuging in a bench top Centrifuge 5415 D (Eppendorf, Hamburg, Germany). The upper aqueous phase was transferred to a new eppendorf and an equal volume of isopropanol (Sigma-Aldrich, Steinheim, Germany) was added to precipitate the RNA. The sample was incubated on ice for 15 minutes and the RNA pelleted by a 5 minute centrifugation. The pellet was washed with 75 % ethanol, air-dried and resuspended in 100 µl water. All procedures were preformed on ice to slow the rate of RNA degradation.

6.2.3. Removal of DNA contamination

The removal of residual DNA from the sample ensures that all products amplified by the RT-PCR reactions originated from RNA. 1 µl RNase OUT (ThermoScript™ RT-PCR system, Invitrogen, Frederick, MA), 1 µl RQI DNase buffer 10x (Promega, Madison, WI), 8 µl DTT (ThermoScript™ RT-PCR system) and 2.5 µl RQI DNase (Promega, Madison, WI) were added to the 100 µl RNA solution, and the mixture incubated at 37 °C for 15 minutes. Digestion was stopped with the addition of 100 µl water and 10 µl RQI DNase Stop solution (Promega, Madison, WI). RNA was extracted twice with phenol:chloroform:isoamyl alcohol and precipitated with 35 µl 3 M sodium acetate (pH 5.2) (Promega, Madison, WI) and ethanol. The RNA yield was determined spectrophotometrically at 260 ηm, where one OD_{260} unit corresponds to 40 µg/ml single stranded RNA. The purity of the sample was established from the relative absorbances by calculating the OD_{260}:OD_{280} ratio (A_{260}/A_{280}). This value should fall between 1.9 and 2.0 to substantiate that there is no protein contamination.

6.2.4. cDNA synthesis

ThermoScript™ RT-PCR kit reagents were used for the RT-PCR reaction. 2-3 µg RNA, 7 µl DEPC-treated water and 1 µl oligo-dT primer were added to a 0.2 ml Thermowell™ PCR tube (Costar®, England). The reaction mix was incubated at 65 °C for 6 minutes in a Mastercycler gradient PCR machine (Eppendorf, Hamburg, Germany) and then placed on ice. 4 µl 5x cDNA buffer, 1 µl DTT, 1 µl RNase OUT, 2 µl dNTPs and 1 µl thermoscript reverse transcriptase were added to the tubes and the tubes incubated for 50 minutes at 55 °C. The enzyme was then inactivated at 85 °C for 6 minutes and the RNA template degraded with the addition of 1 µl RNaseH and incubation at 37 °C for 20 minutes.

6.3. PCR of malarial genes

The complete *Plasmodium falciparum* genome sequencing project enabled the identification of the genes of interest. BLAST searches of the malaria genome database, PlasmoDB (Bahl *et al.*, 2002), were carried out to obtain the relevant gene sequences based on high homology to mammalian counterparts. The selected genes and their PlasmoDB designations were:

µ-chain adaptins: three homologues

- µ1- PF13_0062
- µ2- PFL0885w
- µ4- PF11_0202

σ-chain adaptins: two homologues

- σ1- PF11_0187
- σ4- PFD1090c

Rab6 homologue (*Pf*rab6)

- PF11_0461

6.3.1. Primer design

Primers were designed to selectively anneal to the 5' and 3' ends of the gene. The aim was to design primers with a melting temperature (Tm) above 60 °C, where both the reverse and forward primers have similar Tm. Generally primers should have a guanine and cytosine (GC) content close to 50 %. However, this was not always possible as malaria genes have an unusual adenine and thymine (AT) rich codon preference (Weber, 1987). Restriction sites were included in both the reverse and forward primers to enable insertion into plasmids. Primers were purchased from Integrated DNA Technologies (Coralville, IA).

Oligonucleotide primer sequences:

μ_1-F: 5' CGCGGATCCGATGGCATGTATAAGCGCT 3'
BamHI

μ_1-R: 5'CGGGAATTCCTAGGACATTCTGACCTG 3'
EcoRI

μ_2-F: 5' CGCGGATCCATGCTCATATAAATGGAAGGGTAACC 3'
BamHI

μ_2-R: 5' CGCGAGCTCCTATTTATACTGGTAGATGCCCGATTCTG '3
XhoI

μ_4-F: 5' CGCGGATCCATGGTGATATCCCAATTTTATATTTTGTC 3'
BamHI

μ_4-R: 5' CTAAGGCGCTTTAAAGTTATTATTGATTCG '3

σ1-F: 5' CGCGGATCCACGCGACTAGCCAAATGGTACATC 3'
BamHI

σ1-R: 5' CGCCTCGAGATTCATTAATGAGTCTTGAGCTGCGAC 3'
XhoI

σ4-F: 5' CGCGGATCCTTCTTGTTAATGGTCAATAAACAAGGC 3'
BamH1

σ4-R: 5' CGCCTCGAGTTACATTAACAGAATTGGTCTCAAGAC 3'
Xho1

Rab6-F: 5' CGCGGATCCGATGAAGGTCCTGTACGCTTACAATTG 3'
BamH1

Rab6-R: 5' CGCCTCGAGTTATAATTGTATATCTACAACATTGGCTTC 3'
Xho1

Note: No restriction site was included in the reverse primer for μ4. A restriction site (Not1) in the multiple cloning site of the pGEM®-T Easy Vector System (Promega, Madison, WI) was used with BamH1 to remove the gene and insert it into the pGEX-4T-1 expression vector (GE Healthcare, UK).

6.3.2. PCR

PCR consisted of 5 μl 10x *Ex*Taq buffer (TaKaRa, Shiga, Japan), 4 μl dNTPs mix (10 mM each) (Finnzymes, Finland), 4 μl cDNA , 1.5 μl of each primer (100 μM stock solution in water) and 34 μl water. Reactions were prepared on ice and placed immediately into the Mastercycler PCR machine preheated to 94°C. After a two minute incubation, 0.3 μl *Ex*Taq polymerase (TaKaRa, Shiga, Japan) was added to the tubes and the reactions mixed by repeated pipetting up and down. The PCR cycle comprised of a denaturation step at 94 °C for 40 second, an annealing period for 45 seconds at 60 °C and an extension phase for two minutes at 68 °C. The cycle was repeated 30 times, followed by a final extension step at 72 °C for 5 minutes.

6.4. Cloning of PCR products

PCR products were first cloned into the pGEM®-T Easy Vector System (Promega, Madison, WI) to generate a convenient and abundant source of gene product for subsequent sub-cloning. This system is convenient for PCR cloning as the 3'-T overhang

at the insertion site of the plasmid anneals with 3'-A overhang generated by Taq polymerase enzymes during the PCR reaction. PCR products were then excised from the vector using restriction enzyme sites located either in the original primers of the PCR product or in the flanking vector multiple cloning region, and ligated to the pGEX-4T-1 expression vector (GE Healthcare, UK) for expression as GST-fusion proteins in *E. coli*.

6.4.1. Purification of PCR products

Non-specific PCR products, primer dimers and excess nucleotides were removed from the PCR product by gel purification before ligation to the vector. 6 µl of gel loading dye (0.25 % (w/v) bromophenol blue and 30 % (v/v) glycerol in TBE: 0.05 M Tris, 0.05 M boric acid, 2 ml 0.5 M EDTA in 1 L water, pH 8.5) was added to each PCR product. The entire sample was loaded onto a 1 % agarose gel prepared with 0.5 g agarose (Hispanagar, Madrid, Spain) and 12 µg ethidium bromide (Sigma-Aldrich, Steinheim, Germany) in 50 ml TBE, and electrophoresis carried out at 75 V for approximately one hour in TBE buffer. The samples were run beside a 1 kb DNA ladder (Promega, Madison, WI) to determine the size of the products. After electrophoresis, DNA bands in the gel were viewed under low intensity Ultraviolet (UV) light on a Gibco BRL UV Transilluminator (Life Technologies, USA), and the bands of interest excised with a scalpel blade and transferred to an eppendorf. The gel was exposed to the UV light for the shortest time possible to prevent the formation of pyrimidine dimers and damage to the DNA.

GFX PCR DNA and Gel Band Purification Kit (GE Healthcare) was used to purify the DNA from the excised gel slices. 300 µl capture buffer was added to the gel slice and the tube incubated in a water-bath at 60 °C until the agarose dissolved. The sample was then passed through a GFX spin column by a brief centrifugation. DNA captured by the matrix was washed with an ethanolic buffer to remove contaminants and salts, and the purified DNA eluted in 50 µl water.

The approximate concentration of the purified DNA was determined by an ethidium bromide spot method using the UV transilluminator. The concentration was determined by comparing the fluorescent intensity of 4 µl purified DNA mixed with 4 µl ethidium bromide (10 µg/ml water) with DNA standards of known concentrations.

6.4.2. Cloning into the pGEM®-T Easy plasmid

To optimize cloning efficiency, the amount of insert DNA and the ligation volumes must be adjusted depending on the molar yield of the purified PCR product. Ratios from 3:1 to 1:3 are recommended good initial parameters for the pGEM®-T Easy Vector System. A 3-fold molar excess of insert DNA was used in this project. The pGEM®-T Easy vector is approximately 3 kb and is supplied at 50 ng/µl. The pGEX-4T-1 vector is 4.9 kb.

To calculate the appropriate amount of insert DNA to include in the ligation reaction, the following equation was used:

$$\frac{\text{amount of vector} \times \text{size of insert} \times \text{insert:vector molar ratio}}{\text{size of vector}} = \text{amount of insert}$$

Ligation reactions were carried out using the reagents supplied with the pGEM®-T Easy Vector System. 5 µl 2x T4 DNA ligation buffer, 1 µl pGEM®-T Easy plasmid, 3 µl insert DNA (made up to the desired concentration with water) and 1 µl T4 DNA ligase were combined in an eppendorf tube and the reaction incubated at 4 °C overnight. The ligation reaction was subsequently used to transform *E. coli* (see section 6.5).

6.4.3. Sub-cloning into the pGEX-4T-1 expression vector

The insert DNA was excised from the pGEM®-T Easy plasmid and irrelevant insert DNA removed from the pGEX-T4-1 plasmid by restriction digest. Restriction endonucleases BamH1 and Xho1 (Roche, Mannheim, Germany) were used for µ2, Rab6, and the σ-chain digestions. BamH1 and EcoR1 (Roche, Mannheim, Germany) was used for the µ1 digestion, and BamH1 and Not1 (Roche, Mannheim, Germany) used for µ4. The pGEX-4T-1 plasmid used for each ligation was prepared with the same enzymes used for each insert digestion. Restriction digests were carried out in 20 µl volumes with 10 units of each enzyme and 2 µl 10x restriction buffer, and incubated overnight at 37 °C.

The digested products were gel-purified using the GFX PCR DNA and Gel Band Purification Kit (GE Healthcare, UK) and the purified DNA eluted in 25 µl water. Concentrations were determined using the ethidium bromide spot method and UV transilluminator. The ligation reaction for pGEX-4T-1 was set up using T4 ligase reagents (New England Biolabs, Ipswich, MA) in 20 µl volumes: 60 ηg plasmid DNA, 2 µl 10x T4 DNA ligase buffer, 1 µl T4 DNA ligase and insert DNA made up with water. The reactions were incubated at 15 °C overnight. DNA ligase creates a phosphodiester bond between the 5' phosphate of one nucleotide and the 3' hydroxyl of another. Where the volume of the insert DNA exceeded the final volume of the ligation mixture, the required amount was first dried down overnight and then resuspended in the correct amount of water. PCR products were cloned in-frame either between BamH1 and EcoR1, BamH1 and Xho1, or BamH1 and Not1 restriction sites.

6.5. Transformation of competent *E. coli* cells

DH5alpha™ *E. coli* cells were used for all initial transformations as they are easier to transform and are compatible with blue/white selection. BL21 Star™(DE3) (Invitrogen, Carlsbad, CA) were transformed with completed pGEX-4T-1 constructs as these cells improve protein expression yields since they contain extra copies of rare codon *E. coli* tRNA genes.

6.5.1. Preparing competent *E. coli* cells

An *E. coli* colony from an Ampillicin-free Luria-Bertani (LB) plate was grown overnight in 3 ml sterile LB broth (10 g tryptone, 5 g yeast extract, 5 g $NaCl_2$, 1 ml 1N NaOH in 1 L water). This culture was then transferred to 250 ml LB broth in a 1 L flask and grown until the optical density at 550 ηm (OD_{550}) was between 0.4 and 0.6. The culture was incubated on ice for one hour and the bacterial cells pelleted at 3000 rpm for 15 minutes at 4 °C. The pellet was drained on paper towel and resuspended in 80 ml sterile, ice-cold FB buffer (1.85 g KCL, 1.875 g $CaCl_2.2H_2O$, 25 g glycerol, 2.5 ml 10 mM K.acetate, made up to 250 ml with Millipore water, pH 6.2). The suspension was placed on ice for one hour, the cells pelleted and then re-dispersed gently in 20 ml FB buffer. Aliquots were stored at -80 °C in cryotubes.

6.5.2. Transformation

The frozen competent cells were thawed on ice and 100 µl transferred to a cold 15 ml Greiner centrifuge tube (CellStar, Greiner Bio-One). 10 µl of the ligation mix, or 5 µl purified plasmid, was added to the cells and the tube incubated on ice for 30 minutes. The cells were heat shocked in a circulating water-bath at 42 °C for 70 seconds and replaced on ice for a further 10 minutes. 500 µl LB broth was then added and the culture incubated for one hour at 37 °C in a shaking incubator. The bacteria were then pelleted in an eppendorf tube at 6000 rpm for three minutes and the supernatant removed. The pellet was resuspended in 60 µl LB broth and plated out on LB plates containing 100 µg/ml Ampicillin (Roche, Mannheim, Germany). Plates were inverted and incubated overnight at 37 °C. The presence of Ampicillin ensures that only bacteria harbouring the plasmid survive.

6.5.3. Blue/white selection for pGEM®-T Easy plasmids containing insert

Blue/white selection allowed for the isolation of colonies containing the pGEM®-T Easy vector with an insert. Selection works on the basis that the multiple cloning site in the vector is situated within the LacZ coding region, a gene that encodes the enzyme β-galactosidase. This enzyme is able to hydrolyze a white substrate known as X-gal (5-bromo-4-chloro-3-indolyl-beta-D-galacto-pyranoside). However, when a PCR product is inserted into the gene, the enzyme cannot be expressed and thus the X-gal substrate will not be cleaved. Therefore, the selection of white colonies present on the plate will provide plasmids harbouring an interrupting insert. Colonies containing β-galactosidase activity grow poorly relative to cells lacking the activity, therefore blue colonies may be smaller than the white colonies. LB pates used for blue/white selection were prepared with 50 µl 0.2 M isopropyl-1-thio-D-galactopyranoside (IPTG) (Promega, Madison, WI) and 20 µl 50 mg/ml X-gal (in DMSO) (Promega, Madison, WI).

6.5.4. Assessment of plasmids

To confirm that isolated plasmids contain the correct insert DNA and to establish the orientation in which the DNA was inserted into the plasmid, restriction digests using restriction sites within the gene sequence were performed, followed by gel analysis.

6.5.4.1. Plasmid isolation

Plasmids were isolated from the bacterial cells using an alkaline-lysis method. Colonies from the transformation plates were grown overnight in 3 ml LB broth containing Ampicillin (100 μg/ml) at 37 °C, and the cultures centrifuged at 6000 rpm for three minutes. The pellets were resuspended in 100 μl GTE buffer (50 mM glucose, 25 mM Tris, 10 mM EDTA in 10 ml water, pH 8.0) and 2 μl DNase-free RNAse (500 μg/ml) (Roche, Mannheim, Germany). 200 μl 0.2 N NaOH in 1 % sodium dodecyl sulphate (SDS) was added and the suspensions placed on ice for 4 minutes. 150 μl 5 M potassium acetate was then added, and after a 5 minute incubation on ice, the suspensions were centrifuged at 13 000 rpm for 10 minutes. 400 μl of the supernatant was transferred to a new eppendorf tube and the plasmid DNA precipitated with 800 μl ethanol. The DNA pellet was washed with 75 % ethanol, air-dried, and then resuspended in 50 μl water. An alternative approach for isolating plasmids was with the use of a plasmid isolation kit, QIA prep® Spin Miniprep Kit (Qiagen, Erkrath, Germany).

6.5.4.2. Confirmation of insert presence by restriction enzyme analysis

Restriction digestion reactions were carried out by adding 10 units of each restriction enzyme specific to the particular gene fragment, 2 μl of the appropriate buffer, 10 μl plasmid DNA and 8 μl water, and incubating the tubes for two hours at 37°C. The digests were analyzed by agarose electrophoresis. The restriction enzymes used were:

μ1 –	BamH1 and Spe1	σ chains –	BamH1 and Xho1
μ2 –	BamH1 and Nsi1	Rab6 –	BamH1 and Xho1
μ4 –	BamH1 and EcoR1		

6.5.5. Storing bacterial stocks

Colonies yielding plasmids with the correct restriction pattern were spread onto LB plates containing Ampicillin (10 μg/ml) and grown overnight. A colony from the plate was then grown overnight in 3 ml LB broth containing Ampicillin, combined with sterile glycerol at a 6:1 ratio, and stored at -80°C.

6.6. Expression of recombinant protein

The proteins encoded by the genes where expressed for the purposes of manufacturing antibodies. The pGEX-4T-1 plasmid adds a GST fusion protein to the N-terminus of the expressed protein, and accounts for an increase in size of the recombinant protein by 26 kDa.

6.6.1. Induction of protein expression using IPTG

Bacteria harbouring the correct plasmids were first grown overnight in 2 ml LB containing Ampicillin, then grown in 20 ml broth with Ampicillin overnight. The culture was added to 200 ml pre-warmed broth with Ampicillin and grown for two hours at 37 °C to allow the *E. coli* to enter its log phase. This ensures that the bacteria grow optimally to permit maximum protein expression. Expression was induced with 0.5 mM IPTG for three hours. The bacteria were then pelleted at 4000 rpm for 10 minutes at 4 °C, washed with TBS (40 mM Tris, 150 mM $NaCl_2$, pH 8.0), and the pellet frozen at -80 °C.

6.6.2. Extraction of proteins from BL21 Star™(DE3) cells

E. coli were lysed by lysozyme / Triton lysis. The pellets were thawed on ice and the bacterial outer cell wall lysed by an incubating in 1.5 mg/ml lysozyme (Sigma-Aldrich, Steinheim, Germany), 1 mM phenylmethylsulfonyl fluoride (PMSF) and 0.5 M DTT (Roche, Mannheim, Germany) on ice for 15 minutes. The cell plasma membrane was lysed by the addition of 1 % (v/v) Triton X-100 (Merck, Darmstadt, Germany). This was followed by the addition of 20 µg/ml DNase1 to eliminate DNA, and more PMSF (1 mM). The mixture was then incubated on ice for 45 minutes, centrifuged at 13000 pm for 25 minutes at 4 °C, and the pellet washed in 20 mM Tris (pH 8.0) containing 1 % Triton (w/v). PMFS is a protease inhibitor used to minimize protein degradation.

The expressed GST-fusion proteins were present in Triton-insoluble aggregates known as inclusion bodies, found in the pellet after Triton treatment, and were partially solubilized with 2 ml 20 mM Tris (pH 8.0) containing 1 % N-laurylsarcosine (sarkosyl) (w/v), an ionic detergent. Under these conditions, the recombinant proteins appear to be selectively solubilized, resulting in a semi-pure lysate.

6.6.3. Protein analysis by sodium dodecyl sulphate polyacrylamide gel electrophoresis (SDS-PAGE)

To verify protein expression, the semi-pure lysates were solubilized and then analyzed by polyacrylamide gel electrophoresis. The lower resolving gel was prepared with 10 % (w/v) acrylamide (Merck, Darmstadt, Germany), 0.27 % (w/v) bis-acrylamide (Merck, Darmstadt, Germany), 25 % (v/v) lower gel buffer (150 mM Tris, 0.4 % (w/v) SDS, pH 8.8), 0.03 % (w/v) ammonium persulphate (BioRad, Hercules, CA) and 0.1 % (v/v) TEMED (BDH Laboratory Reagents, England) in water. Following polymerization of the lower gel, the stacking gel was prepared with 25 % (v/v) stacking buffer (50 mM Tris, 0.4 % SDS (w/v), pH 6.8), 4.2 % (w/v) acrylamide, 0.1 % (w/v) bis-acrylamide, 0.03 % (w/v) ammonium persulphate and 0.1 % (v/v) TEMED in water.

Samples were prepared with a 4x sample application buffer (50 % (v/v) stacking buffer, 40 % (v/v) glycerol, 4 % (w/v) SDS, 4 % (v/v) 2-mercapto-ethanol in water) and heated at 100 °C for three minutes. SDS present in the resolving gel buffer (192 mM Glycine, 2.5 mM Tris, 0.1 % (w/v) SDS, pH 8.4) is responsible for conferring a negative charge to the protein to allow migration from the negative cathode, at the top of the gel, to the positive anode at the base, and for the denaturing conditions which permit the separation of proteins according to their molecular size and not charge.

Electrophoresis was performed at a constant current of 20 mA per single gel in a Mini PROTEAN® 3 Cell (BioRad, Hercules, CA) apparatus, with the use of a PowerPac Basic™ Power Supply (BioRad, Hercules, CA). As the dye front approached the base of the gel, the gel was removed and stained with Coomassie blue stain (45 % (v/v) methanol, 10 % (v/v) acetic acid, 0.25 % (w/v) coomassie blue, in 1 L water). The molecular size of the proteins was determined by comparison with a pre-stained Broad Range Protein Molecular Weight Marker (Promega, Madison, WI) run adjacent to the samples. Gel images were captured with a Kodak DC290 Zoom digital camera.

6.6.4. Protein purification

Two procedures were use to purify the GST-fusion proteins: affinity chromatography using glutathione-agarose columns (Sigma-Aldrich, Steinheim, Germany) and electro-elution from SDS-PAGE gel slices

6.6.4.1. Purification by electro-elution

In addition to protein expression confirmation, polyacrylamide gel electrophoresis was used to purify the recombinant proteins. The sarkosyl lysate and/or remaining pellet sample were prepared with the 4x sample application buffer and run on a gel as described previously. The gel was then incubated in 0.2 M imidozole containing 0.1 % (w/v) SDS for 15 minutes, washed with water, stained with 0.2 M zinc sulphate for one minute, and then washed again. The bands of interest were viewed against a dark background and excised from the gel. The gel strip was cut into smaller pieces and destained in clarifier solution (192 mM glycine, 25 mM Tris, pH 8.3). Proteins were then eluted from the gel pieces by electro-elution using an Electro-Eluter Model 422 (BioRad, Hercules, CA). The apparatus was set up as described by the manufacture's instruction and the elution buffer made with the same constituents as the resolving buffer used in SDS-PAGE. Elution was carried out at 30 mA for about 4 hours. Thereafter, the buffer containing the eluted proteins was removed and dialyzed (Cellulose membrane dialysis tubing, size 25 mm x 16 mm) overnight against 0.3x PBS to remove SDS, freeze-dried and resuspended in water. The samples were analyzed by SDS-PAGE.

6.6.4.2. Purification using glutathione-agarose beads

Affinity chromatography using glutathione-agarose permits selective purification of proteins containing glutathione binding sequences, such as GST. The agarose beads were swelled overnight in water and settled into columns, and the columns equilibrated at 4 °C with PBS containing 0.1 % (v/v) Triton (PBS-Triton). 2 ml 20 mM Tris containing 1 % (v/v) Triton and DTT to 10 mM was added to the semi-pure lysate and the mixture centrifuged at 15000 rcf for 25 minutes. The supernatant was diluted in 20 ml PBS, allowed to partially refold overnight at 4 °C and applied to the column. The column was washed with 20 ml PBS-Triton and bound GST-fusion proteins eluted with 3 ml PBS

containing 0.1 % (v/v) Triton and 30 mM glutathione. The pH of the PBS was adjusted to 7.4 after addition of the glutathione to ensure that proteins were not denatured, which would cause them to remain in the column. The eluted protein was freeze-dried, resuspended in water, analyzed by SDS-PAGE, and the approximate concentrations estimated by visual comparison to proteins of the Broad Range Protein Molecular Weight Marker of know concentrations.

6.7. Antibody preparation

BALB/c mice, supplied by S.A. Vaccine Producers (Johannesburg, South Africa), were used to raise antibodies to the recombinant proteins. Five mice were immunized with each antigen. 800 µl antigen solution, containing approximately 200 µg of purified protein, was emulsified with 1 ml complete Freund's adjuvant (Sigma-Aldrich, Steinheim, Germany) by vortexing for one hour. 300 µl of the emulsion was administered to each mouse intraperitoneally. Incomplete Freund's adjuvant was used for a booster immunization three weeks after primary immunization and for subsequent boosters every three weeks.

Blood was collected from the tail vein of each mouse one week after each booster immunization. The blood was allowed to clot and then centrifuged at 13000 rpm for 10 minutes. The supernatant (serum) was removed and centrifuged again to ensure all blood cells and cell fragments had been removed. Sodium Azide (BDH Laboratory Reagents, England) was added to a final concentration of 0.04 % (w/v) to prevent bacterial growth, and the serum stored in aliquots at -80 °C.

In addition, antibodies to µ1, the σ-chains and *Pf*rab6 were raised in rabbits by GeneScript Corporation (USA) using synthesized peptides. The peptide sequences were:

µ1-1	NENKDLYYKRPVNVC
σ1	CIDKGDNELITLEI
σ4	VNKQGQTRLSQYYNC
*Pf*rab6	TTKWIQDILNERGKC

6.8. Enzyme-Linked Immunosorbent Assay (ELISA)

Antibody responses were evaluated by enzyme-linked immunosorbent assay (ELISA). Wells of a 96-well microtitre plate (CellStar, Greiner Bio-One) were coated overnight with 0.1 µg antigen in PBS at 4 °C and washed 4 times with 0.1 % (v/v) Tween 20 (Sigma-Aldrich, Steinheim, Germany) in TBS, before blocking with TBS-Tween containing 1 % (w/v) Bovine Serum Albumin (BSA, Boehringer Mannheim) for one hour. Consecutive two-fold dilutions of pooled sera using blocking solution were incubated for one hour, followed by a further 4 washes. Goat anti-mouse Horseradish peroxidase (HRP) (KPL, Gaithersburg, MD), diluted 1:2000, were added to wells for one hour. Plates were then washed 4 times with TBS-Tween, once with 0.1 M phosphate-citrate buffer (0.05 M citric acid, 0.07 M di-sodium hydrogen phosphate in water, pH 4.8), and quantitated with OPD colorimetric substrate (phosphate-citrate buffer containing 1 mg/ml o-phenylenediamine and 0.5 µl/ml hydrogen peroxide). The colour reaction was stopped with the addition of 50 µl (per well) 2.5 N sulphuric acid and absorbance read at 492 ηm. No primary antibody was used for the negative controls, and for the positive control, rabbit anti-GST (Sigma-Aldrich, Steinheim, Germany) 1:5000 was used with a rabbit secondary anti-HRP. ELISA was performed in duplicate on pooled bleeds from three different mice for µ2 and µ4 sera.

6.9. Western blotting

Western blot analysis was performed to determine if the antisera recognize specific malaria proteins. Proteins obtained from saponin treated parasites (described previously) were solubilized in 4x sample buffer and run on a SDS-PAGE gel, and the gel incubated in transblot buffer (192 mM glycine, 25 mM Tris, 20 % methanol in water) for 15 minutes. The proteins were then electrophoretically transferred to a Polyvinylidene Difluoride (PVDF) membrane (Immobilon™-P, Sigma-Aldrich, Steinheim, Germany) in a Mini Trans-Blot® Electrophoretic Transfer Cell (BioRad, Hercules, CA) at 100 V for one hour. Prior to transfer, the PVDF membrane was cut to the appropriate size and equilibrated in transblot buffer for 15 minutes. The membrane was layered on to the gel, the two placed between wet filter paper and sponge, and enclosed in a blot cassette. The cassette was assembled in the transfer cell and the chamber filled with transblot buffer.

After protein transfer the membrane was cut into strips. Each strip was blocked with incubation buffer consisting of 5 % (w/v) fat-free milk powder (Elite™ Clover, Roodepoort, South Africa) and 0.5 % (v/v) Tween in TBS for 40 minutes. Each antiserum was diluted 1:1000 in incubation buffer and applied to a single strip for one hour on a Duomax 1030 rocking platform shaker (Heidolph®, Schwabach, Germany). The membranes were then washed 4 times in 0.5 % (v/v) Tween-TBS. The secondary antibody, either a goat anti-mouse IgG (whole molecule) peroxidase conjugate (Sigma-Aldrich, Steinheim, Germany) for mouse derived primary antisera or goat anti-rabbit IgG peroxidase conjugate (Sigma-Aldrich, Steinheim, Germany) for rabbit antisera, was diluted 1:5000 and incubated with the membranes for one hour. The membranes were then washed a further 4 times, drained of excess fluid, and covered with a layer LumiGLO® chemiluminescent substrate (KPL, Gaithersburg, MD) for two minutes. They were then drained on tissue paper, covered with clear plastic and exposed to an X-ray film (Kodak BioMax Light Autoradiography Film, Sigma-Aldrich, Steinheim, Germany) for varying amounts of times ranging from 10 seconds to one minute. The film was developed with Kodak GBX Developer and fixed with Fixaplus X-ray Fixer (Champion). Western blots images on developed autoradiograph film were captured using a Kodak DC290 Zoom digital camera.

Antigen competition experiments were performed on strips of membrane containing parasite proteins to verify that the μ1 antiserum contained antibodies recognizing the recombinant μ1 antigen. Two 5 ml antiserum solutions (1:1000 dilutions) were prepared. 10 μg purified μ1 antigen was added to one of the preparations, and both solutions incubated at room temperature for one hour. The preparations were used separately on two strips of membrane and standard western blot procedure carried out.

6.10. Immunofluorescence microscopy assays (IFA)

6.10.1. General IFA

Parasites were released from erythrocytes by saponin treatment (described previously), washed repeatedly with PBS to remove haemoglobin, and immobilized on poly-lysine (1 mg/ml) coated glass coverslips. Unbound parasites were removed with further PBS

washing. Parasites were fixed for 15 minutes with either ice-cold methanol or a 4 % (w/v) paraformaldehyde (PFA) (Sigma-Aldrich, Steinheim, Germany) solution containing 0.25 % (v/v) glutaraldehyde (Fluka, Buchs, Switzerland) in PBS. Following more washes, PFA / glutaraldehyde fixed parasites were permeabilized with 0.1 % (v/v) Triton in PBS, and the coverslips treated with 0.15 M glycine for 20 minutes to quench free aldehyde groups of glutaraldehyde, thereby preventing unspecific binding to amine groups of antibodies. Coverslips were subsequently incubated in block solution (50 % (v/v) foetal calf serum (Highveld Biological, Kelvin, South Africa), 2 % (w/v) BSA, 1 mM $MgCl_2$, 1 mM $CaCl_2$, 0.1 % (v/v) Tween in PBS) for 30 minutes. Primary antibodies, diluted 1:200 in block solution, were spotted onto parafilm in a moistened chamber and coverslips incubated face down on the drops for one hour. After washing, coverslips were inverted on drops containing fluorochrome-conjugated secondary antibody (diluted 1:250) for one hour. For mouse-derived primary sera, either a fluorescein isothiocyanate (FITC)-conjugated goat anti-mouse antibody (KPL, Gaithersburg, MD) or an Alexa fluor® 488 goat anti-mouse IgG (Invitrogen, Frederick, MA) was used, and for rabbit sera, a tetramethylrhodamine B isothiocyanate (TRITC)-conjugated goat anti-rabbit antibody (Invitrogen, Frederick, MA). Coverslips were washed a final 4 times and parasite nuclei stained by incubation for 30 seconds in PBS containing 1 μg/ml 4',6'-diamidino-2-phenylindole dihydrochloride (DAPI). The coverslips were rinsed in water and mounted face-down on glass slides in Permafluor® Aqueous mounting medium (Immunotech, France). All microscopy assays were performed on a Nikon Eclipse E600W fluorescent microscope with a Y-FL EPI-Fluorescence attachment, fitted with a 100x oil-immersion objective. Images were captured with a Media Cybernetics CoolSNAP-Pro monochrome cooled charge-coupled device camera.

6.10.2. Co-localization IFA

Co-localization studies using two different mouse derived antibodies followed the general immunofluorescence microscopy procedure described above. After incubation with the first primary antibody followed by FITC-conjugated or Alexa fluor® 488 goat anti-mouse secondary, the parasites were washed and treated with PFA / glutaraldehyde once again to fix the antibodies in place, and with glycine to block non-specific sites. Samples were subsequently incubated with blocking solution and the second primary antibody and a TRITC-conjugated anti-mouse secondary antibody added sequentially.

Localization of the different fluorochrome-conjugated secondary antibodies was observed with the different fluorescent filters (FITC and TRITC-filters) on the microscope. Negative controls contained no second primary antibody, to confirm that the final TRITC-conjugated secondary antibody does not cross-react with free binding sites on the first primary antibodies, and yield spurious apparent co-localization.

For co-localization where mouse and rabbit derived sera were used, the primary antibodies were added simultaneously, and after washing, both secondary antibodies were added (usually Alexa fluor® 488 goat anti-mouse and TRITC-conjugated anti-rabbit antibodies).

Dual labelling IFA with the mitochondrion stain, MitoTracker® Red CMXRos (Molecular Probes, Invitrogen), followed the procedure suggested by the supplier. Live trophozoite stage parasites were incubated with 100 ηM MitoTracker® for 30 minutes in the dark, washed with complete medium and fixed onto coverslips with paraformaldehyde. The general immunofluorescence microscopy procedure described above was then carried out in minimal light.

6.11. Electron microscopy (EM)

Immuno-EM localization was preformed to validate and extend the IFA results. Trophozoite-infected erythrocytes were enriched using LD columns that become magnetized in a strong magnetic field and a midi-MACS cell separation system (Miltenyi Biotec GmbH, Bergisch Gladbach, Germany). This procedure utilizes the magnetic properties of the iron found in haemozoin in mature stage parasites. Trophozoite-infected erythrocytes are retained in the column, while uninfected and ring stage infected erythrocytes (which lack haemozoin) pass through (Trang *et al.*, 2004). The trophozoite-infected erythrocytes may then be eluted from the column by removing it from the midi-MACS magnet. Alternatively, trophozoites were released from erythrocytes using saponin lysis as described earlier, and were sedimented by centrifugation at 2000 rcf.

The enriched erythrocytes or isolated trophozoites were fixed in fixing buffer (0.1 M sucrose, 0.1 M sodium cacodylate, 2 mM $MgCl_2$, 2 mM $CaCl_2$, pH 7.4) containing 4 %

(w/v) paraformaldehyde and 0.2 % (w/v) glutaraldehyde for one hour. The fixed cells were immobilized in plugs of 2 % (w/v) low melting point agarose in fixing buffer, dehydrated in a series of ascending ethanol concentrations, and embedded in LR White resin (Electron Microscopy Sciences, PA). Ultra-thin sections of about 70 to 80 ηm were prepared from the resin samples using a Reichert Ultracut ultramicrotome and immobilized on nickel grids. The sections were rehydrated in PBS for 10 minutes and unreacted aldehyde groups quenched in PBS containing 5 mM glycine for 5 minutes. All incubations, antibody staining and washing steps were carried out by floating the grids on drops of the relevant buffers in a humidified container.

The sections were first blocked in PBS containing 5 % (v/v) goat serum for 20 minutes, then incubated for one hour in the primary mouse antisera diluted 1:800 in incubation buffer consisting of 0.2 % (v/v) goat serum and 0.2 % (w/v) acetylated BSA (Aurion-BSA; Electron Microscopy Sciences, PA) in PBS. After washing three times with washing buffer (0.2 % goat serum in PBS), they were incubated in incubation buffer containing a 1:250 dilution of rabbit anti-mouse antiserum (Calbiochem, la Jolla, CA) for one hour. After further washes, they were incubated in 10 ηm colloidal gold-conjugated goat anti-rabbit antiserum (GE Healthcare, UK) diluted 1:25 in incubation buffer for one hour. Sections were then sequentially washed twice in washing buffer, PBS containing 0.1 % (v/v) Tween 20, and PBS. Bound antibodies were fixed to the sections by incubating the grids in PBS containing 2 % (w/v) glutaraldehyde for 10 minutes. This was followed by a final wash in water and sequential incubations in 2 % (w/v) uranyl acetate for 8 minutes and 2 % (w/v) lead acetate for 4 minutes to contrast the sections. The grids were viewed with a Jeol 1200EXII transmission electron microscope.

Appendix

A-1. Nucleotide, amino acid and peptide sequences.

A-1.1. Nucleotide sequence of PF13_0062 (µ1)

Amino acid sequence

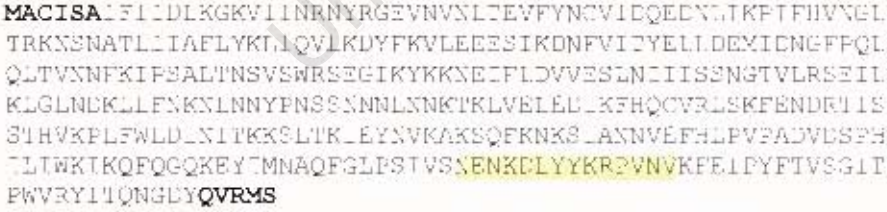

The nucleotide and amino acid sequence of the *Plasmodium falciparum* AP-1 complex subunit µ1. The forward (μ_1-F) and reverse primer (μ_1-R) sequences are highlighted in red. The full length gene was amplified (1314 bp). dsRNA knockdown reverse primer is highlighted in blue. The synthesized peptide fragment of µ1 is highlighted in yellow.

A-1.2. Nucleotide sequence of PFL0885w (μ2)

ATGATCGATGGGCTGTACATATTTTTATTAACGGGCAACTTCTGATACAAAGAAATTATCCAGACACAA
CCAAAAGAACTGATTCAACAGAATACATAAATAAATATATAAAAACGAAACGTTTTTATCAAAATCCGAT
TGTTGAAATAAATAACAGCATTTTTTATAAACGTAAACATAAATGAAACAGTTATAACCGTACTAACAAGA
AGCAATTCAAATATACGTTTGATATTTAACTTTATACATAAATTCATTGAGATATTAAAATATTTTTTA
ATAATGAATTATCTGGAATAAATATTGTAAATAATTCTGTGTTAATACATGAAATATGTGATGAAACAAC
AGATTATGGATATCCACAAACATTAGAAGTGAATATATTAAAAAATAGCTTACTAAACAAAGTTAAATAC
TATAGTAAAACACTCTAGATACTTTCAGAAAATACAAATGAATTATCAAATGTAAATAGTGTGATTGAAG
ATATTGTACATGATCCACATATACATAATACGACAACTAATAATAAAAAGAATAAATCGAATAATAAAAT
TAGAGACTTTTATAATACAAAAAGTGTTAAAAATAAAAATACGTATGATTTAAATGAAACAAATAAATTA
AAACATATAGGTAAACGAAACATTAAACAGAATAAAAAATAAAACAACTAATAATAATAATAATAATAATA
AGACAGCAAATCATCTTAATTATATAACAGGTAATTGTACATGGAGAAATAATAATACTTATTATAAGAA
AAATCAAATATATATACATACATTACAAATATTAAATGTAACTATAAATAGTAATAATTTAATATATGCT
CATATAAATGGAAAGGTAACCTTAAAATGTCACCTCTCCGGAATGCCTTTATGTGAACTAAGCACAAATA
ATAAAACTAATTTACTAAAGAATATTCTCGCCGGTAGTAACACAAGTAACAATAATAATAATACAAGTAA
TAATAATAACAAAACAAATCAAGGAAATGCCCTACGGGGTAGTTGTGGATCGAATAGTTGGTTAATAAT
AAAGTTATGCAAAATAATTTAAAGAAAAAATATACACTCGATGAAAAAGATAATGAAGAAATAATTATTG
ATAATTCCATATTTCATCATTCTCTTACCTTATCCAAATATGAAAATAATAAAGTTATTACCTTCACACC
ACCAGATGGTACATTTGAATTAATGAAATATACCATAACAAAAAATATTCAAATACCTTTCATATCCTA
GCTATATATAATCCTATATTAGAATATTCAAAAAATGTAGAAAAAAAATTCTCTTTAAAAAAATTAACTA
CTAATAATAAAAGCATCTATGGTGAATACAAAAATACAAACAAATATGAATACTCTGTTACCATTAAATC
AAATTATAAAGCAAATATGCATGCATCTGATGTATTAATTAAAATACCAATCTATAAATTCTCAGAAAAT
GTTCAAGTTAAATATAAATCCATAGCAAAACTGAATTTAATAATATACATAGTTTGGTTATATGCAGAA
TCAAAAAATTCCTAAGTTCAAGTGAACATAATATAAAAATACATTTAAGCTTACAAAATCATAATCAAAT
TTATTCTAATACGAATAACACACAAAAAGTAGACGACTTATCAAAAGTTGTGTTACAAGTACATAAAATT
AAAAACATGAATACTGTCAAATCTTCAAACACATACAAAATGCCCATAACACTGAGCTTTAAAATACCTA
TGTTTACCTCAAGCCGCATGTACATAAGATACCTCAAGGTTCCGAAAAATCAAATCATAAGATAATTAA
GTGCATCAAGTATCTAACAGAATCGGGCATCTACCAGTATAAATAG

Amino acid sequence

MIDALYIFFINGQLLTQRNYRDTTKRTDLTQYINKYIKTKRFYENPIVEINKVFFIKVNINEIVITVLTR
SNSNICLIFNEIYKFLELLKYEFNNELSGLNIVNNFVLIYETCDEIIDYGYPQTLEVNILKNSLLNKVKY
YSKTSRYFQKISNELLNVNSVIEDIVHDPHLHNRISNNKKNKSNNKIRDFYNTKSVKNKNTYDINETNKL
KYIGKETLNRIKNKIINNNNNNKTANCFNYITGNCTWRNNNIYYKKNEIYIDILEILNVTINSNNLIYA
HINGKVTLKCHLSGYPLCELSINNKINLLKNIGAGSNISNNNNNISNNNNKTNQGNALRGSGGSNSLVNN
KVMQNNLKKNYTIDEKDNEEIIDNGIFHHGVTLSKYENKKVITFTPPDGIFELMKYTITKNIQIPFHIL
AIYNFILEYSKNVEKKFSLKKLTTNNKSIYGEYKNTNKYEYSVTIKSNYKGNMHASDVLINIPIYKFSEN
VQVKYKSIGKIEFNNIDSIVIWFIKKFLSSSEHNIKIHLTLENHNQIYSNMNNIQKVDDLSKVVLQVHKI
KNMNIVKFLNIYKMPITLSFKIPKFTSSGMYIRYIKVFEKSNYKIIKWIKYILTESGIYQYK

The nucleotide and amino acid sequence of the *Plasmodium falciparum* AP-2 complex subunit μ2. The forward (μ_2-F) and reverse primer (μ_2-R) sequences are highlighted in red. The full length sequence has a length of 1866 bp, though only a portion of the gene was amplified (1031 bp).

A-1.3. Nucleotide sequence of PF11_0202 (μ4)

ATGGTGATATCCCAATTTTATATTTTGTCTCCAAGAGGGGATACCATTATTAATAGAGATTTTCGTGGAG
ATATAATAAAAGGTAGTGCCGAAGTATTTTTTCGAAATGTAAAATTATATAAAGGTGATGCACCTCCAGT
TTTTTATTTGAATCGTATAAATTTTACATATTTGAAAAGTAATAGTTTATATTTGTAGTAACATCATTG
TTTAATATTTCTCCAAGTTATTTAATTGAATTATTACATCGGTTGCTAAAAATATTTAAAGATTTTTGTG
GACAAATTACAGAAGAATTAATACGAACCAATTTTATTTTAATATATGAAATAATAGATGAAATAATAGA
TTATGGTTATTTACAAAATAGTAATACAGAATATATAAAAAATCTAATACATAATGAAATAGCAACAAAT
AATAATACAGTGAAAAAATTTGCCAACCTACCTAATTTTTCTATAAAAAATACAAATACATTACCATCAA
ATGCATCCCAAAAACCTATACAAATTAATGATAAAAAAAATGAAATATTTATAGATATAGTTGAAAAAT
TAATTTAATTATGAATTCGAATGGAGAAATAGTATATTCATATATTGATGGTGTATACAAATAAAATCT
TACTTATTAGGAAATCCATTTATCAAAATAGCTTTGAATGATGATTTATATATTAAAAATATTCATCATG
ATAATTCAAATAATATTATTATTGACGATTGTAATTTTAATCATCTAGTTAATTTATCACAATTTGAAAA
AGATAAAATTCTATCTTTATACCAACCAGATGGTGAATGTGTACTTATGAATTATCGAATCAATAATAAC
TTTAAAGCGCCTTTTCAAAATATATGCTAATGTTATATATAACCAAAATCATACGGTAGAATTGTGTATAA
GAATACGGCTAGATATCCCTTCTCAATATACATGCACAAATGTATTTGTTATTGCAATTTATGTAAACA
CATAACTAATGTACATTTGGACTTGAATACGAATTCGGATTTATTCTCAGCTCAATATATATCAAATGAG
AACAAATTATTATGGACCATCAAAAAATTCAAGGGAGAACACGAATATAGTATTCGATCAAAAATTACCT
TAAGTCCTCATTATGCCTTTTCAAAACGAGATTTTGGACCTATATATATTTATTTGAAATACCAATGTT
TAATTTATCAAAACTTAGAATAAAATATCTGAGCATAATTGAAAATTACAAAACAAGTAATACGCACCGA
TGGGTGCGTTATATAACTCAATCTTCTTCATATGTTTACCGTTTGAACTGA

Amino acid sequence

MVISQFYILSPRGDTILNRDFRGDILKGSAEVFFKNVKLYKGDAPPVFYLNGINFTYLKSNSLYFVVTSL
FNLSPSYLIELLHRLLKIFKDFCGQITEELIRINFILIYEIIDFITDYGYLQNSNTEYIKNLTHNEIATN
NNCVKKFANLPNFSLKNTNTLPSNASQKFLQLNDKKNEIFLDLVEKINLLMNSNGELVYSYIDGVIQIKS
YLLGNFFIKIALNDDLYIKNTHFDNSNNTITDDCNFNHLVNLSQFEKDKILSLYQPDGECVLNNYRINNN
FKAPFKIYANVLYNQNHTVELCIRIRLDIPSQYTCTVFVYCNLCKHITNVFLDINTNSDLPSAQYISNE
NKILWTIKKFKGFHEYSTRSKTTLSPHYAFSKRDFGPIYTLFFIPMFNLSKLRINYLRIIENFKTSNTHR
WVRYITQSSSFVYRLN

The nucleotide and amino acid sequence of the *Plasmodium falciparum* AP-4 complex subunit μ4. The forward (μ_4-F) and reverse primer (μ_4-R) sequences are highlighted in red. The full length sequence has a length of 1311 bp, though only part of the gene was amplified (852 bp).

A-1.4. Nucleotide sequence of PF11_0187 (σ1)

ATGATTCATCTTCTACTACTCATCAGCGGACAAGGAAAAACGCGACTAGCCAAATGGTACATCCCTCTAT
CTCAAAAGCAAAAGCCAAAAATAATAAGACAAACATCACAAATAACCTTAAACACGACTCCAAAACTTCG
TAACTTTGTGGAATGGAGAGAATATAAACTTGTTTTTAAAAGGTATGCAAGTTTATTCTTCATTGCTTGT
ATAGATAAAGGCGACAACGAATTAATCACCCTGGAAATTATACATCACTATGTACAAATCTTAGATAAAT
ATTCTCGTAATCTTCGTCAACTTGATCTAATTCTTAATTCTCATAAAGCTTATTATTTACTACATCAAAT
ATTAGTAACTGGTGAAATGCAAGAAAGTAGTAAAAAAACAATCCTCCGTATTGTCGCAGCTCAAGACTCA
TTAATGGAAGATAATAAAACTACCAAAAAATTAGGAGCCCTTATATAA

Amino acid sequence

MIHFVLLTSRQGK**TRLAKWY**TPLSQKFKAKLTRFTSQTTLNRTPKLCNFVFKRFYKLVFKRYASLFFTAC
LDKGDNFLTTLEICIIIYVEILDKYFCNVCELDLIFNFIIKAYYLLDEILVTGEMQESSKKTILRI**VAAQDS**
LMEDNKTIKKLGALI

The nucleotide and amino acid sequence of the *Plasmodium falciparum* AP-1 complex subunit σ1. The forward (σ_1-F) and reverse primer (σ_1-R) sequences are highlighted in red. The amplified PCR product has a length of 387 bp. The synthesized peptide fragment of σ1 is highlighted in yellow.

A-1.5. Nucleotide sequence of PFD1090c (σ4)

ATGATACAATTCTTGTTAATGGTCAATAAACAAGGCCAAACTACGTCAACCCAATATTACAATCATTTAA
GTATTGAAGAAAAAACTATATTAGAAGGAGAACTTATAAGAAAATGTTTATCAAGAGTGGATTATCAGTG
TTCTTTTTTACAATATAGGGAATATAAAATTATTTACAGAAGGTATGCAAGCTTATATCTCATCGTTGGG
GTATCAGACCAAGACGTTAACGAATTGCTATTCTCGAAATGATTCATAACATAATAGAAATCCTGGATA
AATATTACGAAAATGTTTGTGAATTAGATATCATGTTCAATATTGACAAAACACATTTTATTATAGACGA
AATTATTTGTAATGGAGAAATCTGTGATATGAACAAAACTAATGTCTTGAGACCAATTCTGTTAATGGAT
AAACTTTCTCTAAAAATCTAA

Amino acid sequence

MIEFLIMVNKQGQTRLSQYYNHLSIEEKTILEGELIRKCLSKVDYQCSFLQYREYKIIYRRYASLYLIVG
VSDQDVNEFATLEMTHNIIETLDKYYENVCELDIMFNIDKTHFLIDEICNGELCDMNKTNVLRPILLMD
KVSLKY

The nucleotide and amino acid sequence of the *Plasmodium falciparum* AP-4 complex subunit σ4. The forward (σ_4-F) and reverse primer (σ_4-R) sequences are highlighted in red. The amplified PCR product has a length of 408 bp. The synthesized peptide fragment of σ4 is highlighted in yellow.

A-1.6. Nucleotide sequence of PF11_0461 (*Pf*rab6)

ATGGATGAATTTCAAAACTCGGGACTAAATAAATACAAACTTGTTTTCTTAGGAGAACAAGCTGTTGGTA
AAACATCTATAATTACAAGACTCATGTATGATACCTTTGACAACAATTACCAATCGACTATTGGTATAGA
TTTTTCGAGTAAGACATTATATTTGGATGAAGGTCCTGTACGCTTACAATTGTGGGACACTGCAGGTCAG
GAAAGATTTCGAAGTTTAATTCCAAGTTATATTAGGGACTCCGCAGCAGCAATTGTTGTATATGATATTA
CTAATAGACAATCCTTTGAAAATACCACAAAAAGGATACAGGATATTTCAATGACAGAGCAAAAGATGT
TATAATTGCTTTAGTAGGAAATAAAACAGATTTAGCTGATCTTAGAAAAGTTACATATGAAGAAGGAAAG
CAAAAAGCTCAAGAATATAATACCATGTTTCATGAAACGACTGCTAAAGCTGGACATAATATAAAAGTTT
TGTTTAAAAAAAATTGCATCAAAATTACCAAATTAGATAATACAAATAATAATGAAGCCAATGTTGTAGA
TATACAATTAACTAATAATTCAAATAAAAATGACAAAAATATGTTAAGTAAATGTTTATGTTAA

Amino acid sequence

MDEFQNSGLNKYKLVFLGEQAVGKTSIITRFMYDTFDNTYQSTIGIDFLSKTLYLDEGPVRLQLWDTAGQ
ERFRSLIPSYIRDSAAAIVVYDITNRQSFENTTKWIQDILNERGKDVIIALVGNKTDLGDLRKVTYEEGM
QKAQEYNTMFHETSAKAGHNIKVLFKKIASKLPNLDNTSNNEANVVDIQLTSNSNKSDKYMLSKCCC

The nucleotide and amino acid sequence of the *Plasmodium falciparum* Rab6. The forward (Rab6-F) and reverse primer (Rab6-R) sequences are highlighted in red. The full length sequence has a length of 531 bp, though only part of the gene was amplified (405 bp). The synthesized peptide fragment of rab6 is highlighted in yellow.

A-2. Plasmid maps.

A-2.1. pGEX-4T-1 vector containing the µ1 PCR product

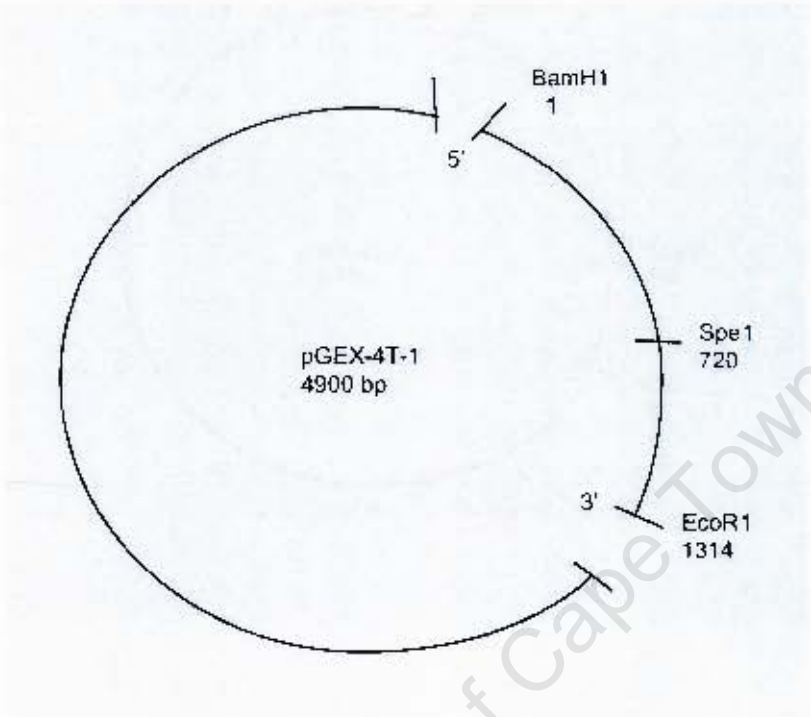

A-2.2. pGEX-4T-1 vector containing the µ2 PCR product

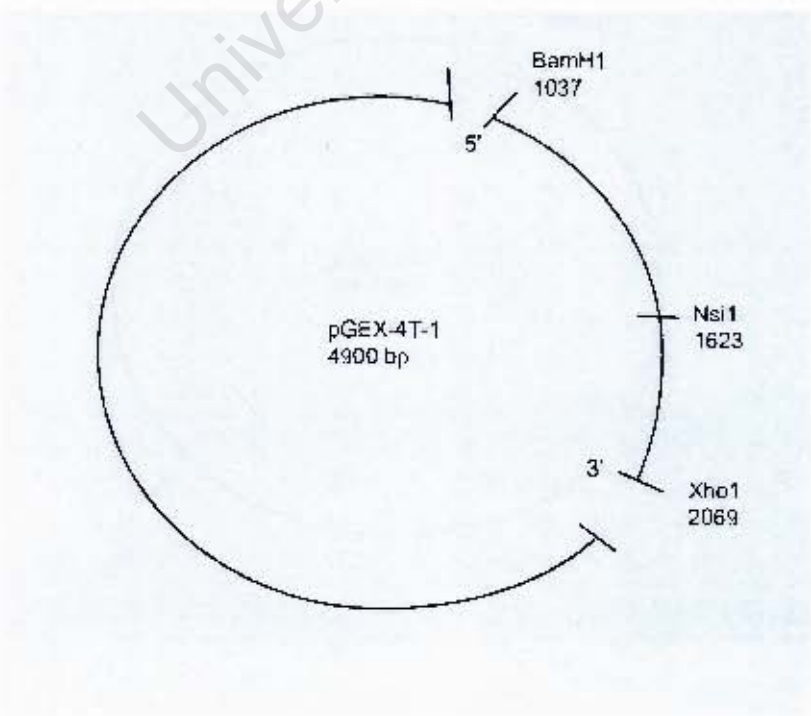

A-2.3. pGEX-4T-1 vector containing the μ4 PCR product

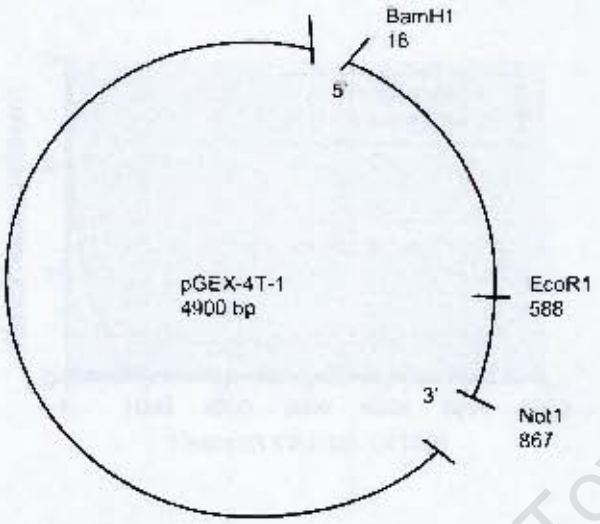

A-2.4. pGEX-4T-1 vector containing one of the σ PCR products or the Rab6 PCR product

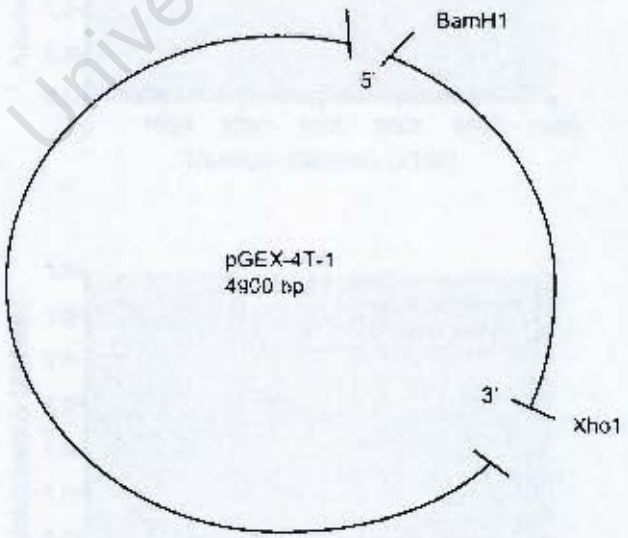

A-3. ELISA by GeneScript Corporation.

A-3.1. ELISA preformed on μ1 anti-peptide antibodies

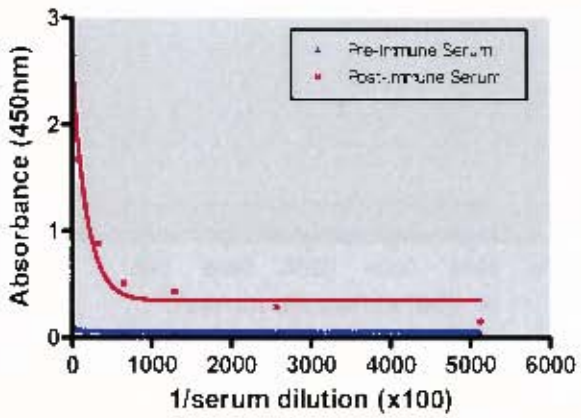

A-3.2. ELISA preformed on σ anti-peptide antibodies

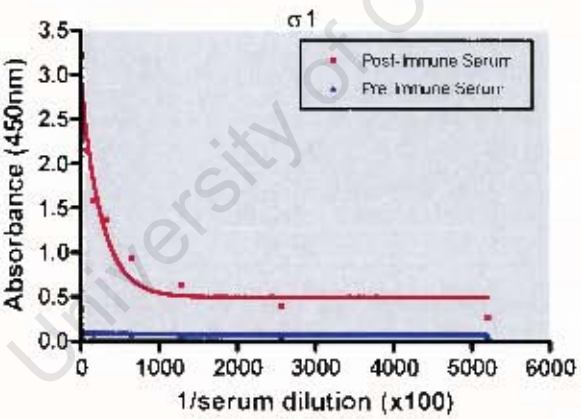

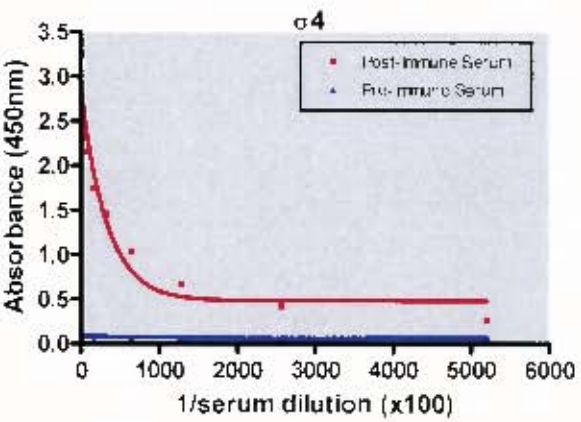

A-3.3. ELISA preformed on Rab6 anti-peptide antibodies

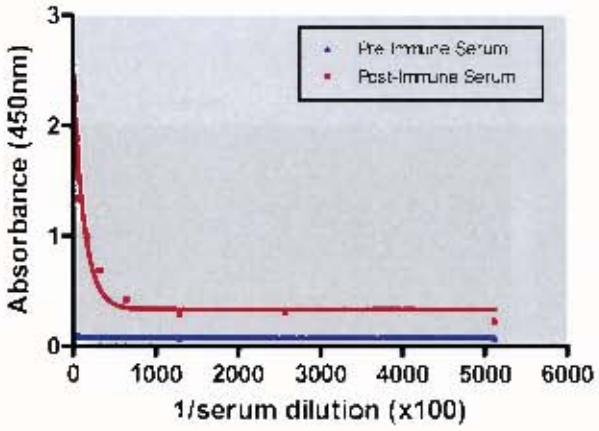

ELISA performed on μ1, σ and Rab6 anti-peptide antibodies.

The graphs illustrate a strong immune response for each antiserum (red) relative to the control pre-immune serum (blue).

A-4. Dual-localization experiment with ERD2-GFP expressing parasites and µ1.

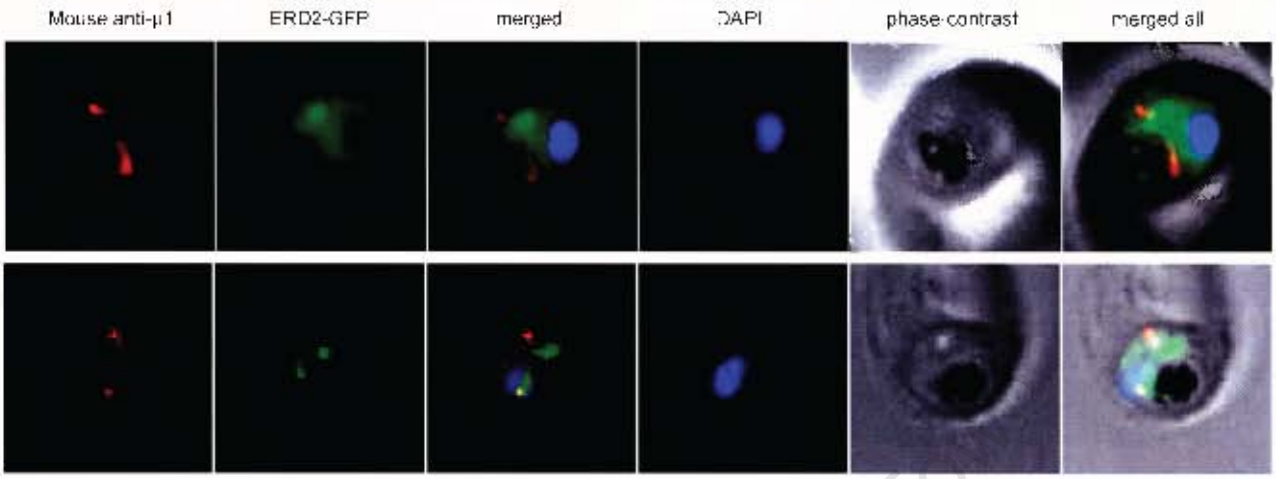

Localization of ERD2-GFP and µ1 in *P. falciparum*.

The ERD2-GFP expressing parasites are shown in green (second frame) and the µ1 antisera in red (first frame). In the merged image, the two signals are separate, however there is some association between the two (second row).

Dual labelling experiments with ERD2-GFP expressing parasites and µ1 antibodies were performed by Dr Nicole Struck (Hamburg, Germany). ERD2 is a *cis*-Golgi marker. The results indicate that ERD2 and µ1 localization are distinct from each other, but in some instances there is some overlap of the signals. This signifies that µ1 does not localize to the *cis*-Golgi but perhaps to distal Golgi membranes.

A-5. Examples of EM images of Golgi staining in the parasite (Witola *et al.*, 2006).

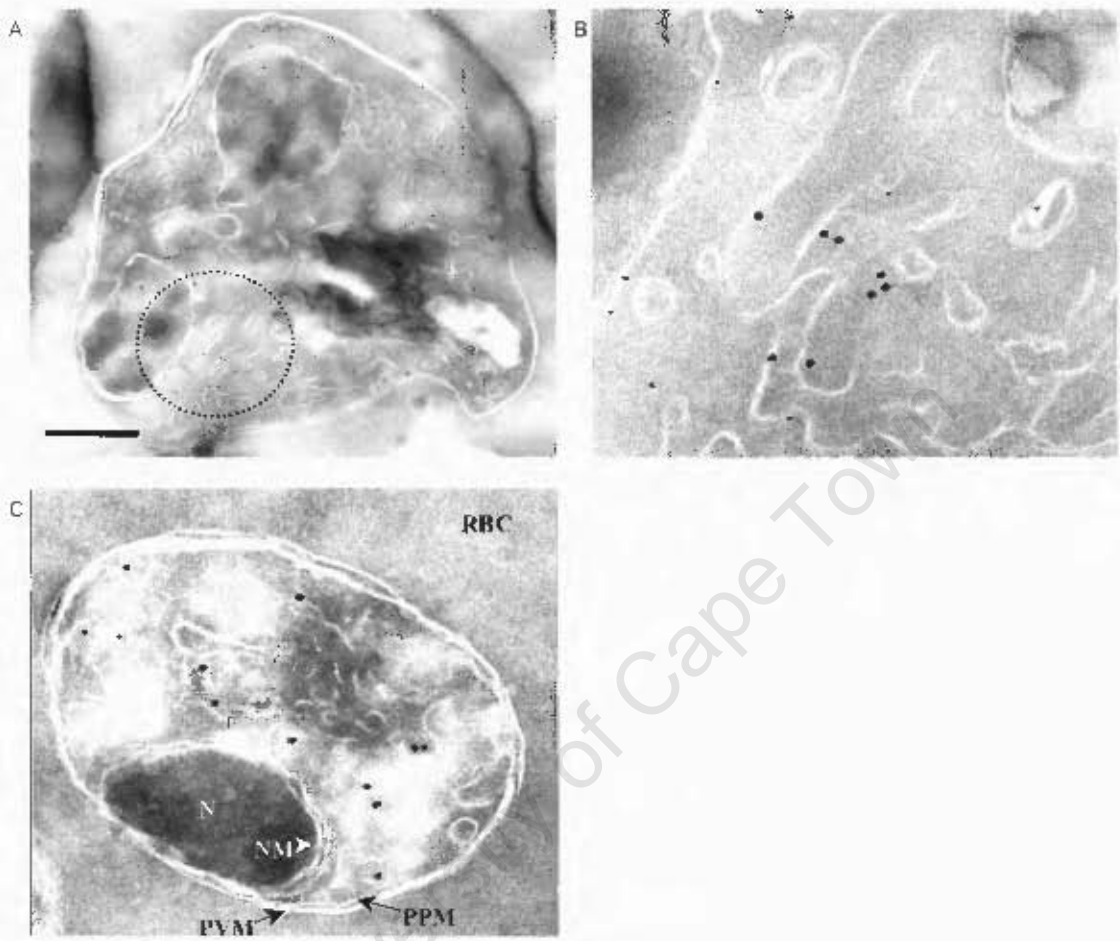

Transmission electron micrographs of cryosections of intra-erythrocytic parasites expressing the Pfpmt-GFP fusion protein. *P. falciparum* phosphoethanolamine methyltransferase (Pfpmt) resides in the Golgi apparatus of the parasite and has complete co-localization with Rab6, a marker of the Golgi. (A) Immunogold labelling (18-nm gold particles) of GFP antibodies bound to parasites. Anti-BiP antibodies (12-nm gold particles) label the ER. (B) Magnification of the region in panel (A) depicted in the dotted line. (C) Immunogold labelling of GFP (18-nm gold particles). *N*, nucleus; *NM*, nuclear membrane; *RBC*, red blood cell cytoplasm; *PVM*, parasitophorous vacuole membrane; *PPM*, parasite plasma membrane. Taken from Witola *et al.*, 2006, page 21308.

A-6. dsRNA knockdown.

RNA interference (RNAi) involves the introduction of double-stranded RNA (dsRNA) or anti-sense RNA corresponding to the target sequence into the parasite. RNAi was used to determine if the µ1 antisera is specific for the µ1 adaptin. This was achieved by specifically reducing the levels of µ1 mRNA by introducing dsRNA, that corresponds to a portion of the µ1 adaptin gene sequence, into the parasite, resulting in the selective degradation of the mRNA and hence the inhibition of protein expression. The target sequence was inserted into the pGEM®-T easy plasmid and the DNA linearized using the Sal1 restriction enzyme. RNA corresponding to the sense and antisense sequences of the target mRNA was produced using Promega translation kits (RiboMAX™ Large Scale RNA Production System- SP6 and T7). The RNA was extracted and the complimentary strands annealed by heating to 78 °C then cooling slowly overnight. The reaction yielded approximately 10 µg/µl dsRNA. 200 µg was added to a 2 ml ring culture (Pst 10 %) and after 24 hr at 37 °C, the parasite pellet collected. Control cultures were set up with equivalent volumes of DEPC-treated water being added instead of dsRNA.

Primer sequences for DNA template for dsRNA synthesis.

Forward 5' ATGGCATGTATAAGCGCT 3'
Reverse 5' GCTTTTATTTTTAAATTGTGATTTTGC 3'

The primers produced a PCR product of 948 bp. A-1.1. shows the forward primer in red and the reverse primer in blue.

Semi-quantitive RT-PCR and agarose gel electrophoresis was used to assess the knockdown observed at RNA level. Samples were taken after 15, 20 and 30 cycles of amplification and the percentage knockdown was calculated using the 20 cycle samples. Western blot analysis shows the effect at protein level. Percentage knockdown was calculated digitally by quantitating band intensity. Actin controls were used for protein level analysis only.

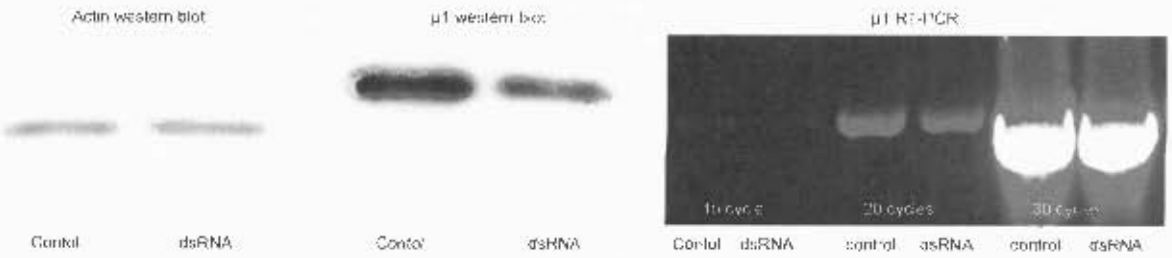

Knockdown at RNA and protein level.

The first two images show protein levels assessed by Western blot. Levels of irrelevant control protein, actin (43 kDa), remain unchanged with the addition of µ1 dsRNA. A clear decrease in protein level is seen when the µ1 adaptin is probed. RNA levels are shown in the third image. Percentage knockdown was calculated using the 20 cycle samples as the 15 cycle samples did not yield sufficient PCR product for comparative analysis, and after 30 cycles, too much product was present.

A 30 % knockdown was observed on RNA and protein level when parasites were treated with µ1 dsRNA. Protein reduction appears specific since the levels of irrelevant control protein remain unchanged, suggesting that the protein probed by the anti µ1 is in fact the µ1 adaptin.

A-7. RACE PCR.

RACE PCR, a method used to determine the 5' and 3' ends of a gene, was performed to establish whether the predicted μ1 gene sequence is correct or if the open reading frame is longer. For 3' RACE, RT-PCR was performed using an oligo(dT) anchor primer, TAP, which initiates synthesis at the poly(A) region of the mRNA. The cDNA was initially amplified using the universal amplification primer (UAP) and a gene-specific forward primer (μ_1-F), and then a nested PCR was completed using the UAP primer and an additional forward primer (μ_1-F2). The PCR products were analysed by agarose gel electrophoresis, gel purified, cloned into the pGEM®-T Easy vector and sequenced with the pUC/M13 forward primer to determine the 3' end of the μ1 transcript.

Primer sequences for 3' RACE

TAP	5' GGCCACGCGTCGACTAGTAC$(T)_{17}$ 3'
UAP	5' GGCCACGCGTCGACTAGTAC 3'
μ_1-F2	5' AGCAGTAACACGTAAGAATAGTAATGC 3'

By analyzing the sequencing data of the nested PCR of 3' RACE, the obtained sequence mapped the 3' stop codon (TAG) to the position predicted. This concluded that the mRNA terminates at the site expected and does not account for the increased size.

5' RACE was unsuccessful, thus no evidence was obtained to show the upstream translation start codon. Therefore, the notion that the 5' end is further upstream can not be confirmed nor denied.

Nucleotide sequence surrounding the μ1 gene

9600
gtagtccccacttttgtatattgtgacatacttgaaaatattatacctttttatgagctt
ttgaaattttttgtttcttttttttttttttttttttttttttttttctatattgagaaa
taattttagtagtaaaaaagagaaggatatctcaatagttttgcttgtaaggtatatt
ttgaattatatataaacatacacatataatataaatatttggtataatataaacatttt
ggtataatataaacattttggtatattatatatatatatatatatatatatgttattttt
atatttttgtgatttgaaatatgaatacaaaattatgaacaagtaaaaaggagaagaaga
atataaaaagaaaataaaagaattaataagattagacaaaatggcatgtataagcgctat
ctttatacttgattttaaaaggaaaagtaataattaatagaaattatcgaggagaagtaaa
tgtaaatttatcagaggtgttttatattgtgttattgatcaagaagaacatttaataaa
accaatatttcatgttatggtttaacatattgtttggtagtcataataatatatactt
tttagcagtaacacgtaagaatagtaatgctacattaattatagcattttatataagct
catacaagtattaaaagattattttaaggtattagaagaagaaagtattaaagataatt
tgtaatcacatatgaattattagatgaaatgattgataatggtttccctcaattaagtga
agtaacaattttaagagtatatataaaaaatataagctcatcaactaacagttaatatttt
taaaatacctttcagctttaacaaattctgtatcatggagaagtgaagtattaaatataa
aaaaaatgaaatttttcttagatgttgttgaaagcttaaatattattatatcttctaatgg
aacagtattaagaagtgaaattttaggatgccttaaaatgaaatcctatttatcagtat
gcctgaattaaaattaggattaaatgataaactacttttttaataaaatcttaataatta
tccaaattcatcaaataataatcttaataataaaacaaaactagtcgaattagaagatat
taaatttcatcagtgtgttagattatcaaaatttgaaaatgatagaactatttcatttat
accacctgatggtatttttaatttaatgacgtatcgtctaagtactcatgtcaaaccatt
attctggctagatattaatatcacaaagaaatccctcacaaaaatcgaatataatgtaaa
agcaaaatcacaatttaaaaataaaagcatagcaaataatgtagaatttcatctacccgt
acctgctgatgttgattcaccacattttcaaacatatataggaacagtcaaatattatcc
tgataaagacatactaatatggaaaattaaacaattccaaggacaaaggaatatattat
gaatgcacaattcggtttaccttccattgtctcaaacgaaaataaagatctttattataa
gagaccagtaaatgtgaaatttgaaatcccttatttcactgtctcaggtattacagtaag
gtatttaaaaattatagaaaaaagtggttatcaagccttgccctgggtcaggtatataac
gcaaaatggcgactatcaggtcagaatgtcctagtaaaataaataatataaataaaatga
aatgaaacatattaattgatggaaaattcaaatgtagcaatatttctgcaattacataat
accacgtgaaaaaaaaaaataaaataaaataaaataaaataaaagacggaaagagagaaa
aaaaaaaaaaaaaaaaaaaaaaatatgatagctagccaaaattaaagacatacataaa
tatatatttatagaactatattgcacacataatatatatatatatatatatatatatatg
tgcgtgcacgttaccttgctgtttatttttctcgtttatatttattaatatagttttt
aagaatatgtcaattttttgtgaaccaaaaaaaattaaagcaaaagttttcaattataaat
11700

The μ1 gene sequence with upstream and downstream intergenic regions (PF13_0062). 3' RACE shows the 3' end of the μ1 gene is at the position predicted, determined by the presence of the TAG stop codon. The predicted full length μ1 gene sequence is in red and the data retrieved from sequencing is in **bold**.

A-8. Alignment of members of the *P. falciparum* Rab family.

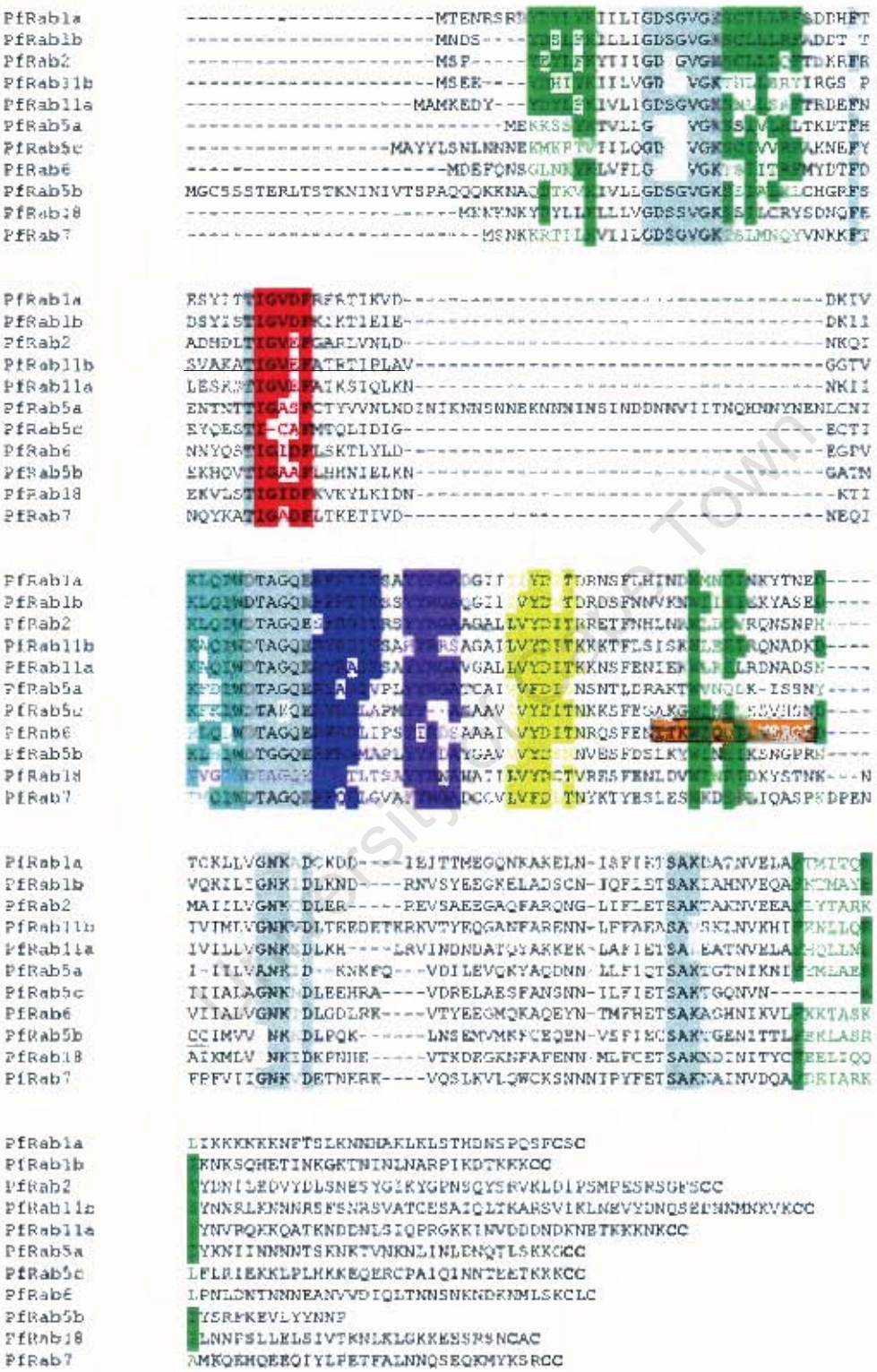

ClustalW alignment of the 11 members of the *P. falciparum* Rab family. The figure was taken from Quevillon *et al.* (2003) and had been amended to indicate the peptide sequence to which the rab6 antiserum was raised (orange).

References

Adessi, C., Chapel, A., Vinçon, M., Rabilloud, T., Klein, G., Satre, M. and Garin, J. (1995). Identification of major proteins associated with *Dictyostelium discoideum* endocytic vesicles. *Journal of Cell Science*. **108**(Pt 10), 3331-3337.

Adisa, A., Albano, F.R., Reeder, J., Foley, M. and Tilley, L. (2001). Evidence for a role for a *Plasmodium falciparum* homologue of Sec31p in the export of proteins to the surface of malaria parasite-infected erythrocytes. *Journal of Cell Science*. **114**(Pt 18), 3377-3386.

Aguilar, R.C., Ohno, H., Roche, K.W. and Bonifacino, J.S. (1997). Functional domain mapping of the clathrin-associated adaptor medium chains μ1 and μ2. *Journal of Biological Chemistry*. **272**(43), 27160-27166.

Aguilar, R.C., Boehm, M., Gorshkova, I., Crouch, R.J., Tomita, K., Saito, T., Ohno, H. and Bonifacino, J.S. (2001). Signal-binding specificity of the μ4 subunit of the adaptor protein complex AP-4. *Journal of Biological Chemistry*. **276**(16), 13145-13152.

Ali, B.R., Wasmeier, C., Lamoreux, L., Strom, M. and Seabra, M.C. (2004). Multiple regions contribute to membrane targeting of Rab GTPases. *Journal of Cell Science*. **117**(Pt 26), 6401-6412.

Allan, B.B. and Balch, W.E. (1999). Protein sorting by directed maturation of Golgi compartments. *Science*. **285**(5424), 63-66.

Amino, R., Giovannini, D., Thiberge, S., Gueirard, P., Boisson, B., Dubremetz, J.F., Prévost, M.C., Ishino, T., Yuda, M. and Ménard, R. (2008). Host cell traversal is important for progression of the malaria parasite through the dermis to the liver. *Cell Host and Microbe*. **3**(2), 88-96.

Angov, E., Hillier, C.J., Kincaid, R.L. and Lyon, J.A. (2008). Heterologous protein expression is enhanced by harmonizing the codon usage frequencies of the target gene with those of the expression host. *PLoS ONE*. **3**(5), e2189.

Aoe, T., Cukierman, E., Lee, A., Cassel, D., Peters, P.J. and Hsu, V.W. (1997). The KDEL receptor, ERD2, regulates intracellular traffic by recruiting a GTPase-activating protein for ARF1. *The EMBO Journal*. **16**(24), 7305-7316.

Araki, N., Johnson, M.T. and Swanson, J.A. (1996). A role for phosphoinositide 3-kinase in the completion of macropinocytosis and phagocytosis by macrophages. *Journal of Cell Biology*. **135**(5), 1249-1260.

Armstrong, C.M. and Goldberg, D.E. (2007). An FKBP destabilization domain modulates protein levels in *Plasmodium falciparum*. *Nature Methods*. **4**(12), 1007-1009.

Asojo, O.A., Gulnik, S.V., Afonina, E., Yu, B., Ellman, J.A., Haque, T.S. and Silva, A.M. (2003). Novel uncomplexed and complexed structures of plasmepsin II, an aspartic protease from *Plasmodium falciparum*. *Journal of Molecular Biology*. **327**(1), 173-181.

Baca, A.M. and Hol, W.G.J. (2000). Overcoming codon bias: A method for high-level overexpression of *Plasmodium* and other AT-rich parasite genes in *Escherichia coli*. *International Journal for Parasitology*. **30**(2), 113-118.

Bahl, A., Brunk, B., Coppel, R.L., Crabtree, J., Diskin, S.J., Fraunholz, M.J, Grant, G.R., Gupta, D., Huestis, R.L., Kissinger, J.C., Labo, P., Li, L., McWeeney, S. K., Milgram, A. J., Roos, D.S., Schug, J. and Stoeckert, C.J. Jr. (2002). PlasmoDB: The *Plasmodium* genome resource. A database integrating experimental and computational data. *Nucleic Acids Research*. **30**(1), 87-90.

Baines, A.C. and Zhang, B. (2007). Receptor-mediated protein transport in the early secretory pathway. *Trends in Biochemical Sciences*. **32**(8), 381-388.

Balu, B. and Adams, J.H. (2007). Advancements in transfection technologies for *Plasmodium*. *International Journal of Parasitology*. **37**(1), 1-10.

Bannister, L.H. and Mitchell, G.H. (2003). The ins, outs and roundabouts of malaria. *Trends in Parasitology*. **19**(5), 209-213.

Bannister, L.H., Hopkins, J.M., Fowler, R.E. Krishna, S. and Mitchell, G.H. (2000). A brief illustrated guide to the ultrastructure of *Plasmodium falciparum* asexual blood stages. *Parasitology Today*. **16**(10), 427-433.

Baum, J., Papenfuss, A.T., Mair, G.R., Janse, C.J., Vlachou, D., Waters, A.P., Cowman, A.F., Crabb, B.S. and de Koning-Ward, T.F. (2009). Molecular genetics and comparative genomics reveal RNAi is not functional in malaria parasites. *Nucleic Acids Research*. April 20. [Epub ahead of print] 1-11.

Bennett, N., Letourneur, F., Ragno, M. and Louwagie, M. (2008). Sorting of the v-SNARE VAMP7 in *Dictyostelium discoideum*: a role for more than one adaptor protein (AP) complex. *Experimental Cell Research*. **314**(15), 2822-2833.

Biagini, G.A., Viriyavejakul, P., O'neill, P.M., Bray, P.G. and Ward, S.A. (2006). Functional characterization and target validation of alternative complex I of *Plasmodium falciparum* mitochondria. Antimicrobial Agents and Chemotherapy. **50**(5), 1841-1851.

Birkeland, H.C. and Stenmark, H. (2004). Protein targeting to endosomes and phagosomes via FYVE and PX domains. *Current Topics in Microbiology and Immunology.* **282**, 89-115.

Birkholtz, L-M., Blatch, G., Coetzer, T.L., Hoppe, H.C., Human, E., Morris, J., Ngcete, Z., Oldfield, L., Roth, R., Shonhai, A., Stephens, L. and Louw, A.I. (2008). Heterologous expression of plasmodial proteins for structural studies and functional annotation. *Malarial Journal.* **7**(1), 197.

Black, M.W. and Pelman, H.R.B. (2001). Membrane traffic: How do GGAs fit in with the adaptors? *Current Biology.* **11**(12), 460-462.

Boehm, M. and Bonifacino, J.S. (2001). Adaptins: the final recount. *Molecular Biology of the Cell.* **12**(10), 2907-2920.

Boehm, M. and Bonifacino, J.S. (2002). Genetic analyses of adaptin function from yeast to mammals. *Gene.* **286**(2), 175-186.

Bonifacino, J.S. and Traub, L.M. (2003). Signals for sorting of transmembrane proteins to endosomes and lysosomes. *Annual Review of Biochemistry.* **72**, 395-447.

Bottomley, M.J., Lo Surdo, P. and Driscoll, P.C. (1999). Endocytosis: how dynamin sets vesicles PHree! *Current Biology.* **9**(8), 301-304.

Cavalli, V., Corti, M. and Gruenberg, J. (2001). Endocytosis and signalling cascades: a close encounter. *FEBS letters.* **498**(2-3), 190-196.

Chang, H.H., Falick, A.M., Carlton, P.M., Sedat, J.W., DeRisi, J.D. and Marletta, M.A. (2008). N-terminal processing of proteins exported by malaria parasites. *Molecular and Biochemical Parasitology.* **160**(2), 107-115.

Chapuy, B., Tikkanen, R., Mühlhausen, C., Wenzel, D., von Figura, K. and Höning, S. (2008). AP-1 and AP-3 mediate sorting of melanosomal and lysosomal membrane proteins into distinct post-Golgi trafficking pathways. *Traffic.* **9**(7), 1157-1172.

Charette, S.J. and Cosson, P. (2008). Altered composition and secretion of lysosome-derived compartments in *Dictyostelium* AP-3 mutant cells. *Traffic.* **9**(4), 588-596.

Chattopadhyay, D., Smith,C.D., Barchueb, J. and Langsley, G. (2000). *Plasmodium falciparum* rab6 GTPase: expression, purification, crystallization and preliminary crystallographic studies. *Acta Crystallographica Section D Biological Crystallography.* **56**(Pt 8), 1017-1019.

Collins, B.M., McCoy, A.J., Kent, H.M., Evans, P.R. and Owen, D.J. (2002). Molecular architecture and functional model of the endocytic AP2 complex. *Cell.* **109**(4), 523-535.

Collins, W.E. and Jeffery, G.M. (2007). *Plasmodium malariae*: Parasite and Disease. *Clinical Microbiology Reviews*. **20**(4), 579-592.

Collins, W.E. and Jeffery, G.M. (2005). *Plasmodium ovale*: Parasite and Disease. *Clinical Microbiology Reviews*. **18**(3), 570-581.

Conner, S.D. and Schmid, S.L. (2003). Regulated portals of entry into the cell. *Nature*. **422**(6927), 37-44.

Conner, S.D. and Schmid, S.L. (2003). Differential requirements for AP-2 in clathrin-mediated endocytosis. *Journal of Cell Biology*. **162**(5), 773-780.

Cooke, B.M., Lingelbach, K., Bannister, L.H. and Tille, L. (2004). Protein trafficking in *Plasmodium falciparum*-infected red blood cells. *Trends in Parasitology*. **20**(12). 581-589.

Cortes, G.T., Winograd, E. and Wiser, M.F. (2003). Characterization of proteins localized to a subcellular compartment associated with an alternative secretory pathway of the malaria parasite. *Molecular and Biochemical Parasitology*. **129**(2), 127-135.

Cowman, A.F. and Crabb, B.S. (2006). Invasion of red blood cells by malaria parasites. *Cell*. **124**(), 755-766.

Crottet, P., Meyer, D.M., Rohrer, J. and Spiess, M. (2002). ARF1·GTP, tyrosine-based signals, and phosphatidylinositol 4,5-bisphosphate constitute a minimal machinery to recruit the AP-1 clathrin adaptor to membranes. *Molecular Biology of the Cell*. **13**(10), 3672-3682.

Damm, E., Pelkmans, L., Kartenbeck, J., Mezzacasa, A., Kurzchalia, T., and Helenius, A. (2005). Clathrin- and caveolin-1–independent endocytosis: entry of simian virus 40 into cells devoid of caveolae. *The Journal of Cell Biology*. **168**(3), 477-488.

de Castro, F.A., Ward, G.E., Jambou, R., Attal, G., Mayau, V., Jaureguiberry, G., Braun-Breton, C., Chakrabarti, D. and Langsley, G. (1996). Identification of a family of Rab G-proteins in *Plasmodium falciparum* and a detailed characterisation of *Pf*rab6. *Molecular and Biochemical Parasitology*. **80**(1), 77-88.

de Smit, M. and van Duin, J. (1990). Secondary structure of the ribosome binding site determines translational efficiency: A quantitative analysis. *Proceedings of the National Academy of Sciences*. **87**(19), 7668-7672.

del Pilar Crespo, M., Avery, T.D., Hanssen, E., Fox, E., Robinson, T.V., Valente, P., Taylor, D.K. and Tilley, L. (2008). Artemisinin and a series of novel endoperoxide antimalarials exert early effects on digestive vacuole morphology. *Antimicrobial Agents and Chemotherapy*. **52**(1), 98-109.

Dell'Angelica, E.C., Mullins, C. and Bonifacino, J.S. (1999). AP-4, a novel protein complex related to clathrin adaptors. *Journal of Biological Chemistry.* **274**(11), 7278-7285.

Dell'Angelica, E.C., Klumperman, J., Stoorvogel, W. and Bonifacino, J.S. (1998). Association of the AP-3 adaptor complex with clathrin. *Science.* **280**(5362), 431-434.

Delplace, P., Bhatia, A., Cagnard, M., Camus, D., Colombet, G., Debrabant, A., Dubremetz, J.F., Dubreuil, N., Prensier, G., Fortier, B., Haq, A., Weber, J. and Vernes, A. 1988). Protein p126: a parasitophorous vacuole antigen associated with the release of *Plasmodium falciparum* merozoites. *Biology of the Cell.* **64**(2), 215-221.

Desai, S.A., Krogstad, D.J. and McCleskey, E.W. (1993). A nutrient-permeable channel on the intraerythrocytic malaria parasite. *Nature.* **362**(6421), 643-646.

Echarri, A., Muriel, O. and Del Pozo, M.A. (2007). Intracellular trafficking of raft/caveolae domains: insights from integrin signalling. *Seminars in Cell and Developmental Biology.* **18**(5), 627-637.

Egan, T.J., Combrinck, J.M., Egan, J., Hearne, G.R., Marques, H.M., Ntenteni, S., Sewell, B.T., Smith, P.J., Taylor, D., van Schalkwyk, D.A. and Walden J.C. (2002). Fate of haem iron in the malaria parasite *Plasmodium falciparum. The Biochemical Journal.* **365**(Pt 2), 343-347.

Egan, T.J., Chen, J.Y. de Villiers, K.A., Mabotha, T.E. Naidoo, K.J., Ncokazi,K.K., Langford, S.J., McNaughton, D., Pandiancherri, S. and Wood, B.R. (2006). Haemozoin (β-haematin) biomineralization occurs by self-assembly near the lipid/water interface. *FEBS Letters.* **580**(21), 5105-5110.

Egea, G., Lázaro-Diéguez, F. and Vilella, M. (2006). Actin dynamics at the Golgi complex in mammalian cells. *Current Opinion in Cell Biology.* **18**(2), 168-178.

Eitzen, G. (2003). Actin remodeling to facilitate membrane fusion. *Biochimica et Biophysica Acta.* **1641**(2-3), 175-181.

Elford, B.C., Cowan, G.M. and Ferguson, D.J. (1997). Transport and trafficking in malaria-infected erythrocytes. *Trends in Microbiology.* **5**(12), 463-465.

Elford, B.C., Cowan, G.M. and Ferguson, D.J. (1995). Parasite-regulated membrane transport processes and metabolic control in malaria-infected erythrocytes. *The Biochemical Journal.* **308**(Pt 2), 361-374

Elliott, D.A., McIntosh, M.T., Hosgood, H.D., Chen, S., Zhang, G., Baevova, P. and Joiner, K.A. (2008). Four distinct pathways of hemoglobin uptake in the malaria parasite *Plasmodium falciparum. Proceedings of the National Academy of Sciences.* **105**(7), 2463-2468,

Elmendorf, H.G. and Haldar, K. (1993). Identification and localization of ERD2 in the malaria parasite *Plasmodium falciparum*: separation from sites of sphingomyelin synthesis and implications for organization of the Golgi. *The EMBO Journal*. **12**(12), 4763-4773.

Engqvist-Goldstein, A.E.Y. and Drubin, D.G. (2003). Actin assembly and endocytosis: From yeast to mammals. *Annual Review of Cell and Developmental Biology*. **19**, 287-332.

Epp, C. and Deitsch, K.W. (2006). Deciphering the export pathway of malaria surface proteins. *Trends in Parasitology*. **22**(9), 401-404.

Esposito, D. and Chatterjee, D.K. (2006). Enhancement of soluble protein expression through the use of fusion tags. *Current Opinions in Biotechnology*. **17**(4), 353-358.

Ewan, G.S. (2004). A dynamic opportunity for drug discovery. *Drug Discovery Today*. **9**(13), 546.

Feinstein, T.N. and Linstedt, A.D. (2008). GRASP55 regulates Golgi ribbon formation. *Molecular Biology of the Cell*. **19**(7), 2696-2707.

Fieser, T.M., Tainer, J.A., Geysen, H.M. and Houghten, R.A. (1987). Influence of protein flexibility and peptide conformation on reactivity of monoclonal anti-peptide antibodies with a protein alpha-helix. *Proceedings of the National Academy of Sciences*. **84**(23), 8568-8572.

Flick, K., Ahuja, S., Chene, A., Bejarano, M.T. and Chen, Q. (2004). Optimized expression of *Plasmodium falciparum* erythrocyte membrane protein 1 domains in *Escherichia coli*. *Malaria Journal*. **3**(50), 1-8.

Foley, M. and Tilley, L. (1998). Protein trafficking in malaria-infected erythrocytes. *International Journal for Parasitology*. **28**(11), 1671-1680.

Francis, S.E., Banerjee, R. and Goldberg, D.E. (1997). Biosynthesis and maturation of the malaria aspartic hemoglobinases plasmepsin I and II. *Journal of Biological Chemistry*. **272**(23), 14961-14968.

Francis, S.E., Gluzman, I.Y., Oksman, A., Knickerbocker, A., Mueller, R., Bryant, M.L., Sherman, D.R., Russell, D.G. and Goldberg, D.E. (1994). Molecular characterization and inhibition of a *Plasmodium falciparum* aspartic hemoglobinase. *The EMBO Journal*. **13**(2), 306-317.

Gallup, J.L. and Sachs, J.D. (2001). The economic burden of malaria. *American Journal of Tropical Medicine Hygiene*. **64**(1,2), 85-96.

Giobbia, M., Tonon, E., Zanatta, A., Cesaris, L., Bisoffi, Z. and Vaglia, A. (2005). Late recrudescence of *Plasmodium falciparum* malaria in a pregnant woman: a case report. *International Journal of Infectious Diseases*. **9**(4), 234-235.

Goldberg, D.E., Slater, A.F., Cerami, A. and Henderson, G.B. (1990). Hemoglobin degradation in the malaria parasite *Plasmodium falciparum*: an ordered process in a unique organelle. *Proceedings of the National Academy of Sciences of the United States of America*. **87**(8), 2931-2935.

Goldman, E., Rosenberg, A.H., Zubay, G. and Studier, W.F. (1995). Consecutive low-usage leucine codons block translation only when near the 5′ end of a message in *Escherichia coli*. *Journal of Molecular Biology*. **245**(5), 467-473.

Goodyer, I.D., Pouvelle, B., Schneider, T.G., Trelka, D.P. and Taraschi, T.F. (1997). Characterization of macromolecular transport pathways in malaria-infected erythrocytes. *Molecular and Biochemical Parasitology*. **87**(1), 13-28.

Gouagna, L.C., Mulder, B., Noubissi, E., Tchuinkam, T., Verhave, J.P. and Boudin, C. (1998). The early sporogonic cycle of *Plasmodium falciparum* in laboratory-infected *Anopheles gambiae*: an estimation of parasite efficacy. *Tropical Medicine and International Health*. **3**(1), 21-28.

Goud, B., Zahraoui, A., Tavitian, A. and Saraste, J. (1990). Small GTP-binding protein associated with Golgi cisternae. *Nature*. **345**(6275), 553-556.

Greenbaum, D.C., Baruch, A., Grainger, M., Bozdech, Z., Medzihradszky, K.F., Engel, J., DeRisi, J., Holder, A.A. and Bogyo, M. (2002). A role for the protease falcipain 1 in host cell invasion by the human malaria parasite. *Science*. **298**(5600), 2002-2006.

Greenwood, B.M., Fidock, D.A., Kyle, D.E., Kappe, S.H.I., Alonso, P.L., Collins, F.H. and Duffy, PE. (2008). Malaria: progress, perils, and prospects for eradication. *Journal of Clinical Investigation*. **118**(4), 1266-1276.

Guerin, P.J., Olliaro, P., Nosten, F., Druilhe, P., Laximinarayan, R., Binka, F., Kilama, W.L., Ford, N. and White, N.J. (2002). Malaria: current status of control, diagnosis, treatment, and a proposed agenda for research and development. *The Lancet Infectious Diseases*. **2**(9), 564-573.

Guilvout, I., Chami, M., Engel, A., Pugsley, A.P. and Bayan, N. (2006). Bacterial outer membrane secretin PulD assembles and inserts into the inner membrane in the absence of its pilotin. *The EMBO Journal*. **25**(22), 5241-5249.

Gürkan, C., Stagg, S.M., Lapointe, P. and Balch, W.E. (2006). The COPII cage: unifying principles of vesicle coat assembly. *Nature Reviews, Molecular Cell Biology*. **7**(10), 727-738.

Haase, S., Cabrera, A., Langer, C., Treeck, M., Struck, N., Herrmann, S., Jansen, P.W., Bruchhaus, I., Bachmann, A., Dias, S., Cowman, A.F., Stunnenberg, H.G., Spielmann, T. and Gilberger, T.W. (2008). Characterization of a conserved rhoptry-associated leucine zipper-like protein in the malaria parasite *Plasmodium falciparum*. Infection and Immunity. **76**(3), 879-887.

Haft, C.R., de La Luz Sierra, M., Hamer, I., Carpentier, J. and Taylor, S.I. (1998). Analysis of the juxtamembrane dileucine motif in the insulin receptor. *Endocrinology*. **139**(4), 1618-1629.

Haldar, K. (1998). Intracellular trafficking in *Plasmodium*-infected erythrocytes. *Current Opinion in Microbiology*. **1**(4), 466-471.

Haldar, K., Samuela, B.U., Mohandasb, N., Harrisona, T. and Hillera, N.L. (2001). Transport mechanisms in *Plasmodium*-infected erythrocytes: lipid rafts and a tubovesicular network. *International Journal for Parasitology*. **31**(12), 1393-1401.

Hanspal, M., Goel, V.K., Oh, S.S. and Chishti, A.H. (2002). Erythrocyte calpain is dispensable for malaria parasite invasion and growth. *Molecular and Biochemical Parasitology*. **122**(2), 227-229.

Harter, C. (1995). COP-coated vesicles in intracellular protein transport. *FEBS Letters*. **369**(1), 89-92.

Hauri, H.P. and Schweizer, A. (1992). The endoplasmic reticulum-Golgi intermediate compartment. *Current Opinions in Cell Biology*. **4**(4), 600-608.

Hawthorne, P.L., Trenholme, K.R., Skinner-Adams, T.S., Spielmann, T., Fischer, K., Dixon, M.W., Ortega, M.R., Anderson, K.L., Kemp, D.J. and Gardiner, D.L. (2004). A novel *Plasmodium falciparum* ring stage protein, REX, is located in Maurer's clefts. *Molecular and Biochemical Parasitology*. **136**(2), 181-189.

Heldwein, E.E., Macia, E., Wang, J., Yin, H.L., Kirchhausen, T. and Harrison, S.C. (2004). Crystal structure of the clathrin adaptor protein 1 core. *Proceedings of the National Academy of Sciences*. **101**(39), 14108-14113.

Hempelmann, E., Motta, C., Hughes, R., Ward, S.A. and Bray, P.G. (2003). *Plasmodium falciparum*: sacrificing membrane to grow crystals? *Trends in Parasitology*. **19**(1), 23-26.

Hill, E., van der Kaay, J., Downes, C.P. and Smythe, E. (2001). The role of dynamin and its binding partners in coated pit invagination and scission. *Cell Biology*. **152**(2), 309-324.

Hinners, I. and Tooze, S.A. (2003). Changing directions: clathrin-mediated transport between the Golgi and endosomes. *Journal of Cell Science*. **116**(Pt 5), 763-771.

Hirst, J., Bright, N.A., Rous, B. and Robinson, M.S. (1999) Characterization of a fourth adaptor-related protein complex. *Molecular Biology of the Cell*. **10**(8), 2787-2802.

Hirst, J. and Robinson, M.S. (1998). Clathrin and adaptors. *Biochimica et Biophysica Acta*. **1404**(1-2), 173-193.

Hirst, J., Lindsay, M.R. and Robinson, M.S. (2001). Golgi-localized, γ-ear-containing, ADP-ribosylation factor-binding proteins: roles of the different domains and comparison with AP-1 and clathrin. *Molecular Biology of the Cell*. **12**(11), 3573-3588.

Höning, S., Ricotta, D., Krauss, M., Späte, K., Spolaore, B., Motley, A., Robinson, M., Robinson, C., Haucke, V. and Owen, D.J. (2005). Phosphatidylinositol-(4,5)-bisphosphate regulates sorting signal recognition by the clathrin-associated adaptor complex AP2. *Molecular Cell*. **18**(5), 519-531.

Hoppe, H.C., Ngô, H.M., Yang, M. and Joiner, K.A. (2000). Targeting to rhoptry organelles of *Toxoplasma gondii* involves evolutionarily conserved mechanisms. *Nature, Cell Biology*. **2**(7), 449-456.

Horrocks, P. and Muhia, D. (2005). Pexel/VTS: a protein-export motif in erythrocytes infected with malaria parasites. *Trends in Parasitology*. **21**(9), 396-399.

Hume, J.C.C., Lyons, E.J. and Day, K.P. (2003). Human migration, mosquitoes and the evolution of *Plasmodium falciparum*. *Trends in Parasitology*. **19**(3), 144-149.

Janson, I.M., Toomik, R., O'Farrell, F. and Ek, P. (1998). KDEL motif interacts with a specific sequence in mammalian erd2 receptor. *Biochemical and Biophysical Research Communications*. **247**(2), 447-451.

Janvier, K. and Bonifacino, J.S. (2005). Role of the endocytic machinery in the sorting of lysosome-associated membrane proteins. *Molecular Biology of the Cell*. **16**(9), 4231-4242.

Janvier, K., Kato, Y., Boehm, M., Rose, J.R., Martina, J.A., Kim, B., Venkatesan, S. and Bonifacino, J.S. (2003). Recognition of dileucine-based sorting signals from HIV-1 Nef and LIMP-II by the AP-1 gamma-sigma1 and AP-3 delta-sigma3 hemicomplexes. *Journal of Cell Biology*. **163**(6), 1281-1290.

Jomaa, H., Wiesner, J., Sanderbrand, S., Altincicek, B., Weidemeyer, C., Hintz, M., Türbachova, I., Eberl, M., Zeidler, J., Lichtenthaler, H.K., Soldati, D and Beck, E. (1999). Inhibitors of the nonmevalonate pathway of isoprenoid biosynthesis as antimalarial drugs. *Science*. **285**(5433), 1573-1576.

Kanzokand, S.M. and Zheng, L. (2003). The mosquito genome – a turning point? *Trends in Parasitology*. **19**(8), 329-331.

Kariuki, M.M., Li, X., Yamodo, I., Chishti, A.H. and Oh, S.S. (2005). Two *Plasmodium falciparum* merozoite proteins binding to erythrocyte band 3 form a direct complex. *Biochemical and Biophysical Research Communications*. **338**(4), 1690-1695.

Kirchgatter, K. and del Portillo, H.A. (2002). Association of severe noncerebral *Plasmodium falciparum* malaria in Brazil with expressed *Pf*EMP1 DBL1 alpha sequences lacking cysteine residues. *Molecular Medicine*. **8**(1), 16-23.

Kirchhausen, T. (1999). Adaptors for clathrin-mediated traffic. *Annual Review of Cell and Developmental Biology*. **15**, 705-732.

Kirchhausen, T., Bonifacino, J.S. and Riezman, H. (1997). Linking cargo to vesicle formation: receptor tail interactions with coat proteins. *Current Opinions in Cell Biology*. **9**(4), 488-495.

Kirk, S.J. and Ward, T.H. (2007). COPII under the microscope. *Seminars in Cell and Developmental Biology*. **18**(4), 435-447.

Kirkham, M. and Parton, R.G. (2005). Clathrin-independent endocytosis: new insights into caveolae and non-caveolar lipid raft carriers. *Biochimica et Biophysica Acta*. **1745**(3), 273-286.

Kisilevsky, R., Crandall, I., Szarek, W.A. Bhat, S., Tan, C., Boudreau, L. and Kain, K.C. (2002). Short-chain aliphatic polysulfonates inhibit the entry of *Plasmodium* into red blood cells. *Antimicrobial Agents and Chemotherapy*. **46**(8), 2619-2626.

Kita, A., Sugiura, R., Shoji, H., He, Y., Deng, L., Lu, Y., Sio, S.O., Takegawa, K., Sakaue, M., Shuntoh, H. and Kuno, T. (2004). Loss of Apm1, the μ1 subunit of the clathrin-associated adaptor-protein-1 complex, causes distinct phenotypes and synthetic lethality with calcineurin deletion in fission yeast. *Molecular Biology of the Cell*. **15**(6), 2920-2931.

Klemba, M., Beatty, W., Gluzman, I. and Goldberg, D.E. (2004). Trafficking of plasmepsin II to the food vacuole of the malaria parasite *Plasmodium falciparum*. *Journal of Cell Biology*. **164**(1), 47-56.

Knuepfer, E., Rug, M., Klonis, N., Tilley, L. and Cowman, A.F. (2005). Trafficking of the major virulence factor to the surface of transfected *P. falciparum*–infected erythrocytes. *Blood*. **105**(10), 4078-4087.

Kobayashi, T., Sato, S., Takamiya, S., Komaki-Yasuda, K., Yano, K., Hirata, A., Onitsuka, I., Hata, M., Mi-ichi, F., Tanaka, T., Hase, T., Miyajima, A., Kawazu, S., Watanabe, Y. and Kita, K. (2006). Mitochondria and apicoplast of *Plasmodium falciparum*: behaviour on subcellular fractionation and the implication. *Mitochondrion*. **7**(1-2), 125-132.

Kooij, T.W.A. and Matuschewski, K. (2007). Triggers and tricks of *Plasmodium* sexual development. *Current Opinion in Microbiology*. **10**(6), 547-553.

Kramer, K.L. and Yost, H.J. (2003). Heparan sulfate core proteins in cell-cell signalling. *Annual Review of Genetics*. **37**(1), 461-484.

Kreis, T.E., Lowe, M. and Pepperkok, R. (1995). COPs regulating membrane traffic. *Annual Review of Cell and Developmental Biology*. **11**, 677-706.

Krettli, A.U. and Miller, L.H. (2001). Malaria: a sporozoite runs through it. *Current Biology*. **11**(10), 409-412.

Krishna, S., Eckstein-Ludwig, U., Joët, T., Uhlemann, A, Morin, C., Webb, R., Woodrow, C., Kun, J.F.J. and Kremsner, P.G. (2002). Transport processes in *Plasmodium falciparum*-infected erythrocytes: potential as new drug targets. *International Journal for Parasitology*. **32**(13), 1567-1573.

Krnajski, Z., Gilberger, T.W., Walter, R.D., Cowman, A.F. and Müller, S. (2002). Thioredoxin reductase is essential for the survival of *Plasmodium falciparum* erythrocytic stages. *Journal of Biological Chemistry*. **277**(29), 25970-25975.

Krugliak. M., Zhang, J. and Ginsburg, H. (2002). Intraerythrocytic *Plasmodium falciparum* utilizes only a fraction of the amino acids derived from the digestion of host cell cytosol for the biogenesis of its proteins. *Molecular and Biochemical Parasitology*. **119**(2), 249-256.

Kyriacou, H.M., Stone, G.N., Challis, R.J., Raza, A., Lyke, K.E., Thera, M.A., Koné, A.K., Doumbo, O.K., Plowe, C.V. and Rowe, J.A. (2006). Differential *var* gene transcription in *Plasmodium falciparum* isolates from patients with cerebral malaria compared to hyperparasitaemia. *Molecular & Biochemical Parasitology*. **150**(2), 211-218.

LaCount, D.J., Vignali, M., Chettier, R., Phansalkar, A., Bell, R., Hesselberth, J.R., Schoenfeld, L.W., Ota, I., Sahasrabudhe, S, Kurschner, C., Fields, S. and Hughes, R.E. (2005). A protein interaction network of the malaria parasite *Plasmodium falciparum*. *Nature*. **438**(7064), 103-107.

Lambros, C. and Vanderberg, J.P. (1979). Synchronization of *Plasmodium falciparum* erythrocytic stages in culture. *Journal of Parasitology*. **65**(3), 418-420.

Land, K.M. (2003). The mosquito genome: perspectives and possibilities. *Trends in Parasitology*. **19**(3), 103-105.

Lankford, S.E., Adams, B.M., Adams, T.E. and Cech, J.J. Jr. (2006). Using specific antisera to neutralize ACTH in sturgeon: a method for manipulating the internal response during stress. *General and Comparative Endocrinology*. **147**(3), 384-390.

Lanzetti, L. (2007). Actin in membrane trafficking. *Current Opinions in Cell Biology*. **19**(4), 453-458.

Lazarus, M.D., Schneider, T.G. and Taraschi T.F. (2008). A new model for hemoglobin ingestion and transport by the human malaria parasite *Plasmodiumfalciparum*. *Journal of Cell Science*. **121**(11), 1937- 1949.

Le, P.U. and Nabi, I.R. (2003). Distinct caveolae-mediated endocytic pathways target the Golgi apparatus and the endoplasmic reticulum. *Journal of Cell Science*. **116**(Pt 6), 1059-1071.

Le Borgne, R. and Hoflack, B. (1998). Mechanisms of protein sorting and coat assembly: insights from the clathrin-coated vesicle pathway. *Current Opinion in Cell Biology*. **10**(4), 499-503.

Le Roch, K.G., Zhou, Y., Blair, P.L., Grainger, M., Moch, J.K., Haynes, J.D., De la Vega, P., Holder, A.A., Batalov, S., Carucci, D.J. and Winzeler, E.A. (2003). Discovery of gene function by expression profiling of the malaria parasite life cycle. *Science*. **301**(5639), 1503-1508.

Lee., M.C.S., Moura, P.A., Miller, E.A. and Fidock, D.A. (2008). *Plasmodium falciparum* Sec24 marks transitional ER that exports a model cargo via a diacidic motif. *Molecular Microbiology*. **68**(6), 1535-1546.

Leech, J.H., Barnwell, J.W., Aikawa, M., Miller, L.H. and Howard, R.J. (1984). *Plasmodium falciparum* malaria: association of knobs on the surface of infected erythrocytes with a histidine-rich protein and the erythrocyte skeleton. *The Journal of Cell Biology*. **98**, 1256-1264.

Lefkir, Y., Malbouyres, M., Gotthardt, D., Ozinsky, A., Cornillon, S., Bruckert, F., Aderem, A.A., Soldati, T., Cosson, P. and Letourneur, F. (2004). Involvement of the AP-1 adaptor complex in early steps of phagocytosis and macropinocytosis. *Molecular Biology of the Cell*. **15**(2), 861-869.

Lefkir, Y., de Chassey, B., Dubios, A., Bogdanovic, A., Brady, R.J., Destaing, O., Brucket , F., O'Halloran, T.J., Cosson, P. and Letourneur, F. (2003). The AP-1 clathrin-adaptor is required for lysosomal enzymes sorting and biogenesis of the contractile vacuole complex in *Dictyostelium* cells. *Molecular Biology of the Cell*. **14**(5), 1835-1851.

Lewin, D.A. and Mellman, I. (1998). Sorting out adaptors. *Biochimica et Biophysica Acta*. **1401**(2), 129-145.

Li, W., Keller, G.A. and Haldar, K. (1995). Recognition of a 170 kD protein in mammalian Golgi complexes by an antibody against malarial intraerythrocytic lamellae. *Tissue Cell*. **27**(4), 355-67.

Luzio, J.P., Rous, B.A., Bright, N.A., Pryor, P.R., Mullock, B.M. and Piper, R.C. (2000). Lysosome-endosome fusion and lysosome biogenesis. *Journal of Cell Science*. **113**(Pt 9), 1515-1524.

Majoul, I., Straub, M., Hell, S.W., Duden, R. and Soeling, H.D. (2001). KDEL-cargo regulates interactions between proteins involved in COPI vesicle traffic measurements in living cells using FRET. *Developmental Cell*. **1**(1), 139-53.

Martinez, O., Schmidt, A., Salaméro, J., Hoflack, B., Roa, M. and Goud, B. (1994). The small GTP-binding protein rab6 functions in intra-Golgi transport. *Journal of Cell Biology*. **127**(6 Pt 1), 1575-1588.

May, R.C. and Machevsky, L.M. (2001). Phagocytosis and the actin cytoskeleton. *Journal of Cell Science*. **114**(6), 1061-1077.

McCormick, P.J., Martina, J.A. and Bonifacino, J.S. (2005). Involvement of clathrin and AP-2 in the trafficking of MHC class II molecules to antigen-processing compartments. *Proceedings of the National Academy of Sciences*. **102**(22), 7910-7915.

McFadden, G.I. and Ross, D.S. (1999). Apicomplexan plastids as drug targets. *Trends in Microbiology*. **7**(8), 328-333.

McIntosh, M.T., Vaid, A., Hosgood, H.D., Vijay, J., Bhattacharya, A., Sahani, M.H., Baevova, P., Joiner, K.A. and Sharma, P. (2007). Traffic to the malaria parasite food vacuole: a novel pathway involving a phosphatidylinositol 3-phosphate-binding protein. *Journal of Biological Chemistry*. **282**(15), 11499-11508.

Mellman, I., Fuchs, R. and Helenius, A. (1986). Acidification of the endocytic and exocytic pathways. *Annual Review of Biochemistry*. **55**, 663-700.

Merrifield, C.J. (2004). Seeing is believing: imaging actin dynamics at single sites of endocytosis. *Trends in Cell Biology*. **14**(7), 352-358.

Miller, L.H., Baruch, D.I, Marsh, K. and Doumbo, O.K. (2002). The pathogenic basis of malaria. *Nature*. **415**(6872), 673-679.

Miller, L.H., Usami, S. and Chien, S. (1971). Alteration in the rheologic properties of *plasmodium knowlesi*-infected red cells. A possible mechanism for capillary obstruction. *Journal of Clinical Investigation*. **50**(7), 1451-1455.

Moffett, A., Shackelford, N. and Sarkar, S. (2007). Malaria in Africa: vector species' niche models and relative risk maps. *PLoS ONE*. **2**(9), e824.

Mogelsvang, S., Marsh, B.J., Ladinsky, M.S. and Howell, K.E. (2004). Predicting function from structure: 3D structure studies of the mammalian Golgi complex. *Traffic*. **5**(5), 338-345.

Munn, A.L. (2001). Molecular requirements for the internalisation step of endocytosis: insights from yeast. *Biochimica et Biophysica Acta*. **1535**(3), 236-257.

Murphy, S.C., Harrison, T., Hamm, H.E., Lomasney, J.W., Mohandas, N. and Haldar, K. (2006). Erythrocyte G protein as a novel target for malarial chemotherapy. *PLoS Medicine*. **3**(12), 2403-2415.

Nelson, W.J. and Yeaman, C. (2001). Protein trafficking in the exocytic pathway of polarized epithelial cells. *Trends in Cell Biology*. **11**(12), 483-486.

Nesterov, A., Carter, R.E., Sorkina, T., Gill, G.N. and Sorkin, A. (1999). Inhibition of the receptor-binding function of clathrin adaptor protein AP-2 by dominant-negative mutant μ2 subunit and its effects on endocytosis. *EMBO Journal*. **18**(9), 2489-2499.

Nevin, W.D. and Dacks, J.B. (2009). Repeated secondary loss of adaptin complex genes in the Apicomplexa. *Parasitology International*. **58**(1), 86-94.

Newmyer, S.L., Christensen, A. and Sever, S. (2003). Auxilin-dynamin interactions link the uncoating ATPase chaperone machinery with vesicle formation. *Developmental Cell*. **4**(6), 929-940.

Newpher, T.M., Idrissi, F.Z., Geli, M.I. and Lemmon, S.K. (2006). Novel function of clathrin light chain in promoting endocytic vesicle formation. *Molecular Biology of the Cell*. **17**(10), 4343-4352.

Ngô, H.M., Yang, M., Paprotka, K., Pypaert, M., Hoppe, H. and Joiner, K.A. (2003). AP-1 in *Toxoplasma gondii* mediates biogenesis of the rhoptry secretory organelle from a post-Golgi compartment. *Journal of Biological Chemistry*. **278**(7), 5343-5352.

Nichols, B.J. and Lippincott-Schwartz, J. (2001). Endocytosis without clathrin coats. *Trends in Cell Biology*. **11**(10), 406-412.

Niedergang, F., and Chavrier, P. (2004). Signalling and membrane dynamics during phagocytosis: many roads lead to the phagos(R)ome. *Current Opinions in Cell Biology*. **16**(4), 422-428.

Ohno, H., Fournier, M.C., Poy, G. and Bonifacino, J.S. (1996). Structural determinants of interaction of tyrosine-based sorting signals with the adaptor medium chains. *Journal of Biological Chemistry*. **271**(46), 29009-29015.

Ohno, H., Aguilar, R.C., Yeh, D., Taura, D., Saito, T. and Bonifacino, J.S. (1998). The medium subunits of adaptor complexes recognize distinct but overlapping sets of tyrosine-based sorting signals. *Journal of Biological Chemistry*. **273**(40), 25915-25921.

Ohno, H., Stewart, J., Fournier, M., Bosshart, H., Rhee, I., Miyatake, S., Saito, T., Gallusser, A., Kirchhausen, T. and Bonifacino, J.S. (1995). Interaction of tyrosine-based signals with clathrin-associated proteins. *Science*. **269**, 1872-1874.

Olliaro, P.L. and Goldberg. D.E. (1995). The *Plasmodium* digestive vacuole: metabolic headquarters and choice drug target. *Parasitology Today*. **11**(8), 294-297.

Omonuwa, S. and Omonuva, S. (2002). Malaria recurrence caused by *Plasmodium falciparum*. *Journal of the American Board of Family Practice*. **15**(2), 159-160.

Owen, D.J. and Luzio, J.P. (2000). Structural insights into clathrin-mediated endocytosis. *Current Opinions in Cell Biology*. **12**(4), 467-474.

Owen, D.J., Vallis, Y., Pearse, B.M., McMahon, H.T. and Evans, P.R. (2000). The structure and function of the β2-adaptin appendage domain. *The EMBO Journal*. **19**(16), 4216-4227.

Owen, D.J. and Evans, P.R. (1998). A structural explanation for the recognition of tyrosine-based endocytotic signals. *Science*. **282**(5392), 1327-1332.

Pagano, A., Crottet, P., Prescianotto-Baschong, C. and Spiess, M. (2004). In vitro formation of recycling vesicles from endosomes requires adaptor protein-1/clathrin and is regulated by rab4 and the connector rabaptin-5. *Molecular Biology of the Cell*. **15**(11), 4990-5000.

Page, L.J. and Robinson, M.S. (1995). Targeting signals and subunit interactions in coated vesicle adaptor complexes. *Journal of Cell Biology*. **131**(3), 619-630.

Parton, R.G. and Richards, A.A. (2003). Lipid rafts and caveolae as portals for endocytosis: new insights and common mechanisms. *Traffic*. **4**(11), 724-738.

Pasvol, G. and Wilson, R.J.M. (1982). The interaction of malaria parasites with red blood cells. *British Medical Bulletin*. **28**(2), 133-140.

Pattnaik, P., Shakri, A.R., Singh, S., Goel, S., Mukherjee, P. and Chitnis, C.E. (2007). Immunogenicity of a recombinant malaria vaccine based on receptor binding domain of *Plasmodium falciparum* EBA-175. *Vaccine*. **25**(5), 806-813.

Pereira-Leal, J.B and Seabra, M.C. (2000). The mammalian Rab family of small GTPases: definition of family and subfamily sequence motifs suggests a mechanism for functional specificity in the Ras superfamily. *Journal of Molecular Biology*. **301**(4), 1077-1087.

Pouvelle, B., Spiegel, R., Hsiao, L., Howard, R.J., Morris, R.L., Thomas, A.P. and Taraschi, T.F. (1991). Direct access to serum macromolecules by intraerythrocytic malaria parasites. *Nature*. **353**(6339), 73-75.

Przyborski, J.M. (2008). The Maurer's clefts of *Plasmodium falciparum*: parasite-induced islands within an intracellular ocean. *Trends in Parasitology*. **24**(7), 285-288.

Ralph, S.A., van Dooren, G.G., Waller, R.F., Crawford, M.J., Fraunholz, M.J., Foth, B.J., Tonkin, C.J., Roos, D.S. and McFadden, G.I. (2004). Tropical infectious diseases: metabolic maps and functions of the *Plasmodium falciparum* apicoplast. *Nature Reviews. Microbiology*. **2**(3), 203-216.

Ramya, T.N.C., Surolia, N. and Surolia, A. (2002). Survival strategies of the malarial parasite *Plasmodium falciparum*. *Current Science*. **83**(7), 818-825.

Rapoport, I., Miyazaki, M., Boll, W., Duckworth, B., Cantley, L.C., Shoelson, S. and Kirchhausen, T. (1997). Regulatory interactions in the recognition of endocytic sorting signals by AP-2 complexes. *The EMBO Journal*. **16**(9), 2240-2250.

Rapoport, I., Chen Chen, Y., Cupers, P., Shoelson, S.E. and Kirchhausen, T. (1998). Dileucine-based sorting signals bind to the beta chain of AP-1 at a site distinct and regulated differently from the tyrosine-based motif-binding site. *The EMBO Journal*. **17**(8), 2148-2155.

Rathore, D., Sacci, J.B., de la Vega, P. and McCutchan, T.F. (2002). Binding and invasion of liver cells by *Plasmodium falciparum* sporozoites. Essential involvement of the amino terminus of circumsporozoite protein. *Journal of Biological Chemistry*. **277**(9), 7092-7098.

Rayner, J.C., Vargas-Serrato, E., Huber, C.S., Galinski, M.R. and Barnwell, J.W. (2001). A *Plasmodium falciparum* homologue of *Plasmodium vivax* reticulocyte binding protein (PvRBP1) defines a trypsin-resistant erythrocyte invasion pathway. *Journal of Experimental Medicine*. **194**(11), 1571-1581.

Reeves, D.C., Liebelt, D.A., Lakshmanan, V., Roepe, P.D., Fidock, D.A. and Akabas, M.H. (2006). Chloroquine-resistant isoforms of the *Plasmodium falciparum* chloroquine resistance transporter acidify lysosome pH in HEK293 cells more than chloroquine-sentitive isoforms. *Molecular and Biochemical Parasitology*. **150**(2), 288-299.

Rhinehart-Jones, T. and Greenwalt, D.E. (1996). A detergent-sensitive 113-Kda conformer/complex of CD36 exists on the platelet surface. *Archives of Biochemistry and Biophysics*. **326**(1), 115-118.

Richard, D., Kats, L.M., Langer, C., Black, C.G., Mitri, K., Boddey, J.A., Cowman, A.F. and Coppel, R.L. (2009). Identification of rhoptry trafficking determinants and evidence for a novel sorting mechanism in the malaria parasite *Plasmodium falciparum*. *PLoS Pathogens*. **5**(3), Epub 2009 Mar 6.

Richardson, T.H., Griffin, K.J., Jung, F., Raucy, J.L. and Johnson, E.F. (1997). Targeted antipeptide antibodies to cytochrome P450 2C18 based on epitope mapping of an inhibitory monoclonal antibody to P450 2C5. *Archives of Biochemistry and Biophysics*. **338**(2), 157-164.

Ricotta, D., Conner, S.D., Schmid, S.L., von Figura, K. and Honing, S. (2002). Phosphorylation of the AP2 μ subunit by AAK1 mediates high affinity binding to membrane protein sorting signals. *Journal of Cell Biology*. **156**(5), 791-795.

Roberts, L., Egan, T.J., Joiner, K.A. and Hoppe, H.C. (2008). Differential effects of quinoline antimalarials on endocytosis in *Plasmodium falciparum*. *Antimicrobial Agents and Chemotheraphy*. **52**(5), 1840-1842.

Robibaro, B., Hoppe, H.C., Yang, M., Coppens, I., Ngô, H.M., Stedman, T.T., Paprotka, K. and Joiner, K.A. (2001). Endocytosis in different lifestyles of protozoan parasitism: role in nutrient uptake with special reference to *Toxoplasma gondii*. *International Journal of Parasitology*. **31**(12), 1343-1353.

Robinson, M.S. and Bonifacino, J.S. (2001). Adaptor-related proteins. *Current Opinion in Cell Biology*. **13**, 444-453.

Rosenthal, P.J. (2004). Cysteine proteases of malaria parasites. *International Journal for Parasitology*. **34**(13-14), 1489-1499.

Rosenthal, P.J., McKerrow, J.H., Aikawa, M., Nagasawa, H. and Leech, J.H. (1988). A malarial cysteine proteinase is necessary for hemoglobin degradation by *Plasmodium falciparum*. 1988. *Journal of Clinical Investigation*. **82**(5), 1560-1566.

Rothman, J.E. (1994). Mechanisms of intracellular protein transport. *Nature*. **372** (6501), 55-63.

Rothman, J.E., Miller, R.L. and Urbani, L.J. (1984). Intercompartmental transport in the Golgi complex is a dissociative process: facile transfer of membrane protein between two Golgi populations. *Journal of Cell Biology*. **99**(1 Pt 1), 260-271.

Royle, S.J. and Lagnado, L. (2006). Trimerisation is important for the function of clathrin at the mitotic spindle. *Journal of Cell Science*. **119**(Pt 19), 4071-4078.

Sahu, N.K., Sahu, S. and Kohli, D.V. (2008). Novel molecular targets for antimalarial drug development. *Chemical Biology and Drug Design*. **71**(4), 287-297.

Salamero, J., Sztult, E.S. and Howell, K.E. (1990). Exocytic transport vesicles generated in vitro from the *trans*-Golgi network carry secretory and plasma membrane proteins. *Proceedings of the National Academy of Sciences*. **87**(19), 7717-7721.

Saliba, K.J., Martin, R.E., Bröer, A., Henry, R.I., McCarthy, C.S., Downie, M.J., Allen, R.J., Mullinm, K.A., McFadden, G.I., Bröer, S. and Kirk, K. (2006). Sodium-dependent uptake of inorganic phosphate by the intracellular malaria parasite. *Nature*. **443**(7111), 582-585.

Salmon, B.L., Oksman, A. and Goldberg, D.E. (2001). Malaria parasite exit from the host erythrocyte: A two-step process requiring extraerythrocytic proteolysis. *Proceedings of the National Academy of Sciences*. **98**(1), 271-276.

Sam-Yellowe, T.Y., Florens, L., Johnson, J.R., Wang, T., Drazba, J.A., Le Roch, K.G., Zhou, Y., Batalov, S., Carucci, D.J., Winzeler, E.A. and Yates, J.R. III. (2004). A *Plasmodium* gene family encoding Maurer's cleft membrane proteins: structural properties and expression profiling. *Genome Research*. **14**(6), 1052-1059.

Sayers, J.R., Price, H.P., Fallon, F.G. and Doenhoff, M.J. (1995). AGA/AGG codon usage in parasites: implications for gene expression in *Escherichia coli*. *Parasitology Today*. **11**(9), 345-346.

Sever, S. (2002). Dynamin and endocytosis. *Current Opinions in Cell Biology*. **14**(4), 463-467.

Sharp, P.M. and Devine, K.M. (1989). Codon usage and gene expression level in *Dictyostelium discoideum*: highly expressed genes do 'prefer' optimal codons. *Nucleic Acids Research*. **17**(13), 5029-5039.

Sheiner, L. and Soldati-Favre, D. (2008). Protein Trafficking inside *Toxoplasma gondii*. *Traffic*. **9**(5), 636-646.

Shin, J.S. and Abraham, S.N. (2001). Caveolae as portals of entry for microbes. *Microbes and Infection*. **3**(9), 755-761

Shinotsuka, C., Waguri, S., Wakasugi, M., Uchiyama, Y. and Nakayama, K. (2002). Dominant-negative mutant of BIG2, an ARF-guanine nucleotide exchange factor, specifically affects membrane trafficking from the *trans*-Golgi network through inhibiting membrane association of AP-1 and GGA coat proteins. *Biochemical and Biophysical Research Communications*. **294**(2), 254-260.

Shorter, J., Watson, R., Giannakou, M.E., Clarke, M., Warren, G. and Barr, F.A. (1999). GRASP55, a second mammalian GRASP protein involved in the stacking of Golgi cisternae in a cell-free system. *The EMBO Journal*. **18**(18), 4949-4960.

Siau, A., Toure, F.S., Ouwe-Missi-Oukem-Boyer, O., Ciceron, L., Mahmoudi, N., Vaquero, C., Froissard, P., Bisvigou, U., Bisser, S., Coppee, J.Y., Bischoff, E., David, P.H. and Mazier, D. (2007). Whole-transcriptome analysis of *Plasmodium falciparum* field isolates: identification of new pathogenicity factors. *The Journal of Infectious Disease*. **196**(11), 1603-1612.

Silvie, O., Charrin, S., Billard, M., Franetich, J.F., Clark, K.L., van Gemert, G.J., Sauerwein, R.W., Dautry, F., Boucheix, C., Mazier, D. and Rubinstein, E. (2006). Cholesterol contributes to the organization of tetraspanin-enriched microdomains and to CD81-dependent infection by malaria sporozoites. *Journal of Cell Science*. **119**(Pt 10), 1992-2002.

Singh, A.P., Puri, S.K. and Chitnis, C.E. (2002). Antibodies raised against receptor-binding domain of *Plasmodium knowlesi* duffy binding protein inhibit erythrocyte invasion. *Molecular and Biochemical Parasitology*. **121**(1), 21-31.

Singh, S., Plassmeyer, M., Gaur, D. and Miller, L.H. (2007). Mononeme: a new secretory organelle in *Plasmodium falciparum* merozoites identified by localization of rhomboid-1 protease. *Proceeding of the National Academy of Sciences of the United States of America*. **104**(50), 20043-20048.

Slater, R. and Bishop, N.E. (2006). Genetic structure and evolution of the Vps25 family, a yeast ESCRT-II component. *BMC Evolutionary Biology*. **6**:59.

Smith, J.D., Craig, A.G., Kriek, N., Hudson-Taylor, D., Kyes, S., Fagen, T., Pinches, R., Baruch, D.I, Newbold, C.I. and Miller, L.H. (2000). Identification of a *Plasmodium falciparum* intercellular adhesion molecule-1 binding domain: A parasite adhesion trait implicated in cerebral malaria. *Proceedings of the National Academy of Sciences*. **97**(4), 1766-1771.

Smythe, W.A., Joiner, K.A. and Hoppe, H.C. (2008). Actin is required for endocytic trafficking in the malaria parasite *Plasmodium falciparum*. *Cellular Microbiology*. **10**(2), 452-464.

Sorkina, T., Bild, A., Tebar, F. and Sorkin, A. (1999). Clathrin, adaptors and eps15 in endosomes containing activated epidermal growth factor receptors. *Journal of Cell Science*. **112**(Pt 3), 317-327.

Spangler, B.D. (1991). Binding to native proteins by antipeptide monoclonal antibodies. *Journal of Immunology*. **146**(5), 1591-1595.

Spycher, C., Rug, M., Pachlatko, E., Hanssen, E., Ferguson, D., Cowman, A.F., Tilley, L. and Beck, H.P. (2008). The Maurer's cleft protein MAHRP1 is essential for trafficking of *Pf*EMP1 to the surface of *Plasmodium falciparum*-infected erythrocytes. *Molecular Microbiology*. **68**(5), 1300-1314.

Stepp, J.D., Huang, K. and Lemmon, S.K. (1997). The yeast adaptor protein complex, AP-3, is essential for the efficient delivery of alkaline phosphatase by the alternate pathway to the vacuole. *Journal of Cell Biology*. **139**(7), 1761-1774

Struck, N.S., Herrmann, S., Schmuck-Barkmann, I., de Souza Dias, S., Haase, S., Cabrera, A.L., Treeck, M., Bruns, C., Langer, C., Cowman, A.F., Marti, M., Spielmann, T. and Gilberger, T.W. (2008). Spatial dissection of the *cis*- and *trans*-Golgi compartments in the malaria parasite *Plasmodium falciparum*. *Molecular Microbiology*. **67**(6), 1320-1330.

Struck, N.S., de Souza Dias, S., Langer, C., Marti, M., Pearce, J.A., Cowman, A.F. and Gilberger, T.W. (2005). Re-defining the Golgi complex in *Plasmodium falciparum* using the novel Golgi marker *Pf*GRASP. *Journal of Cell Science*. **118**(Pt 23), 5603-5613.

Sturm, A., Amino, R., van de Sand, C., Regen, T., Retzlaff, S., Rennenberg, A., Krueger, A., Pollok, J.M., Menard, R. and Heussler, V.T. (2006). Manipulation of host hepatocytes by the malaria parasite for delivery into liver sinusoids. *Science*. **313**(5791), 1287-1290.

Takano, E., Maki, M., Mori, H., Hatanaka, M., Marti, T., Titani, K., Kannagi, R., Ooi, T. and Murachi, T. (1988). Pig heart calpastatin: identification of repetitive domain structures and anomalous behavior in polyacrylamide gel electrophoresis. *Biochemistry*. **27**(6), 1964-1972.

Takatsu, H., Futatsumori, M., Yoshino, K., Yoshida, Y., Shin, H. and Nakayama, K. (2001). Similar subunit interactions contribute to assembly of clathrin adaptor complexes and COPI complex: analysis using yeast three-hybrid system. *Biochemical and Biophysical Research Communications*. **284**(4), 1083-1089.

Takei, K. and Haucke, V. (2001). Clathrin-mediated endocytosis: membrane factors pull the trigger. *Trends in Cell Biology*. **11**(9), 385-391.

Takei, K., Slepnev, V.I., Haucke, V. and De Camilli, P. (1999). Functional partnership between amphiphysin and dynamin in clathrin mediated endocytosis. *Nature, Cell Biology*. **1**(1), 33-39.

Taraschi, T.F., O'Donnell, M., Martinez, S., Schneider, T., Trelka, D., Fowler, V.M., Tilley, L. and Moriyama, Y. (2003). Generation of an erythrocyte vesicle transport system by *Plasmodium falciparum* malaria parasites. *Blood*. **102**(9), 3420-3426.

Taraschi, T.F. and Nicolas, E. (1994). The parasitophorous duct pathway: new opportunities for antimalarial drug and vaccine development. *Parasitology Today*. **10**(10), 399-401.

Taraschi, T.F., Trelka, D., Schneider, T. and Matthews, I. (1998). *Plasmodium falciparum*: Characterization of organelle migration during merozoite morphogenesis in asexual malaria infections. *Experimental Parasitology*. **88**(3), 184-193.

Taraschi, T.F., Trelka, D., Martinez, S., Schneider, T. and O'Donnell, M.E. (2001). Vesicle-mediated trafficking of parasite proteins to the host cell cytosol and erythrocyte surface membrane in *Plasmodium falciparum* infected erythrocytes. *International Journal of Parasitology*. **31**(12), 1381-1391.

Taylor-Robinson, A. (2001). Malaria sporozoite rite of passage. *Trends in Parasitology*. **17**(4), 165.

Templeton, T.J. and Deitsch, K.W. (2005). Targeting malaria parasite proteins to the Erythrocyte. *Trends in Parasitology*. **21**(9), 399-402.

Theos, A.C., Tenza, D., Martina, J.A., Hurbain, I., Peden, A.A., Sviderskaya, E.V.,Stewart, A., Robinson, M.S., Bennett, D.C., Cutler, D.F., Bonifacino, J.S., Marks, M.S. and Raposo, G. (2005). Functions of adaptor protein (AP)-3 and AP-1 in tyrosinase sorting from endosomes to melanosomes. *Molecular Biology of the Cell*. **16**(11), 5356-5372.

Thyberg, J. and Moskalewski, S. (1999). Role of microtubules in the organization of the Golgi complex. *Experimental Cell Research*. **246**(2), 263-279.

Tilley, L., McFadden, G., Cowman, A. and Klonis, N. (2007). Illuminating *Plasmodium falciparum*-infected red blood cells. *Trends in Parasitology*. **23**(6), 268-277.

Tonkin, C.J., Pearce, J.A., McFadden, G.I. and Cowman, A.F. (2006). Protein targeting to destinations of the secretory pathway in the malaria parasite *Plasmodium falciparum*. *Current Opinion in Microbiology*. **9**(4), 381-387.

Tonkin, C.J., van Dooren, G.G., Spurck, T.P., Struck, N.S., Good, R.T., Handman, E., Cowman, A.F. and McFadden, G.I. (2004). Localization of organellar proteins in *Plasmodium falciparum* using a novel set of transfection vectors and a new immunofluorescence fixation method. *Molecular and Biochemical Parasitology*. **137**(1), 13-21.

Trager, W. and Jensen, J.B. (1976). Human malarial parasite in continuous culture. *Science*. **193**(4254), 673-675.

Trang, D.T.X., Huy, N.T., Kariu, T., Tajima, K. and Kamei, K. (2004). One-step concentration of malaria parasite-infected red blood cells and removal of contaminating white blood cells. *Malaria Journal*. **3**(7), 1-7.

Traub, L.M. and Kornfeld, S. (1997). The *trans*-Golgi network: a late secretory sorting station. *Current Opinions in Cell Biology*. **9**(4), 527-533.

Traub, L.M. (2005). Common principles in clathrin-mediated sorting at the Golgi and the plasma membrane. *Biochimica et Biophysica Acta*. **1744**(3), 415-437.

Tripathi, A.K., Sullivan, D.J. and Stins, M.F. (2006). *Plasmodium falciparum*-infected erythrocytes increase intercellular adhesion molecule 1 expression on brain endothelium through NF- κB. *Infection and Immunity*. **74**(6), 3262-3270.

Tripathi, A.K., Garg, S.K. and Tekwani, B.L. (2002). A physiochemical mechanism of haemozoin (β-Hematin) synthesis by malaria parasite. *Biochemical and Biophysical Research Communications*. **290**(1), 595-601.

Udagama, P.V., Atkinson, C.T., Peiris, J.S., David, P.H., Mendis, K.N. and Aikawa, M. (1988). Immunoelectron microscopy of Schüffner's dots in *Plasmodium vivax*-infected human erythrocytes. *American Journal of Pathology*. **131**(1), 48-52.

Ullrich, H.J., Beatty, W.L. and Russell, D.G. (2000). Interaction of *Mycobacterium avium*-containing phagosomes with the antigen presentation pathway. *Journal of Immunology*. **165**(11), 6073-6080.

Ullu, E., Tschudi, C. and Chakraborty, T. (2004). RNA interference in protozoan parasites. *Cellular Microbiology*. 6(6), 509-519.

van den Steen, P.E., Deroost, K., van Aelst, E., Geurts, N., Martens, E., Struyf, S., Nie, K.Q., Hansen, D.S., Matthys, P., van Damme, J. and Opdenakker, G. (2008). CXCR3 determines strain susceptibility to murine cerebral malaria by mediating T lymphocyte migration toward IFN-γ-induced chemokines. *European Journal of Immunology*. **38**(4), 1082-1095.

van Dooren, G.G., Waller, R.F., Joiner, K.A, Roos, D.S. and McFadden, G.I. (2000). Traffic jams: protein transport in *Plasmodium falciparum*. *Parasitology Today*. **16**(10), 421-427.

van Houten, N.E., Zwick, M.B., Menendez, A. and Scott, J.K. (2006). Filamentous phage as an immunogenic carrier to elicit focused antibody responses against a synthetic peptide. *Vaccine*. **24**(19), 4188-4200.

van Wye, J., Ghori, N., Websterb, P., Mitschler, R.R., Elmendorfa, H.G. and Haldar, K. (1996). Identification and localization of rab6, separation of rab6 from ERD2 and implications for an 'unstacked' Golgi, in *Plasmodium falciparum*. *Molecular and Biochemical Parasitology*. **83**(1), 107-120.

Vargas-Serrato, E., Corredor, V. and Galinski, M.R. (2003). Phylogenetic analysis of *CSP* and *MSP-9* gene sequences demonstrates the close relationship of *Plasmodium coatneyi* to *Plasmodium knowlesi*. *Infection, Genetics and Evolution*. **3**(1), 67-73.

Vervoort, E.B., van Ravestein, A., van Peij, N.N., Heikoop, J.C., van Haastert, P.J., Verheijden, G.F. and Linskens, M.H. (2000). Optimizing heterologous expression in *dictyostelium*: importance of 5' codon adaptation. *Nucleic Acids Research*. **28**(10), 2069-2074.

Wakeham, D.E., Ybe, J.A., Brodsky, F.M. and Hwang, P.K. (2000). Molecular structures of proteins involved in vesicle coat formation. *Traffic*. **1**(5), 393-398.

Waller, R.F. and McFadden, G.I. (2005). The apicoplast: a review of the derived plastid of apicomplexan parasites. *Current Issues in Molecular Biology*. **7**(1), 57-79.

Waller, R.F., Keeling, P.J., Donald,R.G.K., Striepen, B., Handman, E., Lang-Unnasch, N., Cowman, A.F., Besra, G.S., Roos, D.S. and McFadden, G.I. (1998). Nuclear-encoded proteins target to the plastid in *Toxoplasma gondii* and *Plasmodium falciparum*. *Proceedings of the National Academy of Sciences*. **95**(21), 12352-12357.

Walliker, D., Quakyi, I.A., Wellems, T.E., McCutchan, T.F., Szarfman, A., London, W.T., Corcoran, L.M., Burkot, T.R. and Carter, R. (1987). Genetic analysis of the human malaria parasite *Plasmodium falciparum*. *Science*. **236**(4809), 1661-1666.

Wang, L.H., Südhof, T.C. and Anderson, R.G.W. (1995). The appendage domain of α-adaptin is a high affinity binding site for dynamin. *Journal of Biological chemistry*. **270**(17), 10079-10083.

Wang, Y., Satoh, A. and Warren, G. (2005). Mapping the functional domains of the Golgi stacking factor GRASP65. *Journal of Biological Chemistry*. **280**(6), 4921-4928.

Ward, G.E., Tilney, L.G. and Langsley, G. (1997). Rab GTPases and the unusual secretory pathway of *Plasmodium*. *Parasitology Today*. **3**(2), 57-62.

Weber, J.L. (1987). Analysis of sequences from the extremely A + T-rich genome of *Plasmodium falciparum*. *Gene*. **52**(1), 103-109.

Wickert, H., Wissing, F., Andrews, K.T., Stich, A., Krohne, G. and Lanzer, M. (2003). Evidence for trafficking of *Pf*EMP1 to the surface of *P. falciparum*-infected erythrocytes via a complex membrane network. *European Journal of Cell Biology*. **82**(6), 271-284.

Wickham, M.E., Culvenor, J.G. and Cowman, A.F. (2003). Selective inhibition of a two-step egress of malaria parasites from the host erythrocyte. *The Journal of Biological Chemistry*. **278**(39), 37658-37663.

Williams, R.L. and Urbé, S. (2007). The emerging shape of the ESCRT machinery. *Nature Reviews. Molecular Cellular Biology*. **8**(5), 355-368.

Wilson, R.J. (2002). Progress with parasite plastids. *Journal of Molecular Biology*. **319**(2), 257-74.

Wilson, R.J., Denny, P.W., Preiser, P.R., Rangachari, K., Roberts, K., Roy, A., Whyte, A., Strath, M., Moore, D.J., Moore, P.W. and Williamson, D.H. (1996). Complete gene map of the plastid-like DNA of the malaria parasite *Plasmodium falciparum*. *Journal of Molecular Biology*. **261**(2), 155-172.

Wiser, M.F., Grab, D.J. and Norbert Lanners, H. (1999). An alternative secretory pathway in *Plasmodium falciparum*: more questions than answers. *Novartis Foundation Symposium*. **226**(discussion 211-214), 199-211.

Wiser, M.F., Norbert Lanners, H., Bafford, R.A. and Favaloro, J.M. (1997). A novel secretory pathway for the export of *Plasmodium* proteins into the host Erythrocyte. *Proceedings of the National Academy of Sciences*. **94**(17), 9108-9113.

Witola, W.H., Pessi, G., El Bissati, K., Reynolds, J.M. and Mamoun, C.B. (2006). Localization of the phosphoethanolamine methyltransferase of the human malaria parasite *Plasmodium falciparum* to the Golgi apparatus. *Journal of Biological Chemistry*. **281**(30), 21305-21311.

Wu Y, Kirkman LA, Wellems TE. (1996). Transformation of *Plasmodium falciparum* malaria parasites by homologous integration of plasmids that confer resistance to pyrimethamine. *Proceedings of the National Academy of Sciences of the United States of America*. **93**(3), 1130-1134.

Xu, W. and. Ellington, A.D. (1996). Anti-peptide aptamers recognize amino acid sequence and bind a protein epitope. *Proceedings of the National Academy of Sciences*. **93**(15), 7475-7480.

Yadava, A. and Ockenhouse, C.F. (2003). Effect of codon optimization on expression levels of a functionally folded malaria vaccine candidate in prokaryotic and eukaryotic expression systems. *Infection and Immunity*. **71**(9), 4961-4969.

Yang, M., Coppens, I., Wormsley, S., Baevova, P., Hoppe, H.C. and Joiner, K.A. (2004). The Plasmodium falciparum Vps4 homolog mediates multivesicular body formation. *Journal of Cell Science*. **117**(Pt 17), 3831-3818.

Yarar, D., Waterman-Storer, C.M. and Schmid, S.L.(2005). A dynamic actin cytoskeleton functions at multiple stages of clathrin-mediated endocytosis. *Molecular Biology of the Cell*. **16**(2), 964-975.

Yeung, S., Pongtavornpinyo, W., Hastings, I.M., Mills, A.J. and White, N.J. (2004). Antimalarial drug resistance, artemisinin-based combination therapy, and the contribution of modeling to elucidating policy choices. *American Journal of Tropical Medicine Hygiene*. **71**(2), 179-186

Yoshida, Y., Kinuta, M., Abe, T., Liang, S., Araki, K., Cremona, O., Di Paolo, G., Moriyama, Y., Yasuda, T., De Camilli, P. and Takei, K. (2004). The stimulatory action of amphiphysin on dynamin function is dependent on lipid bilayer curvature. *EMBO Journal*. **23**(17), 3483-3491.

Zahraoui, A. Joberty, G., Arpin, M., Fontaine, J.J., Hellio, R., Tavitian, A. and Louvard, D. (1994). A small rab GTPase is distributed in cytoplasmic vesicles in non polarized cells but colocalizes with the tight junction marker ZO-1 in polarized epithelial cells. *Journal of Cell Biology*. **124**(1-2), 101-115.

Zhang, J., Long, M. and Li, L. (2005). Translational effects of differential codon usage among intragenic domains of new genes in *Drosophila*. *Biochimica et Biophysica Acta*. **1728**(3), 135-142.

Zhou, Z., Schnake, P., Xiao, L. and Lal, A.A. (2004) Enhanced expression of a recombinant malaria candidate vaccine in *Escherichia coli* by codon optimization. *Protein Expression and Purification*. **34**(1), 87-94.

Zinsmaier, K.E. and Bronk, P. (2001). Molecular chaperones and the regulation of neurotransmitter exocytosis. *Biochemical Pharmacology*. **62**(1), 1-11.